UNIVERSITÀ DEGLI STUDI
DI MODENA E REGGIO EMILIA

Dottorato di ricerca in
MODELS AND METHODS FOR MATERIAL AND ENVIRONMENTAL SCIENCES

Ciclo XXXII

Dating of ancient mortars: the case studies of Pompeii and the medieval Modena cathedral UNESCO sites

Candidato: Giulia Tirelli

Relatore (Tutor): Prof. Stefano Lugli

Coordinatore del Corso di Dottorato: Prof. Giovanna Vezzalini

INDEX

CASE STUDY 2: POMPEII UNESCO SITE

RIASSUNTO

I monumenti storici sono strutture complesse soggette a modiche nel corso del tempo. Per questo motivo la loro tutela è una vera e propria sfida. Per valutare lo stato di conservazione di un edificio è fondamentale ricostruire la sua storia e identificare le principali vulnerabilità e criticità. I siti UNESCO della Cattedrale di Modena e di Pompei ne rappresentano due casi significativi. La datazione assoluta dei materiali da costruzione è stata svolta al fine di ricostruire la storia degli interventi di restauro effettuati come conseguenza di eventi sismici.

La Cattedrale di Modena fu danneggiata dal terremoto avvenuto nel 2012 e le principali vulnerabilità sono state riscontrate nelle volte cinquecentesche. Il progetto di rafforzamento antisismico ha permesso di indagarne le fasi costruttive e di comprendere la sequenza storica dei danni subiti. Dalle campagne di ricognizione svolte direttamente sugli estradossi delle volte, sono state identificate numerose lesioni ed è emersa la presenza di ampie porzioni ricostruite utilizzando malte di allettamento con legante di gesso e calce. Risulta evidente quindi che queste sezioni giustapposte a diverso legante siano da ascriversi ad importanti interventi di restauro strutturale effettuati al fine di riparare i danni provocati da eventi sismici. Lo scopo della ricerca è quello di datare le porzioni originarie delle volte e quelle successivamente restaurate correlando i risultati ottenuti con il catalogo parametrico dei terremoti italiani, al fine di risalire al possibile evento lesivo. È stato quindi applicato un progetto di ricerca innovativo che integra diversi metodi di datazione assoluta: radiocarbonio e Luminescenza Otticamente Stimolata (OSL) per la datazione delle malte, e Termoluminescenza (TL) per la datazione dei mattoni. Al fine della corretta interpretazione dei risultati, è stata eseguita la caratterizzazione petrografica delle malte di calce ed è stata inoltre svolta l'analisi dei pollini presenti all'interno delle malte di gesso. I risultati mostrano che la malta di calce è stata utilizzata sia per la costruzione originaria sia per riparazioni successive, mentre la malta di gesso è stata impiegata o in volte fortemente danneggiate e ricostruite totalmente o per restaurare porzioni di volte originariamente in malta di calce. Si evince così che le aree danneggiate siano più estese di quelle rilevabili esclusivamente mappando le lesioni oggi visibili. Infine la comparazione delle due procedure di preparazione dei campioni di malta di calce da datare al radiocarbonio (Cryo2Sonic e digestione acida graduale), ha permesso di identificare la metodologia più idonea ai fini della datazione di malte di calce con aggregato a composizione carbonatica.

Diversi pavimenti a mosaico, appartamenti ad alcune *domus* e ad aree pubbliche di Pompei, presentano dei risarcimenti, probabilmente effettuati al fine di colmare lacune provocate da danni

subiti o in epoche antiche o più recenti, dopo lo scavo del sito. Questi interventi sono state riscontrati in diverse ed importanti *domus* (Casa di *Paquius Proculus,* Casa del Menandro, Casa della Fontana Piccola, Casa VIII, 3, 24) e nelle Terme del Foro. Al fine di chiarire se questo tipo di restauro sia stato effettuato nell'antichità o si tratti di un intervento moderno, sono state applicate diverse metodologie, quali la caratterizzazione petrografica, la datazione assoluta al radiocarbonio e l'analisi dei pollini. La datazione al radiocarbonio ha fornito due range cronologici (4229-3376 a.C. e 17784-14521 a.C.) che sono molto più antichi di quanto previsto per gli edifici romani, indicando una contaminazione da CO_2 di origine geologica. Poiché la metodologia di digestione acida graduale per la preparazione di malte da sottoporre a datazione radiocarbonica si è dimostrata efficace nell'eliminare la contaminazione da aggregato carbonatico, ne consegue che le malte di Pompei hanno incorporato una fonte di CO_2 derivante del drammatico seppellimento da materiale vulcanico ad alta temperatura durante l'eruzione del Vesuvio nel 79 d.C. Se le malte di restauro fossero state moderne, non ci aspetteremmo questa contaminazione e la datazione al radiocarbonio avrebbe fornito un'età moderna. Da ciò si deduce che questi interventi successivi sono antichi restauri, probabilmente effettuati dopo il terremoto del 62 d.C., che precedette la fatale eruzione del Vesuvio. Un' antica e sconosciuta fase di restauro è stata quindi pienamente identificata come un'altra importante parte della drammatica storia di Pompei, che andrebbe preservata.

ABSTRACT

Historical monuments are complex structures, built and modified over time. For this reason, their preservation is a challenging issue. Reconstructing the history and structural vulnerability of a building is fundamental to assess its state of conservation. The Modena Cathedral and Pompeii UNESCO sites represent significant examples in this regard. Absolute dating of the building materials has been performed in order to provide data on the site chronology and the history of repair interventions, especially after earthquakes.

The Modena Cathedral was damaged by the 2012 earthquake and the main vulnerabilities were identified on the 15th century vaults. An anti-seismic reinforcement project gave the opportunity to investigate the construction phases and to assess the damages suffered in the past. A detailed survey of the vaults binder was carried out and revealed the scars of multiple repair works after several earthquakes, resulting in a complex patchwork of lime and gypsum mortars. The aim of the study was to absolute date the original vaults construction and the restoration portions built after the main earthquakes, correlating them to the earthquake chronology deduced from the historic catalogue. An integrated approach using different techniques has been applied: radiocarbon dating by Cryo2Sonic and by sequential dissolution, and Optically Stimulated Luminescence (OSL) of the sand aggregate to date ancient mortars, and Thermo-luminescence (TL) to date bricks. The petrographic characterization of mortars has been performed as fundamental step for the interpretation of the results and the analysis of the pollen trapped in the gypsum mortar has been tested. The results show that lime mortar was used both as original building material and for later repairs, while the gypsum binder was used to entirely rebuild some vaults or to repair some vaults originally built using lime mortars. This demonstrates that the vaults suffered much larger damage induced by earthquakes than previously assessed just by mapping fracture and crack networks. In addition, the comparison of the two sample preparation procedures of mortar for radiocarbon dating (Cryo2Sonic and sequential dissolution) has allowed to identify the most suitable method for lime mortars rich in carbonate aggregate.

Some mosaic floors in houses and public spaces in Pompeii present late interventions, which were probably carried out to fill gaps in pavements to repair various types of damage, either in ancient time or just after the excavation of the site. Important *domus* (House of *Paquius Proculus*, House of Menander, House of the Small Fountain, House VIII, 3, 24) and the *Forum* baths display these repairs. To clarify the origin of the restoration, ancient vs. modern, petrographic characterization,

radiocarbon dating and pollen analysis have been performed. The result of radiocarbon dating range from 4229 to 3376 BC and from 17784 to 14521 BC, which is much older than expected for roman buildings, demonstrating a geological source for CO_2. Since the sequential dissolution methodology has been proved efficient in eliminating the geological contribution of carbonate grains, it follows that the Pompeii mortars have been incorporated a CO_2 sources probably deriving by the dramatic burial by high temperature volcanic material during the 79 AD eruption of Vesuvius. If the repair mortars were modern, we would not expect this contamination and the radiocarbon dating would have yielded a modern age. It means that these late interventions are ancient restoration, probably carried out after the earthquake of 62 AD that preceded the fatal eruption of Vesuvius. According to these results an ancient unrecognized restoration phase is now fully identified as another important part of the dramatic history of Pompeii, that should be preserved.

ACKNOWLEDGMENTS

Before starting, I would like to thank all who made possible completing the research.

First of all, I want to thank my tutor, prof. Stefano Lugli who followed me during the PhD years, encouraging me to live important experiences that made my PhD productive and stimulating.

Thanks to the Studio Tecnico Silvestri of Modena, in particular arch. Elena Silvestri, and dr. Maria Stella Pisapia (Consulente Soprintendenze di Napoli e Pompei) who have made my doctoral work possible.

I would like to thank all the partners involved in the project for the hospitality, access to their laboratories, equipment, expertise and the essential contribution to my work:

- the Department of Environmental Science and Technology of the University of Campania "Luigi Vanvitelli" in Caserta, in particular prof. Carmine Lubritto and dr. Paola Ricci.

- the Department of Material Sciences, University of Milan Bicocca, in particular dr. Laura Panzeri, prof. Emanuela Sibilia, prof. Marco Martini and dr. Anna Galli.

- the Laboratory of Palynology and Palaeobotany of the University of Modena and Reggio Emilia, in particular prof. Marta Mazzanti, dr. Giovanna Bosi and dr. Paola Torri.

- the Laboratory of Nuclear Techniques Applied to Cultural Heritage (LABEC) of the National Institute for Nuclear Physics, in particular dr. Mariaelena Fedi.

- the AMS ^{14}C Dating Centre at Aarhus University (Denmark), in particular prof. Jan Heinemeir and prof. Jesper Olsen.

-the Laboratory of Ion Beam Physics of ETH Zurich, in particular dr. Irka Hajdas.

It was an honor to be a visiting PhD student at Abo Akademi Univeristy of Turku (Finland). I am grateful to dr. Alf Lindroos who patiently guided me and taught me all the secrets of the mortar dating and for his generous hospitality. Thanks also to prof. Åsa Ringbom for her contagious joy and enthusiasm. Her support at the project has been motivating.

1. INTRODUCTION

Pompeii and the medieval Modena cathedral UNESCO sites have been chosen as case studies to clarify the site chronology and the history of the restoration, by means of absolute dating of building materials. Reconstructing the history and the structural vulnerability of the historical monuments is fundamental for their preservation.

The Modena Cathedral vaults were extremely damaged by the 2012 earthquake and an anti-seismic reinforcement project was planned giving us the opportunity to investigate the construction phases and to assess the damages suffered in the past. A complex patchwork of lime and gypsum mortars have been detected on the vaults, revealing the scars of multiple repair works after several earthquakes. The aim of the study is to absolute date the original vaults construction and the restoration portions, correlating them to the earthquake chronology deduced from the historic catalogue.

Some mosaic floors in houses and public spaces in Pompeii present late interventions carried out to repair various types of damage. The aim of the research is to discriminate the timing of the restoration, ancient vs modern.

Since historical sources leaves unclear issues, a scientific approach is the only way to obtain reliable data. An integrated method using different techniques (petrographic analysis, radiocarbon dating, OLS dating, TL dating, pollen analysis) has been applied for both case studies.

Beside the specific archaeological and historical questions, the present study is also concerned with the capabilities and limits of the different absolute dating techniques. This thesis presents how different methods have been used and how successful they have been. The research deals with the problem of the different contamination sources that can occur in radiocarbon dating of ancient mortar and the comparison of the two sample preparation procedures of mortar for radiocarbon dating has allowed to identify the most reliable method.

2. MORTAR DATING: THE STATE OF THE ART

Mortar is an artificial building material used to link bricks or stones. Mortar is a mixture of binder, aggregate, water and eventually other organic (e.g. charcoal, straw) or inorganic (e.g. ceramic fragments) components. The binder (gypsum, lime, clay or cement) is the material that, mixed with water, form an easily workable mass capable to hardening to form a unique hard structure. The aggregate (sand, gravel or *pozzolana*) is added to the binder in order to reduce the effect of mortar shrinkage and to enhance the mechanical properties (Cazalla et al. 2000; Stefanidou and Papayianni 2005). There are two characteristic types of lime: hydraulic and non-hydraulic. They differ in the manner by which they harden and in the properties they display. Hydraulic limes harden to a greater or lesser extent due to a chemical reaction between their active clay particles, lime and water (hydraulic set) whereas non-hydraulic limes harden due to a reaction between CaO in the mix and atmospheric CO_2 (carbonation) (Pavia et al. 2006). Artificial hydraulic mortars were obtained by mixing lime with *pozzolana* or crushed bricks (*cocciopesto*) (Binda and Baronio 1988; Bugini et al. 1993; Baronio and Binda 1997; Baronio et al. 1997; Moropoulou et al. 2005; Böke et al. 2006; Pavia 2008; Pavia and Caro 2008; Silva et al. 2009; Elsen et al. 2012; Weber et al. 2015).

2.1. Production of historic mortar

Historic mortars are a mixture of lime, $Ca(OH)_2$ (calcium hydroxide as the mineral portlandite) an aggregate, usually sand or volcanic pyroclastic material. The historic mortar manufacture includes different steps, presented schematically in figure 1.

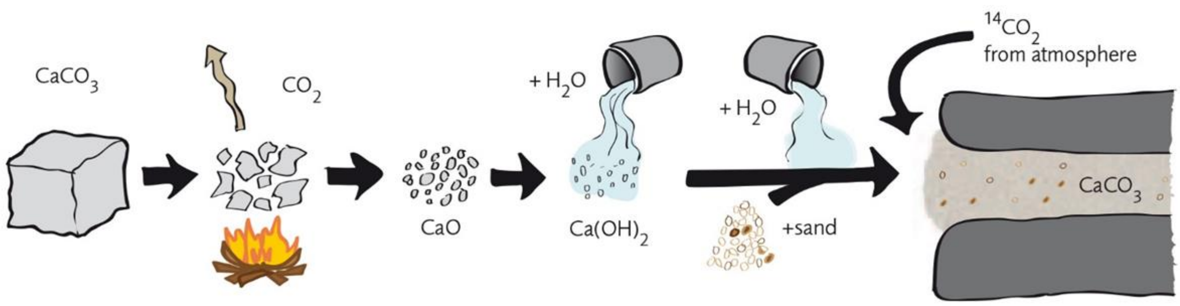

Fig. 1: The $CaCO_3$ cycle from limestone to binder calcite (Hale et al. 2003).

The production process begins with the burning of crushed limestone in a kiln at temperatures of about 800-900 °C or exceeding. At this temperature calcination occurs and the calcium carbonate (mineral calcite) is transformed into quicklime (calcium oxide-CaO) liberating carbon dioxide:

$$CaCO_3 \rightarrow CaO + CO_2 = \text{calcination}$$

Then quicklime is then slaked with water to form the mineral portlandite (calcium hydroxide – $Ca(OH)_2$):

$$CaO + H_2O \rightarrow Ca(OH)_2 = \text{slake}$$

The slaking process is an exothermic reaction and the produced calcium carbonate is stored under water excess as lime putty (aging process). A long-term storage improves the mortar quality and workability due to the particle size reduction and morphology changes of the portlandite crystal (Rodriguez-Navarro et al. 1998; Cazalla et al. 2000; Elert et al. 2002; Margalha et al. 2013). The carbonate crust formed over the slaked lime during the aging process can lead to the lime lumps formation (Bruni et al. 1997).

Subsequently the lime is mixed with geological material or reused inorganic building materials. The mortar is non- hydraulic or hydraulic if the aggregate is respectively sand and gravel (inert) or volcanic glass, burned clay minerals and ceramic splinter. In this latter case the filler material reacts with the strongly alkaline lime and other binder minerals than calcite are formed (Lindroos 2005). After the application, the mortar starts to set and harden when the lime absorbs atmospheric CO_2 to regenerate calcium carbonate ($CaCO_3$).

2.2. Binder related particles (BRP)

In the historic mortars three different type of binder related particles (BRPs) are distinguished according to the grades of calcination: underburned fragments, overburned fragments and lime lumps *sensu stricto* (Elsen 2006).

The underburned fragments are remnants of under burnt limestone that maintain the original rock structure providing information about the type of limestone used for lime production (Hughes and Cuthbert 2000; Hughes et al. 2001; Pavia and Caro 2006; Fratini et al. 2008).

The overburned fragments are sintered particles formed in the hottest zones of traditional kilns where the temperatures are sufficient to melting the lime. Inside the mortar, these fragments will slowly carbonate because the sintered lime is weakly reactive. The overburned fragments provides information about maximum burning temperatures in the kilns (Elsen 2006).

The lime lumps *sensu stricto* are the most commonly observed binder related particles. They are a pure calcium carbonate lump, easily detectable due to the rounded porous structure and the whitish and soft aspect. These are thought to originate from imperfect mixing of the binder due to residues of the carbonate crust formed on the lime putty in the process of maturation (Bruni et al. 1997) or from a poor mixing of the lime putty with the aggregates (Lindroos et al. 2007; Ortega et al. 2008; Pesce et al. 2009). Some other authors attribute their development to dry slaking (Hughes et al. 2001; Carran et al. 2010).

The study of these particles provides significant information about the historic mortar production technology. After the slaking process, lime putty is sieved through a grating system to avoid the inclusion of limestone relicts in the mortar (Bruni et al. 1997; Pecchioni et al. 2014). This means that a surplus of these particle indicates a poor production technology as strong inhomogeneities in the distribution of temperature in the kiln, lack of sieving and difficulty in the calcination of the stone because its composition (Pecchioni at al. 2014). Moreover, their identification is a crucial step in the mortar dating.

2.3. Radiocarbon dating of mortars

Determine the age of ancient buildings and establish construction phases represent important issues in the archeological an architectural research. The lime mortar binder represents a potential tool to assess the construction timing of buildings since it reflects the atmospheric ^{14}C concentration at the time of hardening process. Thus the lime binder can be used as material for ^{14}C dating. This principle is well known but problems to obtained the correct radiocarbon age can arise when other carbonate phases interfere (Lindroos 2005). Underburned limestone fragments, charcoal particles from wood-fired kilns and carbonate aggregate could contaminate the radiocarbon dating result and provide older age. Carbonate rocks, in fact, are mainly made of $CaCO_3$ that, at the beginning of the sedimentary process, contained the carbon isotopes of the earth's atmosphere at the time of the precipitation. So in contrast to the carbon contained in the lime mixtures of archeological interest which have a lifetime shorter than the radiocarbon, $CaCO_3$ of geological origin come from times far earlier than the equivalent to the decay time of radiocarbon. This means that any isotope contained in carbonate rocks is "^{14}C dead" and this implies that any molecule of carbonate rock (carbonate sand or underburned fragments) in the mortar can sensitively affect the result of radiocarbon dating with a heavy ageing (Pesce and Ball 2012). On the other hands, a rejuvenation effect can be induced by delayed hardening in thick walls (Sonninen et al. 1985) or if late exchange with the atmospheric CO_2 occurred after the construction, producing secondary calcite within the calcareous binder. These problems have been described extensively (e.g. Van Strydonck et al. 1983a, b, 1986, 1989; Van Strydonck and Dupas 1991; Ambers 1987; Heinemeier et al. 1997 with further references) and sample procedures have been improved upon since the beginning of radiometric method dating in order to remove the contaminants that invalidate the results.

The first mortar datings were performed in the 1964 by Labeyrie and Delibrias by thermal decomposition of crushed mortar samples at 900°C (Labeyrie and Delibrias 1964; Delibrias and Labeyrie 1965). The carbon dioxide was precipitated in a barium hydroxide solution and reliberated by acid hydrolysis of barium carbonate for decay counting measurement. In the same period, Stuiver and Smith (1965) performed the acid hydrolysis, with diluted HCl at different temperatures, directly on crushed samples. Soon after, Baxter and Walton (1970) realized that, when acid hydrolysis is applied, differences in carbonate phases solubility can be exploit to achieve accurate dating results. The soft and friable carbonate binder dissolves more rapidly than the crystalline carbonate limestone and calcareous sands. Folk and Valastro (1976) tried to identify and remove the contaminating carbonates developing a partial dissolution method, that isolate and date the early fractions of effervescing CO_2. The CO_2 emanating from the residue was dated separately to monitor the degree of contamination. This so-called "Texas method" (Ambers 1987) was tested and developed further by Van Strydonck et al. (1983a, b; 1986; 1989) and Van Strydonck and Dupas (1991). They increased the number of dated CO_2 fractions from one sample by splitting it into several aliquots and using different partial dissolution for the aliquots. In 1990 Tubbs and Kinder introduced the use of Accelerator Mass Spectrometry (AMS) to date organic residues in mortar, and soon late, Van Strydonck et al. (1992) used AMS to date small samples of mortars and lime lumps. The use of AMS to determine ^{14}C in lime mortars significantly reduces the amount of sample required (<1 mg) making it possible to take a very small piece of the samples (e.g. lime lumps) (Ringbom et al. 2014). In the mid-1990s and onward, the 85% phosphoric acid substituted the HCl acid (Heinemeier et al.

1997), previously and mostly used for the chemical separation, also in preparation for AMS analysis (Hodgins et al. 2011; Al-Bashaireh 2013).

Recently the potential of lime lumps has been studied and implemented (Pesce et al. 2009; Pesce and Ball 2012; Pesce at al. 2012; Pesce and Ball 2015; Lindroos et al. 2018). Since lumps formed by clodding of the lime putty before it is mixed with the aggregate, they contain the same lime as the surrounding matrix and they should be free from contamination of dead-carbon geological carbonates from the filler. For this reason, they can be successfully used for mortar radiocarbon dating. However, there are many kind of lime lumps and not all of them are suitable for identifying the age of the mortared structure (Van Strydonck et al. 1992; Pesce et al. 2009, 2012; Lindroos et al. 2014). There are lumps incompletely burned that contained limestone relicts or, due to their soft and porous nature, secondary calcite can be formed within the lumps if they have been in contact with groundwater or percolating water (Lindroos et al. 2007; Lindroos et al. 2011).

Nowadays, the methods most commonly used to eliminate the contaminants, that must be separated from the carbon belonging to the original binder, consist of a mechanical pre-treatment (Nawrocka et al. 2005; Mazaioli et al. 2011; Ortega et al. 2012; Nonni et al. 2013, 2017; Addis et al. 2019) and a chemical treatment (Heinemeier et al. 1997; Sonninen and Jungner 2001; Lindroos et al. 2007 and successive).

Mechanical separation (Cryo2Sonic)

The mechanical separation is based upon the assumption that the limestone of aggregate is stronger and more resistant than the more porous mortar binder carbonate. Nawrocka et al. (2005) introduced cryo-breaking of mortar pieces in a repeated freezing/thawing process to produce fine-grained material collected as water suspension, but the results of ^{14}C dating showed that improvement of the binder-aggregate separation process was necessary. This concept was developed further by Marzaioli et al. (2011) according the principle that the carbonate belonging to the binder fraction is characterized by a more easily breakable structure compared to the dead carbon. The procedure includes a sequence of physical separations (cryobreaking, ultrasonication, and centrifugation) in order to isolate a suspension of binder carbonates from bulk mortar. Only the suspended fraction collected after centrifugation is used for the ^{14}C dating. They tested the protocol (CryoSoniC), based on a single step of ultrasonication of 30 min, on synthetic mortars, prepared according to the traditional production process. In this case, it was known the isotope signature of laboratory CO_2 and it was guaranteed the absence of any other contaminant sources (e.g. lack of added aggregates) with the exception of unburned limestone residues. Shortly after, Marzaioli et al. (2013) applied the procedure to genuine mortars samples from archeological sites of known or independently constrained age (i.e. other ^{14}C dates on different materials) with the aim of checking the effectiveness of the methodology on field samples, including the suppression of eventual ''aggregates effects''. The protocol was also tested on lime lumps in order to reduce the risk of contamination from calcinations relicts. The results revealed the efficacy of the protocol for the lime lumps, selecting the calcite portion representative of the binder, but also the necessity to update the classical CyoSoniC procedure for mortar samples by adding a double step of ultrasonication, producing different time-evolved suspension fractions from the same mortar matrix (Marzaioli et al. 2013; Nonni et al. 2013). Moreover, the protocol was improved by performing mineralogical characterization of the mortars before the entire procedure in order to understand the nature of the sample and to assess the presence of contamination.

Starting from the principle assumed for CryoSonic, that used the ultrasonication as the key step to select the right fraction to date, the improvement of the procedure, developed in Cryo2Sonic, was carried out testing differential ultrasonication time interval on the same archaeological sample. A time trend of 10, 30, 45 and 60 minutes of ultrasonication was set. The resulting suspended fractions were isolated and dated. The first ultrasonication step of 10 minutes produce a fraction much older than the others, which however show all similar results. The hypothesis put forward was that a first very old fraction suddenly enters the suspension and is mixed with younger fractions. Since the first produced fraction was related to fine aggregates contribution (or possibly to secondary calcite crystallization), the original ultrasonication procedure (Marzaioli et al. 2011) was split into two sub-phases obtaining a fraction called "sand" from the first ultrasonication of 10 minutes and fraction called "susp" from the second step of 30 minutes. According to this theory the first fraction including fine and/or diagenetic calcite, should be more easily affected by contaminations than the second, which, on the contrary, should reach an age closer to the real value (Nonni et al. 2014).

The improved Crio2sonic procedure is detailed as follows (fig. 2) (Nonni et al. 2017):

1. Cryogenical breaking**.** According to Nawrocka et al. (2005) and Marzaioli et al. (2011, 2013), about 5 g of mortar is submerged in liquid nitrogen until reaching a thermal equilibrium, and immediately transferred to an oven at 80°C and kept at a constant temperature for 1 min. After repeating this

freezing/thawing cycle three times, the mortar is crumbled by hand or by applying pressure by a very gentle hammering in order to avoid the production unwanted fine grain-size particles not belonging to the binder.

2. Size selection**.** The resulting material is sieved under 500 µm and stored in a 75 mL beaker with ~40 mL of deionized water. The system is left to settle for 12 hr.

3. 1st ultrasonic selection**.** After complete sedimentation, the water portion is removed using a micropipette, followed by addition of 40 mL of deionized water to the beaker, and left to settle for 1 hr. Then an ultrasonic bath is run for 10. The suspended mortar particles are totally removed and transferred to a Falcon 50 mL centrifuge tube. This fraction of binder represents the fraction potentially affected by dead carbon contamination and/or diagenetic calcite (sand) due to the probable presence of very fine carbonaceous grain sand entering the suspension easily and before binder particles.

4. 2nd ultrasonic selection**.** A new volume of 40 mL of deionized water is added to the residual powder, decanted on the bottom of the beaker after the first sonic attack, and it is left to settle for 1 hr. Then a second ultrasonic bath is run for 30 min. About 30 mL of water suspension is collected in a centrifuge tube (50 mL), avoiding any agitation of the sediments. This last fraction represents the suspension guaranteeing accurate dating (susp).

5. Centrifugation**.** The Falcon centrifuge tube containing susp carbonates and the other containing the sand fraction are centrifuged at 8.0 krpm in a rotor of 10 cm mean radius for 5 min. The watery part is removed and the tubes is left oven-dried overnight at a constant temperature of 80°C. This type of fraction is considered to be representative of the binder.

Each sample of 40 mg of carbonate fractions (susp and sand) and carbonate standards samples (i.e. IAEA C1 and C2; Rozanski et al. 1992) are digested under vacuum to develop CO_2, by means of a complete orthophosphoric acid attack for 2 hours at 85 °C. The developed CO_2 is cryogenically purified from other gasses, reduced to graphite on iron powder catalyst according to the CIRCE sealed-tube reaction protocol (the zinc process) following Marzaioli et al. (2008), and analyzed to measure ^{14}C isotopic ratios using the CIRCE AMS system (Terrasi et al. 2008).

Fig. 2: schematic representation of the Cryo2SoniC procedure (Nonni 2014).

The main advantages of the Cryo2SoniC methodology are 1) the complete digestion of the laboratory isolated mortar fraction, avoiding difficulties in handling time-evolved fractions, and 2) the limited number of analyses per mortar to be performed, one for each sample after methodology accuracy evaluation (Nonni et al. 2013).

Recently, the method has been implemented by modifying some steps of the purification protocol and adding a more extensive characterization of the mortars before and after the purification treatment (Addis et al. 2019). At present, the protocol (Cryo2Sonic version 2.0) consists of four steps:

1. Mortar characterization in order to assess the nature of the contaminants and adopt the correct procedure in order to remove them. Both petrographic and mineralogical analyses are performed by means of several techniques, such as optical microscopy (OM), cathodoluminescence-induced optical spectroscopy (CL-OS) and x-ray powder diffraction (XRPD). Using the information obtained from mortar characterization, the purification protocol is better defined in terms of number of cycles and duration of each step.;

2. Purification treatment by means of sonication, centrifugation and gravimetric sedimentation. The mortar is ultra-sonicated in an ultrasonic bath by using ultra-pure water and centrifuged. Then, it is suspended in ultra-pure water for 20 hours, in order to obtain a dimensional separation of the binder particles. At the end of the sedimentation time, the uppermost suspension is sampled and filtered by using a vacuum pump system and inorganic 0.1 µm filters;

3. Characterization of the obtained powder using x-ray powder diffraction and cathodoluminescence-induced optical spectroscopy in order to evaluate effectiveness of the purification treatment (i.e. the purity of the binder and the absence of geological carbonates);

4. ^{14}C dating of the powder that is composed by pure lime binder.

Sequential dissolution

The method, based on the principle presented by Folk and Valastro (1967) and developed by Van Strydonck and Dupas (1991), was completed by Lindroos (2005) with cathodoluminescence inspection of the samples and further developed incremental CO_2 extractions during dissolution.

According to the procedure, the samples are broken into small pieces with plastic covered pliers, avoiding hammering that can produce splinter from the aggregates (contaminants). The crushed material is sieved using increasingly fine mesh widths ranging between 20-500 µm. The grain-size fraction <100 µm that may be used for dating are subsequently wet sieved. At present the routine method uses the 46-75 µm fine-grained fraction, since the dissolution time decreases with the grain size (Ringbom et al. 2011).

Coarser grain size fraction (300-500 µm) is checked for alkalinity test with phenolphthalein dissolved in alcohol (Hajdas et al. 2017). An alkaline reaction may indicate the presence of calcium hydroxide, which will react with the modern CO_2 in the atmosphere, affecting the result and leading to a younger age. For this reason, alkaline samples are not usually dated (Lindroos 2005). Preliminary petrographic analysis under polarizing light microscopy is also performed in order to determine the different mineralogical phases of mortar samples.

After sieving, cathodoluminescence (CL) is carried out on the fine grain size fraction to identify the presence of contaminants. The fine grains are spread over a glass backing glued with a polysaccharide and placed in a vacuum chamber and irradiated with an electron beam. The CL enables to distinguish between different carbonate phases with slightly different crystallinity and trace element chemistry (Marshal 1988; Machel 2000; Pagel 2000). The causes of the luminescence of carbonates are defects in the crystal structure or impurities hosted in the crystal lattice. The most important factor determining the colour and intensity of the luminescence is the Mn^{2+}/Fe^{2+} ratio in the calcite (Habermann et al. 2000). Binder presents usually a dark brown colour with variations from tile red to nearly black, while limestone and calcite CL colour is orange and the quartz CL colour is blue (Lindroos 2005). In some cases, however, the contaminants are not luminescent or they have lost their luminescence due the weathering, fire damage, etc. (Heinemeier et al. 2010).

The dissolution is done in a vacuum system with 85% phosphoric acid at 0° poured on the sample powder (fig. 3). The CO_2 fractions are collected on the basis of reaction times (Heinemeier et al. 1997). The phosphoric acid reaction is the following:

$$CaCO_3 + H_3PO_4 \rightarrow CaHPO_4 + CO_2 + H_2O$$

The process starts out with a violent reaction, liberating CO_2 from the fast dissolution of the pure binder carbonate, and then the reaction gradually slows down, reflecting the slow dissolution of the remaining binder carbonate and the slowly dissolving sedimentary filler carbonates and the underburned limestone (Heinemeier et al. 2010). The first fraction is usually produced and captured in ten seconds or less. Two consecutive CO_2 fractions of similar size are collected usually within 100 s and the next increments are collected during the following hours (Lindroos et al. 2019). Typically, five CO_2 increments from about 100 mg samples powders are collected in order to create the age profiles of the samples, and usually the first three are dated.

During the reaction, the dissolution times and the CO_2 pressure are monitored and registered. The CO_2 pressure is determined for each increment and the amount of carbon it contains is calculated. Thereafter, the CO_2 increments are split into two parts, one converted to graphite for AMS ^{14}C measurement, and the other for the determination of stable isotope ratios of carbon and oxygen (Lindroos 2005). The conventional ^{14}C dates are calibrated using OxCal v 4.3.2 program (Bronk-Ramsey 2017).

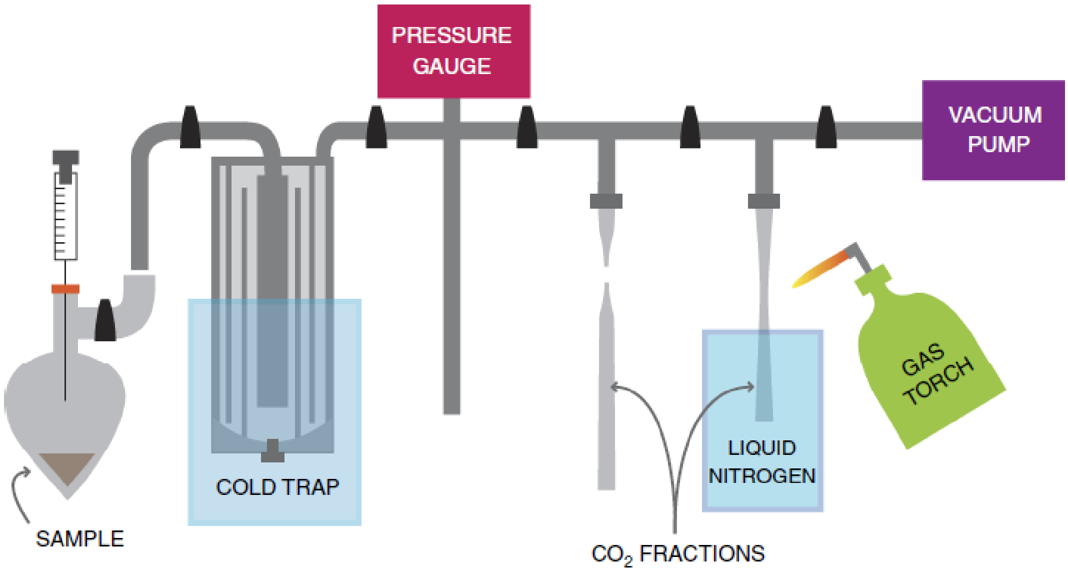

Fig. 3: CO_2 preparation line used in the laboratory of the Abo Akademi. The sample is held in the reactor vessel to the left and the acid is introduced as excess 85% H_3PO_4 with a burette. The cold trap contains isopropanol cooled down to -70°C. CO_2 is collected in glass vials cryogenically with liquid nitrogen (LN). Not shown in the figure is the LN cold trap in front of the vacuum pump (Lindroos et al. 2018).

The ^{14}C profiles are the most reliable and sensitive indicators of the activity of the different contaminants and their correct interpretation is the key to successful dating. In the profile the ^{14}C age is plotted as a function of the proceeding hydrolysis. A typical profile displays a concave curvature, characterized by rapidly dissolving mortar binder and slowly dissolving contaminants. The first CO_2 fraction, released by the mortar binder, will have a ^{14}C age close to the right archeological age (the two “good mortars” in fig. 4). In contrast, a convex profile dipping steeply near the y-axis indicates the presence of rapidly dissolving young contaminants (the “bad mortar” in fig. 4) (Lichtenberger et al. 2015). As shown in figure 5, if calcareous sand or gravel are used as aggregate in the mortar, the contamination is detectable in the profile, such as the presence of under burned limestone fragments (fig. 5A, Lindroos et al. 2007) and the effect of re-crystallization (fig. 5B, Ringbom et al. 2011).

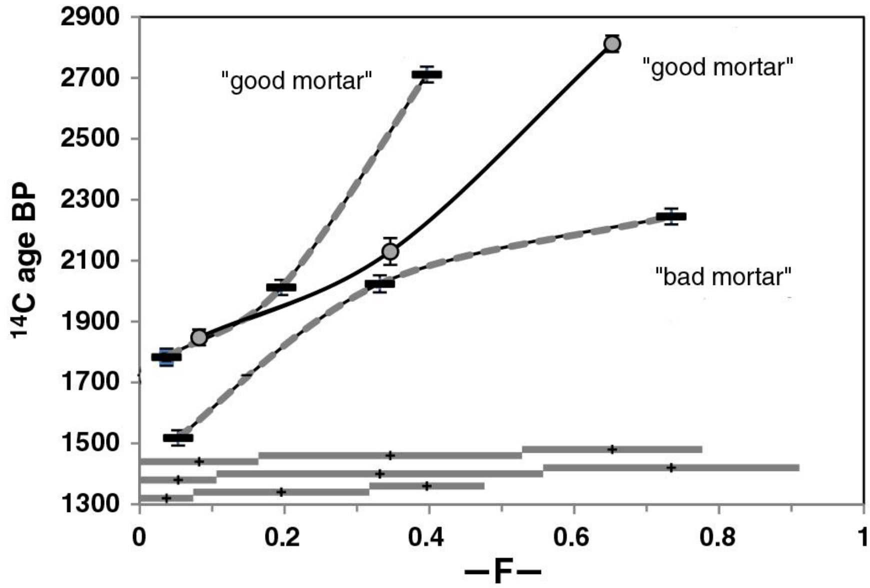

Fig. 4: ^{14}C profile showing either convex and concave curvatures. F is the fraction of reactive material transformed from carbonate to carbon dioxide. The horizontal gray bars along the x-axis denote the size of the extracted CO_2 fractions relative to the total carbon yield (=1) (Lichtenberger et al. 2015, modified).

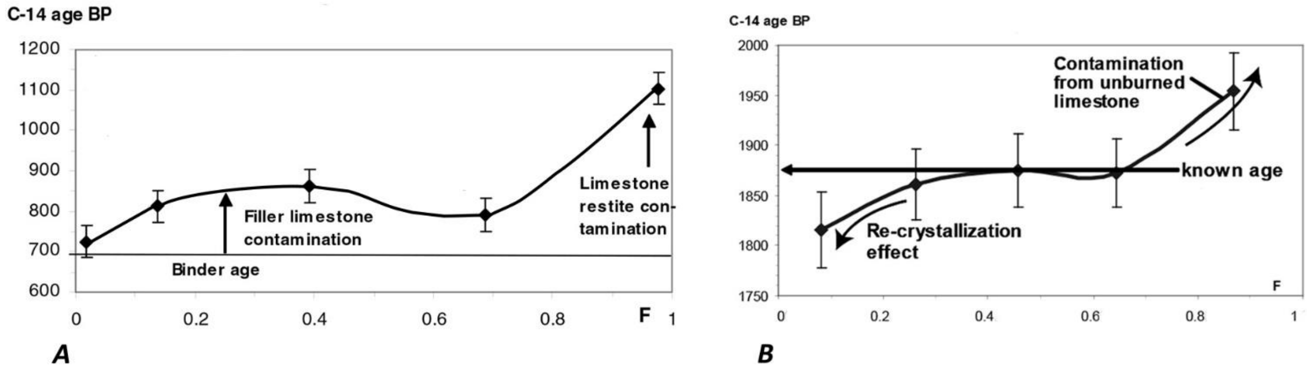

Fig. 5: A) modeled contaminant effects caused by filler limestone and slowly dissolving unburned limestone residues (Lindroos et al. 2007, modified); B) ^{14}C profile showing the effect of young and old carbonate contaminants (Ringbom et al. 2011, modified).

In case of *pozzolana* mortars, age profiles revealed a more complex pattern as shown in figure 5B. The correct age is revealed usually in the middle of the profile, while the first fraction is affected by young carbonate contamination and the last fractions reflect contamination of slowly dissolving geological carbonate (Ringbom et al. 2011, 2014).

In order to evaluate the results and define the true age of the samples, different reliability criteria (listed below) have been defined (Heinemeier et al. 2010; Ringbom et al. 2011).

Criterion I (CI): The ^{14}C ages of the first two CO_2 fractions are the same (one sample per building unit is in principle sufficient for a conclusive result). The rationale behind this criterion is that if there is no age gradient (i.e. no increase in limestone contamination) from fraction 1 to fraction 2, then both fractions are most likely free of contamination and therefore date the time when the mortar hardened. The quoted date of the mortar sample is based on fraction 1 only in order not to exaggerate the precision of the result (Heinemeier et al. 2010).

Most age profiles show an increase of contamination in later CO_2 fractions. If, however, the first fractions from the same building unit consistently yield the same age, the result is considered successful according to Criterion II (CII) (Ringbom et al. 2014).

Criterion II (CII): Mutual agreement between the dates of the first CO_2 fractions in a series of three or more samples from one single building unit. The rationale behind this criterion is the following: although the age gradient indicates a degree of contamination in fraction 2 (and therefore possibly also in fraction 1) it is more likely that all first fractions have insignificant limestone contamination than all of them having the same amount of significant contamination, leading to the same age excess for all samples (Heinemeier et al. 2010).

Many samples yield valuable data that are not sufficient for conclusive dating, but when put into a context it may help to clarify the chronology. However, they are not independently valid for dating, but need support of age control from other dating methods and other materials, such as dendrochronology and ^{14}C analysis of organic materials embedded in the mortar (Ringbom et al. 2014).

Criterion III (CIII): Mutual agreement between the dates of the first CO_2 fractions in two samples from a single building unit (Heinemeier et al. 2010).

Criterion IV (CIV): The last criterion includes samples where the first CO_2 fraction from one sample in a building unit yields a date that fits into a relative chronology (Heinemeier et al. 2010).

2.4. Luminescence dating of mortar and bricks

Luminescence dating is a powerful tool for age determination of the last heating or the last exposure to light of archaeological and geological materials. The physical mechanism consists in the trapping of electron charges as a consequence of the interaction with radiation and, in the subsequent light emission, upon heating at high temperature or expose to light (bleaching event). The quartz and feldspar grains found in pottery, bricks and mortars acted as dosimeters and they were able to record the amount of radiation to which they had been exposed (Wintle 2008). The analysis of this radiation provide the age of the manufacturing of the object. However, between the two minerals, the use of the quartz is preferred because feldspars are affected by the phenomenon of anomalous fading (Wintle 1973), consisting in the loss of the signal over time due to instability of the deep traps that can lead to an underestimation of the age. For dating, the amount of absorbed energy per mass of mineral ($1\ J\ kg^{-1} = 1\ Gy$ (Gray)) due to natural radiation exposure since bleaching (Palaeodose or Equivalent Dose, D_e) is determined by comparing the natural luminescence signal of a sample with that induced by artificial irradiation. The time elapsed since the last daylight exposure or heating is calculated by dividing the palaeodose by the dose rate. The latter representing the amount of energy deposited per mass of mineral due to radiation exposure acting on the sample over a certain time (radiation absorbed annually, Gy/year).

This relation is represented by the following equation:

$$\text{Luminescence age} = \text{Palaeodose (Gy)} / \text{Annual dose rate (Gy/year)}$$

Luminescence dating in Archaeology

The possibility of dating ceramics objects by the use of their thermoluminescence (TL) properties was firstly proposed by Grogler et al. (1960) and Kennedy and Knopff (1960) and then developed by the group headed in Oxford University by Martin Aitken (Aitken et al. 1964; Aitken et al. 1968). In the 70's, two sample preparation techniques were studied: the so-called fine-grain (Zimmermann 1971) and coarse-grain (Fleming 1970) techniques. These methods consider grains of different sizes extracted from the ceramics. Soon after TL became a dating tool for archaeological ceramics, Fleming (1979) discovered the potential of TL for dating brickwork. In this case, the TL dating refers to the moment of the bricks firing. The first step of the application of this technique to historical building was made by Goedicke et al. (1981). The results appear both precise and accurate using the polymeral fine-grain technique. This was confirmed by other dating works on European historical buildings located in Denmark (Abrahamsen et al. 1998), Czech Republic (Cechák et al. 2000), Finland (Hutt et al. 2001), Germany (Göksu and Schwenk 2001) and Italy (Martini and Sibilia 2001). Nevertheless, thermoluminescence cannot solve all the problems concerning the dating of historic buildings. In fact, TL is able to determine the period of manufactured of a brick which may not coincide with the construction of the structure itself, because bricks are often reused (Martini and Sibilia 2006). Furthermore, there are structures that are made with unfired brick or natural materials such as natural stones and mud bricks that can obviously not be dated with thermoluminescence (Goedicke 2011). To overcome these limits, studies on the possibility of dating historical mortars through optically stimulated techniques (OSL) have been developed. The possibility to use mortars to evaluate the time of construction, repair works or modifications of a structure represents an important breakthrough in dating historical buildings. Mortar was first recognized as a suitable dosimeter (for the reconstruction of accident doses after incidents at nuclear power plants) by Bøtter-Jensen et al. (2000). Many of them noted the problem of age over-estimation being a logical consequence of the analytical technique employed. This is known as a Multi Grain (MG) aliquot analysis and it consists in measuring the average luminescence signals emitted by tens or hundreds of grains together (Goedicke 2003). The multi-grain technique gave acceptable values of absorbed dose only with well-bleached samples while it obviously overestimated in poorly bleached grains. In fact, many mortars contain grains that were not sufficiently set to zero by light (optically bleached) during mortar preparation and consequently they emit too high luminescence signals (Urbanová et al. 2018). The development of the Single Grain technique (SG-OSL) (Murray and Roberts 1997; Duller and Murray 2000; Murray and Wintle 2000; Bøtter-Jensen and Murray 2002) based on the OSL signal of each single quartz grain, has allowed the identification of the best-bleached grains in a heterogeneously and/or incompletely bleached mixture. This technique is highly time-consuming because usually only less than a few percent of the grains give acceptable signals. The analysis of a huge number of grains is therefore required (Duller et al. 2000; Goedicke 2003, 2011). Recently published studies on mortar dating (Urbanová et al. 2015; Urbanová et al. 2016; Urbanová and Guibert 2017; Panzeri 2017) demonstrate the efficacy of this method.

Thermoluminescence (TL)

Thermoluminescence (TL) describes the light emitted by a mineral when heated. The light originates from captured electron being freed due to heat stimulation and subsequent recombination. In order to perform TL measurements from ceramic samples, the so called fine-grain technique (Zimmermann, 1971) is mainly used. It consists in the selection of the grain size fraction between 1 and 8 µm, without any mineral separation. After a 2 mm layer from the surface has been removed, the pottery fragment is crushed with a mortar or the powder is sampled using a drill. By washing the products of this operation in acetone, a suspension of fine grains is obtained. Making use of the fact that the settling time is determined by diameter, grains in the size range of 1 to 8 mm are separated. The grains obtained are resuspended in acetone and allowed to deposit on stainless steel discs in a thin layer of a few microns thickness. Then the sample is typically heated to about 500°C to release the trapped electrons. The curve representing the intensity of emitted light as a function of the temperature is called glow-curve, that usually comprises a series of peaks. The glow-curve shape and intensity depend on the type and energy of radiation. The resulting TL signal is proportional to the number of the trapped electrons and thus to the sample age.

Optical Stimulated Luminescence (OSL)

The Optical Stimulated Luminescence (OSL) is the light emitted by a mineral by shining a beam of light onto it (Huntley et al 1985). OSL is applied on the quartz sand extracted from the mortar sample and it allows the dating of the last exposure of the mortar aggregate to light and this corresponds to the moment of mortar making (Zacharias et al. 2002). The sample preparation method mainly uses for OSL dating is the coarse grain technique (Fleming 1970). It consists in a first step in which the sample is sieved to a particle size between 100 and 300 µm. Then the powder is washed in water that removes the eventual presence of clay and a series of chemical attacks (HCl and H_2O_2) for eliminate carbonates and organic materials are carried out. It is then performed a density separation using sodium polytungstate solution to eliminate heavy minerals and, subsequently, to separate quartz from feldspars etching the quartz grain in concentrated HF, which is also needed to remove the external layers of quartz grains that received an α dose (Mejdahl 1985). Finally, another treatment in HCl is performed to eliminate any fluorides produced (Zacharias et al. 2002; Preusser et al. 2008). It is thus obtained a powder composed of grains of “pure” quartz with a selected size.

All the sample preparation phases are made in semi darkness, using a red light, since the light could bleach the OSL signal retained in quartz grains. This procedure is a standard for the OSL dating protocols.

One of the major problems in OSL dating is the incomplete bleaching of the latent signal. An incomplete zeroing of the OSL signal can be due to the presence of quartz of different origin whose bleaching characteristics can highly vary, as well as to the short duration of the exposure to light during the manufacturing process, especially for what concern the mixing and working procedures at the construction site (Goedicke 2003, 2011; Panzeri 2013; Panzeri et al. 2017; Stella et al. 2018; Panzeri et al. 2019). The plateau test is one of the approaches to investigate if the sample has been completely bleached prior the mortar setting. The test consists to plot the palaeodose as a function of optical stimulation time. The basic idea behind this approach is that the signal during initial stimulation and at lower temperature, respectively, is more light-sensitive than the subsequent following signal. As a consequence, one would expect an increase of palaeodose with stimulation time (temperature) for incompletely bleached samples and a flat shine-plateau-plot for samples that were completely reset (Preusser et al. 2008).

Determination of the palaeodose (D_e)

The measurement of palaeodose comprises three different steps: irradiation, preheating and measurement of luminescence. Irradiation is carried out to induce a latent luminescence signal in the quartz grains and is performed by using either beta or gamma calibrated sources. During artificial irradiation all traps, including those unstable over longer time periods, capture electrons. To allow comparison with the palaeodose absorbed over the burial time, the unstable component of the luminescence signal has to be removed, and it is achieved by heating the sample causing eviction of the electrons caught at shallow traps (Murray and Wintle 1999). Once this preheating of the sample has been performed, the luminescence is measured by stimulating the sample with light.

The evaluation of the dose absorbed by the sample (D_e) consists of a comparison between the luminescence signal obtained from sample, without having been subjected to any artificial irradiation in the laboratory, with the signal obtained artificially, in order to find the relation between the intensity of luminescence with the dose absorbed by the sample. In principle there are two different approaches to determine the palaeodose: additive dose and regenerative dose. In the additive dose approach an artificial laboratory-induced signal is added to the natural signal, while in the regenerative dose method the latent luminescence signal is first removed and the sample is then irradiated and a laboratory signal regenerated. For both approaches, a so called dose response curve is calculated reflecting the increase of latent luminescence in the mineral grains with increasing dose. The additive dose method is used for TL dating, while regenerative dose method for OSL dating.

<u>The additive dose method</u>

The additive method utilizes the multiple aliquots methodology (MAAD, Aitken 1985). A number of equal portions (aliquots) are prepared and divided into groups, with typically 4/6 aliquots or more in each group. One group is reserved for measurement of the natural OSL and the other groups are artificially irradiated before being analyzed, with the addition of an artificial dose to the natural dose. The luminescence signal from the natural dose, as well as the natural plus added doses is plotted against the added doses (zero added dose for the natural) and the relation is fitted with a linear curve, which describes the growth of the luminescence signal with increasing dose (growth curve). The additive growth curve is extrapolated to the dose axis to provide an estimate of the Paleodose. The major disadvantage of a multiple aliquot approach is that each aliquot often behaves differently (due to e.g., variable sensitivity changes, incomplete and variable bleaching, etc.) giving rise to scatter in the data (Preusser et al. 2008). In this case, it could be necessary a normalization, irradiating all aliquots with same dose (Duller 1994; Wintle 1997) and repeating the luminescence measure. This method is therefore suitable for samples for which heterogeneity is zeroing may be excluded.

<u>The regenerative dose method</u>

The main aspect of this approach is that all measurements are carried out on a single aliquot of sample, avoiding problems related to the normalization. The main advantages of the methodologies are the improved precision, rapid measurements and less sample needed (Bøtter-Jensen and Murray 2002). The most widely used protocol for single aliquots for OSL measurements is the Single Aliquot Regeneration protocol (SAR), mainly developed by Murray and Wintle (2000, 2003). In this protocol, the natural luminescence signal is measured from all single aliquot and then the laboratory doses are given, with several cycles of artificial radiation and reading of the signal. The obtained values are used for the construction of the response curve for each single aliquot. Once the curve is drawn, it is possible to have the value of the paleodose by interpolation, by means the intersection of the OSL natural signal with the growth curve. The critical disadvantage is that an error in paleodose will occur if there is a change of sensitivity between measurement of natural OSL and the laboratory regenerated OSL (Murray and Wintle 1997). The luminescence sensitivity of the aliquot changes depending on the laboratory procedures (e.g. the temperature and duration of the preheat treatment), and conditions during burial (e.g. ambient temperature) (Duller 2008). To carry out the sensitivity correction, a so-called test dose, which remains constant during the whole protocol, is given after measuring each regenerative (including natural and zero) dose (Wintle and Murray 2000). Thus the SAR protocol comprises different steps: give dose Di, preheat, OSL reading (Li), test dose Dt, preheat, measured OSL (Ti) (Murray and Wintle 2000). The performance of each individual SAR cycle is also verified by two internal tests: recuperation and recycling ratio. The first test (recuperation) consists of a new OSL measurement, at the end of each cycle, to check if the sample has been emptied after each irradiation reaching the complete bleaching (Duller 2008). The second test (recycling ratio) confirms whether correction for sensitivity change was successful. The recycling test consists in applying the same regeneration dose in two different cycles, and giving the ratio of the sensitivity corrected luminescence signals from the two measurements. A basic requirement that proves the suitability of the SAR protocol is that a known dose that is given in the laboratory can be retrieved by the measurement procedure. For testing this, a so-called dose recovery test is carried out during which the natural signal is first optically bleached and then a known laboratory dose is given to the sample. This known dose is then treated as unknown, applying again the SAR protocol. If the result of this measurement is still the same, then the parameters used for the determination of equivalent dose are appropriate (Duller 2008; Preusser et al. 2008).

Determination of the dose rate

After obtaining the palaeodose, the next step for the age determination for a sample is the assessment of the rate at which the radiation dose was delivered to the mineral grains. In most cases, the accumulated dose per unit time, the dose rate, is constant throughout the period of “life” of the tested sample. The annual dose-rate absorbed by the samples is the sum of the contributions of the internal radioactivity of the material and of that of the radioactivity of the surrounding environment. In both cases, the responsible radioisotopes are the radioactive families ^{238}U, ^{232}Th, ^{40}K and, to a much lesser extent, ^{87}Rb. To these, the contribution of a cosmic ray (mainly γ) dose has to be added.

The annual dose can be written as the sum of different contributions α, β, γ:

$$D = D\alpha + D\beta + D\gamma + D\gamma\ (\text{cosmic})$$

The dose-rate is evaluated by assessment of the radioactivity of the sample and by on site measurement. An important aspect is the estimation of dose-rate in the presence of water. Therefore, for a realistic estimation of total annual dose, it is necessary to take into account the water content of the sample because the moisture in the interstices of sediments absorbs part of the radiation that would otherwise reach the grains. Hence, the dose rate in sample containing moisture is low than that in the same dry sediment and if the effect is ignored, there may be an underestimation of the age (Zimmerman 1971). Another parameter to be considered in the final calculation of the dose rate is the grain size of sample because the dimension of grains varies the capacity of absorption of the sample, as explained below (Wintle 2008).

Dose rate for fine grain

For samples prepared following the protocol fine grain for TL dating, the annual dose value can be evaluated from the α, β and γ radiation due to the internal radioactivity concentration of the sample and from the cosmic radiation and the γ dose coming from the environment (Zimmerman 1971; Wintle 2008). In fact, during the sample preparation the 2 mm outer are removed and the radiation α and β due the external environment is negligible, since α radiations can penetrate the quartz only of about 20-30 µm, while the β penetrate 2-3 mm. The total annual dose for samples prepared according to the fine grain technique can then be written as:

$$\text{Age} = \text{paleodose}/\ D\alpha + D\beta + D\gamma + Dc$$

Dα= α from the sample (with humidity correction); Dβ= β from the sample (with humidity correction); Dγ= γ component of the sample and the environmental; Dc= cosmic ray component.

Dose rate for coarse grain

For samples prepared following the coarse grain protocol for OSL dating, the unique contributions to consider are those from the β and γ radiation (Wintle 2008; Goedicke 2011) the contribution of α particles can be neglected: they can penetrate only the outermost layer of the grains (10μm, Preusser et al. 2008), which is removed during the physical-chemical preparation phase of the sample through the attack with HF. The total annual dose for samples prepared according to the coarse grain technique is:

$$Age = paleodose/\ D_\beta + D_\gamma + D_c$$

D_β= β from sample; D_γ= γ component of the sample and environment; D_c= cosmic ray component.

CASE STUDY 1: MEDIEVAL MODENA CATHEDRAL UNESCO SITE

3. INTRODUCTION AND AIMS

3.1. Introduction

The seismic event that hit the Emilian plain in 2012 caused an extensive damage to the historical and artistic heritage (Candigliota et al. 2012; Decanini et al. 2012; Indirli et al. 2012; Parisi and Augenti 2013; Andreini 2014; Graziani et al. 2015). More than two thousand earthquakes occurred from May 16 to June 26, 2012 and seven of these with a magnitude greater than 5. Two main shocks took place on May 20, 2012 (02:03:52 UTC, Finale Emilia (MO), Mw 5.9, PGA 0.078) and May 29, 2012 (07:00:03 UTC, Medolla (MO), Mw 5.8, PGA 0.107) (ISIDe, http://iside.rm.ingv.it/; Dolce et al 2012 Report I and II).

The cathedral masonry cross-vaults of the UNESCO World Heritage Site of Modena suffered several damages and their conditions appeared alarming. The 29 May 2012 Emilia earthquake caused some masonry blocks falling from the nave and aisles vaults, especially next to the facade and the apses. The survey of the cracking patter shows the presence of new fractures and that previous ones have been reopened (Baraccani et al. 2015; Baraccani et al. 2017; Baraccani et al. 2019).

An anti-seismic reinforcement project was planned with the aim to determine the vulnerability of the cathedral analyzing the damages suffered in the past. The structural restoration and the strengthening plan were formulated and carried out by Studio Tecnico Silvestri of Modena (Elena Silvestri, Architect, and Professor Tomaso Trombetti, Engineer) and funded by Regione Emilia Romagna (Baraccani et al. 2015).

My research has pursued in parallel with the consolidation work and it has found the support by UNESCO. The aim of the study is to investigate the building materials and to clarify the history of the vaults building and repairs. According to historical documents (Dondi 1896; Baracchi and Giovannini 1988; Baracchi 1993), the vaults were progressively added to the main framework during the 15th century but the issues regarding the construction phases and the restoration works are uncertain and unclear. Therefore, the absolute dating of building materials represents the only way to obtain reliable data.

The thesis applies an integrated approach using three independent methods: radiocarbon dating and Optically Stimulated Luminescence for dating mortars and Thermo-luminescence to date bricks.

The comparison of two accredited different sample preparation technique of mortar (Cryo2Sonic and sequential dissolution) for radiocarbon has been performed in order to identify the most successful and suitable method for lime mortars rich in carbonate aggregate.

3.2. Problem definition

At the beginning of the research, when the restoration project began, preliminary surveys have been carried out on the extrados of the vaults in order to investigate the building. The study has been performed removing the thin plaster layer that covered the bedding mortars and the bricks. The surveys revealed that large portions of the vaults were constructed using two different type of mortars: gypsum mortars and lime mortars. These unexpected data suggest different structural restoration carried out in the past using different materials and techniques, probably related to damages suffered after the main earthquakes which struck the area.

The first part of the research was focused on the mapping of the building materials and a systematic sampling was performed for the compositional study. Moreover, the CPTI15 earthquakes catalogue (Rovida et al. 2016) was examined in order to identify the seismic events that have actually affected the Cathedral vaults.

The second part of the research was focused in applying the absolute dating techniques of building materials in order to clarify the history of interventions. Radiocarbon dating by Cryo2sonic and by sequential dissolution and Optically Stimulated Luminescence have been carried out to date the lime mortars and Thermo-luminescence to date bricks. For the correct application of the radiocarbon dating and for the interpretation of results, petrographic characterization of mortars has been performed. Moreover, the analysis of the pollen trapped in the mortar has been tested in order to identify chronological markers, in particular for the gypsum mortar that is not directly datable. The dates known from historical documents have been used to constrain the results of the absolute dating methodologies.

3.3. Aims

The objectives of the study are:

- Obtain information on the provenance of raw materials and the features of the building materials used for the construction of the vaults and their restoration;
- Provide new consideration about the timing of the original vaults construction and the history of the later interventions;
- Correlate the renovation works to the earthquake chronology deduced from the historic catalogue (Rovida et al. 2016);
- Assess the vulnerability of the actual state of the Cathedral and clarify the damages suffered in the past;
- Perform the absolute dating of the phases of construction and repair;
- Verify which absolute dating method is the most suitable for this research and test different preparation technique to the same set of samples in order to compare the capabilities and identify the most successful method.

4. MODENA MEDIEVAL UNESCO SITE

The Modena Medieval monumental complex consists in the Cathedral, the Civic tower Ghirlandina and the buildings facing square “Piazza Grande” (fig. 6). In 1997 it was declared “UNESCO Cultural Heritage” site. The monumental complex was built between 1099, date of the Cathedral’s foundation marked on a stone on its façade, and 1319, when the construction on the Ghirlandina was completed (Piccinini 2009).

Fig. 6: the UNESCO site of Modena. The main façade, the southern side of the Cathedral and Civic tower Ghirlandina.

Due the lack of documentation and the several transformation and addition that occurred over time (Acidini Luchinat et al. 1984), the chronological sequence of construction of the Cathedral is difficult to interpret and is still subject of discussion (Silvestri 2013).

The laying of the first stone of the Cathedral happened on 6th June 1099 and the construction was carried out under the coordination of the architect Lanfranco and sculptor Wiligelmo, proceeding in parallel with the erection of the lower portion of the tower Ghirlandina (Dieghi 2009; Labate 2009). The inscription on the southern side of the Cathedral celebrates the consecration of the building on 12nd July 1184, suggesting that the construction was completed. Between the 12th and the 13th centuries the Campionesi Masters performed significant modifications to the edifice’s original structure adding some gothic architectural elements and they completed the construction of the Ghirlandina Tower, building the body of the bell tower (Piccinini 2009).

The cathedral is liturgically oriented basilica with three naves closed by three semicircular apses and a false transept. It has a presbytery in an elevated position, due to the presence of a crypt containing the corpse of the city's patron, Saint Geminianus. The central nave has five large spans while the lateral aisles have eight, whose dimensions are half the size of the central ones. The interior space is divided by sturdy pillars and large columns used alternated for the support of the 15th century vaults (fig. 7).

Fig. 7: the 15th century vaults of the Modena cathedral.

4.1. Construction timing of the vaults

According to Baracchi and Giovannini (1988) the vaults were built in order to prevent dangerous water infiltration from the wooden roof of the Cathedral and their construction started in the 1404. Baracchi (1993) reports a contract of 1404 in which is expressed the will of Rangone Petrazzini, *Massaro* of the *Fabbriceria* (who is responsible for the administration and preservation of the Cathedral), to build the five vaults of the central nave, with the agreement of the bishop Nicolò Boiardi. The work was assigned to the Master Bartolomeo de Foco who was committed to start the construction of the five vaults in May 1404 and to finish it in November 1404. However, the project was not completed. The contract is included in a deed of 4 May 1414, in which is documented the suspension of the work few years after the beginning, due to the dead of the Master Bartolomeo de Foco and the *Massaro*, and the resumption of work with the election of the new *Massaro* Alberto Rangone. The deed of 15 February 1415 reports that only the most eastern vault was completed and that the construction for the other vaults was suspended. Therefore, it can deduce that the first vault was built between 1404 and 1415.

The construction of the vaults proceeded 30 years later. The will to build a new vault next to the one already in existence is reported in the testament of 26 December 1436 of the new *Massaro* of the Fabbriceria Lodovico Roncosifrego. It is likely that he died several years later because his heirs made the deed for the construction of the vault on June 1443. The work was completed in 1445, as reported the deed of 25 March 1445, in which is indicated that the vault was already built and painted by Giovanni da Modena.

After the conclusion of the second vault, the widow of Lodovico Roncosifrego, Costanza Albicini, decided to continue the work. She dictated in her testament the wish to build a new vault next to the one built by the will of the departed husband. The testament is included in a deed of 4 November 1446, in which is also reported the dead of the woman and the expected beginning of the work in the same year. At the end of the deed, the agreement concluded between the son of the woman and the bricklayers is described. The latter (Stefano da Ferrara and Giacomo da Rubiera) undertook to finish the construction on August 1447 but no document indicates if the project was really realized following this timeframe (Baracchi 1993).

The last two central vaults were built, respectively, for the will of the family Forni and Fontana and the bricklayer Giacomo da Rubiera was commissioned the work (Baracchi 1987). On September 1453 the vaults were completed and painted by Giovanni da Modena (Baracchi and Giovannini 1988).

Although the initial intention was to build the five vaults of the central nave in few months, the construction took several decades, from 1404 to 1453, thanks to the contribution of private benefactors.

Unlike the central vaults, the construction timing of the lateral aisles is not plenty documented. Only few information appeared in Baracchi and Giovannini (1988), where is reported a deed of 25 February 1433 in which the will of family Guidoni to build the two most western vaults of the northern lateral aisle is expressed. The deed also mentions that the two parallel vaults, in the southern lateral aisle, have already been built. According to Dondi (1896), the construction of the lateral aisle was concluded in 1454.

The construction phases of the vaults, deduced from the historic documents, is shown in figure 8.

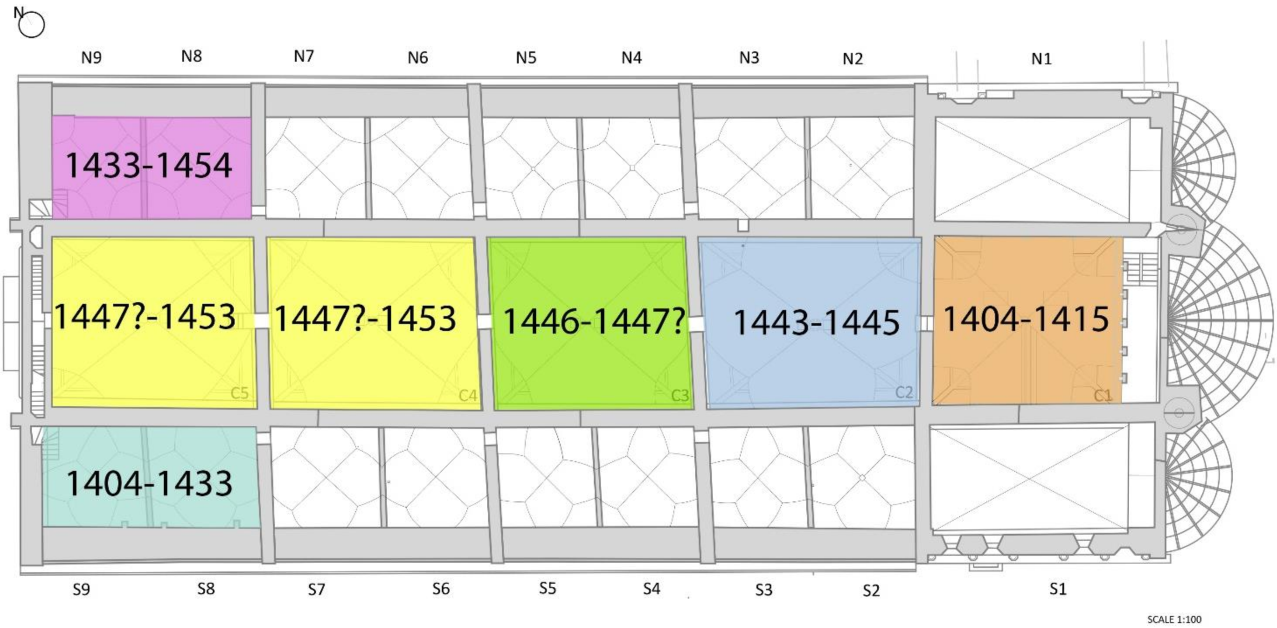

Fig. 8: building phases of the Modena cathedral vaults.

4.2. History of the restorations of the vaults

In order to determine the vulnerability of the Cathedral, it is fundamental identify the damages suffered in the past and reconstruct the history of the restoration. In this phase of the research the catalogue of the historic earthquake was consulted in order to identify the damaging earthquakes that may have affected the Cathedral and the historical sources were investigated. The documents (Dondi 1896; Baracchi and Giovannini 1988) report that several restorations were carried out during the 16th century immediately after the vault construction but no more information are given for the subsequent interventions until the 19th century when the consolidation project of the Cathedral and the Tower started (Acidini Luchinat et al. 1984).

4.2.1. Catalogue of ancient earthquakes

The research was carried out examining the CPTI15 earthquakes catalogue (Rovida et al 2016). According to criteria following in Baraccani et al. (2014), several damaging, great moment magnitude (Mw) and high Peak Ground Acceleration (PGA) value earthquakes have been selected. These significant historical earthquakes occurred after the vaults construction and with epicenters located in various areas. In table 1 the chosen earthquakes are reported.

Year	Epicenter	PGA	Magnitude (Mw)
1474	Modena	0.232	4.30
1501	Castelvetro (MO)	0.187	5.82
1505	Bologna	0.055	5.41
1584	Tuscan-Emilian Apennines	0.025	5.99
1586	Spilamberto	0.091	4.53
1660	Modena	0.172	4.25
1671	Rubiera	0.129	5.23
1688	Romagna	0.028	5.85
1811	Sassuolo	0.072	5.09
1828	Staffora valley	0.012	5.55
1832	Reggio Emilia		5.51
1850	Modena	0.144	4.53
1873	Reggiano	0.059	4.93
1873	Eastern Liguria	0.032	5.47
1909	Bassa padana	0.028	5.48
1919	Mugello	0.043	6.18
1920	Garfagnana	0.062	6.48

1923	Formigine	0.105	5.05
1928	Carpi	0.059	4.54
1931	Modenese	0.066	4.54
1934	Vignola	0.037	4.06
1967	Formigine	0.072	4.09
1996	Correggio	0.064	5.26
2012	Finale Emilia	0.078	5.90
2012	Medolla	0.107	5.80

Tab. 1: list of the earthquakes occurred after vaults construction with great Mw and high PGA values.

4.2.2. 16th century restoration works

The first intervention after the vaults construction is attested in 1455 when one of the vaults in the norther aisle (N7) was damaged ("Cadé il coverto sopra la volta de li castaldi"; Dondi 1896). Few years later, in 1462, Giacomo da Rubiera was commissioned to repair one of the northern vaults, probably the vault N2, where the new organ was placed, while in 1481 the northern vault N5 was mended after the collapse of the roof ("Per far conzare uno pezo del cuperto sopra laltare dela Comuna che era chascato per la neve"; Baracchi and Giovannini 1988). The northern aisle near the Tower Ghirlandina is the most precarious because of the weight of the snow that melts slowly in the north side, and the falling of marble slabs from the Tower (Baracchi and Giovannini 1988). Another restoration was performed in 1490, this time on the southern vault of the altar of Saint Bartolomeo, identified with the vault S4 ("Per far conzare uno pezo de coverto dele volte de la giexa sopra la volta de laltare de San Batolome era caduto…"; Baracchi and Giovannini 1988).

As reported in the sources (Dondi 1896; Baracchi and Giovannini 1988) the vaults suffered the greatest damage after two strong earthquakes occurred in the 16th century. The earthquake of 1501 (Castelvetro (Mo), Mw 5.98, PGA 0.18; Rovida et al. 2106) aggravated the vulnerable conditions of some vaults and different interventions were performed:

- tie-rods were added to vaults of the altar of "Nostra Dona" (vaults S7-S6) (Baracchi and Giovannini 1988);

- the central vaults close to the façade (C5) was repaired and the damaged wooden beams of the roof were replaced ("una culmegna sopra la giesa verso le pelizarie"; Baracchi and Giovannini 1988);

- the pillars of the central nave that withstand the weight of the vaults were reinforced ("impiombar li pilastri"; Baracchi and Giovannini 1988);

- the new sacristy in the northern side of the Cathedral in proximity of the vaults N3-N2 was renovated (Dondi 1896)

After 4 years, another damaging earthquake occurred (Bologna, Mw 5.57, PGA 0.05; Rovida et al. 2106) and further works were needed:

- tie-rods were added to the northern vault of the altar of Saint Caterina and the northern vault of the pulpit (N7-N6) (Baracchi and Giovannini 1988);

- the fractures on the façade were mended (Dondi 1896).

In the following years, the condition of the roof deteriorated and many restorations are documented because of its collapse on the vaults. In particular, in 1511 the northern vault of the organ (N2) was damaged due the abundant snowfall, while in 1513 the central vault C4 was rebuilt ("Spexe per fare il coperto del domo dala volta de quili del Forno quale si era cascata e rota"; Baracchi and Giovannini 1988). Again, in 1515, the northern vault N2 was repaired ("per far cunzare la volta dove è li mantexi de lorgano"; Baracchi and Giovannini 1988) and in 1533 the reconstruction of the wooden roof was carried out (Baracchi and Giovannini 1988).

Figure 9 shows the several vaults that have suffered damages in the past as reported in the historical sources.

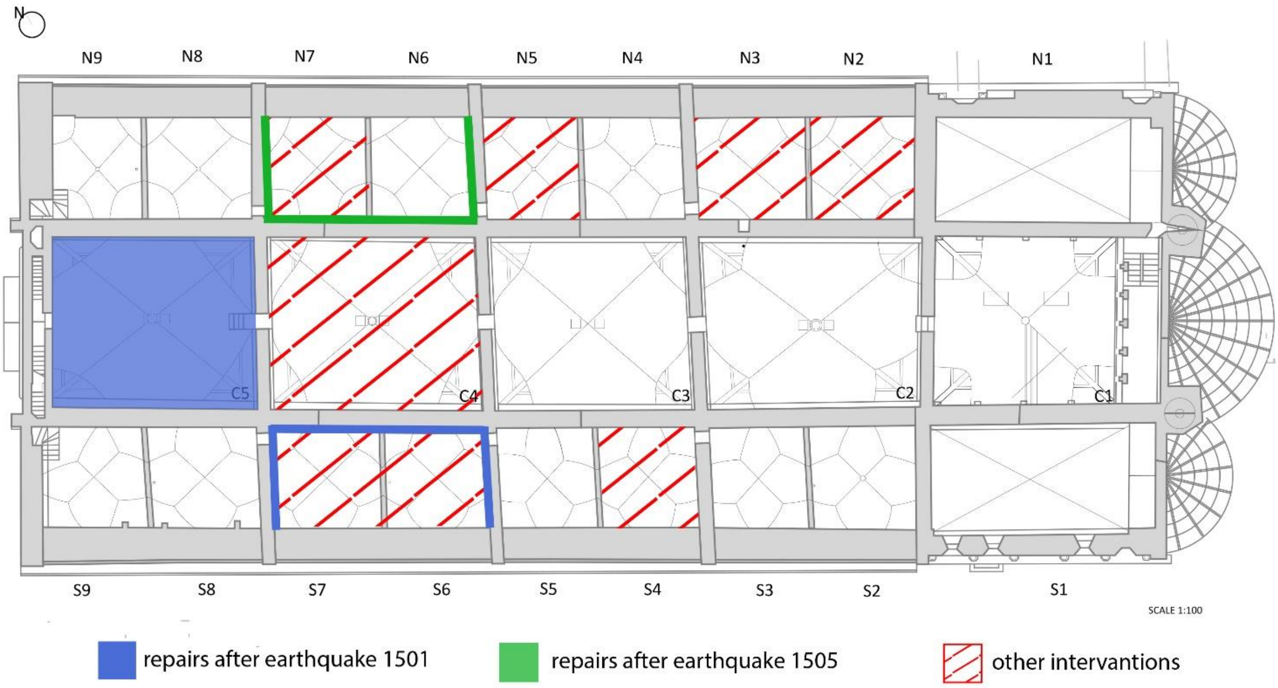

Fig. 9: late interventions on the Modena cathedral vaults.

4.2.3. 19th century restoration project

In the first half of the 19th century, a conservation project of the Cathedral was planned and different surveys were carried out on the 15th century vaults. The inspections were performed in order to verify the state of preservation of the roof structure, especially after the earthquake of 1832 (Reggio Emilia, Mw 5.51; Rovida et al. 2016). Several fractures were detected on the vaults and the impairment of the wooden roof were identified. In particular, it was recognized that the presbyterial vault (C1) and the lateral northern vaults were the worst preserved, while the central vault close to the façade (C5) appeared more recent and well preserved (Pistoni 1977; Acidini Luchinat et al. 1984).

In 1840 the finale report of the strengthening interventions recommended to renovate the roof of the central nave, to rebuild the central vaults C1, C3 e C4 and to reconstruct the roof of the sacristy (Pistoni 1977).

According to Acidini Luchinat et al. (1984), in 1841 the consolidation work was concluded but it should be noted that not all the activities that were projected were carried out and that is difficult to pinpoint which interventions were actually performed.

To conclude, it should be take into account also the damages caused to the vaults during the Second World War. The aerial bombing of 13 May 1944 affected the southern side of the Cathedral, in particular the door “Porta dei Principi” damaging the two vaults near the door (S7-S6) (Acidini Luchinat et al. 1984).

4.3. Damages 2012 earthquake

After the 2012 sequence seismic, the main vulnerabilities have been identified on the 15th century vaults. The mapping of the fracture and crack networks revealed an alarming situation since most of the fractures, previously assessed, were re-opened, as shown in figure 10 (Baraccani et al. 2015; Baraccani et al. 2017; Baraccani et al. 2019). The anti-seismic reinforcement project has been planned in order to increase the safety level of the Cathedral and several interventions have been carried out. The extrados of the vaults has been consolidated by injections of lime and by putting a new layer of lime reinforced with carbon-fiber mesh, while the plaster of the intrados has been consolidated and the cracks have been filled with lime (Baraccani et al. 2015).

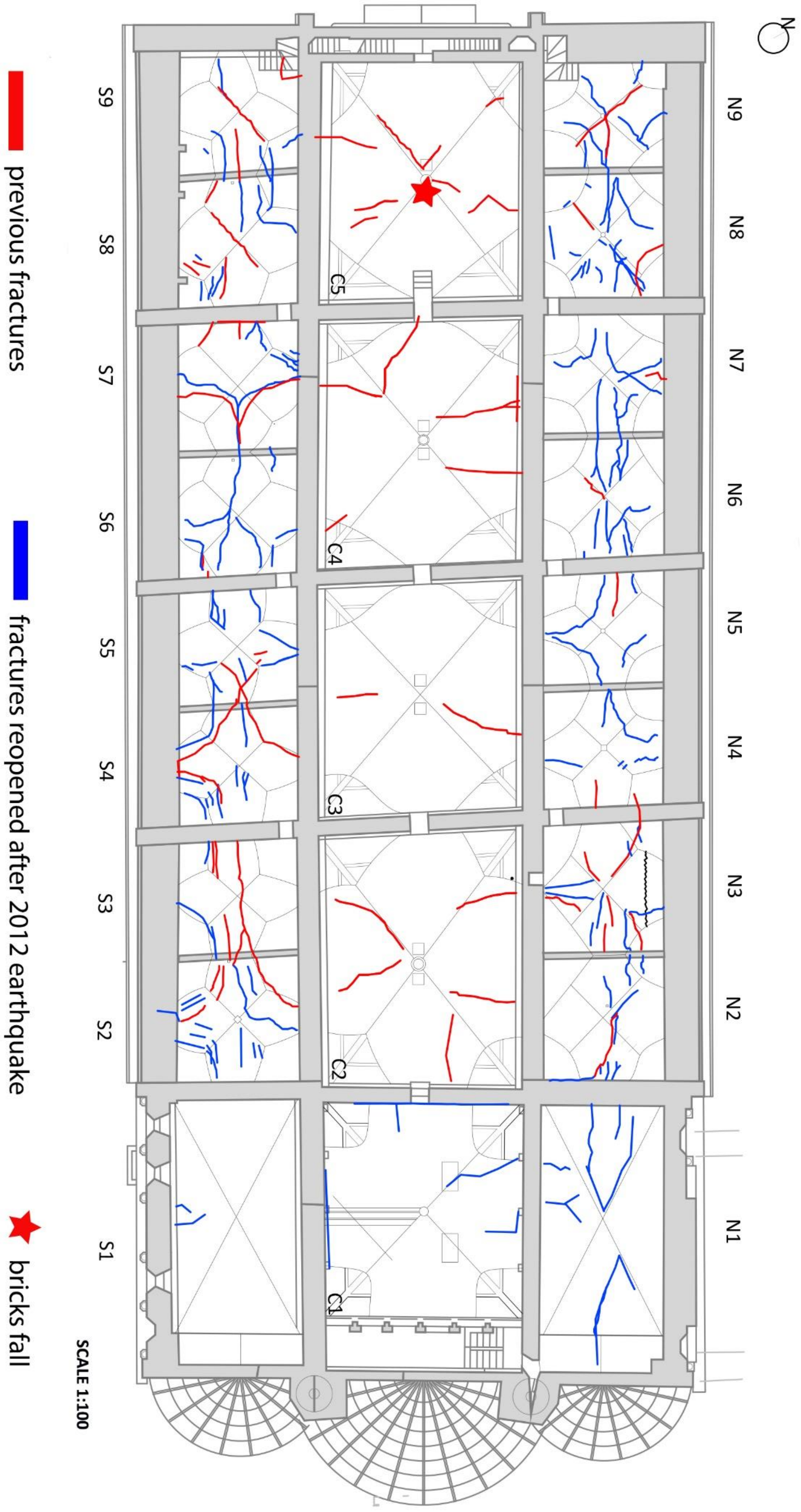

Fig. 10: map of the damages and the cracks detected on the vaults after the 2012 earthquakes.

5. MATERIALS AND METHODS

At the beginning of the reinforcement work, the thin lime layer that covered the vaults was removed and a detailed survey was carried out on the extrados of the vaults in order to identify the type of mortars embedded with the bricks. The first part of this chapter concerns the mapping and the systematic sampling of the building material. The compositional study has been performed trough the petrographic characterization of the mortars following the methodology applied for the Tower Ghirlandina (Lugli at al 2010) and Finale Emilia Town Hall (Lugli et al. 2016). The method allows to identify the raw material sources of the mortars and the history of the building techniques.

In the second part of the chapter, the absolute dating methods of the building materials is reported. The radiocarbon dating of lime mortars is presented and the two sample preparation techniques (Cryo2Sonic and sequential dissolution) are described. OSL on lime mortars and TL on bricks have been used to test the radiocarbon results using independent methodologies. Moreover, the analysis of the pollen, trapped in the mortars, has been applied for the reconstruction of the environment at the time of the mortar preparation.

5.1. The sampling

Several surveys have been carried out on the extrados of the vaults. The first investigations were performed removing the lime layer of the vaults only in few and small sections. For each uncovered area of the vaults, the mortar type was identified. The survey revealed that portion of the vaults were constructed using both lime and gypsum mortar (fig. 11). In order to clarify the building and restoration chronology, a systematic sampling was performed for the absolute dating of the building material (fig. 12). The choice of the samples has been made considering the materials and the type of analysis to perform. Mortars and bricks were sampled from the same places. For each lime mortar sample, the embedded brick was collected with the aim to compare the absolute dating results. In the case of portions built using gypsum mortar, that is not directly datable, the brick fragments were sampled for TL dating. The mortar samples for OSL dating and bricks for TL dating were sampled using a chisel and a hammer under dim red light and they were put into a black plastic bag.

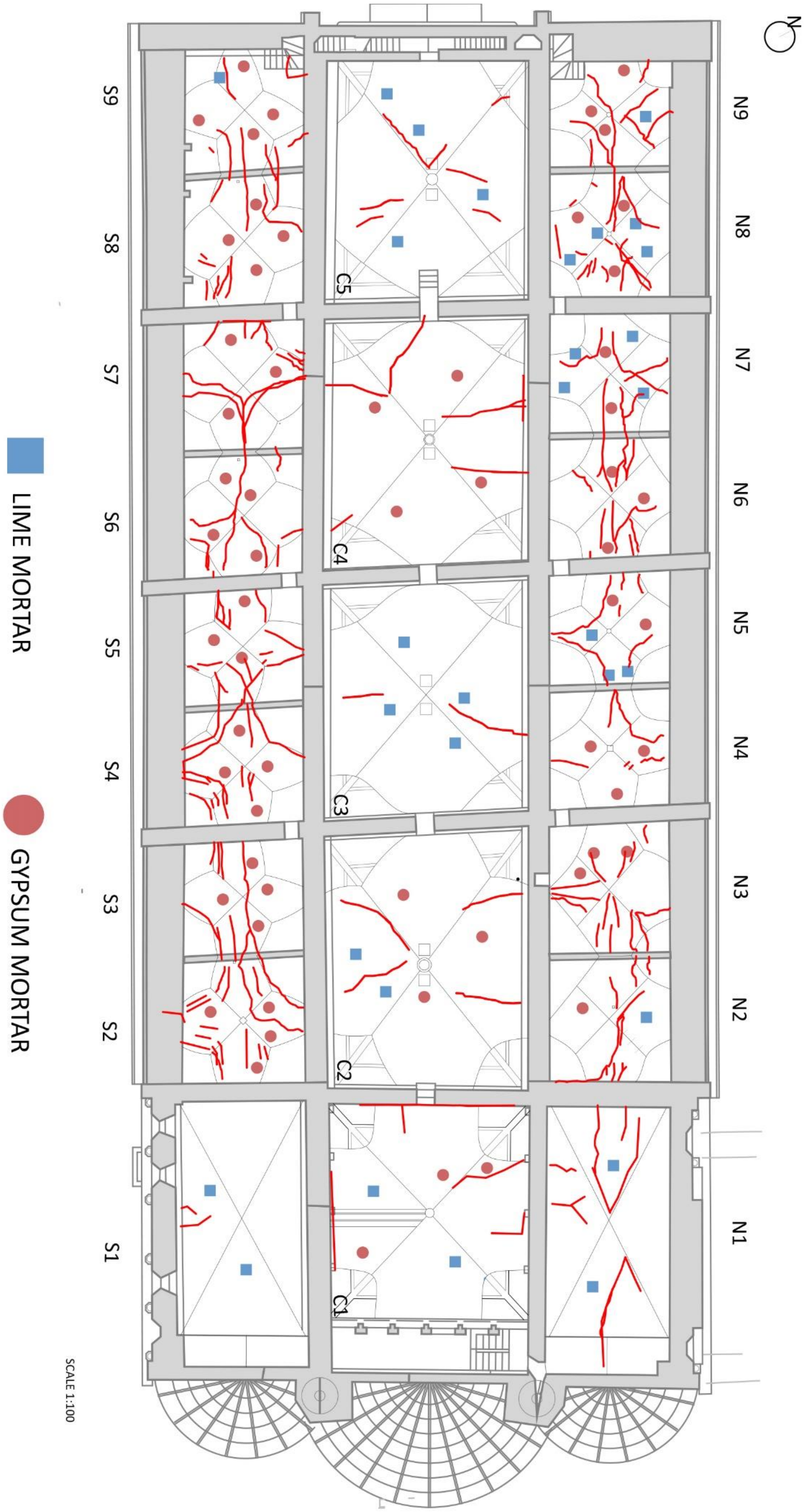

Fig. 11: mapping of the binder detected.

A total of forty-seven samples have been collected: twenty-nine mortar samples (gypsum and lime) and eighteen bricks fragments (fig.13).

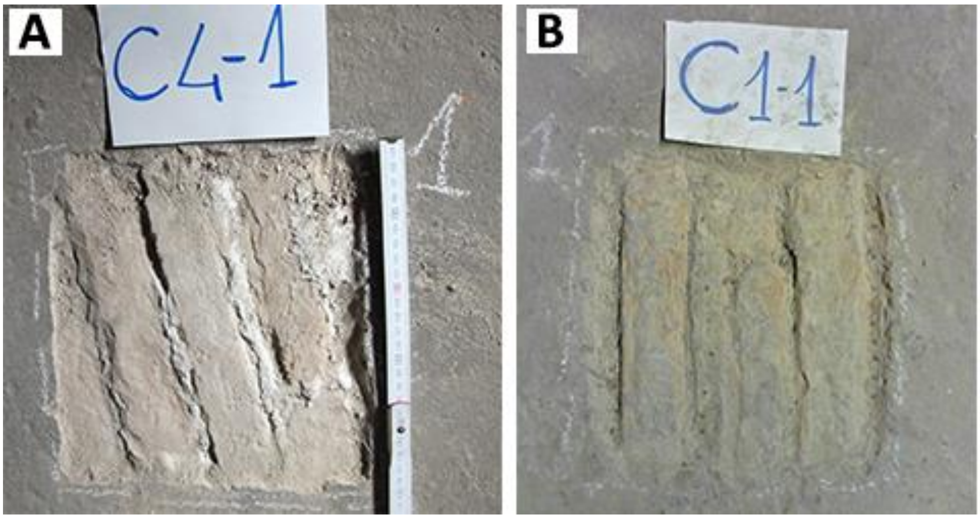

Fig. 12: sampling point of the central vault C1: A) area C4-1 gypsum mortar; B) area C1-1 lime mortar.

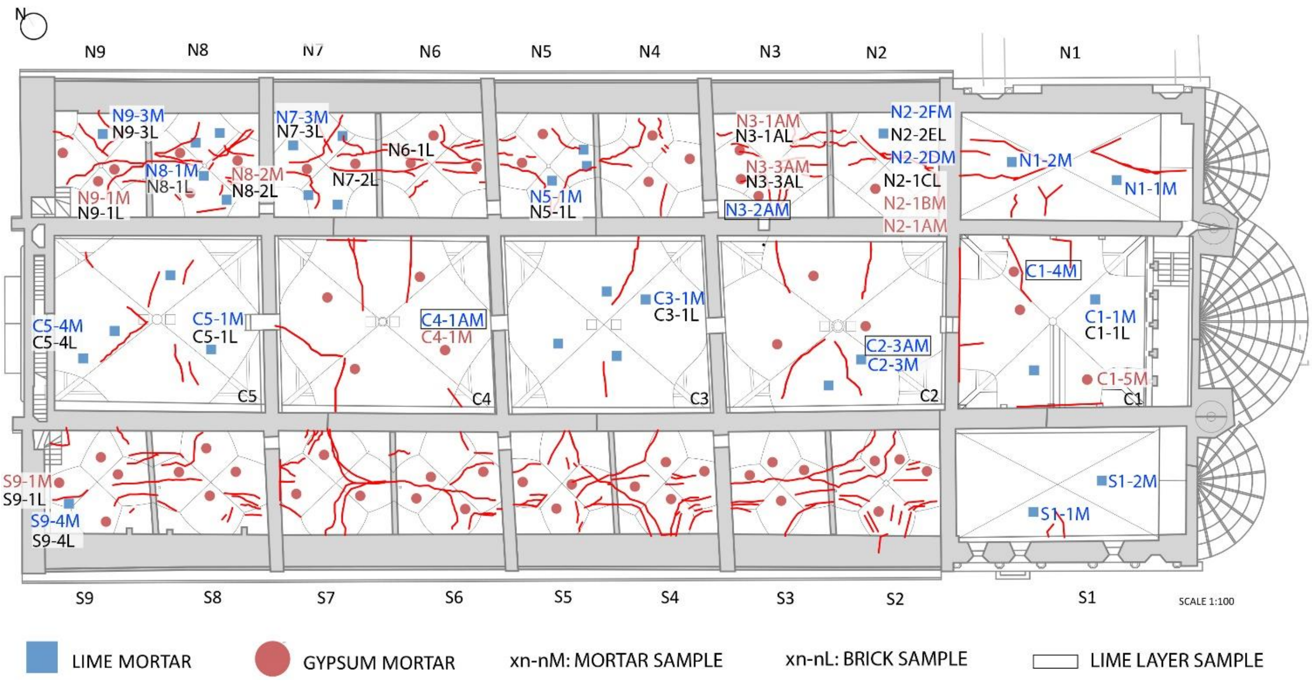

Fig. 13: sampling points of mortars and bricks.

Once the lime layer that covered the vaults was totally removed, a detailed mapping of the vaults has been completed. Figure 14 shows the complex scenario that was detected: large portions of the vaults were built using either a gypsum or a lime binder and the scars of several earthquakes, repaired using different binders, were revealed. The result is a complex patchwork of lime repairs over original gypsum vaults and gypsum repairs over original lime vaults. No apparent systematic construction criteria were followed to dictate the use of lime or gypsum binders.
In particular, the central vault C5 appeared to be the most modified over time: as shown in figure 15 three different type of mortar (lime, gypsum G1 and gypsum G2) were identified and for each portion new samples (mortar and brick) were collected. The gypsum mortar G1 and the gypsum mortar G2 present different grain size, detectable during the macroscopic survey. Sample G1 appear a coarse-grain size gypsum mortar, while sample G2 fine-grain size gypsum mortar. These two type of gypsum mortars (G1 and G2) were recognized also in the central vault C4. According to the restoration work schedule, it was possible to carry out an accurate study of the gypsum portion only on the central vaults C4 and C5. Thus, it can not be excluded that also the remaining vaults were build and/or modified using different type of gypsum mortars, such as G1 and G2.

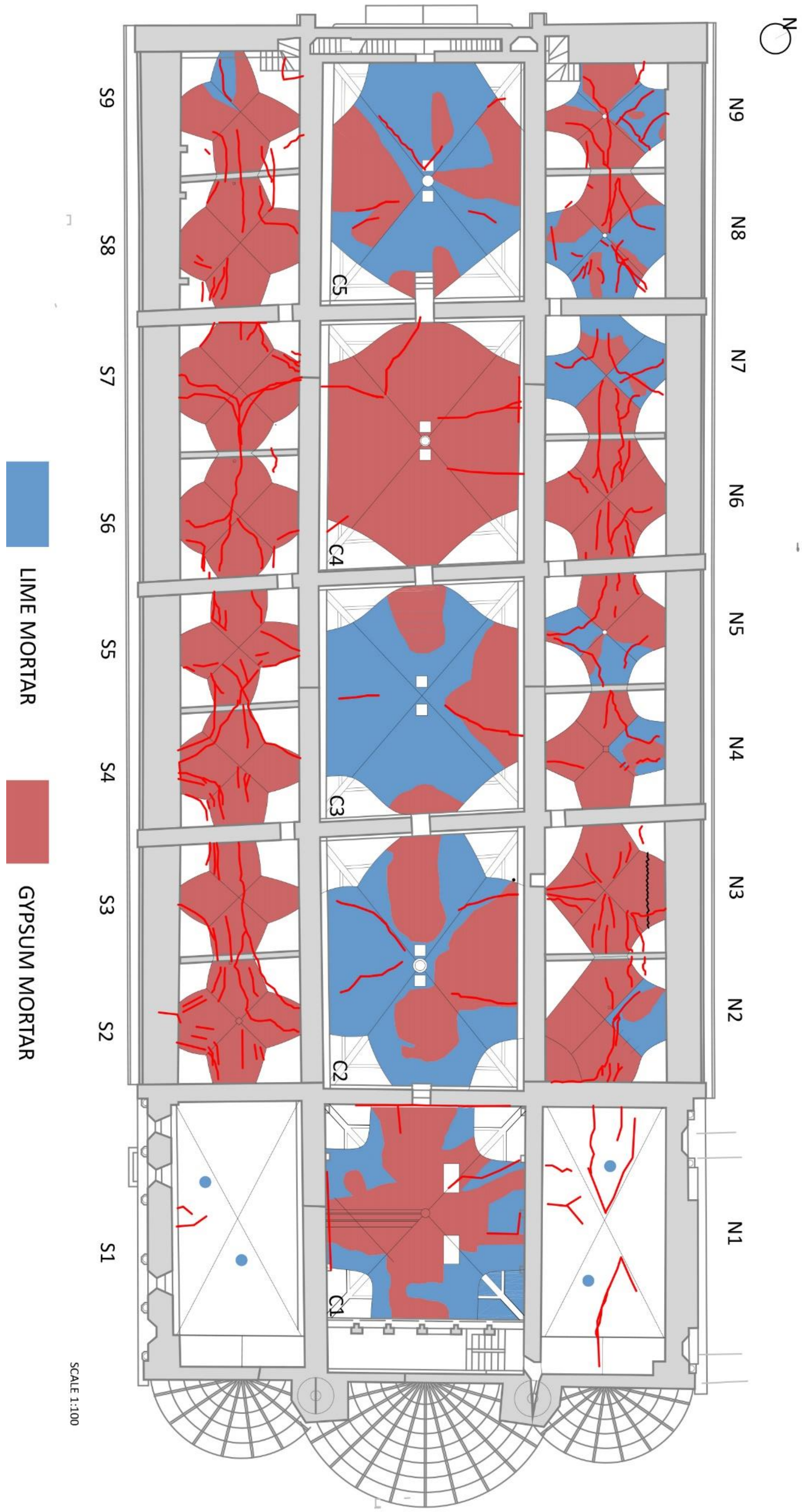

Fig. 14: detailed mapping of the portions built using different binder: lime and gypsum.

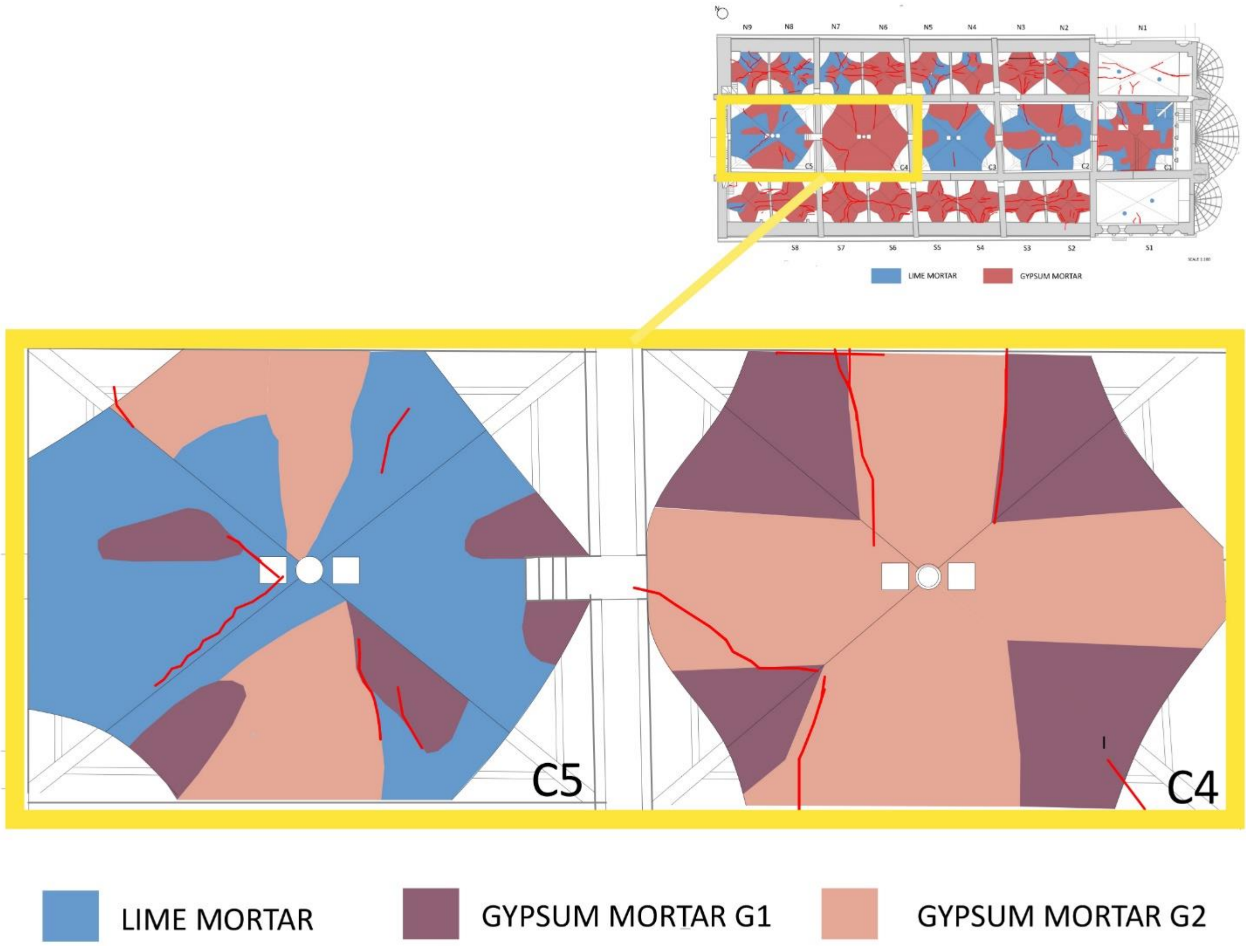

Fig. 15: accurate mortar recognition of the vaults C4 and C5. The figure shows the portions build using lime mortar, gypsum mortar G1 and gypsum mortar G2.

The final amount of samples collected is fifty-three, thirty-two of mortar samples (lime and gypsum) and twenty-one brick samples. The samples selected for absolute dating and pollen analysis is listed in table 2. The absolute dating was performed on the same set of samples in order to compare the results and test the different methodologies.

Nine lime mortar samples were selected to be prepared for radiocarbon dating following the two methodologies of sample preparation. The samples belong to the central nave vaults and to four lateral aisles, three northern vaults and one southern vault, where the most complex and interesting situation was recognized. In particular, the vault N3 is one of the most vulnerable of the northern vaults, as reported by the historical sources, and the vault S9 is the only southern vault that presents a portion built using lime mortar.

The Luminescence dating was performed on the same vaults selected for ^{14}C dating. Fifteen brick samples were chosen for TL dating and two lime mortar samples for OSL dating.

The pollen analysis was tested on six mortar samples chosen according to the absolute dating results.

In figure 16 the samples selected for absolute dating are highlighted on the extrados plan of the vaults.

Vault	Sample name	Sample	Expected age	Method
C1	C1-1M	lime mortar	1404-1415	^{14}C dating by Sequential dissolution
	C1-1L	bricks (lime mortar)		TL
C2	C2-3M	lime mortar	1443-1445	^{14}C dating by Sequential dissolution
C3	C3-1M	lime mortar	1446-1447?	^{14}C dating by Cryo2sonic and Sequential dissolution
	C3-1L	bricks (lime mortar)		TL
C5	C5-1L	bricks (lime mortar)	1447?-1453	TL
	C5-4M	lime mortar		^{14}C dating by Cryo2sonic and Sequential dissolution
	C5-4L	bricks (lime mortar)		TL
	C5-5M	lime mortar		^{14}C dating by Sequential dissolution
	C5-5L	bricks (lime mortar)		TL
	C5-6M	gypsum mortar		Pollen analysis
	C5-6L	bricks (gypsum mortar)		TL
	C5-7M	gypsum mortar		Pollen analysis
	C5-7L	bricks (gypsum mortar)		TL

N3	N3-1AL	bricks (gypsum mortar)	/	TL
	N3-2AM	lime mortar		14C dating by Cryo2sonic
	N3-3AM	gypsum mortar		Pollen analysis
	N3-3AL	bricks (gypsum mortar)		TL
N8	N8-1L	bricks (lime mortar)	1433-1454	TL
	N8-1M	lime mortar		^{14}C dating by Cryo2sonic and Sequential dissolution
	N8-1M	lime mortar		OSL multi grain
	N8-2M	gypsum mortar		Pollen analysis
	N8-2L	bricks (gypsum mortar)		TL
N9	N9-1L	bricks (gypsum mortar)	1433-1454	TL
	N9-3M	lime mortar		^{14}C dating by Cryo2sonic and Sequential dissolution
	N9-3L	bricks (lime mortar)		TL
S9	S9-1M	gypsum mortar	1404-1433	Pollen analysis
	S9-1L	bricks (gypsum mortar)		TL
	S9-4M	lime mortar		^{14}C dating by Cryo2sonic and Sequential dissolution
	S9-4M	lime mortar		OSL multi grain
	S9-4M	lime mortar		OSL single grain
	S9-4M	lime mortar		Pollen analysis
	S9-4L	bricks (lime mortar)		TL

Tab. 2: list of the samples selected for absolute dating and pollen analysis.

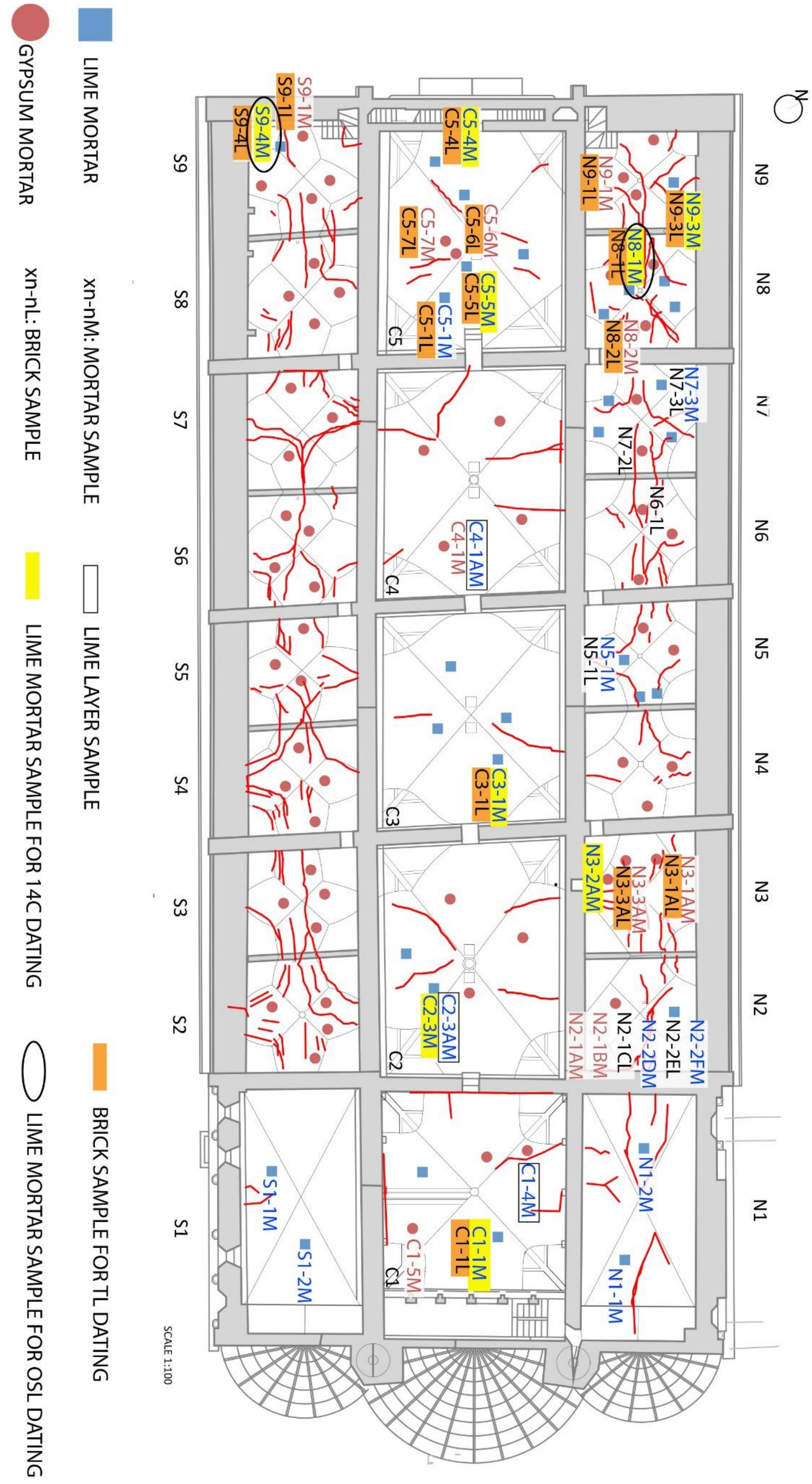

Fig. 16: samples selected for absolute dating.

5.2. Characterization of mortars

The petrographic analysis of mortars provides valuable information on ancient mortars technology (Pavia and Caro 2008) and it represents a fundamental tool for the determination of the supplying sources of the raw materials (sand and rocks for lime production) (Hughes et al. 2001; Lugli et al. 2007; Fratini et al. 2008). This information is to take into account during the manufacture of new building materials for the restoration works. Mortar cannot be reused, as bricks, and its characteristic can be utilized to indirectly distinguish different construction phases of historic buildings (Lugli et al. 2010; Lugli et al. 2013; Lugli et al. 2016).

The mortar samples were vacuum impregnated with epoxy resin to obtain thin-sections, that were observed under the optical microscope in transmitted light. The main mortars features were described using as a reference the Document UNI-Normal 11176. The investigation enables to determine the composition of the aggregate, the grain size and the morphology, the sorting grade, the type of binder, the presence of additives, the porosity and the cracking. Furthermore, radiocarbon dating requires the petrographic characterization for identify the presence of contaminants. The petrographic analysis was performed using optical microscope LEITZ Orthoplan polarizing transmitted light. The optical microscope is equipped with a Nikon Coolpix 990 digital camera for the acquisition of micrographs.

Image analysis of thin sections was performed to determine the aggregate binder ratio and the aggregate grain size by means of Image J free software (Carò e Di Giulio 2004; Michalska et al. 2017; Nonni et al. 2017). The aggregate binder ratio was calculated following the recommendation produced by the RILEM TC 167-COM (2001). Three photomicrographs of about 5 mm per side for each lime mortar samples were analyzed. The method allows to calculate the particle size distribution and the percentage of the area of aggregate, binder, binder related particles (BRPs) and pores. The average on the data obtained from the three analysis is calculated and reported. In figures 17A and B an example of the graphs in which the data obtained are summarized is shown. In the first the main characteristics of the mortar, such as the binder quantity, the aggregate, the BRPs and the porosity are plotted, while in the second the particle size distribution is reported.

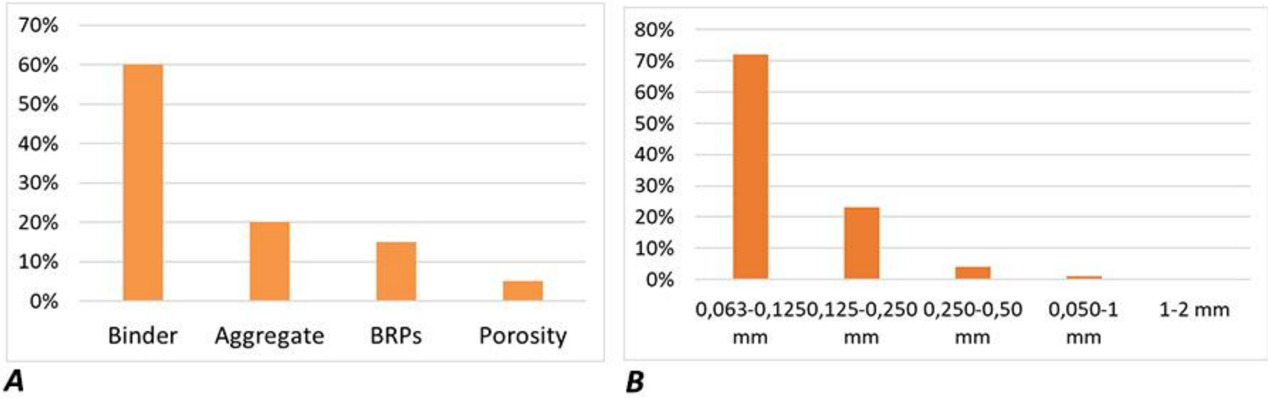

Fig. 17: A) graph of the mortar texture; B) graph of the aggregate grain size.

5.3. Absolute dating

Radiocarbon dating of lime mortar samples was performed with the collaboration of the University of Campania "Luigi Vanvitelli" (Department of Environmental Science and Technology) and the Åbo Akademi University of Turku (Finland). The radiocarbon dating results have been tested using optically stimulated luminescence (OSL) on mortars and thermoluminescence (TL) on bricks, performed by the Department of Material Science, University of Milan Bicocca.

5.3.1. Preliminary mortars characterization for radiocarbon dating

The preliminary petrographic analysis with the optical microscope of mortars thin sections allows the identification of the different carbonate elements in a mortar, as the aggregates nature (fig. 18A and B), BRPs (fig. 18C), secondary calcite crystallization, straw and charcoal fragments (fig. 18E and F), which are most probably a remnant of the burning process (Elsen 2006; Pavia and Caro 2008; Ortega et al. 2012; Pecchioni et al. 2014). To obtain the accurate age of a mortar it is crucial to eliminate components that would cause an offset of the ages, such as unburned limestone relicts, calcareous aggregates and new formed calcite, considered as contaminants. The identification of lime lumps (fig. 18D) is also carried out since lime lumps that could be separated from the mortar avoiding contamination from dead carbon. The preliminary petrographic analyses also help in characterizing the samples in order to select the best preparation procedure and to interpret the radiocarbon data.

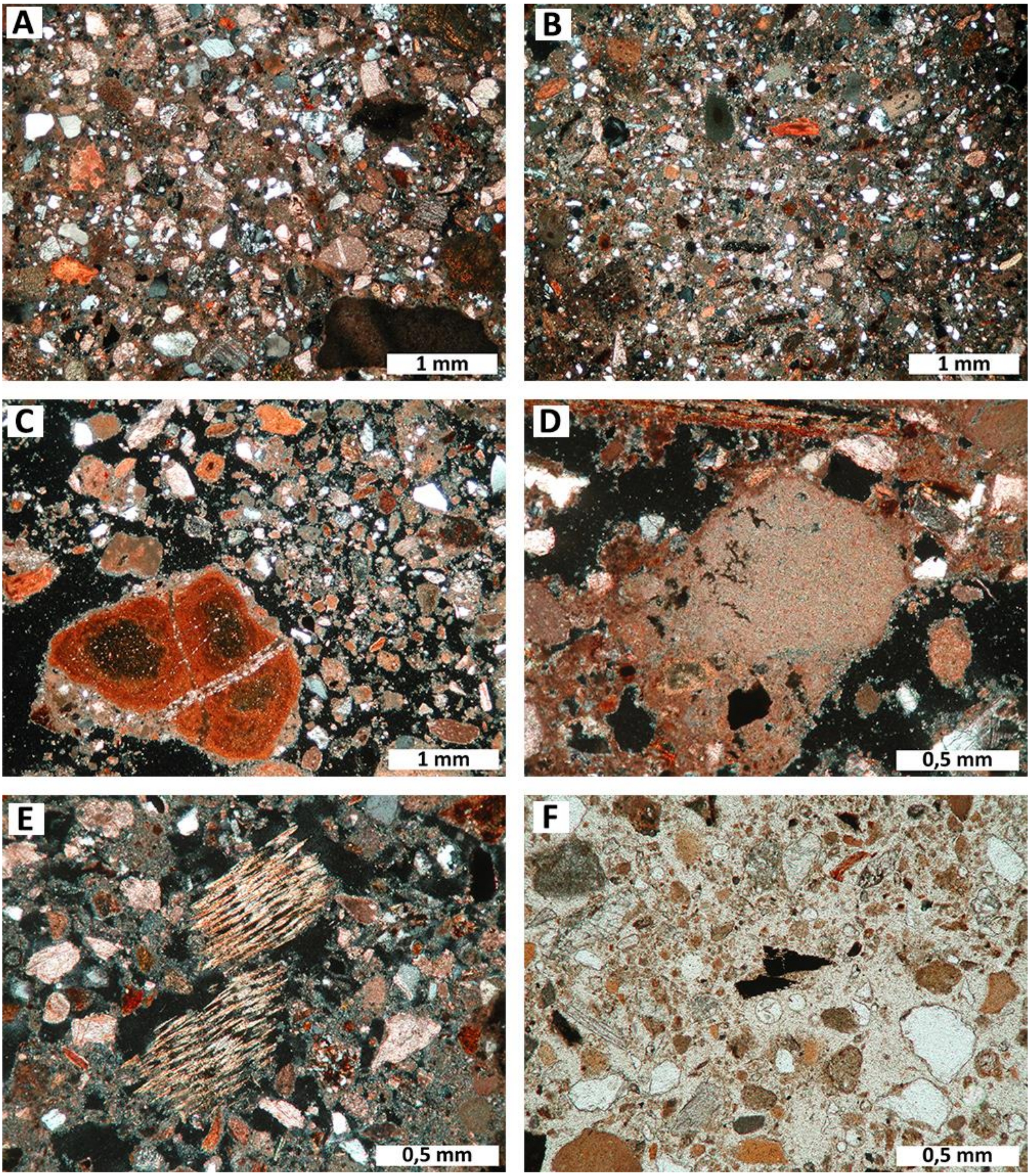

Fig. 18: photomicrographs of lime mortar thin sections: A) the aggregate of the mortar has high percentage of limestone, crossed polars; B) mortar with fine aggregate, crossed polars; C) at the bottom left a fragment of partially burned limestone, crossed polars; D) at the center a lime lump *sensu strictu* crossed polars; E) at the center straw fragments, crossed polars; F) at the center a black charcoal fragment, natural light.

5.3.2. AMS Radiocarbon dating

Once the contamination is identified, it must be separated from the carbon belonging to the original binder. The methods most commonly used for sample preparation consist of a mechanical pre-treatment (Nawrocka et al. 2005; Mazaioli et al. 2011; Ortega et al. 2012; Nonni et al. 2013, 2017; Addis et al. 2019) and a chemical treatment (Heinemeier et al. 1997; Sonninen and Jungner 2001; Lindroos et al. 2007 and successive). Both techniques (Cryo2sonic and sequential dissolution) have been applied on the same mortar samples in order to identify the most suitable method. Nine lime mortar samples have been selected belonging to eight different vaults (C1-1M, C2-3M, C3-1M; C5-4M, C5-5M, N3-2AM, N8-1M, N9-3M, S9-4M). The samples are characterized by carbonate aggregate and presence of underburned particles. In addition, the samples C2-3M, C3-1M, C5-4M and C5-5M contain many *cocciopesto* fragments. Therefore, the mortars could be contaminated by dead carbon and the presence of *cocciopesto* could produces weakly hydraulic mortars. As reported by several authors (Hodgins et al. 2011; Lindroos et al. 2011; Ringbom et al. 2011, 2014; Michalska and Czernik 2015; Hajdas et al. 2017; Hayen et al. 2017; Michalska et al. 2017), the radiocarbon dating of hydraulic mortars could be complicated and problematic.

First, the mortars have been carefully processed and observed with a stereomicroscope in the laboratory of the University of Modena and Reggio Emilia (UNIMORE). The ones containing sufficient quantity of lime lumps have been selected and the lumps have been mechanically separated from the bulk under the stereomicroscope. Lumps of pure lime are clearly identifiable in old lime mixtures as they exhibit a white, rounded and a floury complexion (fig. 19, Pesce and Ball 2012).

Fig. 19: pure lime lumps in a specimen of air lime mortar (left hand side) and detail of the lime lump (right hand side) (Pesce and Ball 2012).

The hardness of this type of lump is very low making them extremely delicate to handle and easily damaged (Pesce and Ball 2012). The surfaces of lime lumps have a floury appearance while those of under burned lumps and sand grains appear denser resembling stone. Evaluation of the superficial hardness is a useful method for distinguishing between similar lumps (incompletely burn limestone or roundly grains of milky quartz). Even performing a crude test, by hand, using a needle point, allows these different types of lumps to be effectively distinguished. This selection is very time consuming and even if it is possible to recognize the carbonate contaminants it is not always possible to completely remove them, due to their very small sizes.

Cryo2SoniC procedure

The procedure has been applied on six lime mortar samples (C3-1M, C5-4M, N3-2AM, N8-1M, N9-3M, S9-4M) at the University of Campania "Luigi Vanvitelli" (Department of Environmental Science and Technology).

<u>Bulk</u>

Around 20 g of mortar per sample (C3-1M, C5-4M, N9-3M) have been submerged in liquid nitrogen for few minutes and transferred into an oven at 80°C. These cycles were repeated 3 times for each sample and then the mortars have been gently crushed with a hammer (Fig. 20). The sieved powder (under 500 µm) has been put into the beaker with an excess (about 75 mL) of deionized water. The first ultrasonic bath for 10 minutes produced the so-called "sand" fraction. The water surface was collected by pipette and centrifuged for 5 minutes at 6.0 krpm to eliminate the water and then it was dried overnight in an oven at 80°C. Then, the sample was filled up again with distilled water (about 75 mL). The development of the Cryo2Sonic procedure involved a second ultrasonic bath of 30' creating the "susp" fraction. This fraction was siphoned in tubes, centrifuged for 5 minutes at 6.0 krpm to eliminate the water (fig. 21) and then it was dried overnight in an oven at 80°C. The dried samples were removed from the tube with a spatula and they were weighed (tab. 3).

Fig. 20: Cryo2Sonic mechanical preparation.

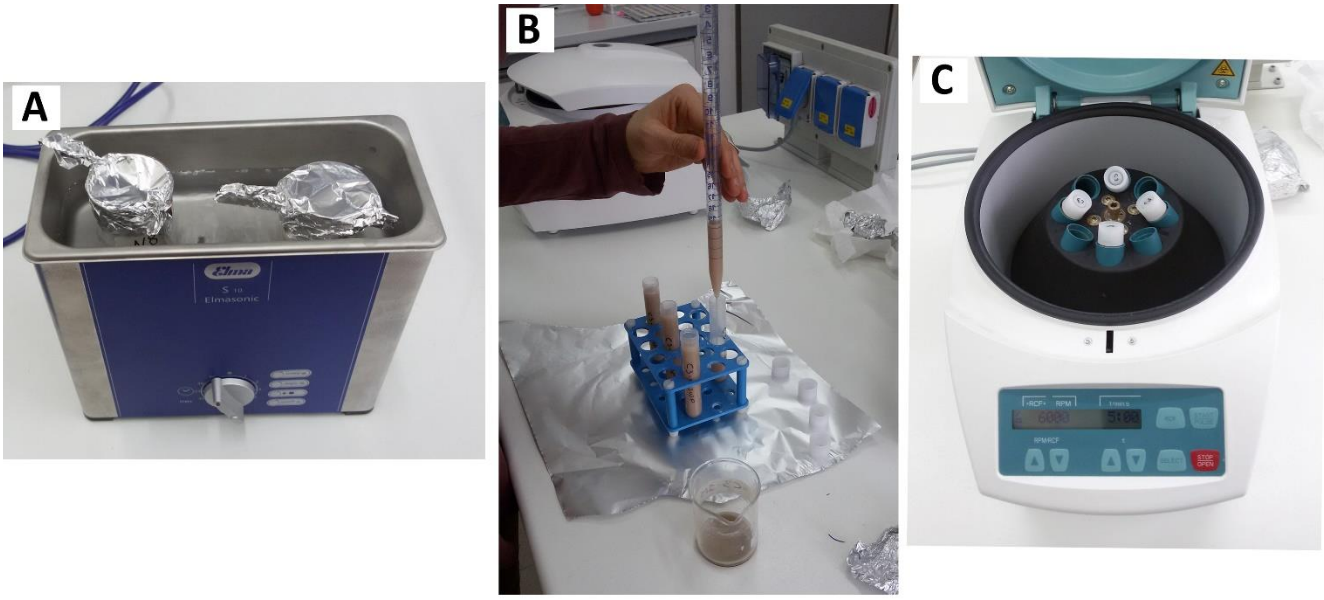

Fig. 21: Cryo2Sonic procedure involves an ultrasonic bath of 30’ creating the susp fraction (A). The fraction is siphoned in tubes (B) and centrifuged for 5 minutes (C).

CRYO2SONIC							
SAMPLES	**m INITIAL SAMPLE (gr)**	**m AFTER cryo-breaking (gr)**	**m (cryo)/ m (sample)**	**SAND (gr) (10' ultrasonic bath)**	**m (sand)/ m (cryo)**	**SUSP (gr) (30' ultrasonic bath)**	**m (susp)/ m (cryo)**
C3-1M	21,94	4,293	19,56%	0,0801	1,86%	0,3102	7,23%
C5-4M	18,10	5,303	29,30%	0,1228	2,31%	0,1082	2,04%
N9-3M	34,24	10,822	31,60%	0,1861	1,72%	0,3883	3,58%

Tab. 3: Cryo2Sonic pretreatment data.

Susp lump fraction

Lumps from the samples C5-4M, N3-2AM, N8-1M and N9-3M were selected and they have been submerged into an excess (about 30 mL) of distilled water and ultrasonicated for 30’. The suspension has been selected by syphoning immediately after ultrasonication to avoid the sedimentation. The obtained suspension was centrifuged for 5 min at 6.0 krpm and the surface water has been eliminated. Samples were put in an oven at 80°C overnight. The dried samples have been removed from the tube with a spatula to obtain the susp_lump fraction and they have been weighed. Due to the scarce amount of material, only the samples N8-1M and N9-3M have been dated (tab.4).

CRYOSONIC			
SAMPLE	**m LUMPS (gr)**	**SUSP (gr) (30' ultrasonic bath)**	**m (susp)/ m (lumps)**
C5-4M	0,0482	0,0037	7,68%
N3-2A	0,0457	0,0011	2,40%
N8-1M	0,0486	0,0085	17,49%
N9-3M	0,0661	0,0195	29,55%

Tab. 4: CryoSonic pretreatment data.

Bulk lumps

Other lumps of the samples (C3-1M, N3-2AM and S9-4M) have been weighed (C3-1M_lump: 30,5 mg; N3-2AM_lump: 21 mg; S9-4M_lump: 20 mg) and they directly underwent to acid digestion.

The dried suspension, the untreated lime lumps and the carbonate standard samples (i.e. IAEA C1 and C2, Rozanski et al. 1992) have been attacked with 85% phosphoric acid under vacuum for 2 h in a drying oven at 85°C. Produced gasses underwent cryogenic purification by means of a vacuum line to separate evolved CO_2 and then graphitized (Fedi et al. 2013), to obtain graphite pellets to be inserted into the accelerator source. Accelerator Mass Spectrometry measurements were performed on the dedicated beam line of the 3 MV tandem accelerator of INFN-LABEC, Florence (Fedi et al. 2007). Calibration of AMS measurement (radiocarbon age) was performed using the software OxCal 4.2 (Bronk Ramsey and Lee 2013; Bronk Ramsey 2016) and using the calibration curve IntCal13 (Remier et al. 2013).

Sequential dissolution

Considering the results obtained using Cryo2Sonic, the radiocarbon dating of the same samples was repeated following the sequential dissolution procedure (Åbo Akademi University). Also, three new samples have been dated given the promising results of the previous ones.

The procedure has been applied on the eight following lime mortar samples: C1-1-M, C2-3M, C3-1M, C5-4M, C5-5M, N8-1M, N9-3M, S9-4M. Seven mortar bulks (C1-1-M, C2-3M, C3-1M; C5-4M, C5-5M, N9-3M, S9-4M) and two lime lump (C3-1MLi and N8-1MLi) have been prepared at Åbo Akademi University, Turku.

<u>Bulk</u>

The samples have been broken in a plastic bag using nipper pieces, not to produce fine splinter of the aggregate (Fig. 22A). The crushed material has been vibrated in a sieve series (mesh widths ranging between 20-500 µm) (Fig. 22B). The grain-size fraction <100 µm has been subsequently wet sieved and the grain-size fraction range of 46-75 µm has been chosen for dating.

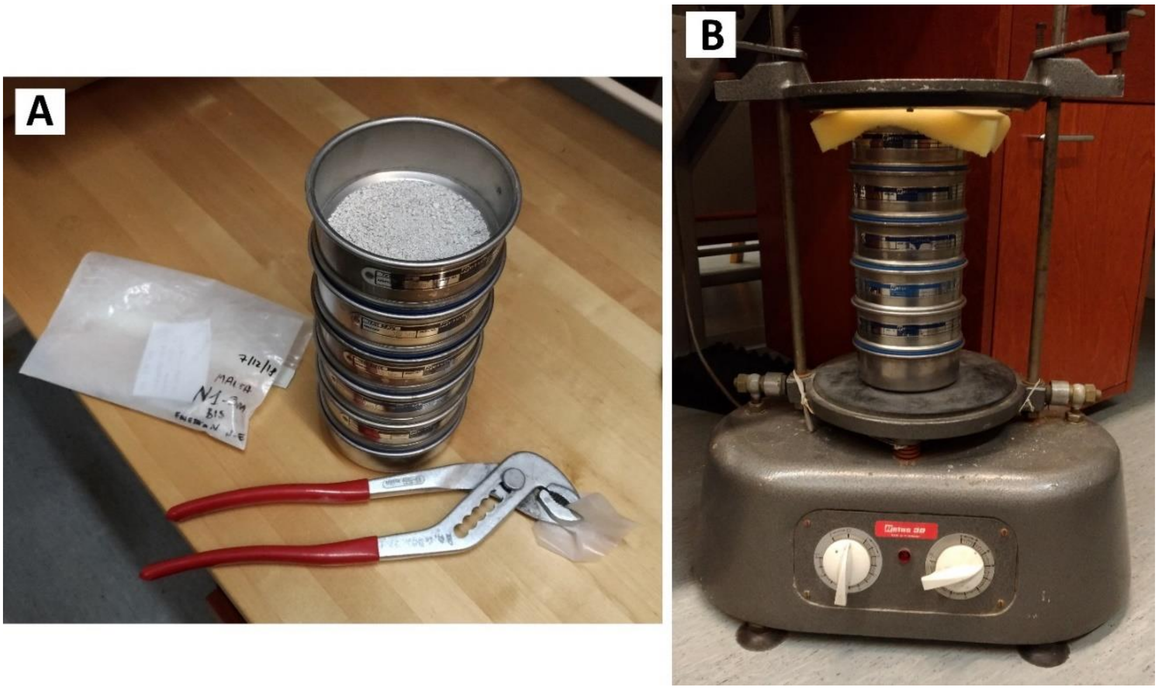

Fig. 22: A) the samples are broken in a plastic bag using nipper; B) The crushed material is vibrated in a sieve series.

The coarser grain size fraction (300-500 µm) has been used for testing the alkalinity of the samples. Approximately 200 mg of sample powder has been put into a glass vessel and two drops of 2% phenolphthalein solution (in ethanol) have been dropped on the sample and then 10 mL of distilled water has been added. A pale pink colour as shown in figure 23 is considered acceptable. All the samples have resulted to be with a low alkalinity and therefore suitable to be dated.

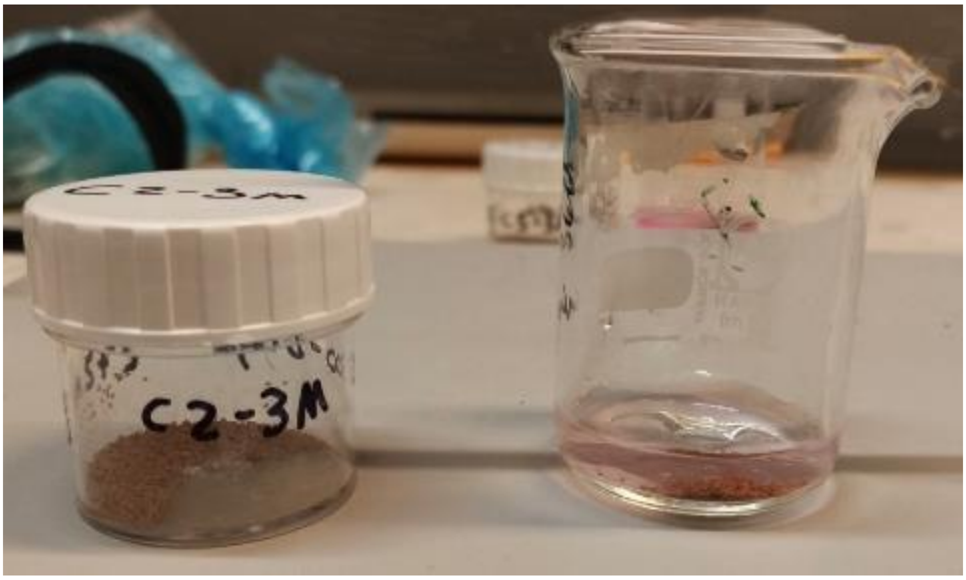

Fig. 23: alkalinity test.

Before hydrolysis the 46-75 µm gran size fraction has been examined with a stereomicroscope combined with a Cambridge Image Technology LTD (CITL) CL8000 MK4 cold cathode cathodoluminescence device and a camera.

The samples have been prepared to carbon dioxide in a specially designed preparation line shown in figure 24. The selected powders have been put into the reactor vessel and, when a sufficient vacuum is reached, around 3 mL of 85% chilled at 0°C phosphoric acid has been let in excess on the powder from a burette. Samples have reacted rapidly and, after 10s or less, the first CO_2 fractions have been isolated, chilled out and captured in glass vials. The next CO_2 fractions have been isolated after 20-30s. The third fractions have been collected within 100s. The reaction has been finished when no more effervescence was visible and the total carbon yield has been calculated from the total CO_2 captured. The partial pressure of the total amount of CO_2 has been measured and used as references when calculated the relative size of dated CO_2 fractions. The samples behavior during the dissolution process is summarized in table 5.

Lump

The two lime lump selected have been crushed before hydrolysis.

Fig. 24: CO_2 extraction line in the laboratory of the Abo Akademi

The vials containing the CO_2 gas of the samples C3-1MLi, C5-4M, N8-1MLi and N9-3M have been sent to the AMS 14C Dating Centre at Aarhus University (Denmark) (Heinemeier et al. 2010; Lichtenberger et al. 2015), while the vials of the samples C1-1M, C2-3M, C3-1M (bulk), C5-5M and S9-4M have been sent to ETH Zurich (Switzerland) (Hajdas et al. 2004; Hajdas et al. 2017). The CO_2 gas has been converted to graphite for AMS ^{14}C measurements via reduction with H_2 using cobalt as a catalyst (Vogel et al. 1984). The calibration of the ^{14}C ages to calendar years has been done using the IntCal13 calibration curve (Remier et al. 2013) and the OxCal 4.3 program (Bronk Ramsey 2017). All calibrated results are reported at 95.4% confident level.

Sample	Grain-size C content *(µm)*	Sample aliquot *mg*	CO2 fraction *(nr)*	Diss. Time *(s)*	P in the CO2 line *(mbar)*	F	Calc.C cont. *(mg)*	Dating
C1-1M	46-75	80	1	6	18,7	0,09	0,24	**X**
85% H_3PO_4	**3.40% C**		2	17	30,5	0,14	0,39	**X**
0 degrees			3	110	44,4	0,21	0,57	**X**
			4	600	60,8	0,29	0,78	
			5	1540	38,0	0,18	0,49	
			6	2060	19,0	0,09	0,24	
			7	2530	11,1	0,05	0,14	
			8	9000	12,8	0,06	0,16	
C2-3M	46-75	50	1	7	21,6	0,10	0,28	**X**
85% H_3PO_4	**5,69%C**		2	17	33,2	0,15	0,43	**X**
0 degrees			3	70	36,2	0,16	0,47	**X**
			4	690	58,00	0,26	0,75	
			5	1610	35,9	0,16	0,46	
			6	2080	17,9	0,08	0,23	
			7	10755	18,3	0,08	0,24	
C3-1MLi	Crushed	39	1	15	48,8	0,19	0,63	**X**
85% H_3PO_4	not sieved		2	21	59,4	0,24	0,76	**X**
0 degrees	**8.27 % C**		3	140	50,3	0,20	0,65	
			4	1450	57,4	0,23	0,74	
			5	2030	12,6	0,05	0,16	
			6	3240	9,51	0,04	0,12	
			7	12060	12,6	0,05	0,16	
C3-1M.1	46-75	60,4	1	6	13,7	0,12	0,18	(X)
85% H_3PO_4	**2.53% C**		2	30	29,5	0,25	0,38	**X**
0 degrees			3	120	29,6	0,25	0,38	**X**
			4	520	27,5	0,23	0,35	
			5	1470	16,5	0,14	0,21	
			6	8310	2,30	0,02	0,03	
C3-1M.2	46-75	100	1	14	14,7	0,08	0,19	**X**
85% H_3PO_4	**2.44% C**		2	8160	175	0,92	2,25	
0 degrees								
C5-4M	46-75	129,3	1	6	53,2	0,09	0,68	**X**
85% H3PO4	**5.36 % C**		2	24	95,7	0,17	1,23	**X**
0 degrees			3	90	86,0	0,15	1,11	**X**
			4	710	139	0,24	1,79	
			5	1880	82,0	0,14	1,06	
			6	3030	45,6	0,08	0,59	
			7	3560	18,2	0,03	0,23	
			8	4250	11,6	0,02	0,15	
			9	5505	6,88	0,01	0,089	
C5-5M	46-75	58	1	5	26,40	0,10	0,34	**X**
85% H_3PO_4	**6,08%C**		2	22	41,00	0,15	0,53	**X**
0 degrees			3	60	42,5	0,15	0,55	**X**
			4	695	91,60	0,33	1,18	
			5	1730	40,30	0,15	0,52	
			6	2302	21,40	0,08	0,28	
			7	2820	11,00	0,04	0,14	
N8-1MLi	Crushed	64,3	1	10	41,4	0,27	0,53	**X**
85% H_3PO_4	not sieved		2	24	37,3	0,24	0,48	**X**
0 degrees	**3.05 % C**		3	460	50,7	0,33	0,65	
			4	8880	23,1	0,15	0,30	

N9-3M	46-75	104,4	1	7	14,0	0,04	0,18	**X**
85% H_3PO_4	**4.48 % C**		2	24	62,6	0,17	0,81	**X**
0 degrees			3	75	58,6	0,16	0,75	**X**
			4	645	110	0,30	1,42	
			5	1850	63,7	0,18	0,82	
			6	2490	30,2	0,08	0,39	
			7	3280	19,0	0,05	0,24	
			8	3630	5,49	0,02	0,07	
S9-4M.2	46-75	106,6	1	20	43,00	0,16	0,55	**X**
85% H3PO4	**3.35 % C**		2	100	56,90	0,21	0,73	**X**
0 degrees			3	395	56,10	0,20	0,72	**X**
			4	1260	60,80	0,22	1,07	
			5	6900	60,60	0,22	0,78	
S9-4M.3	46-75	140	1	13	48,4	0,170	0,62	**X**
85% H_3PO_4	**2.62 % C**		2	35	53,8	0,189	0,69	**X**
0 degrees			3	150	56,1	0,197	0,72	**X**
			4	1270	57,4	0,202	0,74	
			5	1560	27,4	0,096	0,35	
			6	1950	20,2	0,071	0,26	
			7	2400	9,4	0,033	0,12	
			8	4410	7,57	0,027	0,10	
			9	4980	4,46	0,016	0,06	

Tab. 5: Hydrolysis data of the samples dated.

5.3.3. Stimulated luminescence

Optically stimulated luminescence (OSL) on mortars and thermoluminescence (TL) on brick have been performed by the Department of Material Science, University of Milan Bicocca. The mortar samples N8-1M and S9-4M have been selected for OSL dating and fifteen brick samples for TL dating (C1-1L, C3-1L, C5-1L, C5-4L, C5-5L, C5-6L, C5-7L, N3-1AL, N3-3AL, N8-1L, N8-2L, N9-1L, N9-3L, S9-1L, S9-4L).

Milan TL protocol

The fine-grain dating technique (Zimmermann, 1971), requiring relative small amount of material, was used for TL dating of bricks. The samples have been prepared under dim red light, using the standard procedure and the polymineral fine grain (1-8 µm) fraction was deposited on stainless steel discs. For the evaluation of the palaeodose, the TL Multiple Aliquot Additive Dose protocol (MAAD, Aitken, 1985) has been applied.

TL measurements were performed using a home-made system based on the photon counting technique with a photomultiplier tube (EMI 9235QB) coupled to a blue filter (Corning BG12). The samples have been heated from RT to 480°C at 15°C s^{-1}. Artificial irradiations have been carried out by a 1.85 GBq 90Sr-90Y beta source (dose-rate: 3.57 Gy min^{-1}), a 37 MBq 241Am alpha source (dose-rate: 14.8 Gy min^{-1}).

Milan OSL protocol

The Single Aliquot Regenerative dose protocol (SAR; Murray and Wintle, 2000) has been applied. OSL measurements (40 s) have been made at 125°C, after pre-heating aliquots for 10 second at 180°C. The preheat value has been experimentally derived on the basis of the results of a dose recovery pre-heat plateau test. A cut-heat of 160°C was applied to each aliquot before the test dose measurement. To evaluate the Equivalent Dose (ED), the initial part of the OSL decay curve has been used, specifically the first 0.6 s. The background has been assumed as the mean signal of the last 10 s of stimulation. The quartz extracted from mortars was checked for the absence of feldspar contamination using IR stimulation on laboratory irradiated samples. OSL measurements have been undertaken using a Risø TL-DA-20 equipped with a 90Sr/90Y beta source delivering 0.129 ± 0.012 Gy/s to quartz coarse grains. The samples have been stimulated by an array of blue LEDs (470 ± 30 nm) with a constant stimulation power of 54 mW/cm^2 or with IR LEDS (830 ± 10 nm) with a constant stimulation power of 360 mW/cm^2. Photons were detected by a bialkali photomultiplier tube (EMI 9235QB) coupled to a 7.5mm Hoya U-340 filter (280-380 nm).

Dose-rate determination

For dose-rate determination, ^{238}U and ^{232}Th concentrations were derived from alpha counting using ZnS (Ag) scintillator discs and assuming a Th/U concentration ratio equal to 3.16 (Aitken 1985). Contribution due to ^{40}K content was obtained from the total concentration of K measured by flame photometry. The attenuation of the beta particles in coarse grain quartz used for mortar dating was taken into account (Bell 1979).

5.4. Pollen analysis

The pollen analysis has been performed on six mortar samples: C5-6M, C5-7M, N3-3AM, N8-2M, S9-1M, S9-4M. The technique was tested analyzing both gypsum mortar and lime mortar. All the samples are gypsum mortars expect the lime mortar sample S9-4M. The choice of the samples has been made considering the absolute dating results. Mortar samples belonging to portions attributed at different building phases have been selected in order to recover pollen grains. Pollen preserves a record of the local vegetation at the time of mortar setting and it can be an indirect indication of the construction timing. This technique was especially applied on gypsum mortars that are not directly datable. The information obtained from pollen analysis can be then linked and compared with the absolute dating results.

Since the literature dealing with pollen analysis of mortar is not abundant, a first attempt was made to ascertain whether this type of substrate could contain and preserve pollen granules and NPPs (non pollen palynomorphs). Preliminary investigations were carried out on three mortar samples (N3-3AM, S9-1M and S9-4M) and subsequently, given the promising result, on the remaining samples (C5-6M, C5-7M and N8-2M).

The pollen analysis has been performed by the Laboratory of Palynology and Palaeobotany of the University of Modena and Reggio Emilia (UNIMORE).

Samples were treated according to the routine method for pollen extraction and analyses in use by the UNIMORE laboratory (Florenzano et al. 2012). The method was imported and adapted from the Institute of Earth Sciences, Vrije Universiteit Amsterdam in the 1990s (PALICLAS project; Lowe et al. 1996; van der Kaars et al. 2001).

According to the available material, few grams, usually 5 g, of dry sediment from each sample was prepared as follows:

1.Treatment with sodium pyrophosphate to deflocculate the sediment matrix in 100 mL beakers.

2. One *Lycopodium* spore tablet was added to each sample to calculate the concentration of microremains from the ratio of the counted number of pollen grains to the counted number of added spores, multiplied by the known number of spores added (Stockmarr 1971). Concentrations are expressed as number of pollen (p/g) per gram.

3. Each sample was transferred to a 7-µm nylon handheld sieve, closed, and washed under running water. The residual sieved sediment was then transferred to a 100 mL beaker with the help of distilled water, and left to stand overnight; then the supernatant was removed by aspiration.

4. About 40 mL of 10% hydrochloric acid were added to remove carbonates, until no further reaction occurred. After one night, the supernatant was removed by aspiration.

5. The residues were concentrated by repeated centrifugation at 2500 rpm for 2 minutes in 10 mL test tubes.

6. After dehydration with glacial acetic acid, 4-5 mL of acetolysis mixture (9:1 ratio of acetic anhydride and sulfuric acid) was added to the residues; the tubes were transferred to a water bath at 90◦C for 10 minutes, and stirred.

7. Heavy liquid separation (useful to concentrate pollen in samples very poor in organic matter) was performed with sodium metatungstate hydrate of specific gravity (sg) 2.0 and centrifugation at 2000 rpm for 20 minutes. After collecting the upper portion of the supernatant in a different centrifugation tube, this step was repeated.

8. The retained fractions were treated with 1 mL of cold 40% hydrofluoric acid for one night to remove silicates.

9. The residue was washed in 98% ethanol, supplemented with glycerol and, finally the remaining ethanol was evaporated. The final residues were mounted on permanent slides in glycerol jelly, and cover slips sealed with paraffin.

An optical microscope with magnifications of 1000x was used for identifying the pollen grains. In each sample all the pollen grains extracted were counted and identified with the help of the reference pollen collection, keys and atlases (e.g. Moore et al. 1991; Reille 1992).

6. RESULTS

In this section the results of the laboratory analyses carried out on mortar and brick samples are presented. The first part concerns the characterization of the mortar aggregate and binder, carried out with polarizing microscopy. The detailed petrographic characterization has been used as the basic scientific knowledge for the absolute dating methodologies discussed in the second part of the chapter.

6.1. Results of petrographic analysis

Lime mortars

Each thin section was first photographed and then described according to the UNI 11176 Document (2006) - Petrographic description of a mortar. About each thin section is specified: type of binder, aggregate binder ratio, composition of the aggregate, grain size and sorting grade, presence of BRPs and hypotheses on the origin of the sand (Lugli et al. 2007).

The petrographic analysis revealed that all lime mortar samples present BRPs particles. The most frequent are the underburned fragments of the carbonate stones used to produce the lime, which do not completely calcine during the burning and are left inside the slaked lime as inert (Elsen 2006). They are rounded limestone (fig. 25A) or marly limestones that show the effect of partial burning especially in the outer part (fig. 25B). These fragments commonly show micritic reaction edges that fade into the surrounding binder (fig. 25C) and also some of them display traces of cleavage (fig. 25D). Overburned lime fragments (fig. 25E) are also frequent.

The lime lumps *sensu strictu* are mainly scares and variable in size, typically few millimeters in diameter or less. Under the polarizing microscope they exhibit porous structures with the same appearance of the surrounding binder (fig. 25F).

Moreover, other particles are found in three mortar samples (C3-1M, N2-2FM and S1-2M). They contain prismatic crystals with high interference colour, iron-rich minerals and bubbles (Fig. 26 A, B, C, D, E, F). The optical features are in between an effusive rock (bubbles) and an intrusive one (well-formed minerals). These particles can be interpreted as burning waste for the irregular reaction rims. These fragments are quite similar to those found in the Cathedral and in the Ghirlandina tower (Caroselli 2015).

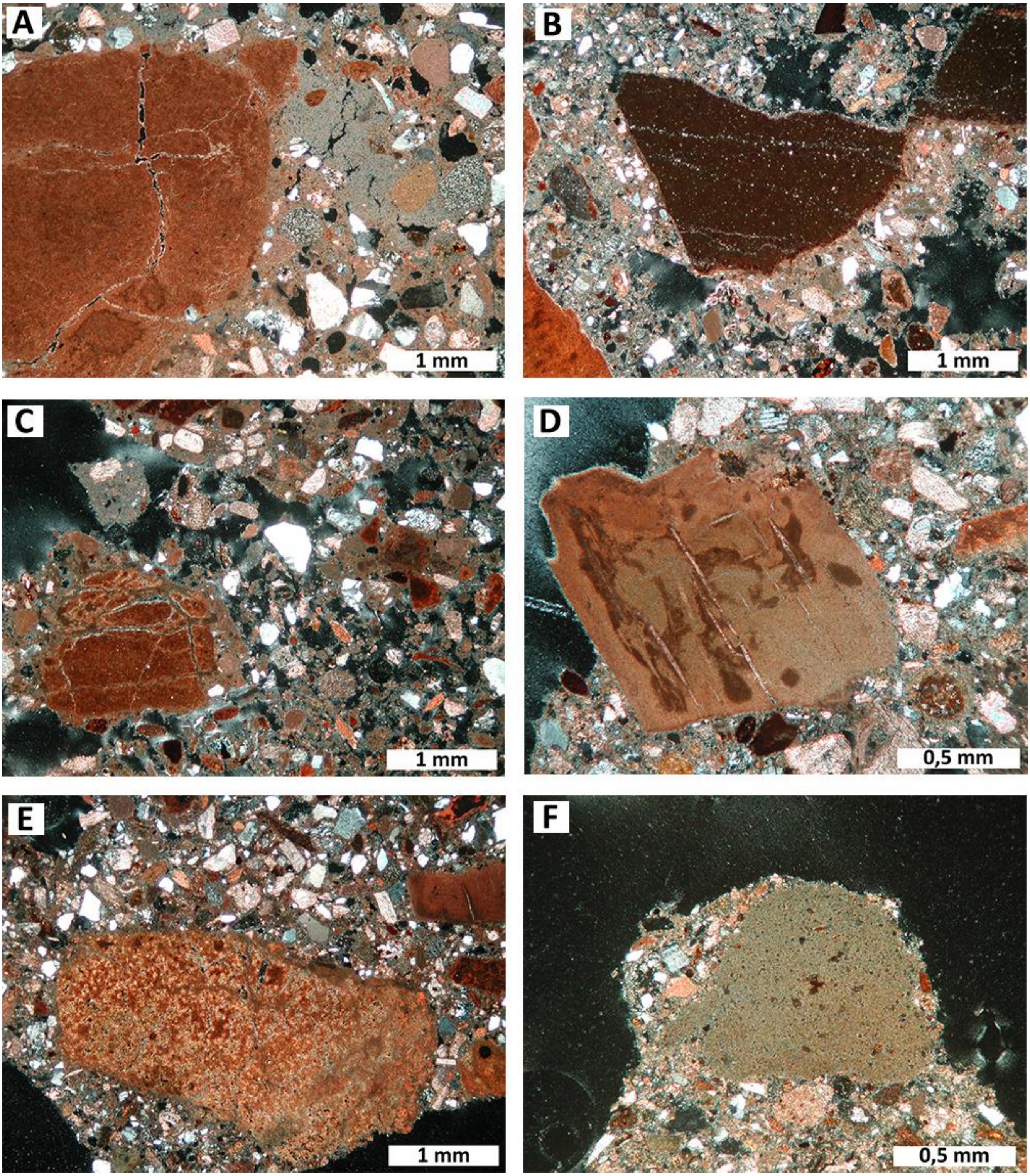

Fig. 25: photomicrographs in crossed polars of binder related particles A); at the left of the imagine rounded limestone; B) fragments of marly limestone underburned with signs of firing and brown-reddish colors. They kept the original structures and textures of the rock and show reaction edges that fade in the binder; C) fragment on the left shows micritic reaction edges that fade into the surrounding binder; D) relict calcite cleavage traces; E) overburned lime fragment; F) lime lumps *sensu strictu* with porous structure with similar appearance to the binder.

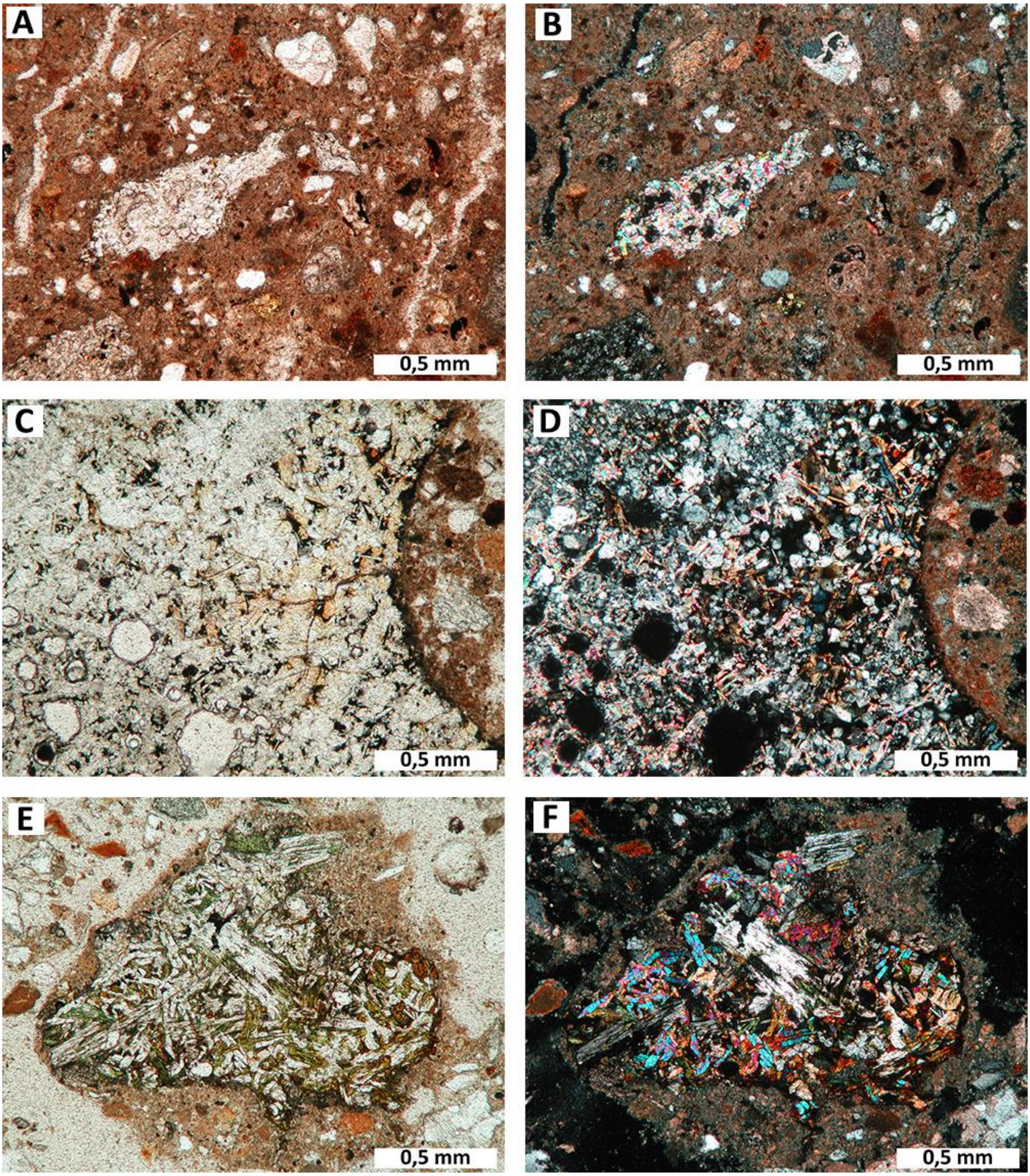

Fig. 26: photomicrograph of particles of unknown origin A) sample C3-1M, transparent crystals and bubbles, natural light; B) sample C3-1M, crystals with high interference colour and bubbles, crossed polars; C) sample S2-1M, transparent elongated crystals and bubbles, natural light; D) sample S2-M, elongated crystals with high interference colours and bubbles, crossed polars; E) sample N2-2FM, prismatic and elongated crystals and brownish interstitial phase, natural light; F) sample N2-2FM, elongated crystals with high interference colours and squared crystals with greyish interference colours, crossed polars.

All lime mortar samples present generally the same aggregate components, although in different proportions. The main ones are: angular clasts of monocrystalline or polycrystalline quartz, angular clasts of feldspars (k-feldspar and plagioclase), rounded fragments of carbonate microcrystalline rocks (micrites), angular fragments of spathic calcite, rounded fragments of serpentinite fragments, fossil fragments, rounded particles of glauconite and fragments of quartz siltstone in carbonate cement. Six samples also present abundant rounded bricks fragments.

The aggregates are fluvial sands taken from the rivers of the Modena area and the evaluation of their supply sources have been performed according to the classification proposed by Lugli et al. 2007. The modern stream sands in the Modena Plain have similar overall compositions, but show significant variations in quartz, feldspar, carbonate and lithic fragment contents. For this reason, the sand from different rivers can be clearly distinguished. Streams draining the eastern sector of the Modena Plain area (Panaro, Tiepido, Guerro) have a generally higher carbonate content than those draining the western part, which are enriched in quartz and feldspar (Secchia and Grizzaga). The Guerro and Tiepido streams have the highest carbonate content, mainly represented by single calcite crystals, while the Grizzaga stream shows the greatest variation in terms of the measured parameters, and therefore has the broadest compositional field (fig. 27). The point counting analysis of the aggregate was not performed and a probable sand provenance for each mortar samples is suggested.

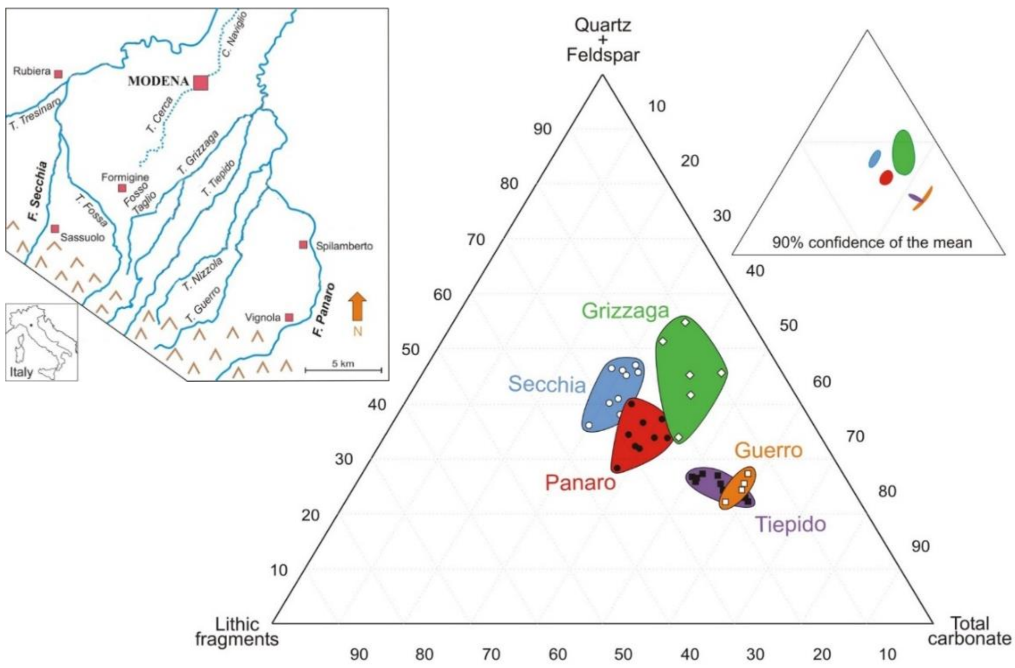

Fig. 27: Ternary diagrams showing modern sand composition of the Modena Plain streams. Simplified sketch of the fluvial drainage network in the Modena Plain (above) (Lugli et al. 2007, modified).

In the following pages the description of each mortar sample is reported.

Central vault C1

Sample C1-1M

The sample C1-1M is a lime-based mortar with underburned/overburned particles up to 4 mm in size. Lime lumps are scarce and small (< 1 mm). The aggregate binder ratio is 1.5. The aggregate grain size is very fine to medium sand (0.1-0.4 mm) and poorly sorted. The composition is: micritic limestone and sparry calcite, quartz, feldspar, siltstone, abundant fossil fragments, serpentinite fragments, iron oxide and/or hydroxide. Straw fragments are also visible. The probable sand provenance is from the Panaro River (Lugli et al. 2007). Pores are very frequent and they show irregular shape (fig. 28A).

Sample C1-4AM

The sample C1-4AM is a lime-based mortar with lime lumps scarce and small (< 1 mm) and devoid of underburned and overburned fragments. The aggregate binder ratio is 2.8. The aggregate grain size is fine to medium sand (0.2-0.5 mm) and well sorted. The sand composition is: micritic limestone and sparry calcite, quartz, feldspar, siltstone, abundant fossil fragments, serpentinite fragments, glauconite, iron oxide and/or hydroxide. Straw fragments are also visible. The probable sand provenance is from the Panaro River (Lugli et al. 2007). Pores are frequent and most of them have irregular shape (fig. 28B).

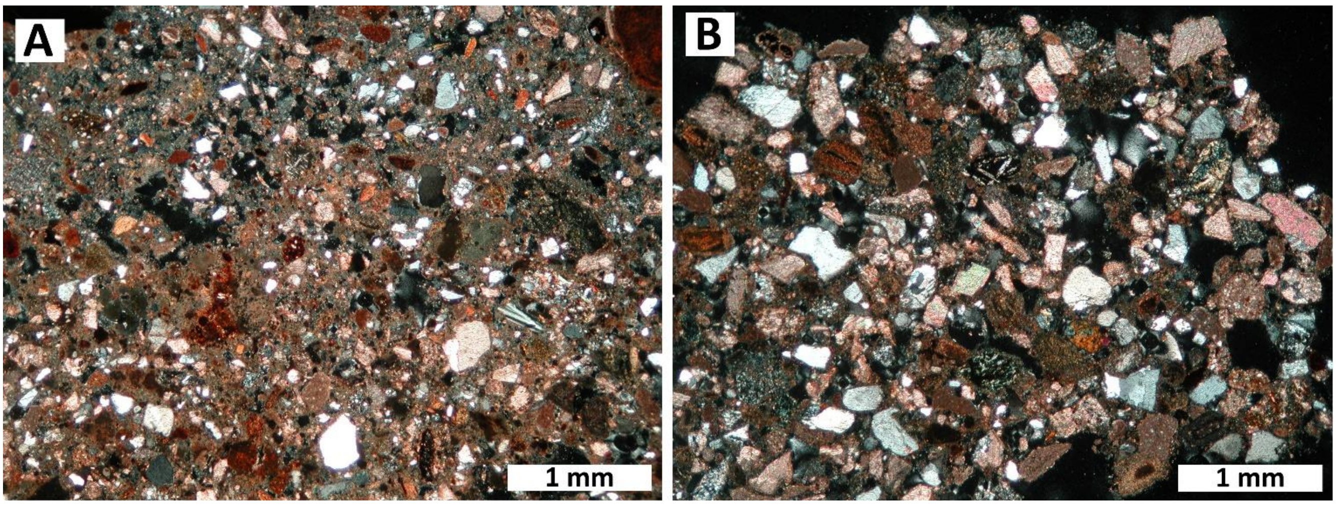

Fig. 28: A) photomicrograph in crossed polars of the mortar sample C1-1M; B) photomicrograph in crossed polars of the mortar sample C1-4AM.

Central vault C2

Sample C2-3M

The sample C2-3M is a lime-based mortar with underburned/overburned particles up to 2 mm in size. Lime lumps are scarce and reach dimensions up to 2 mm. The aggregate binder ratio is 1.4. The aggregate composition is abundant brick fragments (*cocciopesto*) with dimensions up to 5 mm, micritic limestone, sparry calcite, quartz, serpentinite fragments, iron oxide and/or hydroxide. The probable sand provenance is from the Panaro River (Lugli et al. 2007). Pore are scarce and they show an elongated shape (fig. 29A).

Sample C2-3AM

The sample C2-3AM is a lime-based mortar with underburned/overburned particles up to 3 mm in size. Lime lumps are scarce and reach dimensions up to 3 mm. The aggregate binder ratio is 1.4. The aggregate composition is abundant brick fragments (*cocciopesto*) with dimensions up to 3 mm, micritic limestone, sparry calcite, quartz, serpentinite fragments, iron oxide and/or hydroxide. The probable sand provenance is from the Panaro River (Lugli et al. 2007). Pore are scarce and they show an elongated shape (fig. 29B).

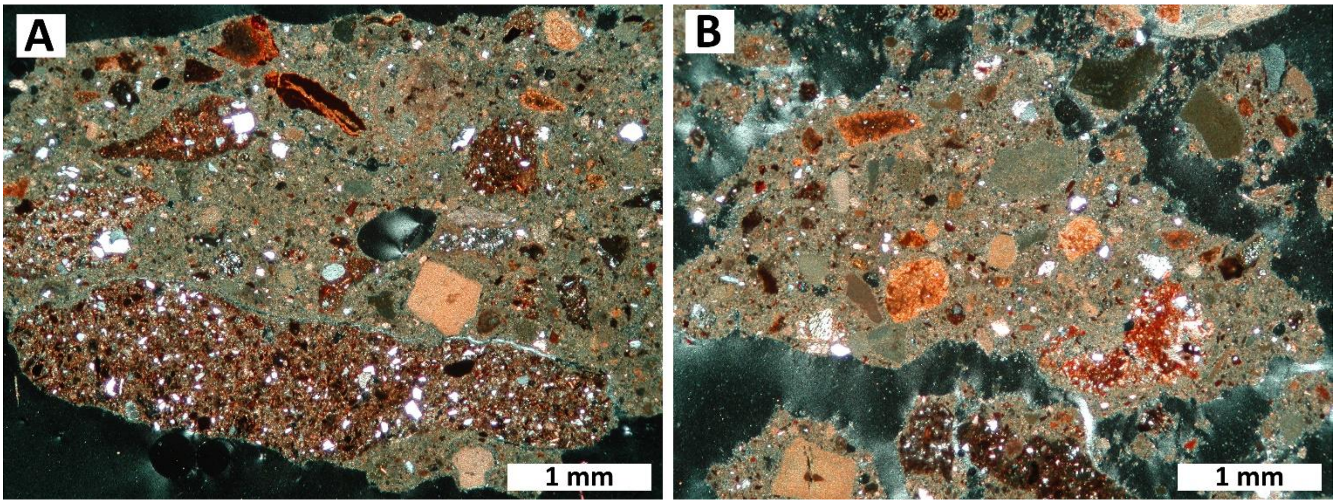

Fig. 29: A) photomicrograph in crossed polars of the mortar sample C2-3M; B) photomicrograph in crossed polars of the mortar sample C2-3AM.

Central vault C3

Sample C3-1M

The sample C3-1M is a lime-based mortar with underburned/overburned particles up to 5 mm in size. Lime lumps are abundant and small (< 1 mm). The aggregate binder ratio is 1.3. The aggregate grain size is very fine to fine sand (0.063-0.3 mm) and moderately sorted. The sand composition is: micritic limestone and sparry calcite, quartz, feldspar, siltstone, fossil fragments, serpentinite fragments, glauconite, iron oxide and/or hydroxide. Brick fragments (*cocciopesto*) are frequent, with dimensions up to 3 mm. The probable sand provenance is from the Panaro River (Lugli et al. 2007). Pore are scarce and they show an elongated shape (fig. 30).

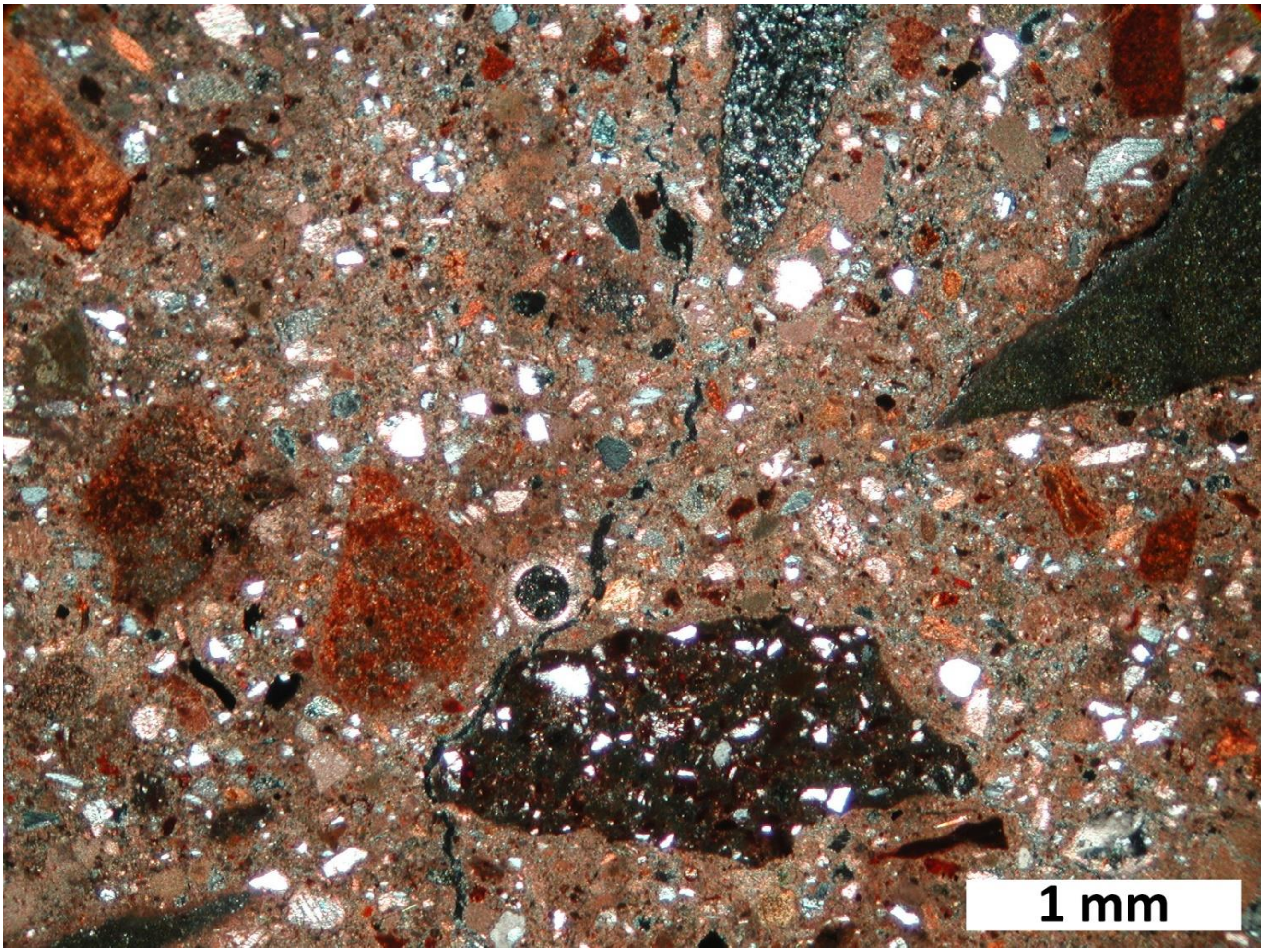

Fig. 30: photomicrograph in crossed polars of the mortar sample C3-1M.

Central vault C4

Sample C4-1AM

The sample C4-1AM is a lime-based mortar devoid of BRPs particles. The aggregate binder ratio is 2. The aggregate grain size is fine to coarse sand (0.2-0.8 mm) and well sorted. The sand composition is: quartz, feldspar, siltstone, micritic limestone and sparry calcite, serpentinite fragments, iron oxide and/or hydroxide. The probable sand provenance is from the Secchia River (Lugli et al. 2007). Pore are scarce and they have irregular shape (fig. 31).

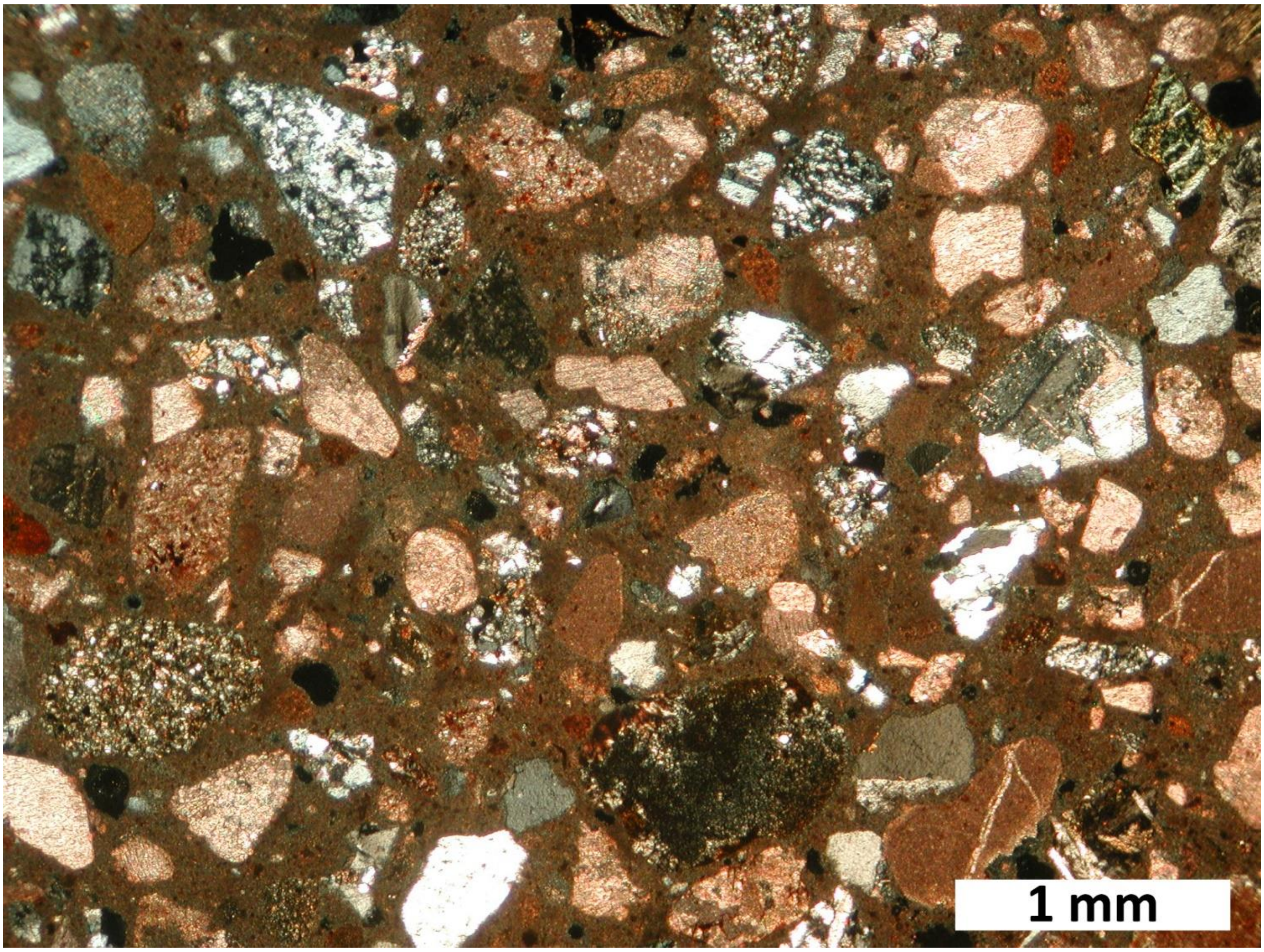

Fig. 31: photomicrograph in crossed polars of the mortar sample C4-1AM.

Central vault C5

Sample C5-1M

The sample C5-1M is a lime-based mortar with underburned/overburned particles up to 4 mm in size. Lime lumps are scarce and small (< 1 mm). The aggregate binder ratio is 1.4. The aggregate composition is abundant brick fragments (*cocciopesto*) with dimensions up to 4 mm, micritic limestone, sparry calcite, quartz, iron oxide and/or hydroxide. Straw fragments are also visible. The probable sand provenance is from the Panaro River (Lugli et al. 2007). Pore are frequent and they show elongated and round shapes (fig. 32A).

Sample C5-4M

The sample C5-4M is a lime-based mortar with underburned/overburned particles up to 3 mm in size. Lime lumps are frequent and reach dimensions up to 3 mm. The aggregate binder ratio is 1.3. The aggregate grain size is very fine to fine sand (0.063-0.3 mm) and moderately sorted. The sand composition is: micritic limestone and sparry calcite, quartz, feldspar, fossil fragments, serpentinite fragments, iron oxide and/or hydroxide. Brick fragments (*cocciopesto*) are abundant, with dimensions up to 3 mm. Straw fragments are also visible. The probable sand provenance is from the Panaro River (Lugli et al. 2007). Pore are frequent and they show elongated and round shapes (fig. 32B).

Sample C5-5M

The sample C5-5M is a lime-based mortar with underburned/overburned particles up to 5 mm in size. Lime lumps are scarce and small (< 1 mm). The aggregate binder ratio is 1.4. The aggregate composition is abundant brick fragments (*cocciopesto*) with dimension up to 4 mm, micritic limestone, sparry calcite, quartz, iron oxide and/or hydroxide. The probable sand provenance is from the Panaro River (Lugli et al. 2007). Pore are frequent and they show elongated and round shapes (fig. 32C).

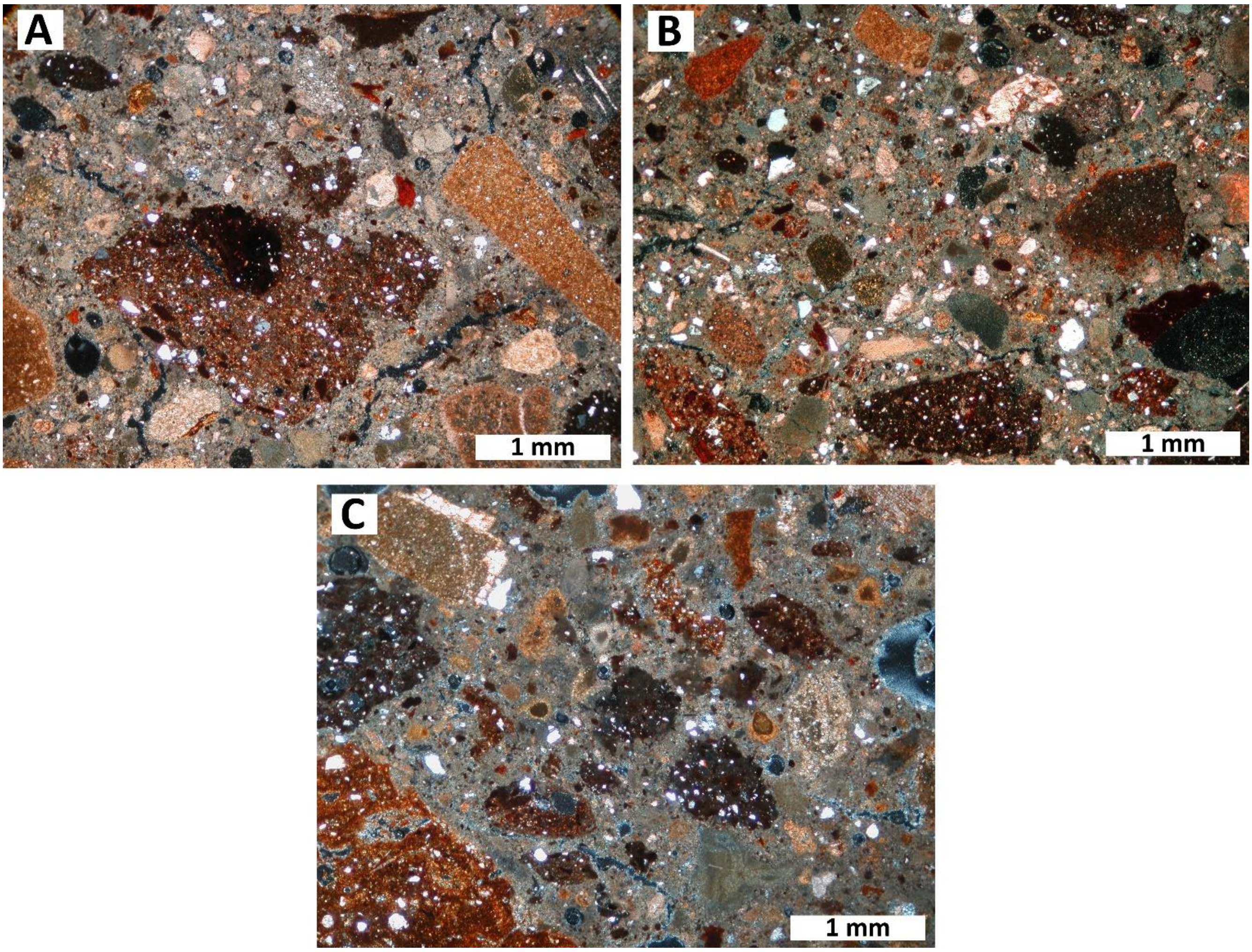

Fig. 32: A) photomicrograph in crossed polars of the mortar sample C5-1M; B) photomicrograph in crossed polars of the mortar sample C5-4M; C) photomicrograph in crossed polars of the mortar sample C5-5M.

Northern vault N1

Sample N1-1M

The sample N1-1M is a lime-based mortar with underburned/overburned particles up to 5 mm in size. Lime lumps are scarce and reach dimensions up to 2 mm. The aggregate binder ratio is 1.5. The aggregate grain size is very fine to medium sand (0.1-0.4 mm) and moderately sorted. The sand composition is: micritic limestone and sparry calcite, quartz, feldspar, siltstone, fossil fragments, serpentinite fragments, iron oxide and/or hydroxide The probable sand provenance is from the Panaro River (Lugli et al. 2007). Pores are frequent and they show irregular shape (fig. 33A).

Sample N1-2M

The sample N1-1M is a lime-based mortar with underburned/overburned particles up to 5 mm in size. Lime lumps are scarce and small (< 1 mm). The aggregate binder ratio is 1.5. The aggregate grain size is very fine to medium sand (0.1-0.4 mm) and moderately sorted. The sand composition is: micritic limestone and sparry calcite, quartz, feldspar, siltstone, fossil fragments, serpentinite fragments, iron oxide and/or hydroxide. The probable sand provenance is from the Panaro River (Lugli et al. 2007). Pores are frequent and they show irregular shape (fig. 33B).

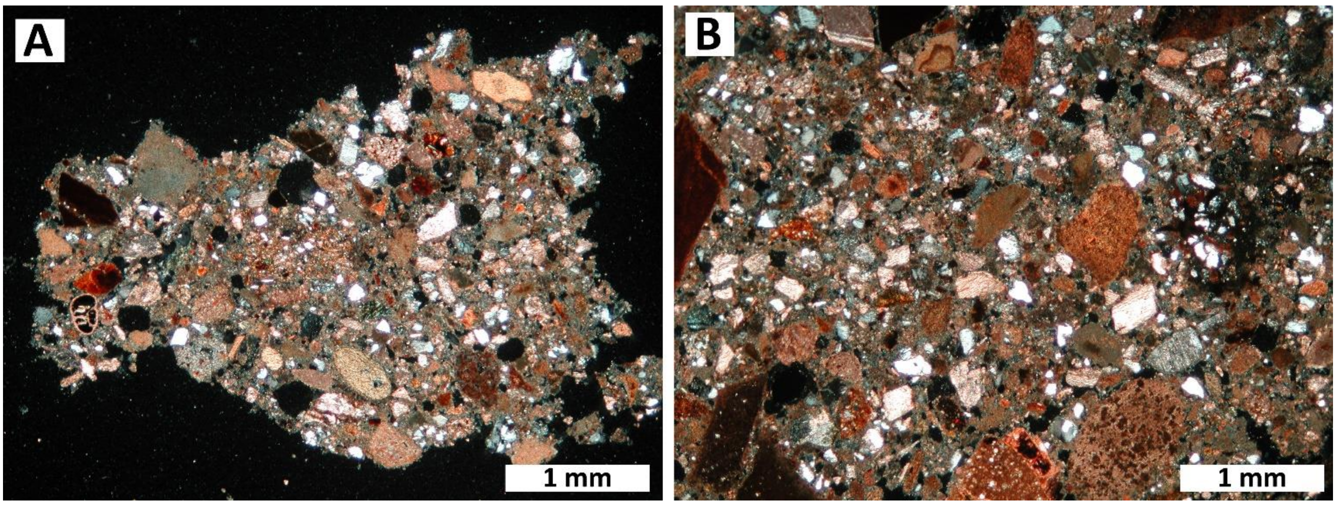

Fig. 33: A) photomicrograph in crossed polars of the mortar sample N1-1M; B) photomicrograph in crossed polars of the mortar sample N1-2M.

Northern vault N2

Sample N2-2DM

The sample N2-2DM is a lime-based mortar with underburned/overburned particles up to 2 mm in size. Lime lumps are frequent and small (< 1 mm). The disintegration phenomena prejudice the correct evaluation of aggregate binder ratio. The aggregate grain size is very fine to medium sand (0.1-0.4 mm) and moderately sorted. The sand composition is: micritic limestone and sparry calcite, quartz, feldspar, fossil fragments, serpentinite fragments, iron oxide and/or hydroxide. The probable sand provenance is from the Panaro River (Lugli et al. 2007) (fig. 34A).

Sample N2-2FM

The sample N2-2FM is a lime-based mortar with underburned/overburned particles up to 3 mm in size. Lime lumps are frequent and small (< 1 mm). The aggregate binder ratio is 1.5. The aggregate grain size is very fine to medium sand (0.1-0.4 mm) and moderately sorted. The sand composition is: micritic limestone and sparry calcite, quartz, feldspar, abundant fossil fragments, serpentinite fragments, charcoal fragment, iron oxide and/or hydroxide. The probable sand provenance is from the Panaro River (Lugli et al. 2007). Pores are frequent and they show irregular shape (fig. 34B).

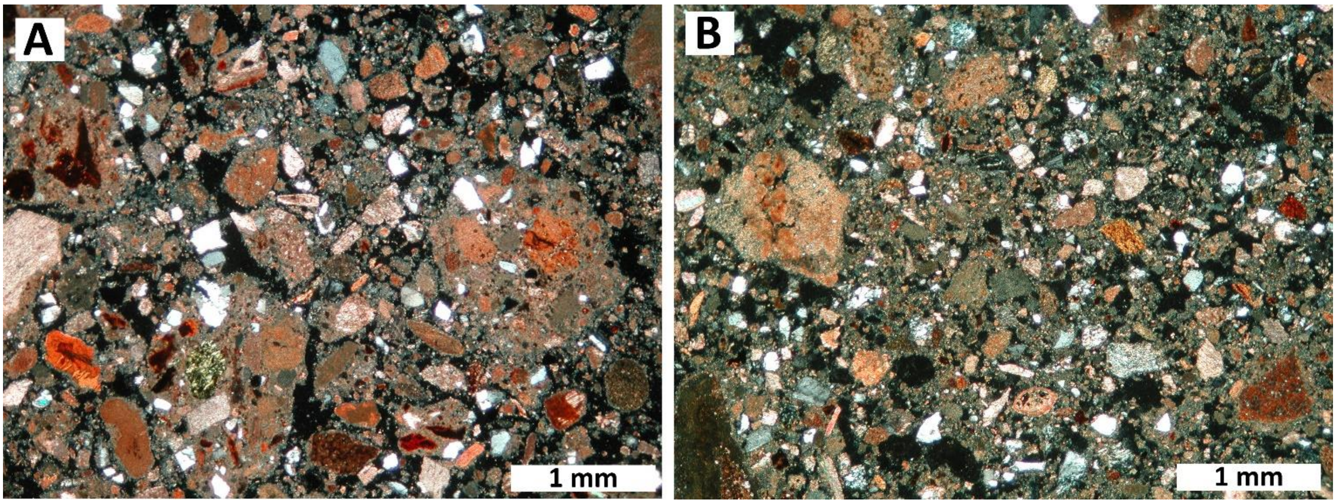

Fig. 34: A) photomicrograph in crossed polars of the mortar sample N2-2DM; B) photomicrograph in crossed polars of the mortar sample N2-2FM.

Northern vault N3

Sample N3-2AM

The sample N2-3AM is a lime-based mortar with frequent lime lumps with dimension up to 1 mm and devoid of underburned and overburned particles. The aggregate binder ratio is 2. The aggregate grain size is fine to coarse sand (0.2-0.9 mm) and well sorted. The sand composition is: quartz, feldspar, siltstone, micritic limestone and sparry calcite, fossil fragments, serpentinite fragments, iron oxide and/or hydroxide. The probable sand provenance is from the Secchia River (Lugli et al. 2007). Pores are frequent and they show irregular shape (fig. 35).

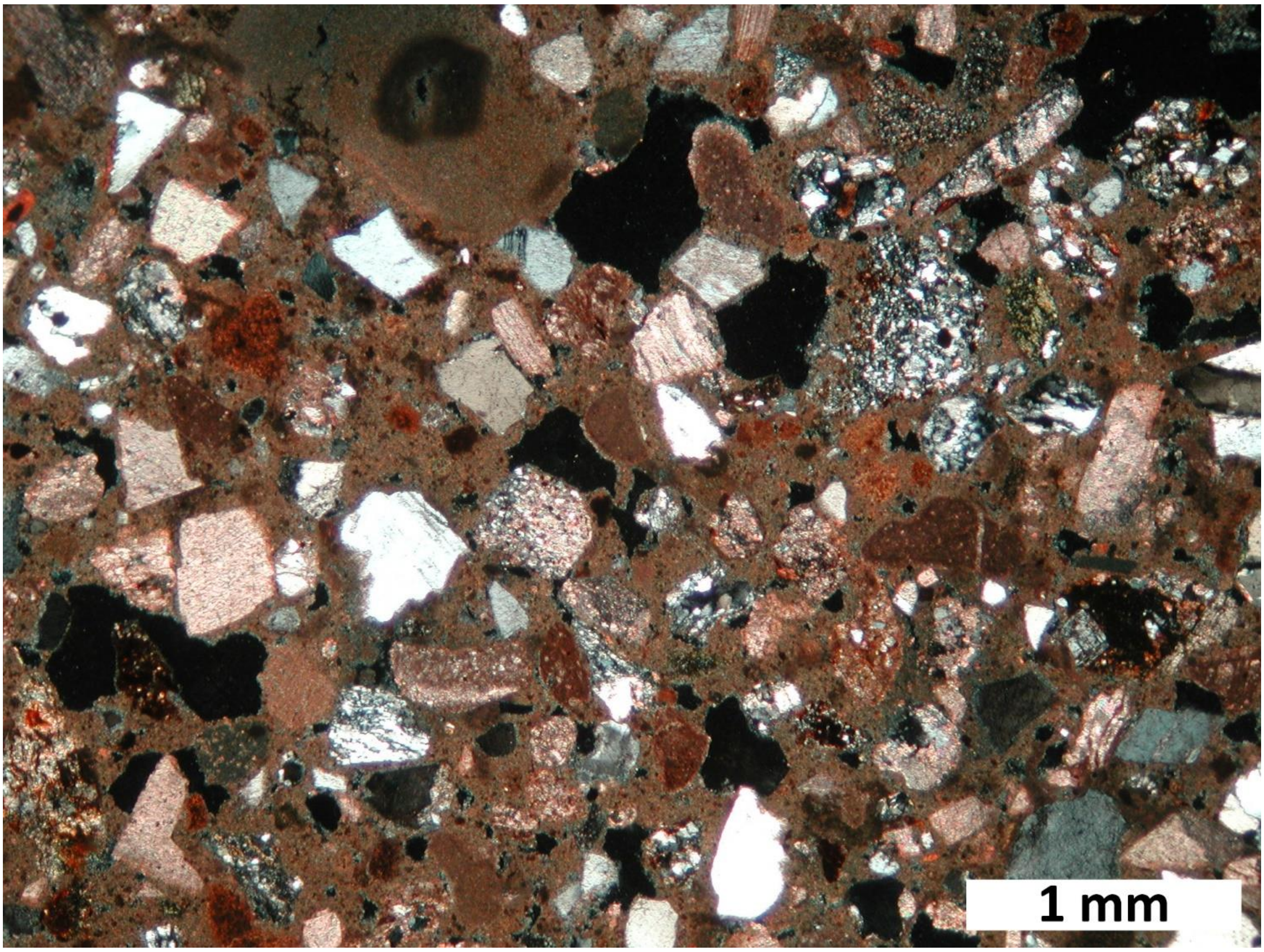

Fig. 35: photomicrograph in crossed polars of the mortar sample N3-2AM.

Northern vault N5

Sample N5-1M

The sample N5-1M is a lime-based mortar with underburned/overburned particles up to 4 mm in size. Lime lumps are frequent and reach dimensions up to 2 mm. The aggregate binder ratio is 2.1. The aggregate grain size is fine to medium sand (0.2-0.5 mm) and moderately sorted. The sand composition is: micritic limestone and sparry calcite, quartz, feldspar, fossil fragments, siltstone, argillite, serpentinite fragments, iron oxide and/or hydroxide. The probable sand provenance is from the Panaro River (Lugli et al. 2007). Pores are very frequent and they show round shape (fig. 36).

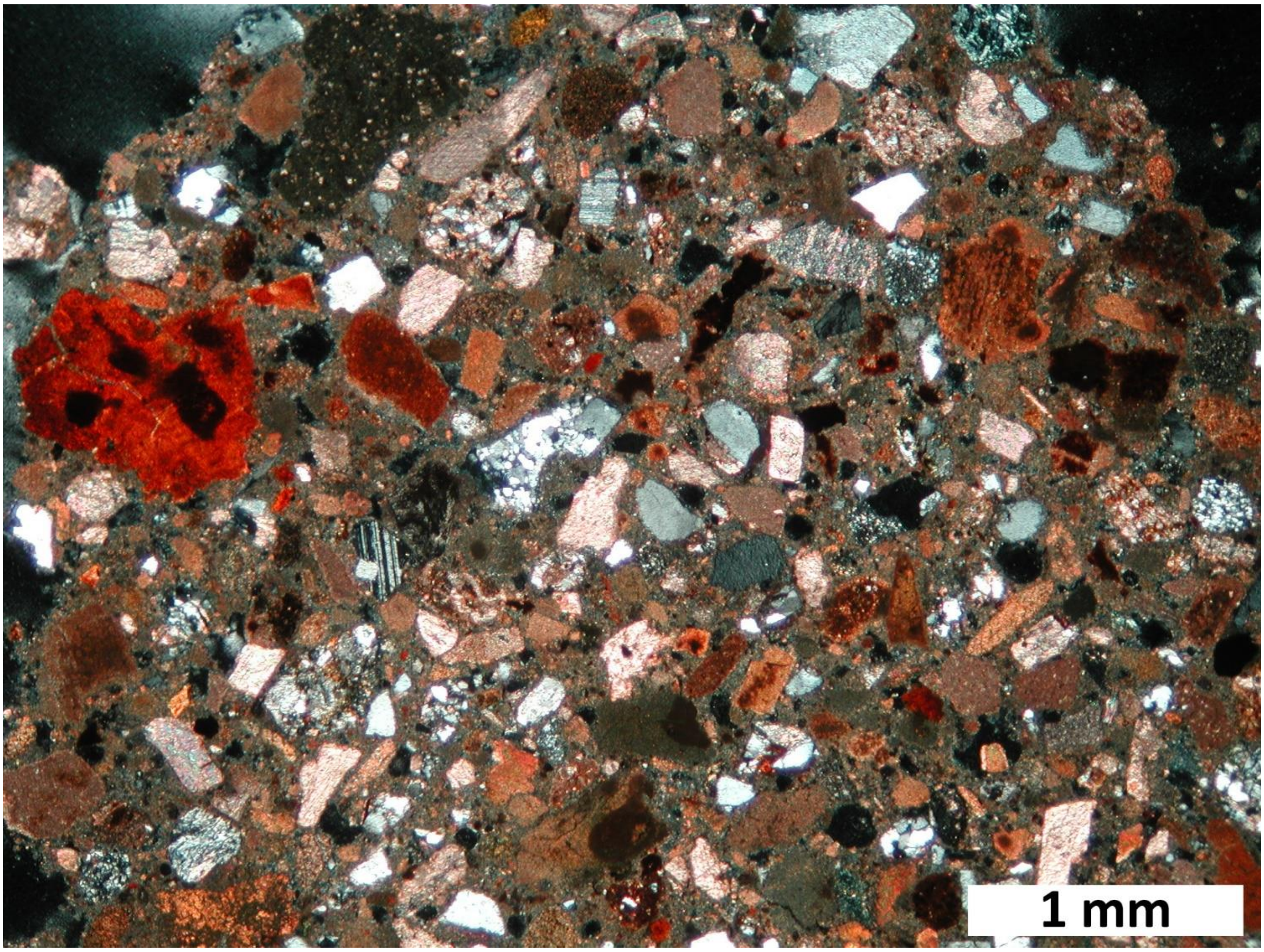

Fig. 36: photomicrograph in crossed polars of the mortar sample N5-1M.

Northern vault N7

Sample N7-3M

The sample N7-3M is a lime-based mortar with underburned/overburned particles up to 3 mm in size. Lime lumps are scarce and reach dimensions up to 1 mm. The aggregate binder ratio is 1.1. The aggregate grain size is very fine to fine sand (0.063-0.2 mm) and well sorted. The sand composition is: micritic limestone and sparry calcite, quartz, feldspar, fossil fragments, serpentinite fragments, glauconite, iron oxide and/or hydroxide. The probable sand provenance is from the Panaro River (Lugli et al. 2007). Pores are frequent and they show round and irregular shape (fig. 37).

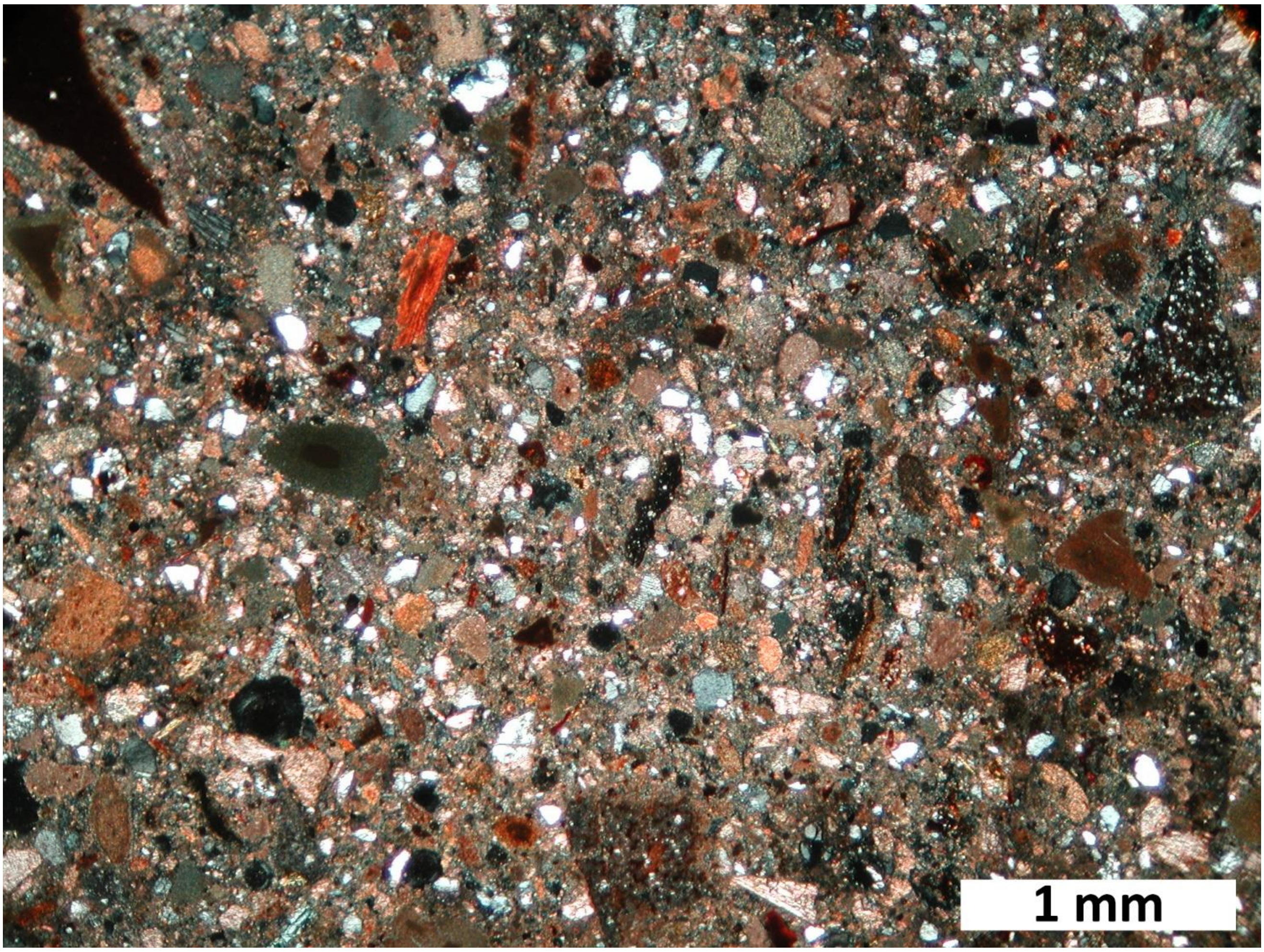

Fig. 37: photomicrograph in crossed polars of the mortar sample N7-3M.

Northern vault N8

Sample N8-1M

The sample N8-1M is a lime-based mortar with underburned/overburned particles up to 4 mm in size. Lime lumps are frequent and reach dimensions up to 1 mm. The aggregate binder ratio is 2.2. The aggregate grain size is fine to medium sand (0.2-0.5 mm) and moderately sorted. The sand composition is: micritic limestone and sparry calcite, quartz, feldspar, siltstone, fossil fragments, serpentinite fragments, glauconite, iron oxide and/or hydroxide The probable sand provenance is from the Panaro River (Lugli et al. 2007). Pores are scarce and they show irregular shape (fig. 38).

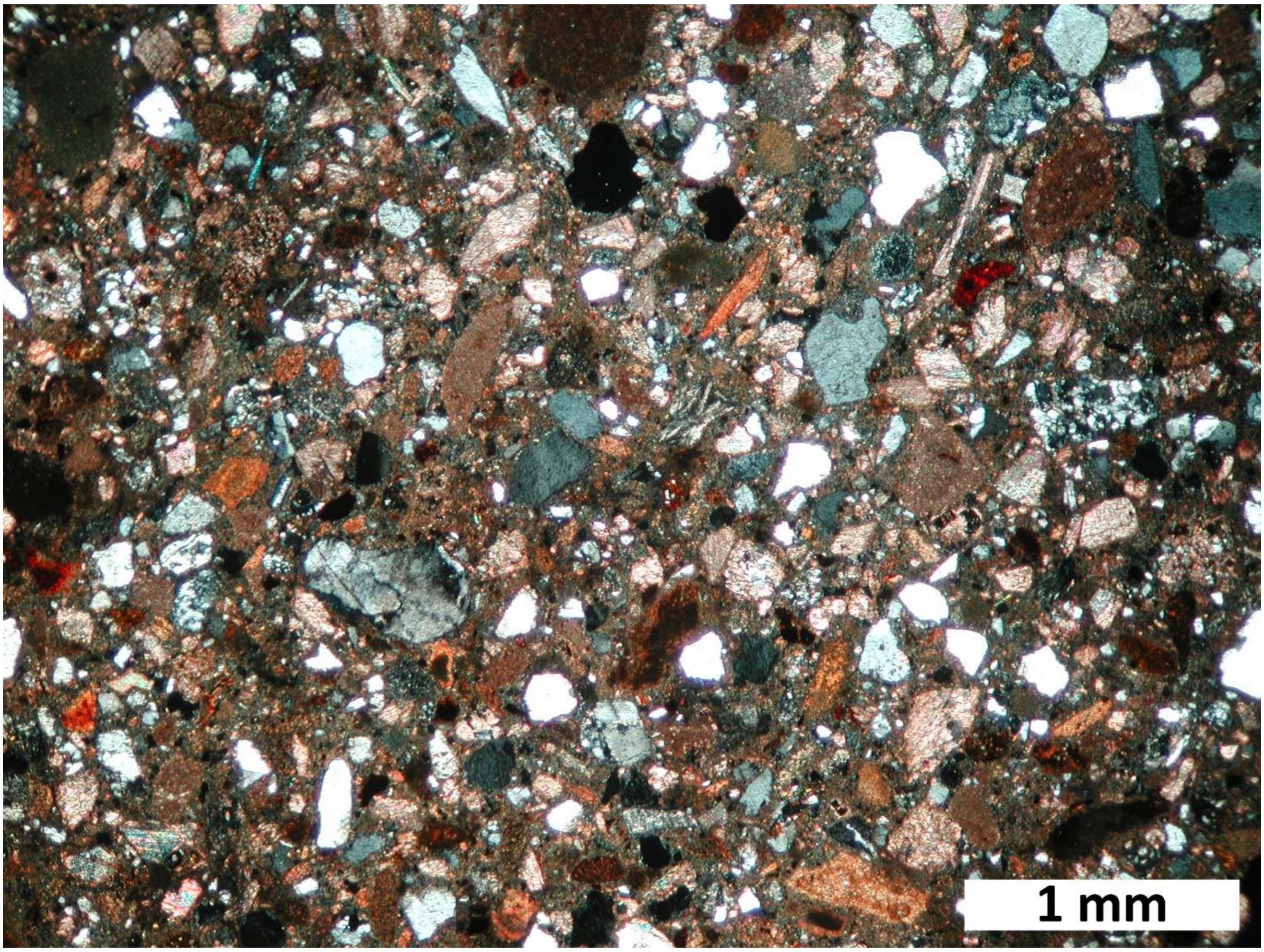

Fig. 38: photomicrograph in crossed polars of the mortar sample N8-1M.

Northern vault N9

Sample N9-3M

The sample N8-1M is a lime-based mortar with underburned/overburned particles up to 4 mm in size. Lime lumps are frequent and reach dimensions up to 3 mm. The aggregate binder ratio is 2.2. The aggregate grain size is fine to medium sand (0.2-0.5 mm) and moderately sorted. The sand composition is: micritic limestone and sparry calcite, quartz, feldspar, siltstone, fossil fragments, serpentinite fragments, biotite, iron oxide and/or hydroxide. The probable sand provenance is from the Panaro River (Lugli et al. 2007). Pores are frequent and they show irregular shape (fig. 39).

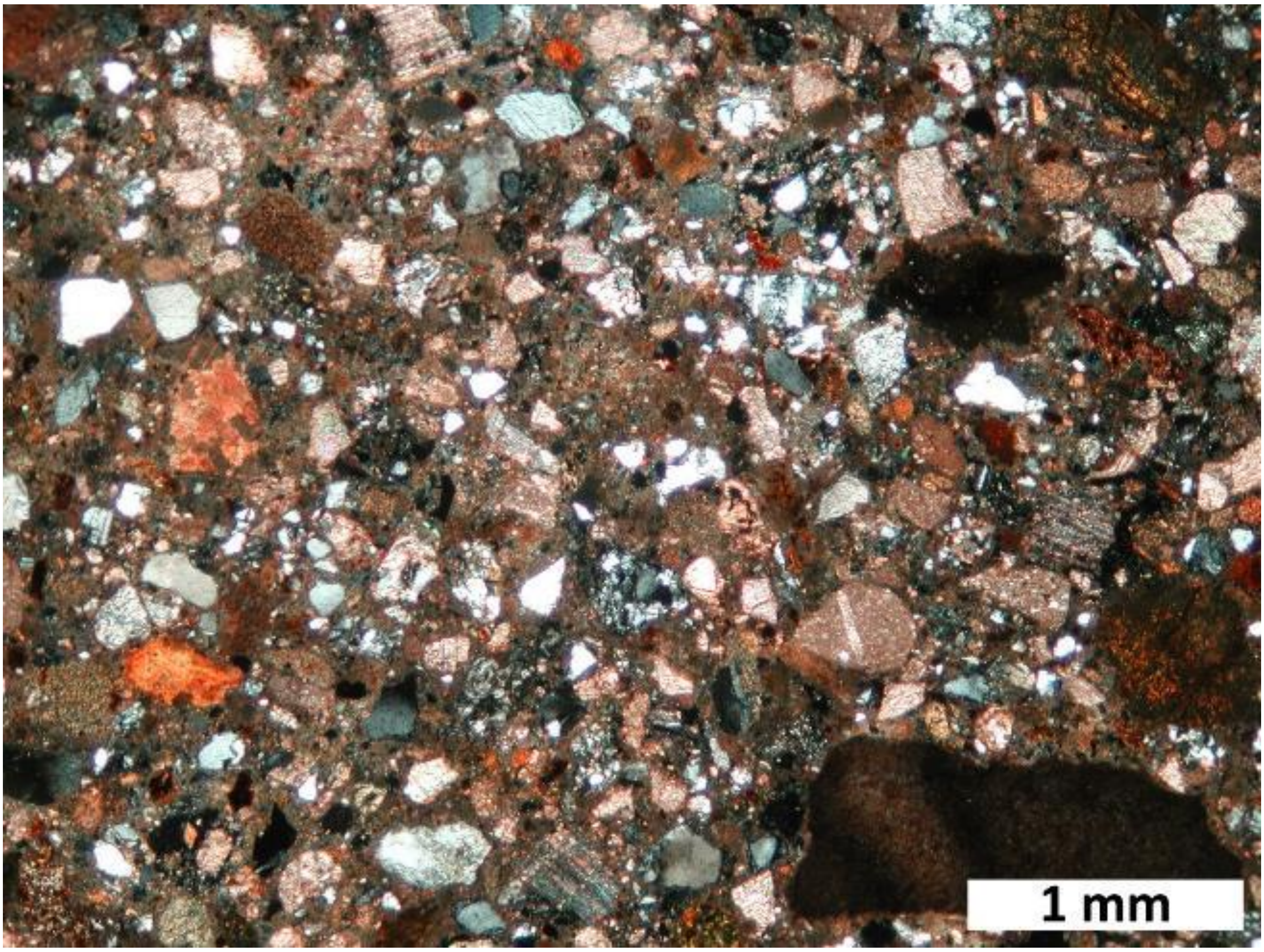

Fig. 39: photomicrograph in crossed polars of the mortar sample N9-3M.

Southern vault S1

Sample S1-1M

The sample S1-1M is a lime-based mortar with underburned/overburned particles up to 5 mm in size. Lime lumps are scarce and small (< 1 mm). The aggregate binder ratio is 1.5. The aggregate grain size is very fine to medium sand (0.1-0.4 mm) and poorly sorted. The sand composition is: micritic limestone and sparry calcite, quartz, feldspar, siltstone, fossil fragments, serpentinite fragments, biotite, iron oxide and/or hydroxide. The probable sand provenance is from the Panaro River (Lugli et al. 2007). Pores are frequent and they show irregular shape (fig. 40A).

Sample S1-2M

The sample S1-2M is a lime-based mortar with underburned/overburned particles up to 5 mm in size. Lime lumps are frequent and small (< 1 mm). The disintegration phenomena prejudice the correct evaluation of aggregate binder ratio. The aggregate grain size is very fine to medium sand (0.1-0.3 mm) and poorly sorted. The sand composition is: micritic limestone and sparry calcite, quartz, feldspar, siltstone, fossil fragments, serpentinite fragments, iron oxide and/or hydroxide. Straw fragments are also visible. The probable sand provenance is from the Panaro River (Lugli et al. 2007) (fig. 40B).

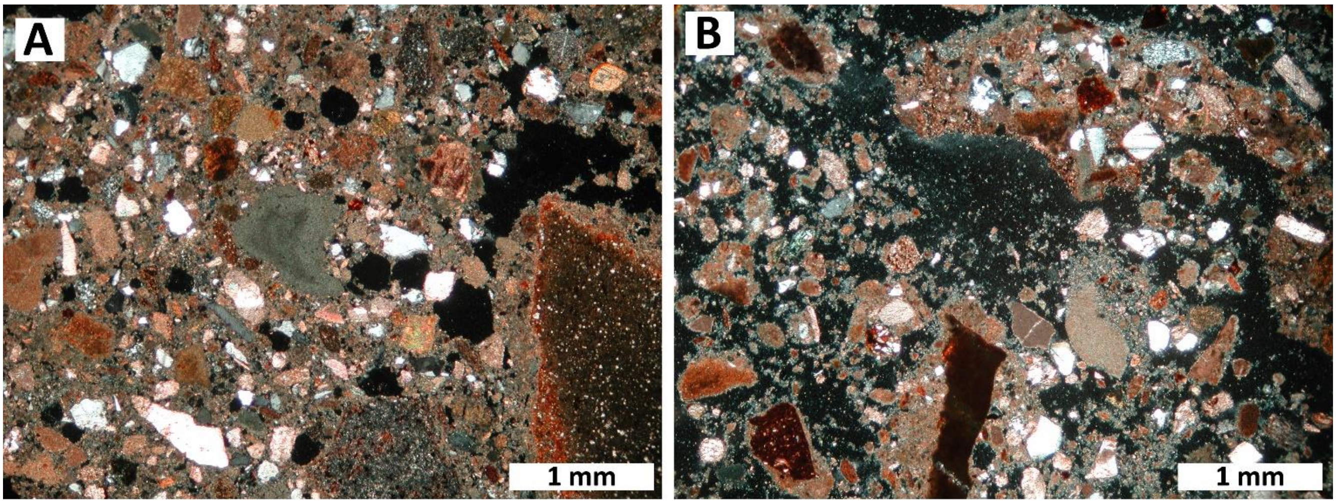

Fig. 40: A) photomicrograph in crossed polars of the mortar sample S1-1M; B) photomicrograph in crossed polars of the mortar sample S1-2M.

Southern vault S9

Sample S9-4M

The sample S9-4M is a lime-based mortar with underburned/overburned particles up to 3 mm in size. Lime lumps are scarce and small (< 1 mm). The aggregate binder ratio is 1.5. The aggregate grain size is very fine to medium sand (0.063-0.4 mm) and moderately sorted. The sand composition is: micritic limestone and sparry calcite, quartz, feldspar, fossil fragments, serpentinite fragments, glauconite, iron oxide and/or hydroxide. The probable sand provenance is from the Panaro River (Lugli et al. 2007). Pores are frequent and they show irregular shape (fig. 41).

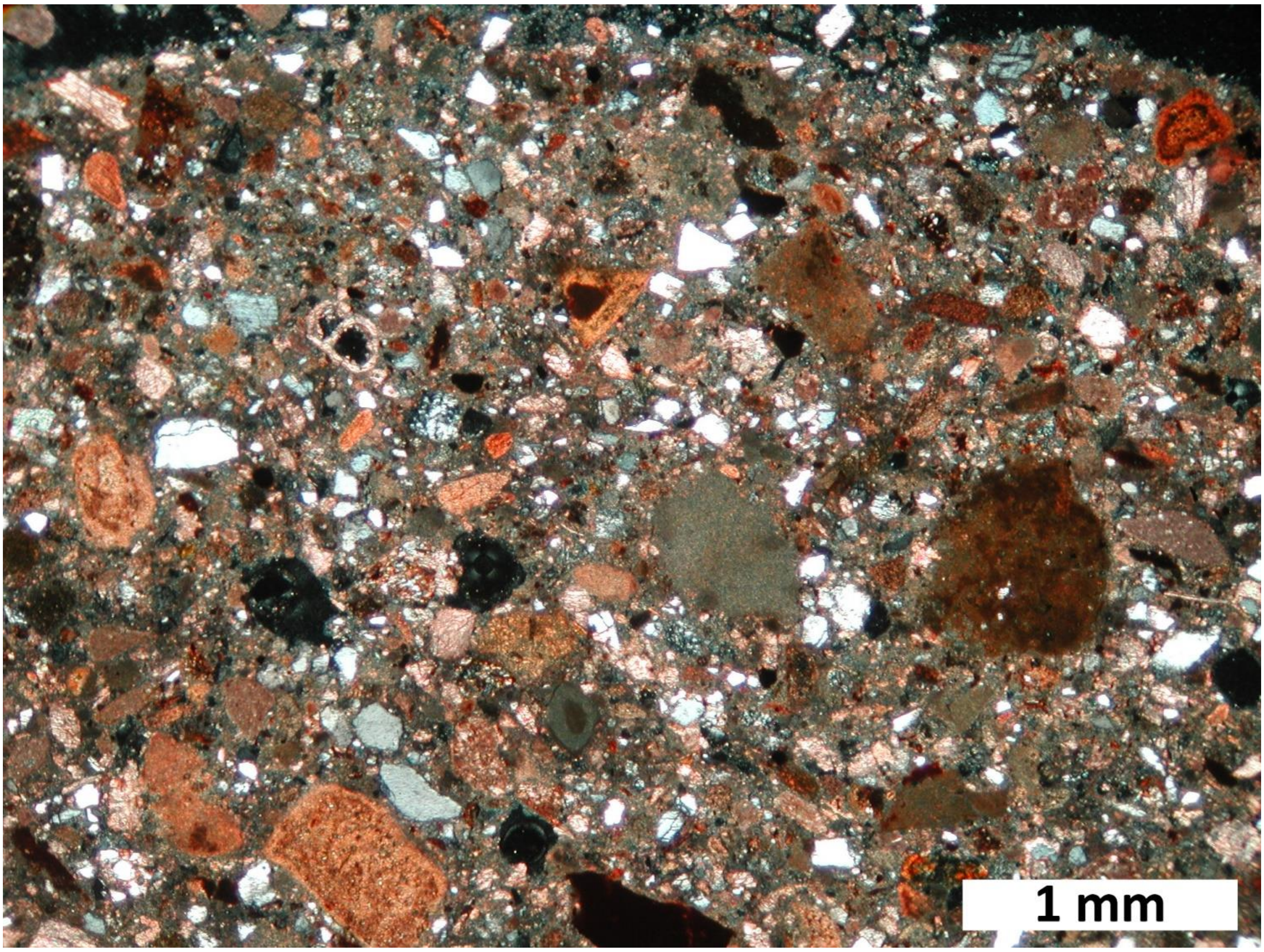

Fig. 41: photomicrograph in crossed polars of the mortar sample S9-4M.

The observation under the optical microscope of mortars thin sections allowed to recognize four groups of lime mortar. The parameters used for discerning different types are the grain size aggregate, the origin of the aggregate mixed with lime and the aggregate binder ratio.

- group 1: samples C2-3M, C2-3AM, C3-1M, C5-1M, C5-4M, C5-5M. All mortars show an aggregate binder ratio of 1.4 and a high presence of *cocciopesto* added to the sand aggregate. The sand provenance is probably from the Panaro River.

- group 2: samples C1-1M, N1-1M, N1-2M, N2-2DM, N2-2FM, S1-1M, S1-2M, S9-4M. All mortars show an aggregate binder ratio of 1.4 and a high presence of BRPs. The aggregate grain size is very fine to medium sand. The sand provenance is probably from the Panaro River. The sample N7-3M displays the same composition but different aggregate binder ratio (1.1) and aggregate grain size (very fine to fine).

- group 3: samples N5, 1M, N8-1M and N9-3M. The mortars show an aggregate binder ratio of 2.2 and frequent BRPs. The aggregate grain size is fine to medium sand. The sand provenance is assumed to be from the Panaro River.

- group 4: samples C4-1AM and N3-2AM. Both mortars present an aggregate binder ratio of 2, an aggregate well sorted and the absence of BRPs. These characteristic suggest an advanced knowledge of building material preparation and therefore a different stage, probably made by more specialized and skilled workers. These samples belong to the thin plaster layer that covered the bedding mortars and the bricks of the vaults. The aggregate is a fine-medium grained sand and the provenance is supposed from the Secchia River.

The sample C1-4AM has the same characteristics of the samples of the group 4 but the sand provenance is possibly from Panaro River.

Mortars belong the groups 1, 2 and 3 have the same aggregate composition but different grain size. This difference may be due to collection of sand in the Panaro River but in different sedimentary areas (meander bars, longitudinal bars or terraces). The particle size differentiation could therefore indicate a collection in different times: during the minimum flow of Panaro River it is possible to collect sand of larger particle size directly within the riverbed, while in other seasons the collection may be conducted only in unflooded areas that in some cases may yield different grain size sands.

The massive presence of underburned BRPs, especially in the mortar samples of the group 2, is due to uneven cooking processes. Clay-bearing limestone relicts identified in all samples are evidence of the burning of impure limestone (marly limestone) that could provide weakly hydraulic proprieties to the mortars, such as the presence of *cocciopesto* in the mortar samples of the group 1 (Binda and Baronio 1988 and successive).

Gypsum mortar

Petrographic investigation of gypsum mortar samples revealed that all samples analyzed display homogeneous composition. They are characterized by a binder of microcrystalline gypsum and by a scarce aggregate composed by selenite crystals, fragments of micritic carbonate rocks and argillite fragment which are impurity in the initial gypsum rock (fig. 42A, B, C and D). Black charcoal particles have been recognized among the aggregate, residue of the kiln fuel (fig. 42E). Anhydrite crystals are also present in two samples (C4-1M and S9-1M), evidence of high firing of gypsum (fig. 42F).

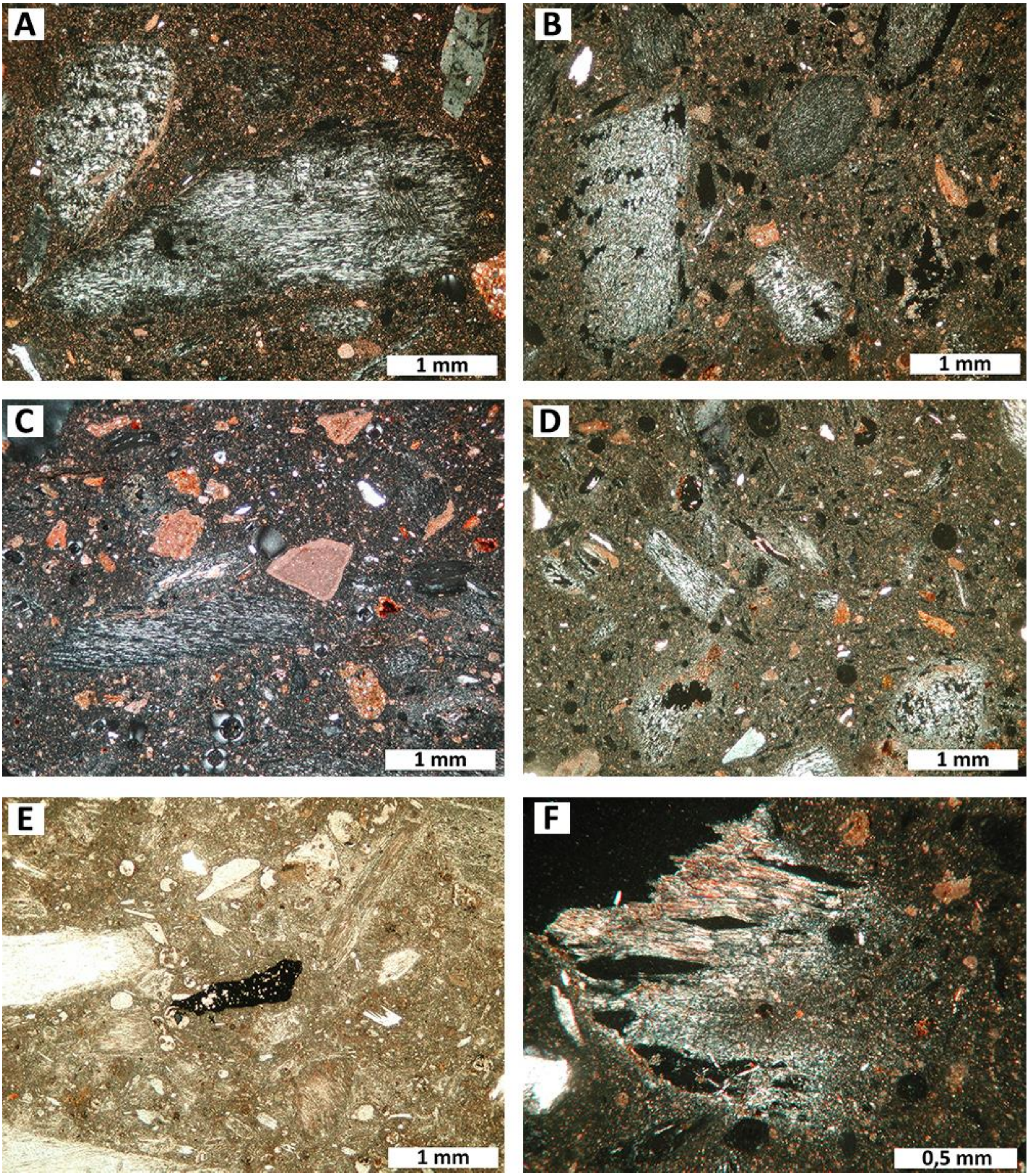

Fig. 42: photomicrograph of gypsum mortar thin sections: A) selenite crystals in the sample C1-5M, crossed polars; B) selenite crystals in the sample N3-3AM, crossed polars; C) selenite crystals, fragments of micritic carbonate rocks and argillite fragment in the sample S9-1M, crossed polars; D) selenite crystals, fragments of micritic carbonate rocks and argillite fragment in the sample N2-1AM, crossed polars; E) at the center of a black charcoal fragment in the sample C1-5M, natural light; F) anhydrite crystal in the sample S9-1M, crossed polars.

In detail, the samples C5-6M and C5-7M, respectively, gypsum mortar G1 and G2 detected on the central vaults C4 and C5, have the same composition (fig. 43A and B) but different aggregate grain size and porosity. The sample G1 present selenite crystal measuring up to 2,5 mm and higher porosity with large rounded pores (fig. 43C and D). This sample also present a selenite crystal with peloids (fig. 43E). An anhydrite crystal in instead identified in the sample C5-7M (fig. 43F).

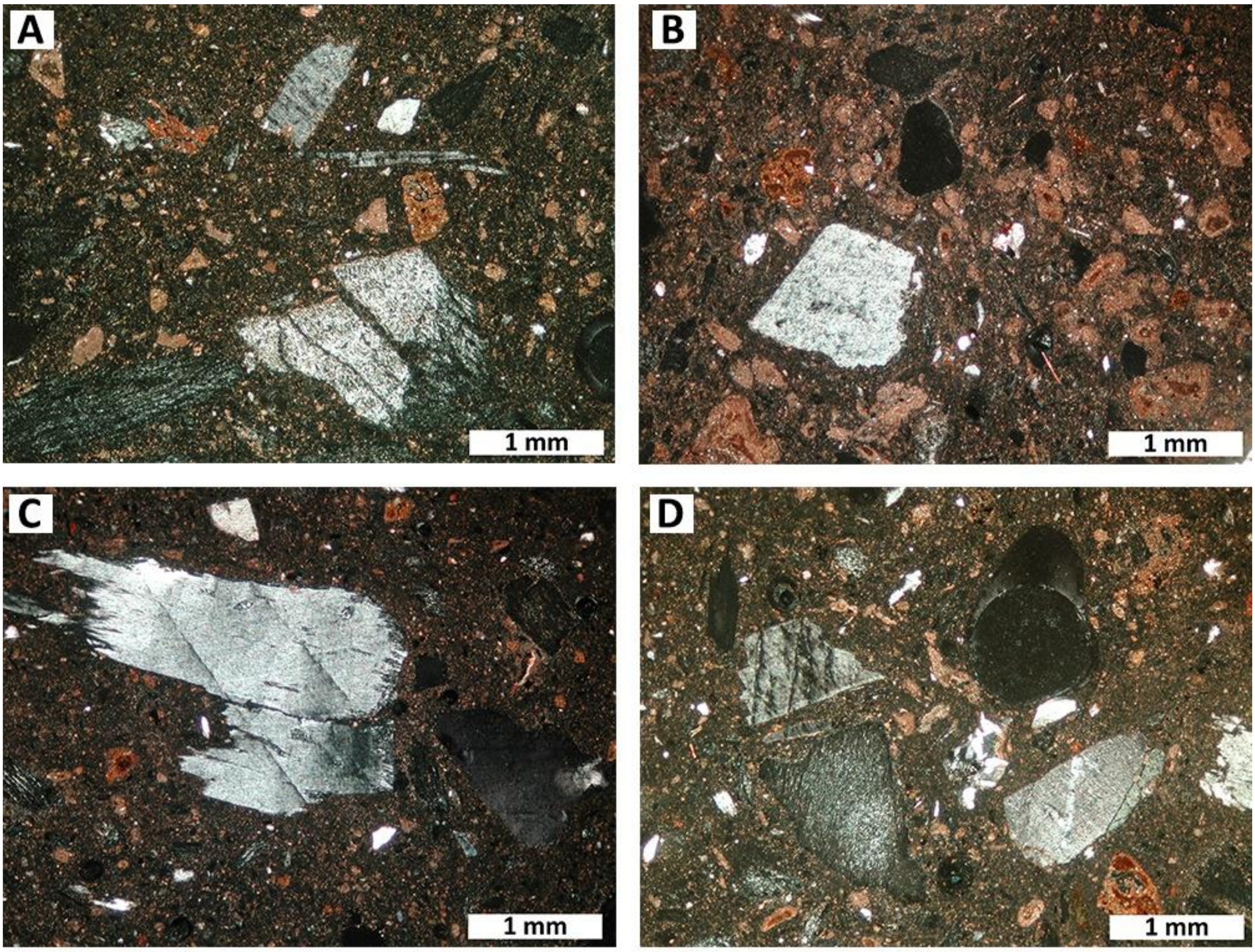

Fig. 43: photomicrograph in crossed polars of the gypsum mortar thin sections C5-6M and C5-7M. A) gypsum mortar sample C5-6M (G1) characterized by selenite crystals, fragments of micritic carbonate rocks and argillite fragments; B) gypsum mortar sample C5-7M (G2) characterized by selenite crystals, fragments of micritic carbonate rocks and argillite fragments; C) gypsum mortar sample C5-6M (G1): at the center selenite crystals; D) gypsum mortar sample C5-6M (G1): large rounded pores.

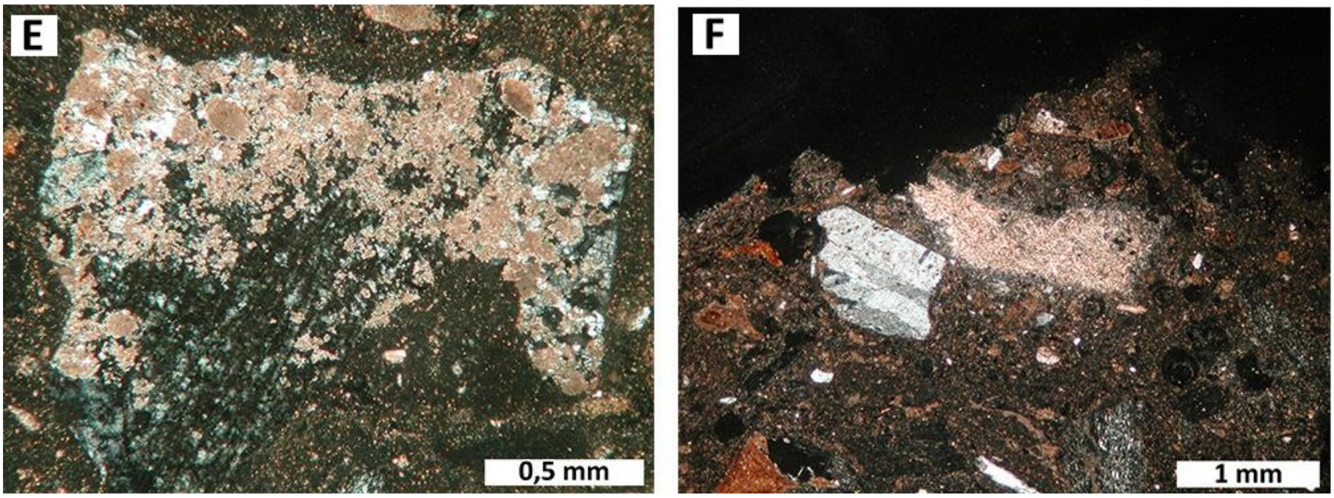

Fig. 43: E) photomicrograph in crossed polars of gypsum mortar sample C5-6M (G1): selenite crystal with peloids; F) photomicrograph in crossed polars of gypsum mortar sample C5-7M (G2): anhydrite crystal at the right side of the image.

6.2. Results of AMS Radiocarbon dating

The petrographic analysis revealed some potential problems for the ^{14}C dating. Firstly, the aggregate is rich in fine limestone clasts and this may be a problem in the case of Cryo2Sonic preparation. According to Nonni (2014) a mortar with a calcareous aggregate can be dated using Cryo2Sonic pre-treatment only if the size of aggregate grain is coarse and hard. The fine size grains should be avoided because the size is similar to the one of binder particles and they may contribute with geological carbon yielding a ^{14}C age that is older than the true age. Secondly, the samples are in general full of BRPs. However, incomplete calcination is generally not a problem since these contaminants usually dissolve slowly and they do not go in suspension with the Cryo2Sonic preparation (Marzaioli, 2011) and in the case of sequential dissolution procedure the effect of the contaminants can be detected in the ^{14}C profile**.** Thirdly, the samples could be slightly hydraulic. It is known that hydraulic mortars are less permeable to atmospheric CO_2, that they contain less dateable carbonate, and that they are constantly active chemically and can generate carbonates whenever they are disturbed (Lindroos et al. 2011; Ringbom et al. 2011, 2014).

6.2.1. Results of Cryo2Sonic procedure (University of Campania "Luigi Vanvitelli")

Results of radiocarbon dating by Cryo2Sonic procedure carried out at the University of Campania "Luigi Vanvitelli" laboratory are listed in table 6.

Sample	Building age	^{14}C age (BP)	Calibrated age 2σ	Notes
C3-1M bulk	1446-1447?	740 ± 55	1168-1315 (86.7%) 1356-1389 (8.7%)	the date is NOT in agreement with building age
C3-1M pure lump		800 ± 48	1058-1074 (1.3%) 1154-1286 (94.1%)	the date is NOT in agreement with building age
C5-4M bulk	1447?-1453	940 ± 70	982 – 1246 (95.4%)	the date is NOT in agreement with building age
N8-1M susp_lump	1433-1454	720 ± 80	1155 – 1413 (95.4%)	the date is NOT in agreement with building age
N9-3M bulk	1433-1454	1130 ± 70	711-745 (3.6%) 764– 1025 (91.8%)	the date is NOT in agreement with building age
N9-3M susp_lump		657 ± 54	1269-1405 (95.4%)	the date is NOT in agreement with building age
S9-4M pure lump	1404-1433	550 ± 90	1267 – 1514 (94.2%) 1600-1617 (1.2%)	the date is in AGREEMENT with building age/ later repair after earthquake 1474, 1501, 1505, 1584 or 1586

Tab.6: results of radiocarbon dating by Cryo2Sonic procedure.

As shown in figure 44, the calibrated results do not coincide with the building age of the vaults (1404-1454), except for the sample S9-4M.

The ^{14}C age of the sample C3-1M_bulk (740 ± 55 BP) corresponds with a calibrated calendar age 1168-1315 (86.7%) and 1356-1389 (8.7%) AD, older than expected age for the original construction (1446-1447?). In order to verify the result obtained by the bulk sample, the hydrolysis of the pure lime lump has been performed, but also in this case, the calibrated age, 1058-1074 (1.3%) and 1154-1286 (94.1%) AD, does not overlap with the expected age.

The measurement of the sample C5-4M_bulk has revealed ^{14}C ages of 940 ± 70 BP corresponding with a calibrated calendar age of 982-1246 AD (95.4%), older than expected age for the original construction (1447?-1453).

The radiocarbon age of the sample N8-1M susp_lump is 720 ± 80 BP, calibrated 1155-1413 AD (95.4%), is not in agreement with the expected building age (1433-1454).

The ^{14}C age of the sample N9-3M_bulk (1130 ± 70 BP) corresponds with a calibrated calendar age 711-745 (3.6%) and 764-1025 (91.8%) AD. Given the incorrect result, the radiocarbon dating was performed on susp_lump sample. The measurements revealed ^{14}C ages of 657 ± 54 BP corresponding with a calibrated calendar age of 1269-1405 AD (95.4%), that do not coincide with the expected age for the original construction (1433-1454).

The measured radiocarbon age on S9-4M_pure lump (550 ± 90 BP) gave a calendar age of 1267 - 1514 (94.2%) and 1600-1617 (1.2%) AD, that coincides with the estimate building age of the vault S9 (1404-1433). However, the calibrated age overlaps also with several earthquakes (1474, 1501, 1505, 1584 or 1586) that occur after the vaults construction, deduced from the historic earthquakes catalogue (see tab. 1). This result therefore suggests that the portion dated could be also a later repair carried out after damaging seismic evets.

The sample N3-2AM has not been dated because the pressure released during the acid digestion was not enough for AMS dating.

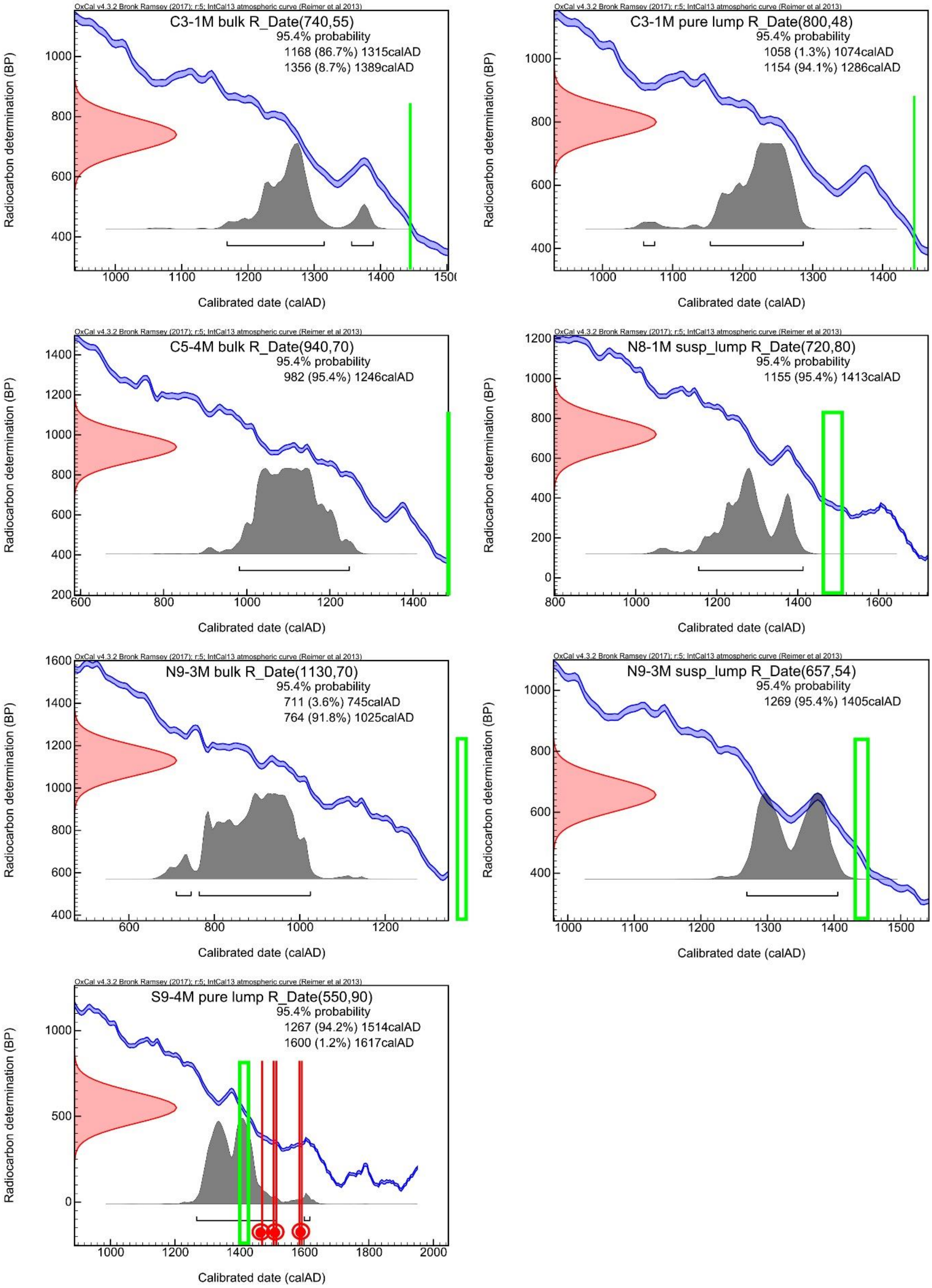

Fig. 44: calibrated results of the samples prepared using Cryo2Sonic procedure. The building age of each vault is marked as green rectangles or lines. The earthquakes, that overlap with the date of the sample S9-4M, are marked as red vertical lines.

6.2.2. Results of sequential dissolution (Abo Akademi University, Turku)

The alkalinity test using phenolphthalein dissolved in alcohol, performed on the coarser grain size fraction (300-500 µm), revealed that all the samples result with a low alkalinity and therefore suitable to be dated (see fig. 23).

CL inspection has been performed on the selected grain size fraction (46-75 µm) after sieving and on the same powder after sequential dissolution. The aim was to determine if there were any contaminants sources within the powder and whether they were dissolved during the hydrolysis. This consideration can be used to interpret the dating results. Sample powders before and after acid dissolution were spread over a glass backing glued with a polysaccharide and analyzed.

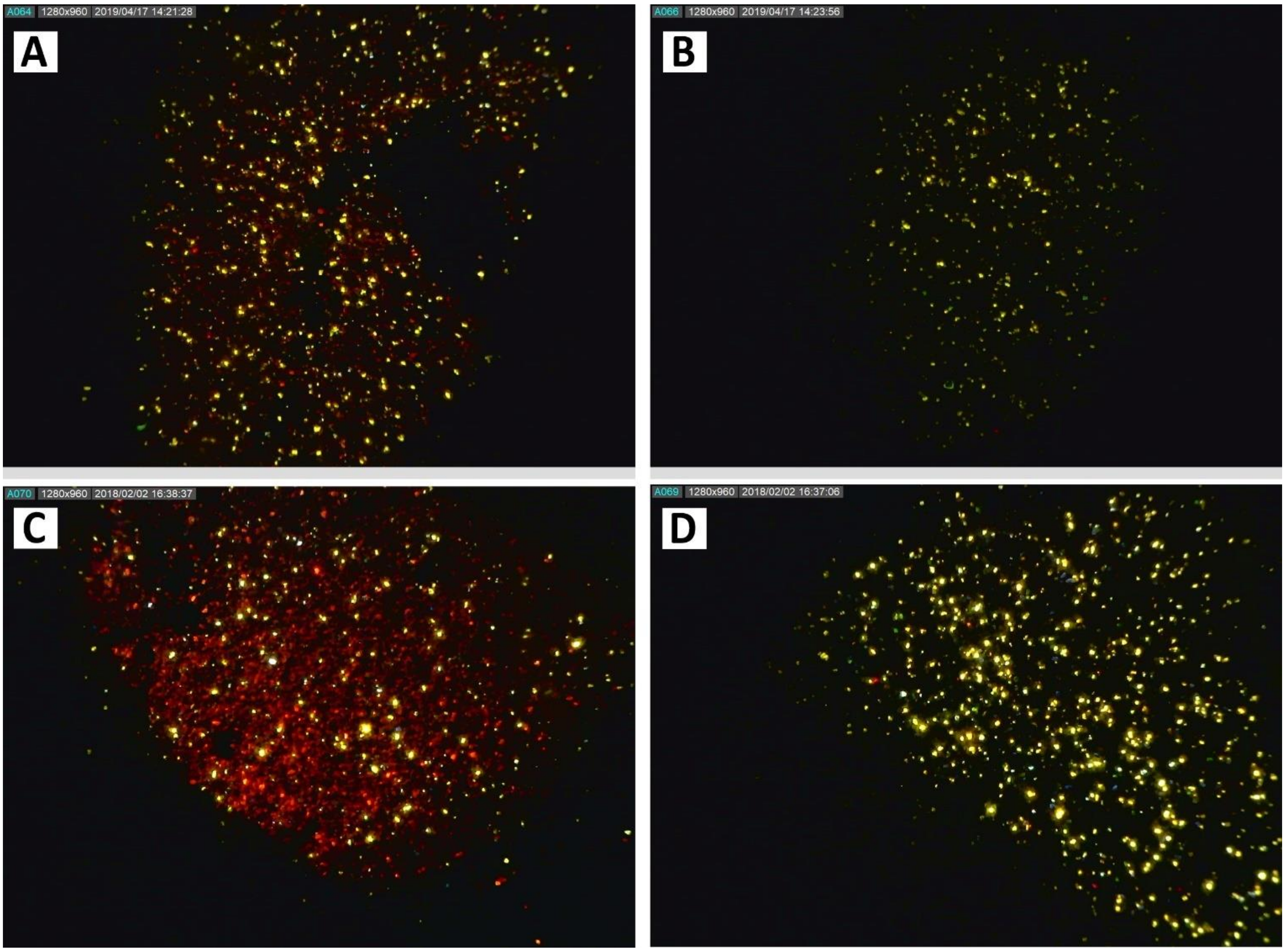

Fig. 45: CL micrograph of the sample C2-3M and C1-1M thin sections. The binder to be dated appears as tile red-brown, orange grains are limestone, blue grains are quartz aggregates and green are feldspars. A) and C) powder of the samples before dissolution. They contain carbonate contaminants and part of silicic aggregates; B) and D) powder of the samples. after dissolution. It is only visible the aggregate composed by quartz and feldspars.

Figure 45 shows CL micrographs of the sample C1-1M and C2-3M thin sections. The powder before dissolution contains carbonate contaminants and part of silicic aggregates. After the dissolution, it is only visible the aggregate while the binder and the carbonate contaminants were dissolved.

Results of radiocarbon dating by sequential dissolution procedure are reported in tables 7 and 8. Figure 46 shows the ^{14}C profiles and the calibrated results.

Sample subsample / CO_2-fraction	**Material**	**Grain size** (µm)	**Reaction time** (s) from t_0	**Carbon yield (tot)** (%)	**Fraction size** (relative 1)	**C-14 age** (BP)	**±**	**δ13C ‰** VPDB	**Laboratory** nr
C1-1M.1.1	Bulk mortar	46-75	6	3.40% C	0-0.09	590	24	-28,2	ETH-86835
C1-1M.1.2			17		0.09-0.24	816	23	-13,3	ETH-86829
C1-1M.1.3			110		0.24-0.45	2876	23	2,6	ETH-86830
C2-3M.1.1	Bulk mortar	46-75	7	5,69%C	0-0.10	516	34	-20,1	ETH-96989
C2-3M.1.2			17		0.10-0.25	471	32	-8,8	ETH-96990
C2-3M.1.3			70		0.25-0.41	589	31	-6,4	ETH-96991
C3-1MLi1.1	Lime lump	Crushed	15	8.27 % C	0-0.20	268	52	n.r.	AAR-25640.1
C3-1MLi1.2			21		0.20-0.44	147	51	n.r.	AAR-25640.2
C3-1M.1.1	Bulk mortar	46-75	6	2.53% C	0-0.12	593	27	-20,3	ETH-86836
C3-1M.1.2			30		0.12-0.37	645	23	-16,2	ETH-86932
C3-1M.1.3			120		0.37-0.62	1601	23	-8	ETH-86933
C3-1M.2.1	Bulk mortar	46-75	14	2.44% C	0-0.08	506	26	-23,8	ETH-86837
C5-4M.1.1	Bulk mortar	46-75	6	5.36 % C	0-0.09	125	75	n.r.	ARR-25642.1
C5-4M.1.2			24		0.09-0.26	592	37	n.r.	ARR-25642.2
C5-4M.1.3			90		0.26-0.41	924	89	n.r.	ARR-25642.3
C5-5M.1.1	Bulk mortar	46-75	5	6,08%C	0-0.10	508	34	-19,8	ETH-96986
C5-5M.1.2			22		0.10-0.25	562	32	-10,3	ETH-96987
C5-5M.1.3			60		0.25-0.40	879	32	-8,6	ETH-96988
N8-1MLi.1.1	Lime lump	Crushed	10	3.05 % C	0-0.27	291	56	n.r.	AAR-25839.1
N8-1MLi.1.2			24		0.27-0.52	223	66	n.r.	AAR-25639.2
N9-3M.1.1	Bulk mortar	46-75	7	4.48 % C	0-0.04	534	35	n.r.	AAR-25638.2
N9-3M.1.2			24		0.04-0.56	829	44	n.r.	AAR-25638.3
N9-3M.1.3			75		0.56-0.72	1773	35	n.r.	AAR-25638.1
S9-4M.2.1	Bulk mortar	46-75	20	3.35 % C	0-0.16	394	67	n.r.	ARR-25641.1
S9-4M.2.2			100		0.16-0.37	1794	94	n.r.	ARR-25641.2
S9-4M.2.3			395		0.37-0.57	4715	71	n.r.	ARR-25641.3
S9-4M.3.1	Bulk mortar	46-75	13	2.62 % C	0-0.17	523	23	-17,4	ETH-83816
S9-4M.3.2			35		0.17-0.36	1207	24	-6,4	ETH-83817

carbon yield (tot) (%) = total carbon yield after about one hour of dissolution
n.r. = not reported
AAR = Aarhus AMS lab; ETH = ETH Zurich

Tab. 7: Hydrolysis data, ^{14}C results and $d^{13}C$ values for the dated samples.

Sample	Building age	^{14}C age (BP)	Calibrated age 2σ	Notes
C1-1M.1.1	1404-1415	590 ± 24	1302-1368 (69.2%) 1382-1411 (26.2%)	the date of the fraction 1 is in **AGREEMENT** with building age
C1-1M.1.2		816 ± 23	1170-1174 (1.3%) 1180-1265 (94.1%)	
C1-1M.1.3		2876 ± 23	1124-976 BC (95.4%)	
C2-3M.1.1	1443-1445	516 ± 34	1321-1348 (12.4%) 1392-1446 (83.0%)	the date of the combined calibration of fractions 1 and 2 is in **AGREEMENT** with building age
C2-3M.1.2		471 ± 32	1407-1462 (95.4%)	
C2-3M.1.3		589 ± 31	1299-1370 (67.4%) 1380-1414 (28.0%)	
C2-3M combine		492 ± 24	1409-1445 (95.4%)	
C3-1MLi.1.1	1446-1447?	268 ± 52	1469-1683 (78.5%) 1737-1805 (13.3%) > 1936 (3.6%)	**incorrect result**. Fraction 1 is older than fraction 2
C3-1MLi.1.2		147 ± 51	1665-1785 (43.6%) 1793-1895 (34.3%) > 1904 (17.5%)	
C3-1M.1.1	1446-1447?	593 ± 27	1299-1370 (69.7%) 1380-1411 (25.7%)	the date of the fraction 1 is in **AGREEMENT** with building age
C3-1M.1.2		645 ± 23	1285-1321 (40.8%) 1349-1392 (54.6%)	
C3-1M.1.3		1601 ± 23	404-477 (47.3%) 482-536 (48.1%)	
C3-1M.2.1		506 ± 26	1399-1445 (94.5%)	
C5-4M.1.1	1447?-1453	125 ± 75	> 1665 (95.4%)	**incorrect result**. Convex ^{14}C profile and the date of the fraction 1 is YOUNGER than building age
C5-4M.1.2		592 ± 37	1296-1415 (95.4%)	
C5-4M.1.3		924 ± 89	909-912 (0.2%) 969-1271 (95.2%)	
C5-5M.1.1	1447?-1453	508 ± 34	1325-1345 (7.4%) 1393-1449 (88.0%)	the date of the fraction 1 is in **AGREEMENT** with building age
C5-5M.1.2		562 ± 32	1305-1365 (52.1%) 1384-1429 (43.3%)	
C5-5M.1.3		879 ± 32	1040-1110 (27.7%) 1115-1224 (67.7%)	
C5-5M combine		537 ± 24	1320-1350 (20.3%) 1391-1435 (75.1%)	
N8-1M.Li.1.1	1433-1454	291 ± 56	1452-1676 (89.3%) 1768-1771 (0.2%) 1777-1800 (4.4%) > 1941 (1.5%)	the date of the combined calibration of fractions 1 and 2 is **YOUNGER** than building age. **LATER REPAIR** after eathquake: 1474, 1501, 1505, 1584, 1586, 1660, 1671
N8-1M.Li.1.2		223 ± 66	1495-1601 (15.6%) 1616-1710 (26.3%) 1717-1891 (41.0%) > 1909 (12.6%)	
N8-1MLi.combine		263 ± 43	1487-1681 (79.2%) 1739-1743 (0.4%) 1763-1802 (12.4%) > 1938 (3.5%)	

N9-3M.1.1	1433-1454	534 ± 35	1315-1356 (28.1%) 1388-1441 (67.3%)	the date of the fraction 1 is in **AGREEMENT** with building age
N9-3M.1.2		829 ± 44	1050-1083 (5.7%) 1126-1136 (1.2%) 1151-1276 (88.5%)	
N9-3M.1.3		1773 ± 35	135-345 (95.4%)	
S9-4M.2.1	1404-1433	394 ± 67	1424-1643 (95.4%)	poor precision in the Aarhus AMS data
S9-4M.2.2		1749 ± 94	6-426 (95.4%)	
S9-4M.2.3		4715 ± 71	3638-3368 BP (95.4%)	
S9-4M.3.1	1404-1433	523 ± 23	1328-1341 (5.2%) 1396-1439 (90.2%)	the date of the fraction 1 is in **AGREEMENT** with building age
S9-4M.3.2		1207 ± 24	722-740 (5.3%) 766-889 (90.1%)	

Tab. 8: ^{14}C results in comparison with the building ages.

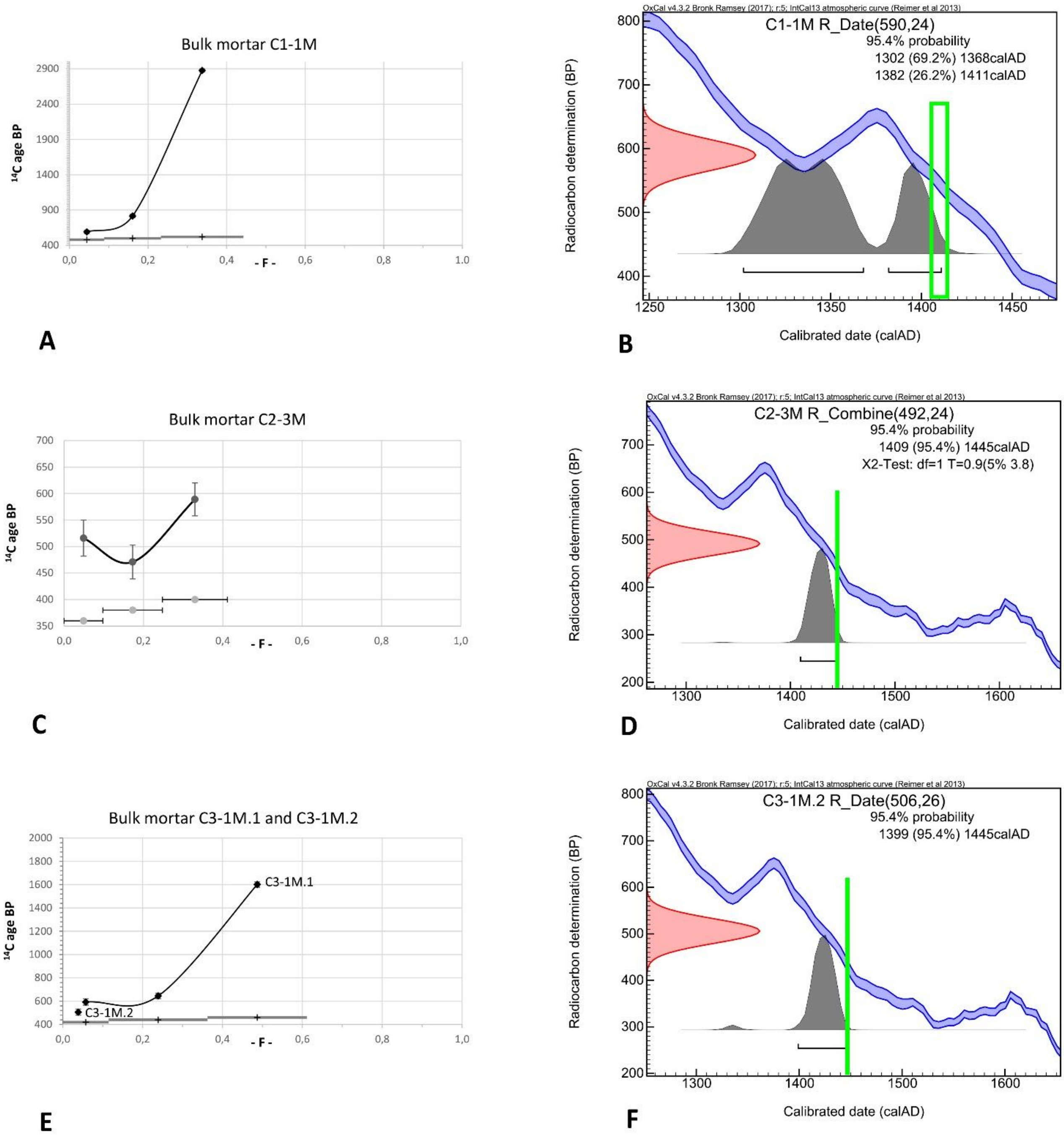

Fig.46: A) ^{14}C age profile of the sample C1-1M; B) calibrated result of the bulk mortar C1-1M, 1302-1368 (69.2 %) and 1382-1411 (26.2 %) AD. The date coincides with the expected age span (1404-1415) marked as a green rectangle; C) ^{14}C age profile of sample C2-3M; D) calibrated result of the bulk mortar C2-3M, 1409-1445 AD (95.4%). The date coincides with the expected age span (1443-1445) marked as a green line; E) ^{14}C age profile of the sample C3-1M; F) calibrated result of the bulk mortar C3-1M.2, 1399-1445 AD (94.5%). The date coincides with the expected age span (1446-1447?) marked as a green line.

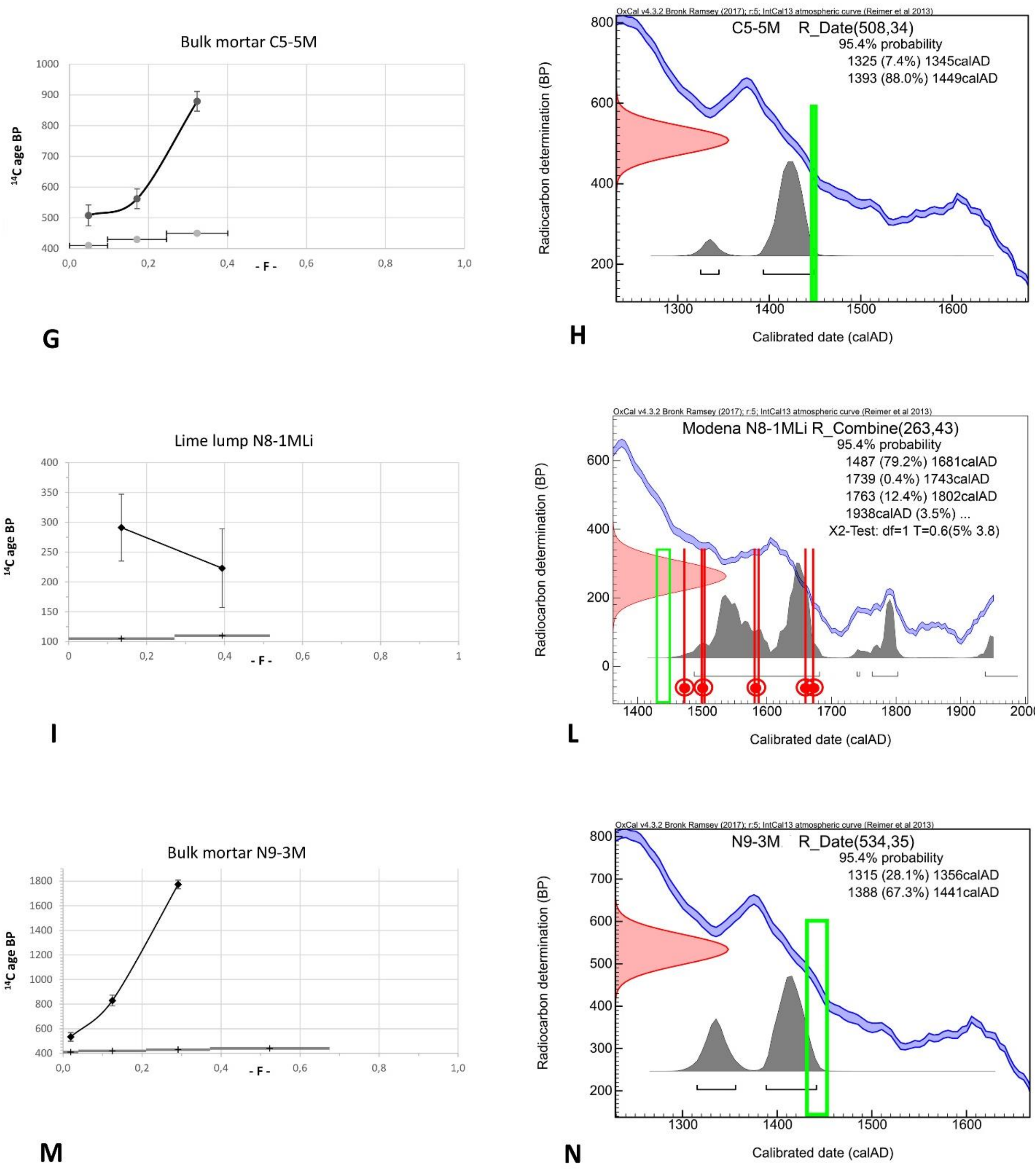

Fig.46: G) ^{14}C age profile of the sample C5-5M; H) calibrated result of the bulk mortar C5-5M, 1325-1345 (7.4%) and 1393-1449 (88.0%) AD. The date coincides with the expected age span (1447?-1453) marked as a green rectangle; I) ^{14}C age profile of the sample N8-1M; L) calibrated result of the lime lump N8-1MLi, 1487-1681 (79.2%), 1739-1743 (0.4%), 1763-1802 (12.4%), >1938 (3.5%) AD. The dates are younger than the expected construction age (1433-1454) marked as a green rectangle. Several earthquakes, marked as red vertical lines, overlap with the ^{14}C age, indicating later repair after significant seismic damage; M) ^{14}C age profile of sample N9-3M; N) calibrated result of the bulk mortar N9-3M, 1315-1356 (28.1%) and 1388-1441 (67.3%) AD. The date coincides with the expected age span (1433-1454) marked as a green rectangle.

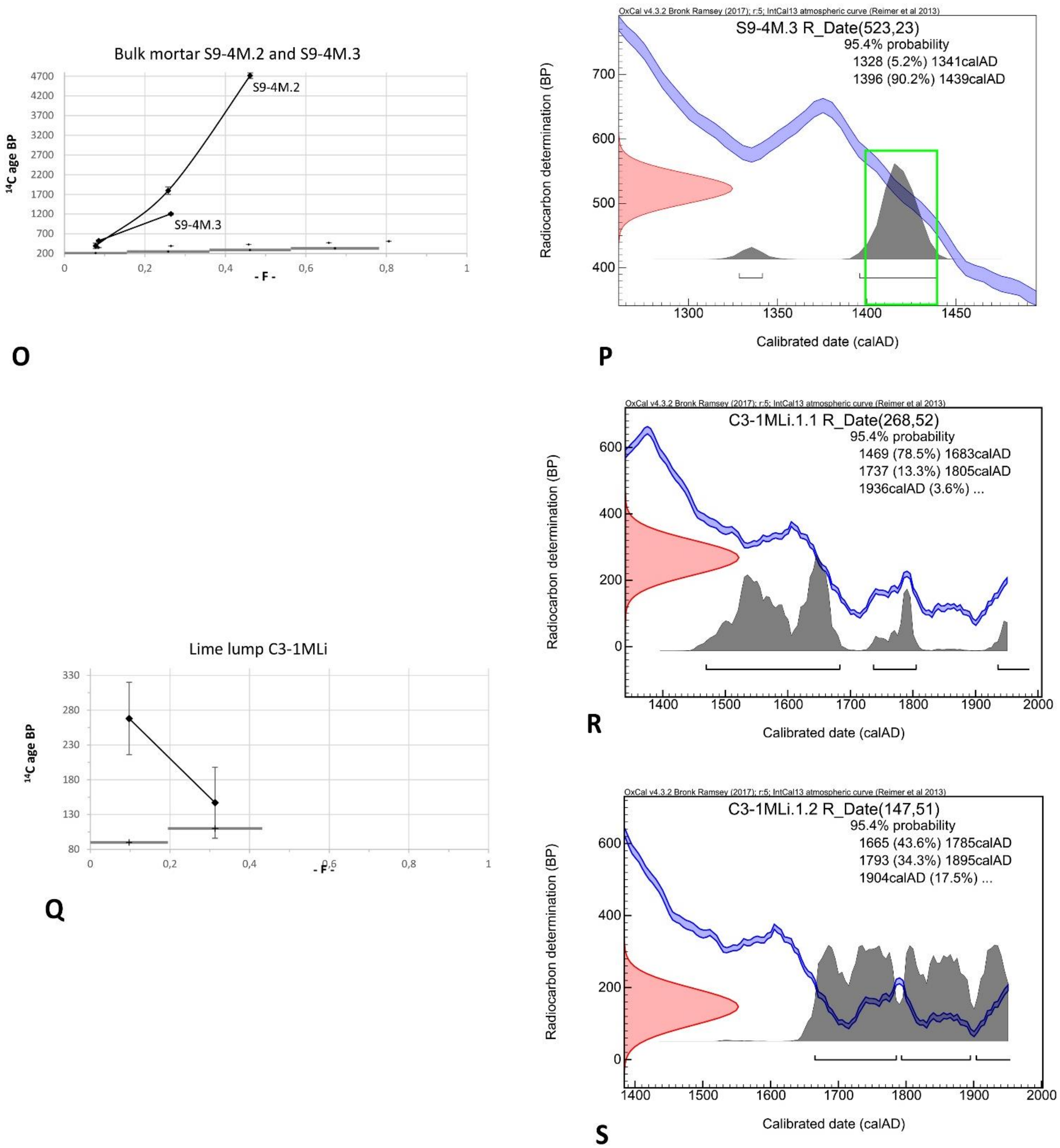

Fig.46: O) ^{14}C age profile of the sample S9-4M; P) calibrated result of the bulk mortar S9-4M.3, 1328-1341 (5.2%) and 1396-1439 (90.2%) AD. The date coincides with the expected age span (1404-1433) marked as a green rectangle; Q) ^{14}C age profile of the sample C3-1MLi; R) calibrated result of fraction 1 (C3-1MLi.1.1); S) calibrated result of the fraction 2 (C3-1MLi.1.2).

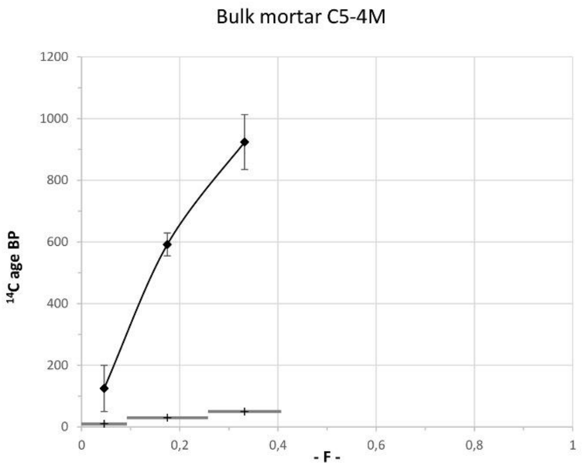

T

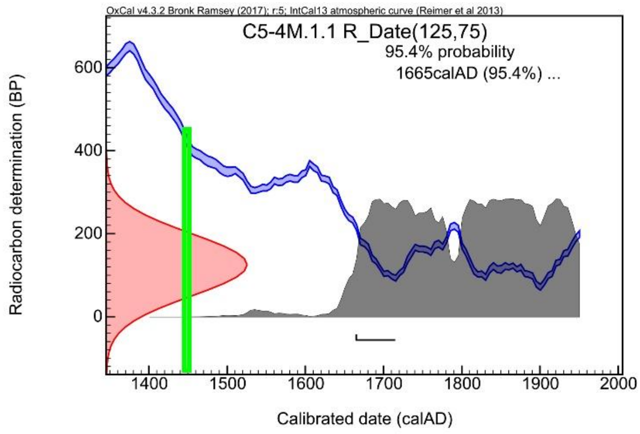

U

Fig.46: T) ^{14}C age profile of the sample C5-4M; U) calibrated result of the fraction 1 (C5-4M.1.1) >1665 AD (95.4%). The dates are younger than the expected construction age (1447?-1454) marked as a green rectangle.

The obtained dating results are evaluated from ^{14}C profiles in figure 46. The majority of the profiles displays a concave curvature, or increasing slope (Lichtenberger et al. 2015) characterized by rapidly dissolving mortar binder and slowly dissolving contaminants (fig. 46A, C, E, G, M, O). In this case the first CO_2 fraction has a ^{14}C age in agreement with the expected building age, marked as a green rectangle in the calibration graphs.

The ^{14}C age of the fraction 1 (590 ± 24 BP) of the sample C1-1M corresponds with a calibrated calendar age 1302-1368 (69.2 %) and 1382-1411 (26.2 %) AD, that coincides with the expected age from historic documents (1404-1415) (fig. 46B).

Due to the low P value of the fraction 1 of the sample C3-1M.1 (see tab. 5), the hydrolysis was performed a second time in order to obtain a bigger CO_2 fraction 1 (C3-1M.2.1) to date. The measurement of this fraction has revealed ^{14}C ages of 506 ± 26 BP corresponding with a calibrated calendar age of 1399-1445 AD (94.5%), that is close to the expected age for the original construction of the vault C3 (1446-1447?) (fig. 46F).

The radiocarbon age of the fraction 1 of the sample C5-5M is 508 ± 34 BP, calibrated 1325-1345 (7.4%) and 1393-1449 (88.0%) AD, is in agreement with the expected building age (1447?-1453) (fig. 46H). Whereas, the combined age of CO_2 fraction 1 and 2 results in ^{14}C age of 537 ± 24, calibrated 1320-1350 (20.3%) and 1391-1435 (75.1%), that is slightly older than the expected age (tab. 8).

Radiocarbon dating of the sample N8-1M was performed on a crushed lime lump analyzed in two CO_2 fractions. As show in figure 46I, the ^{14}C profile revealed that the dates seem to be inverted i.e. fraction 1 produced an age slightly older than fraction 2. However, CO_2 fractions 1 and 2 have overlapping ages and according to the Criterion I (Heinemeier et al. 2010; Ringbom et al. 2011; Lindroos et al. 2018) if the first two CO_2 fractions agree within the given error margins (and so the ages are overlapping), it demonstrates absence of contamination and it is considered a reliable result. In this case the combined calibration is assumed to give the true age of the mortar. The combined age of the CO_2 fractions 1 and 2 results in ^{14}C age of 263 ± 43 BP, corresponding with a calibrated calendar age 1487-1681 (79.2%), 1739-1743 (0.4%), 1763-1802 (12.4%), >1938 (3.5%) AD, younger than the expected age for the original construction (1433-1454), indicating a later re-construction. The catalogue of earthquakes reports several seismic evets that occurred after the vaults construction (see tab. 1). Seven damaging earthquakes in 1474, 1501, 1505, 1584, 1586, 1660, 1671 overlap with the radiocarbon dating (fig. 46L) and they may be the direct responsible for the reparation works, which are not documented in the historical records.

Also sample C2-3M fulfills the Criterion I. A combined calibration of CO_2 fraction 1 and 2 of the sample C2-3M yields the ^{14}C age 492 ± 24 BC corresponding with a calibrated calendar age 1409-1445 AD (95.4%), that is in agreement with the building age span (1443-1445) (fig. 46D).

The ^{14}C age of the fraction 1 (534 ± 35 BP) of the sample N9-3M corresponds with a calibrated calendar age 1315-1356 (28.1%) and 1388-1441 (67.3%) that coincides with the expected age for the original construction (1433-1454) (fig. 46N).

Due to poor precision in the Aarhus AMS data (tab. 8), the sample S9-4M was prepared a third time and dated at ETH Zurich. The radiocarbon age of the CO_2 fraction 1 (523 ± 23 BP) of the sample S9-4M.3 gave a calibrated calendar age 1328-1341 AD (5.2%) and 1396-1439 AD (90.2%), that overlap perfectly with the expected age from historic documents (1404-1433 AD) (fig. 46P).

The dating of samples C3-1MLi (lime lump) and C5-4M were rejected. The former has the second CO_2 fraction significantly younger than the first fraction and sample C5-4M has a CO_2 profile with a decreasing slope, suggesting delayed hardening (Lindroos et al. 2007, 2011; Lichtenberger et al. 2015).

The radiocarbon measurement on the lime lump C3-1MLi was performed analyzing two CO_2 fractions. The ^{14}C dating was unsuccessful because the first fraction released is older than the second fraction (fig. 46Q) and so the dating is invalidated. In this case the analyzed lime lump could have partially carbonated after the mortar was set in place or it could contain calcium hydroxide which carbonates when exposed to air, producing secondary calcite. The young carbonate leads to a rejuvenation of the result for fraction 1. In figures 46R and S the calibrated dates of the two fractions are shown.

The sample C5-4M does not yield a useful profile because it has a convex beginning (fig. 46T). The fraction 1 gave an age younger than expected (1447?1453) (fig. 46U). This result is probably due to delayed hardening. In fact, the sample C5-4M is a lime base mortar with *cocciopesto* added to the aggregate. This mean that the mortar could be weakly hydraulic and less permeable to atmospheric CO_2 (Lindroos et al. 2011; Lichtenberger et al. 2015; Hajdas et al. 2017).

Finally, it is remarkable how consistently the known ages (green rectangles) hit the right flank of the age distributions when the dating is successful. This must be because there is a lot of dead carbon contamination causing steep ^{14}C profiles and a minor bias towards older ages even for the initial CO_2 fractions.

6.3. Results of Luminescence dating

6.3.1. OSL dating results

The results of the OSL dating carried out by the University of Milan Bicocca are reported in table 9.

Sample	Technique	Measured aliquots	Accepted aliquots	E.D. (Gy)	Error E.D.	Dose rate (mGy/a)	Error dose rate	Age (years BP)	Date	Error
N8-1M	OSL multi grain	44	31	2,30	0,2	0,97	0,03	2370	350 BC	220
S9-4M	OSL multi grain	48	20	4,2	0,9	1,32	0,04	3180	1160 BC	700
S9-4M	OSL single grain	3400	86	1,4	0,3	1,32	0,04	1061	960	200

Tab. 9: results of OSL mortar dating carried out by the University of Milano Bicocca.

The obtained OSL ages are much older than the expected ones, regardless the techniques used. The sample S9-4M in fact yielded an OSL age of 1160 BC ± 700 when MG technique is applied. The weighted mean was used in order to evaluate the Equivalent Dose. Instead if we used the SG technique an age of 960 AD ±200 was obtained. In this case the SG technique is applied and the MAM model (Galibraith et al. 1999; Arnold et al. 2009) was used to calculate the Equivalent Dose.

For the sample N8-1M only the MG technique was applied due to the scarce amount of available sample. The obtained OSL age was 350 BC ± 220. This age overestimation is due to the partial or inhomogeneous bleaching of the quart grains during the mortar manufacturing process. At present the reason of the incomplete bleaching is not clear, but Sawakuchi et al. (2011) suggested that vegetated floodplains and permanent flow of turbid waters together with fast transportation reducing the number of episodes of erosion and deposition along the river stream do not favor quartz bleaching. These characteristics are compatible with the sand supply areas of the UNESCO site.

6.3.2. TL dating results

The results of the TL dating carried out by the University of Milan Bicocca are reported in table 10.

Sample code Milano	Sample code Modena	E.D. (Gy)	Error E.D.	Dose rate (mGy/a)	Error dose rate	Age (years BP)	Date	Error
D2686	C1-1L	2,24	0,16	5,86	0,18	380	1640	40
D2622	C3-1L	2,7	0,9	4,67	0,17	580	1440	60
D2623A	C5-1L	3,8	0,3	4,76	0,16	790	1220	65
D2623B	C5-4L	3,5	0,3	4,68	0,16	750	1265	65
D2683	C5-5L	9,3	0,7	5,26	0,16	1770	250	170
D2684	C5-6L	6,8	0,5	3,9	0,12	1740	280	170
D2685	C5-7L	1,25	0,09	6,96	0,21	180	1840	20
D2624A	N3-1AL						not datable	
D2624B	N3-3ALc						not datable	
D2624C	N3-3ALa	1,2	0,2	5,74	0,19	210	1810	40
D2624D	N3-3ALb	1,2	0,2	6,39	0,22	190	1830	40
D2625A	N8-1L	5,3	0,5	5,47	0,19	970	1050	90
D2625B	N8-2Lc	1,5	0,1	5,44	0,19	280	1730	20
D2625C	N8-2La	1,40	0,18	5,13	0,17	270	1740	30
D2625D	N8-2Lb	1,2	0,3	5,72	0,2	210	1805	20
D2626A	N9-1L	4,20	0,5	5,65	0,19	740	1270	75
D2626B	N9-3L	4,50	0,41	6,07	0,21	740	1275	70
D2627A	S9-1La	4,30	0,48	5,52	0,19	780	1240	80
D2627B	S9-4L	3,6	0,3	4,67	0,16	770	1245	65
D2627C	S9-1Lb	3,00	0,4	3,91	0,14	770	1250	80

Tab. 10: results of TL mortar dating carried out by the University of Milano Bicocca.

As reported in table 11, most of the bricks show an age that is not in agreement with the construction timing of the cathedral vaults.

In the case of the vault S9 the bricks manufactured in the 13th century (1245 ± 65 and 1240 ± 80, 1250 ± 80) were re-used later in both lime and gypsum portions of the vault. The same is true for the vault N9.

The TL dating results of the vault C5 attest several interventions. Five brick samples were dated, bound with lime mortar and gypsum mortar G1 (C5-6L) and G2 (C5-7L). Bricks manufactured in the 13th century (1220 ±65 and 1265 ±65) were re-used in lime portion as well as bricks from the Roman period (250 ± 170). Bricks dated back to the Roman age (280 ± 170) were also identified in the gypsum mortar portion G1, while bricks from gypsum portion G2 gave younger result (1840 ± 20) than the original building age (1447?-1454), suggesting that a later repair, using gypsum mortar, was carried out in the 19th centuries, possibly to mend the damages caused by the earthquakes that occurred in 1811, 1828, 1832, 1850. These seismic events, deduced from the historic earthquakes catalogue (see tab. 1), overlap with the dating.

The dates acquired from the vault N8 revealed that the lime portion of the vault was built with re-used bricks from the 11th century (1050 ± 90), while bricks from the gypsum portion are younger (1730 ± 20, 1740 ± 30, 1805 ± 20) than the original construction phase of the vault. Comparing the TL dating results with the earthquake catalogue (see tab. 1), it has been concluded that significant restoration works were carried out using gypsum mortar in the 19th century after the damaging earthquake of 1811.

Similar data has been obtained by TL dating of the brick samples of the vault N3 (1810 ± 40 and 1830 ± 40). The vault was probably reconstructed using gypsum mortar in the 19th century after the damaging earthquakes of 1811, 1828, 1832, 1850 (see tab. 1). However, as reported by the historical sources, the vault N3 could be also damaged by the abundant snowfalls. Baracchi and Giovannini (1988) mention that the northern aisle of the Modena cathedral, closer to the Tower Ghirlandina, is the most vulnerable because of the weight of the snow that melts slowly in the north side.

In the same manner, according to the TL dating result of the sample C1-1L (1640 ± 40), the vault C1 was rebuilt in the 17th century after damaging earthquakes occurred in 1660 and 1671.

Only one sample (C3-1L: 1440 ± 60), belonging to the vault C3, results in agreement with the expected age of the original construction (1446-1447?). The bricks, bound with lime mortar, were produced in the 15th century when the construction of the vault C3 took place.

Example of TL glow curves for the brick samples C3-1L, N3-3ALa and S9-4L are reported in figure 47. These three samples gave different ages (C3-1L: 1440 ± 60; N3-3ALa: 1810 ± 40; S9-4L: 1245 ± 65).

Sample	Type of mortar	Building age	Date	Note
C1-1L	lime	1404-1415	1640 ± 40	later **repair** after earthquake: 1660,1671
C3-1L	lime	1446-1447?	1440 ± 60	the date is in **AGREEMENT** with building age
C5-1L	lime	1447?-1453	1220 ± 65	**Re-used** bricks
C5-4L	lime		1265 ± 65	**Re-used** bricks
C5-5L	lime		250 ± 70	**Re-used** bricks
C5-6L	gypsum		280 ± 170	**Re-used** bricks
C5-7L	gypsum		1840 ± 20	later **repair** after earthquake: 1811, 1828,1832,1850
N3-3ALa	gypsum	/	1810 ± 40	later **repair** after earthquake: 1811, 1828, 1832,1850
N3-3ALb	gypsum		1830 ± 40	
N8-1L	lime	1433-1454	1050 ± 90	**Re-used** bricks
N8-2Lc	gypsum		1730 ± 20	later **repair** after earthquake: 1811
N8-2La	gypsum		1740 ± 30	
N8-2Lb	gypsum		1805 ± 20	
N9-1L	gypsum	1433-1454	1270 ± 75	**Re-used** bricks
N9-3L	lime		1275 ± 70	**Re-used** bricks
S9-1La	gypsum	≤1433	1240 ± 80	**Re-used** bricks
S9-4L	lime		1245 ± 65	**Re-used** bricks
S9-1Lb	gypsum		1250 ± 80	**Re-used** bricks

Tab. 11: TL dating results in comparison with the building ages.

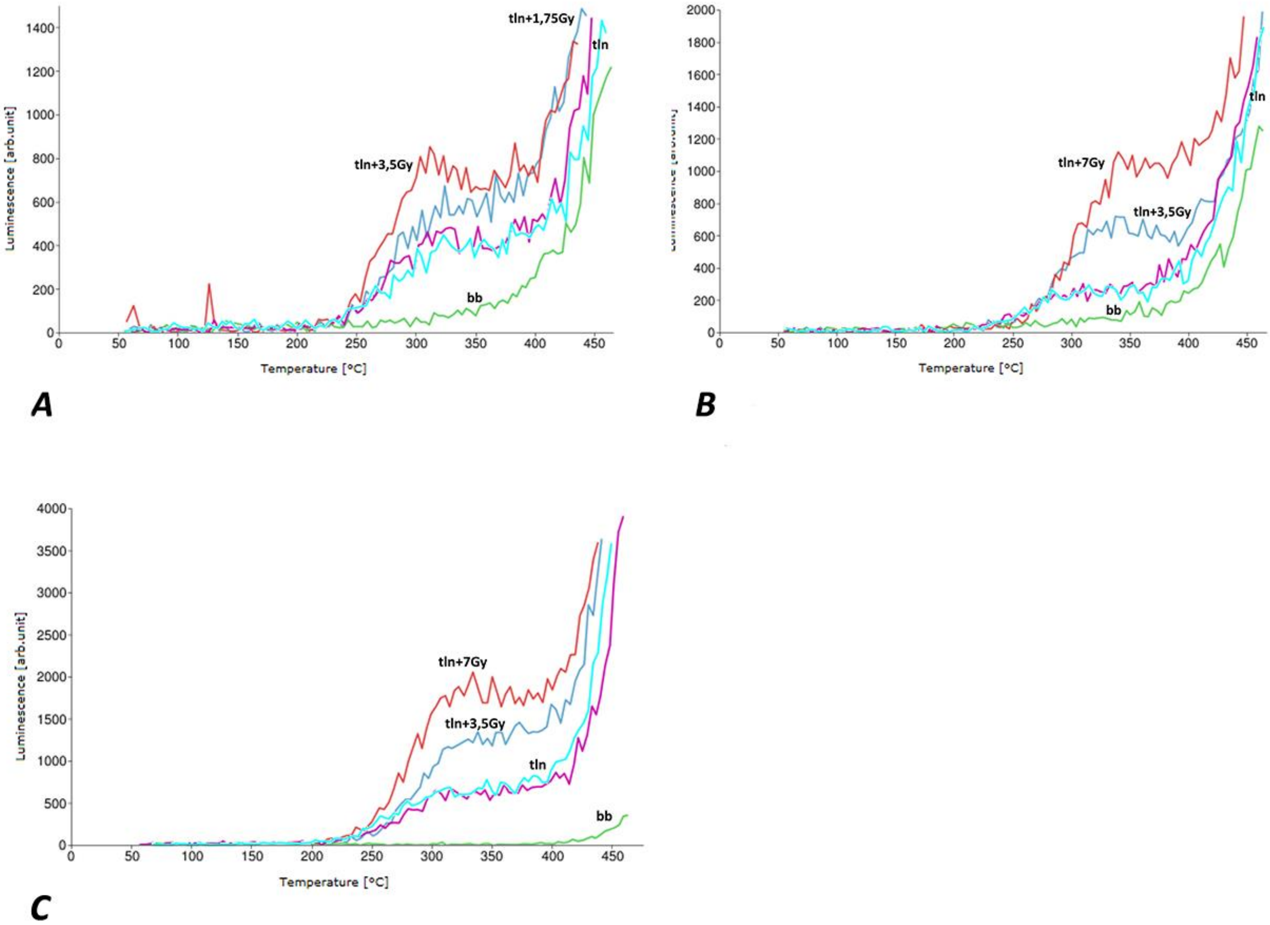

Fig. 47: TL glow curves for samples C3-1L (A), N3-3ALa (B) and S9-4L (C).

6.4. Results of pollen analysis

SAMPLES N3-3AM, S9-1M, S9-4M

Total pollen concentration values are low, ranging from 819 p/g in S9-4M to 2956 p/g in S9-1M (tab. 12), in line with what reported in works on similar materials (e.g. Langgut et al. 2013). Also the number of taxa identified is limited, between 16 and 18 taxa per sample, but given the low number of granules counted (from 30 to 40 per sample), it suggests a possible future good floristic variety in accordance with the increase of the pollen sum. A total of 32 taxa (18 among woody and 14 among herbaceous) were identified. All three samples are in any case fertile and it will be possible to obtain sufficient statistic count (at least around 120-150 granules). However, while percentage pollen spectra are statistically unreliable, some interesting information can be achieved by the qualitative data:

-in the sample S9-4M the plane tree (*Platanus*) and the pear tree (*Pyrus*) were identified. The plane tree is an ornamental plant already well known and used in the Roman period in Modena (Bosi et al. 2017), until the present time. The pear tree is a fruit tree that has carpological finds (seeds) in the nearby site of the garden bishopric of Modena (12th century AD), in front of the Cathedral (Benatti et al. 2011), as evidence of its medieval diffusion even within the walls. The same applies to the walnut tree (*Juglans regia*), present in this sample and in the next one, whose remains (endocarpi, sometimes wood/coal) are common in all towns since Roman times;

-The sample S9-1M is the one with the least floral peculiarities, except for the exclusive presence of chestnut tree (C*astanea sativa*). Although the presence of this plant is attested in the bishopric of the Cathedral (Benatti et al. 2011) and in medieval times in the vicinity of urban centers or religious complexes even in the low plain (Zucchini 1967), it is conceivable that the pollen, found in the samples, comes from the anthropic woods of the hill for atmospheric pollen transport. Among NPPs, fungal remains related to clay sediments formed by events of soil erosion (types UAB 30 and UAB 48) or characteristic of dead plants (type EMA 129 and *Epicoccum hdv* 1011) were identified. In addition, a significant amount of fungal hyphae, greater than the other two samples, is present. These pollen may have to be linked, at least in part, to the techniques used to produce the mortar sample;

- in the sample N3-3AM pollen of *Ginkgo biloba* is present. This plant has arrived in Italy as botanical curiosity in the second half of the 18th century (Targioni Tozzetti 1853; De Toni 1887; Saccardo 1909; Maniero 2000). *Ginkgo biloba* was so widely used as an ornamental plant that in the mid-1800s it was considered cultivated throughout Europe (Crane et al. 2013). The presence of its pollen in this sample is a rather effective chronological marker, caught between the laying and the setting of the mortar. Moreover, this sample is the one that has the most exclusive elements compatible with an “evolved” urban green areas such as ivy (*Hedera helix*), holm oak (*Quercus ilex*) and roses (*Rosa*); it also presents the plane tree (already identified in S9-4M).

It should be noted that all three samples have pollen of *Cyperaceae*, as evidence of the presence of water in the urban environment (Bosi et al. 2015). In addition, as it is reasonably expected, all samples have a high component of anemophilous granules that have arrived at the site for air transport, partly from relatively near locations, partly from transport away from hilly/sub mountain areas. Among the first, the deciduous oaks are present in all samples, sometimes accompanied by the white hornbeam, sometimes by the ashwood and sometimes by the hazel tree, typical of the planitial oak woods. From higher altitudes the chestnut, beech and fir trees have been identified and perhaps the pines, which however could have an ornamental function. All these taxa are still documented today in the pollen rain of the Modena city center (Ferrari et al. 1986).

Samples C5-6M, C5-7M, N8-2M

The analysis is still ongoing and the final results are not available. However, the preliminary study of the samples C5-6M (G1) and C5-7M (G2) has provided interesting information. The amount of pollen is abundant and the remains are in a good state of preservation in both samples. There is pollen that reflect the period during which the mortar was prepared and pollen of plants extinct in the Italian flora (but nowadays re-introduced as ornamental plants), belonging to the rocks used to obtain the mortar. The sample G1 shows pollen evidence of ornamentals plants, trapped in the mortar during its setting, giving evidence of the environment that surrounded the Cathedral. Whereas the sample G2 presents pollen of cultivated plants as fava, cereals and hemp, that are evidence of a rural environment where the mortar was produced.

Moreover, the features of these two mortar samples are different from the previous analyzed (N3-3AM, S9-1M and S9-4M) that do not present pollen of extinct plants. It means that different raw materials were used for the production of the mortar samples and that, in particular, the gypsum of the samples N3-3AM, S9-1M and S9-4M probably belongs to the Triassic gypsum outcrop of the Secchia River Valley.

In conclusion, the analysis of the pollen trapped in the mortar samples of the Modena cathedral vaults allows to reconstruct the context during mortar production and identify the raw material sources.

Modena Cathedral vaults				
samples		S9-4M	S9-1M	N3-3AM
weight (g)		3,80	1,42	3,70
added *Lycopodium* spore		20848	20848	20848
counted *Lycopodium* spore		201	149	166
pollen sum		30	30	40
concentration (p/g)		**819**	**2956**	**1358**
Arboreal pollen (AP) taxa: 18				
ARALIACEAE	*Hedera helix*			2,50
CORYLACEAE	*Corylus*	6,67		
	Carpinus betulus		6,67	2,50
	Ostrya - Carpinus orientalis type	3,33		
CANNABACEAE	*Humulus lupulus*	3,33		
FAGACEAE	*Castanea sativa*		3,33	
	Fagus		3,33	2,50
	Quercus caducifolia indiff.	6,67	23,33	5,00
	Quercus ilex			2,50
GINKGOACEAE	*Ginkgo*			2,50
JUGLANDACEAE	*Juglans regia*	6,67	3,33	
OLEACEAE	*Fraxinus excelsior* type	3,33		2,50
PINACEAE	*Abies*		6,67	7,50
	Pinus indiff.		3,33	7,50
PLATANACEAE	*Platanus*	6,67		2,50
ROSACEAE	*Rosa*			2,50
	Pyrus	10,00		
SALICACEAE	*Populus*	3,33		
Non-arboreal pollen (NAP) taxa: 14				
APIACEAE	*Apiaceae* indiff.		6,67	
ASTERACEAE	*Cichorioideae*	10,00		
BRASSICACEAE	*Hornungia* type			2,50
CHENOPODIACEAE	*Chenopodiaceae* indiff.	3,33		2,50
CYPERACEAE	*Cyperaceae* indiff.	3,33	10,00	12,50
FABACEAE	*Lotus* type	3,33		
PLANTAGINACEAE	*Plantago* indiff.	6,67	3,33	
POACEAE	*Avena/Triticum* group			2,50
	Hordeum group		3,33	
	Poaceae spontanee group	16,67	13,33	35,00
RANUNCULACEAE	*Ranunculus acris* type		3,33	
ROSACEAE	*Fragaria/Potentilla* type		3,33	2,50
	Agrimonia		3,33	
URTICACEAE	*Urtica dioica* type	6,67	3,33	2,50
% AP		50,00	50,00	40,00
% NAP		50,00	50,00	60,00
NPP (non-pollen palynomorphs) (% pollen sum)				
FUNGI	HdV 54 (hypha)	26,67	70,00	7,50
	EMA 129 (characteristic of dead plants- alder tree)		3,33	
	UAB 30 (clay sediments formed by events of soil erosion)		3,33	
	UAB 48 (clay sediments formed by events of soil erosion)		3,33	
	HdV 1011 *Epicoccum* (saprophyte)		3,33	
	EMA 36 (abundant on dead wood)			2,50
	EMA 13 (smut fungus)			2,50
	HdV 20	3,33		
	Sordaria HdV 55 A (coprophile)		6,67	2,50
	Coniochaeta cf. *lignaria* (HdV 172)(dead wood)			2,50
ANIMALIA	EMA 46 (hair)			2,50
PLANT REMAINS	brachisclereidi	3,33		
	annulate vessels/ spiral vessels	3,33	6,67	
	charcoal		*	**
OTHER	HdV 1058	3,33		

Tab. 12: pollen and NPP remains in the mortar samples N3-3AM, S9-1M and S9-4M.

7. DISCUSSION

7.1. AMS Radiocarbon dating comparison

The results obtained from the radiocarbon dating using Cryo2Sonic procedures are showed in figure 48.

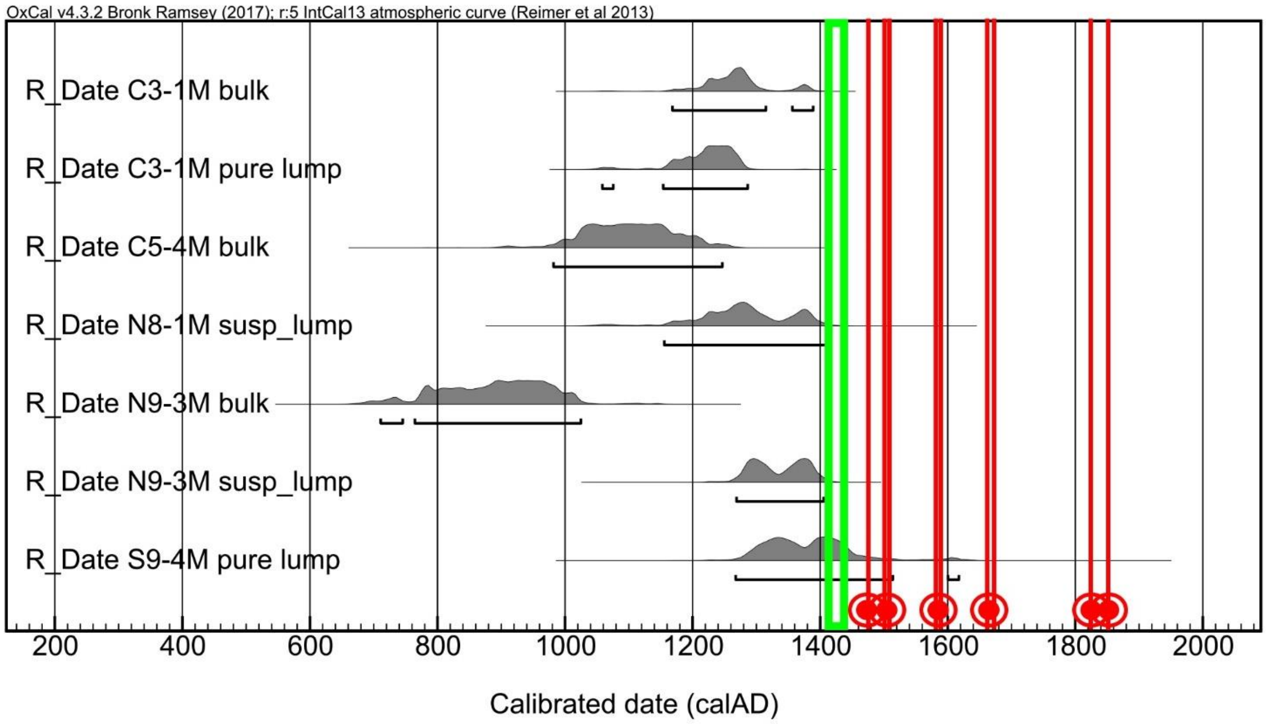

Fig. 48: overview of the calibrated results of the samples prepared using Cryo2Sonic procedure. The building age of the vaults (1404-1454) is marked as green rectangle. The several earthquakes, that occurred after the vaults construction, are marked as red vertical lines. Five of them overlap with the calibrated date of the sample S9-4M.

The only case where the age of mortar is comprehended within the documented construction span is from the sample S9-4M. The dated lime lump was not prepared following the CryoSonic procedure, but it underwent directly to the acid digestion. The S9-4M calibrated date is 1267-1514 (94.2%) and 1600-1617 (1.2%) AD. Unfortunately, this date does not permit to discriminate if the only lime portion detected on the vault S9 is a remain of the original construction or it is a later restoration. The catalogue of earthquakes (see tab. 1) reports several seismic events that occurred after the vaults construction and five damaging earthquakes in 1474, 1501, 1505, 1584, 1586 overlap with the radiocarbon dating, as shown in figure 48. They may be the direct responsible for the repairs works, that are not documented in the historical records. However, the calibrated age also is in agreement with the original building age of the vault S9 (1404-1433).

As concern all other samples, they were subjected to Cryo2Sonic treatment and the dating gave incorrect results because of a dead carbon contamination. The C3-1M, C5-4M and N9-3M bulk mortars yielded an older age than expected (fig. 48) and this means that Cryo2Sonic procedure has been not able to remove the contamination from underburned limestone fragments and carbonate sand of geologic origin. The ^{14}C results also revealed the difficulty to discern the lime lumps from the underburned BRPs. The radiocarbon dating of C3-1M lump, N8-1M and N9-3M susp_lumps gave older results compared to the original building age (fig.48). It can be supposed that the selected lumps contained an underburned core inside, not easy detectable with a stereomicroscope, caused by the incomplete reaction of the original limestone. These calcination relicts provide a significant aliquot of dead carbon that aged the results.

The results obtained from the radiocarbon dating using sequential dissolution procedures are showed in figure 49.

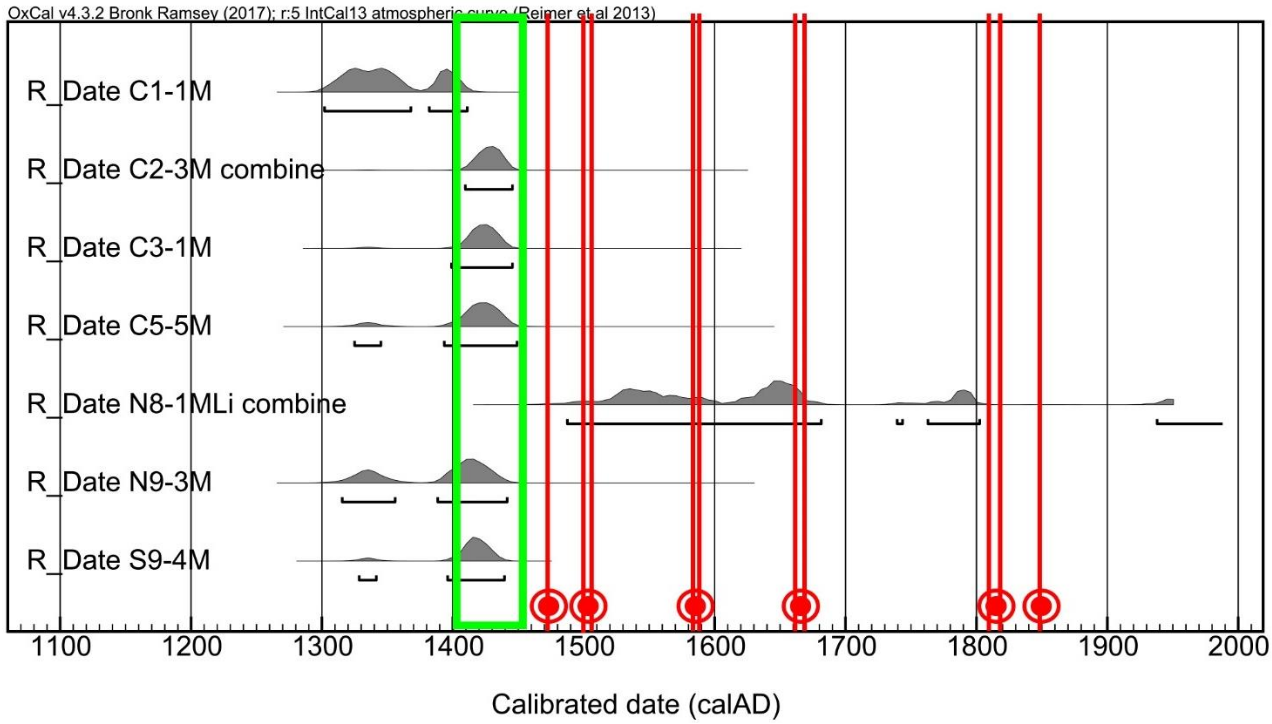

Fig. 49: overview of the calibrated results of the samples prepared using sequential dissolution procedure. The building age of the vaults (1404-1454) is marked as green rectangle. The several earthquakes, that occurred after the vaults construction, are marked as red vertical lines. Seven of them overlap with the calibrated date of the sample N8-1MLi.

Radiocarbon dating using sequential dissolution procedure provides calendar ages that perfectly match with chronological references, showing an optimum reliability of this technique (fig.49).

Despite the potential contamination by dead carbon due to the underburned limestone fragments and carbonate grains in the aggregate identified in the mortar samples with the petrographic analysis, the procedure has succeeded in selecting the good fraction representative of setting moment. The sample N8-1M is the only one that yielded an age younger (1487-1681 (79.2%), 1739-1743 (0.4%), 1763-1802 (12.4%), >1938 (3.5%) AD) than the original construction age (1433-1454). This result attests that a later intervention was carried out after significant damage, probably as a result of the 1474, 1501, 1505, 1584, 1586, 1660, 1671 earthquakes (see tab. 1).

7.2. Luminescence dating

The thermoluminescence analysis on bricks provided interesting information about the restoration history of the vaults. Only one sample, belong to the vault C3, has got a date compatible with the original building period. Several re-used bricks, manufactured in the 11th and 13th century, have been identify in the vaults C5, N8, N9 and S9. Moreover, two brick samples from the vault C5 belong to the Roman period. Unfortunately, the re-used of older bricks do not allow to pinpoint the timing of the intervention, especially if the bricks are embedded with gypsum mortar that can not be directly dated. Conversely, the TL dating result of the vault C1, C5, N3, N8 revealed that many later repairs have been carried out during the 17th, 18th and 19th centuries. As reported in the catalogue of the ancient earthquake (tab.1), several damaging seismic events occurred after the vaults construction and they may be the responsible for the restoration works, which are not documented in the historical records. In fact, Acidini Luchinat et al. (1984) only report that possible strengthening interventions were carried out in the 19th century on the vaults C1, C3 and C4, after the earthquake occurred in 1832, but there is no certainty of that.

The OSL dating of lime mortar did not provide reliable data. The obtained OSL ages are much older than expected ones, regardless of the techniques used, indicating a poor and partial bleaching of the quart grains (Sawakuchi et al. 2011).

7.3. Pollen analysis

The pollen data obtained from the vaults mortar samples reflect the period during which the mortar was produced and applied. The samples display a pollen record of ornamental plants that surrounded the Modena cathedral in the medieval time (plane, pear and walnut trees) and pollen findings of plants belonged to the areas nearby the city such as white hornbeam, ashwood and hazel trees from the planitial woods and chestnut, beech and fir trees from the hilly zones. The analysis also testifies a rural environment with finds of cultivated plants, as evidence of the mortar production context.

The most interesting information is provided by the gypsum mortar sample N3-3AM. A pollen evidence of *Ginkgo biloba* has been identified in the sample and it was probably trapped during the laying and the setting of the mortar. This plant has arrived in Italy in the second half of the 18th century and it was widely used as ornamental plant. The presence of its pollen is an effective chronological marker. Moreover, the TL dating result of the bricks embedded in the gypsum mortar revealed an age that is in agreement with the pollen analysis result. The brick fragments gave an age of 1810 ± 40 and 1830 ± 40, suggesting that a later repair of the vault N3 was carried out in the 19 century using gypsum mortar.

8. CONSTRUCTION AND RESTORATION PHASES OF THE MODENA CATHEDRAL VAULTS

The detail survey carried out on the extrados of the 15th century vaults of Modena cathedral revealed a complex unexpected structure by the use of different mortars for the original construction and for later multiple modifications.

The petrographic analysis allows to recognize two phases of the vault construction, according to the technology of mortar production. Most of the bedding lime mortars present a large amount of binder related particles and variable grain-size sand probably supplied from the Panaro River. The difference in the particle size of the aggregate may indicate the collection in distinct areas of the Panaro River, possibly in different seasons. These mortars belong to the vaults C1, N1, N2, N5, N7, N8, N9, S1 and S9. A different group is identified by the mortar of the vaults C2, C3 and C5, characterized by abundant *cocciopesto* and BRPs. Also in this case the sand provenance is supposed to be from the Panaro River. According to the radiocarbon dating results by sequential dissolution, both mortar types have been used for the original building of the vaults.

The successive phase is identified by the lime mortar samples of the group 4. The samples show a more refined technique of preparation: absence of BRPs and a more sorted aggregate. The provenance of the aggregate sand has also changed and it is presumed from the Secchia River. Unlikely, it was not possible to obtain any reliable radiocarbon dating of this later phase, due to the small amount of sample available (sample N3-2AM).

The radiocarbon dating using sequential dissolution of lime mortars and the TL dating of bricks helped to clarify the chronology of the construction phases and the history of the complex restorations, which are probably related to damages suffered in the past after the main earthquakes which struck the area. The comparison of the absolute dating results allows to draw the following conclusion.

The vault C1 was originally built using lime mortar in 1404-1415 and older bricks, and was subsequently partially reconstructed using lime mortar in the 17th century, possibly as a result of the 1660, 1671 earthquakes.

The vault C2 was originally built using lime mortar in 1443-1445. In this case only the radiocarbon dating was performed.

The vault C3 was originally built using lime mortar and new bricks produced in the 15th century for the vault construction in 1446-1447.

The vault C5 was originally built using lime mortar and re-used bricks in 1447-1453. Two different restoration phases were also identified. A first partially reconstruction was carried out using gypsum mortar G1 and older bricks. As gypsum mortar can not be directly dated, the re-use of older bricks does not allow to detect the timing of the vault repair and the possible triggering earthquake. A second intervention was performed using gypsum mortar G2 in the 19th century, probably to repair the damage caused by the 1811, 1828, 1832, 1850 earthquakes.

The vault N3 was modified in the 19th century using gypsum mortar, probably as a result of the 1811, 1828, 1832, 1850 earthquakes. As reported by the historic sources, also the abundant snowfalls may have caused damages (Baracchi and Giovannini 1988).

Two different restoration phases were recognized on the vaults N8. A first restoration by lime mortar and re-used bricks, was carried out immediately after the original construction, possibly as a result of the 1474, 1501, 1505, 1584, 1586, 1660, 1671 earthquakes. A second intervention was then necessary to repair damage probably caused by the 1811 earthquake. As building materials for this second repair new bricks were used, kept together by a gypsum mortar.

The vault N9 was originally built using lime mortar and older bricks in 1433-1454, while gypsum mortar was used for later repair with re-used bricks. Unfortunately, also in this case it was not possible to trace the restoration timing.

The vault S9 was originally built using lime mortar and older bricks in 1404-1433, and was subsequently partially reconstructed with gypsum mortars and re-used bricks. As for the previous vaults modified using gypsum mortar and re-used bricks, the dating of the later intervention can not be defined.

All absolute dating results and their interpretation are reported in table 13. Figure 50 shows the mapping of the portions built using different binder with the dating results.

Sample	Sample type	Building age	Absolute dating method	Date	Notes	Interpretation
C1-1M	lime mortar	1404-1415	^{14}C Sequential dissolution ETH Zurigo	1302-1368 (69.2%) 1382-1411 (26.2%)	the date is in **AGREEMENT** with building age	lime mortar for original construction (1404-1415) and for later repair after earthquake 1660 or 1671
C1-1L	brick lime mortar		TL	1640 ± 40	**later repair** after earthquake 1660, 1671	
C2-3M	lime mortar	1443-1445	^{14}C Sequential dissolution ETH Zurigo	combine: 1409-1445 (95.4%)	the date is in **AGREEMENT** with building age	lime mortar for original construction (1443-1445)
C3-1M	lime mortar	1446-1447?	^{14}C Cryo2sonic	Bulk: 1168-1315 (86.7%) 1356-1389 (8.7%) Pure Lump: 1058-1074 (1.3%) 1154-1286 (94.1%)	the date is **NOT** in agreement with building age	lime mortar for original construction (1446-1447?) with new bricks
C3-1M	lime mortar		^{14}C Sequential dissolution Aarhus AMS Centre	1: 1469-1683 (78.5%) 1737-1805 (13.3%) >1936 (3.6%) 2: 1665-1785 (43.6%) 1793-1895 (34.3%) >1904 (17.5%)	incorrect results. fraction 1 older than fraction 2	
C3-1M	lime mortar		^{14}C Sequential dissolution ETH Zurigo	1399-1445 (95.4%)	the date is in **AGREEMENT** with building age	
C3-1L	brick lime mortar		TL	1440 ± 60	the date is in **AGREEMENT** with building age	
C5-1L	brick lime mortar	1447?-1453	TL	1220 ± 65	**RE-USED** bricks	lime mortars for original construction (1447?-1453) with re-used bricks. gypsum mortar for later repair with re-used bricks and gypsum mortar for later repair after earthquake (1811, 1828, 1832 or 1850)
C5-4M	lime mortar		^{14}C Cryo2sonic	Bulk: 982 – 1246 (95.4%)	the date is **NOT** in agreement with building age	
C5-4M	lime mortar		^{14}C Sequential dissolution Aarhus AMS Centre	>1665 (95.4 %)	incorrect result. Convex 14C profile and the date of the fraction 1 is **YOUNGER** than building age	
C5-4L	brick lime mortar		TL	1265 ± 65	**RE-USED** bricks	
C5-5M	lime mortar		^{14}C Sequential dissolution ETH Zurigo	1325-1345 (7.4%) 1393-1449 (88.0%)	the date is in **AGREEMENT** with building age	
C5-5L	brick lime mortar		TL	250 ± 170	**RE-USED** bricks	
C5-6L	brick gypsum mortar		TL	280 ± 170	**RE-USED** bricks	
C5-7L	brick gypsum mortar		TL	1840 ± 20	**later repair** after earthquake: 1811, 1828, 1832, 1850	

N3-1AL	brick gypsum mortar	/	TL	not datable	/	gypsum mortar for later repair after earthquake (1811, 1828, 1832 or 1850)
N3-2AM	brick lime mortar		^{14}C Cryo2sonic	not datable	/	
N3-3ALa	brick gypsum mortar		TL	1810 ± 40	**later repair** after earthquake: 1811, 1828, 1832, 1850	
N3-3ALb	brick gypsum mortar		TL	1830 ± 40		
N8-1L	brick lime mortar	1433-1454	TL	1050 ± 90	**RE-USED** bricks	lime mortar for later repair with re-used bricks after earthquake (1474, 1501, 1505, 1584, 1586, 1660 or 1671) . gypsum mortar for interventions of 19th century
N8-1M	lime mortar		^{14}C Cryo2sonic	Susp_lump: 1155 – 1413 (95.4%)	the date is **NOT** in agreement with building age	
N8-1M	lime mortar		OSL multi grain	390 a.C. ± 220	the date is **NOT** in agreement with building age	
N8-1M	lime mortar		^{14}C Sequential dissolution Aarhus AMS Centre	combine: 1487-1681 (79.2%) 1739-1743 (0.4%) 1763-1802 (12.4%) >1938 (3.5%)	the date is **YOUNGER** than building age. Later repair after eathquake: 1474, 1501, 1505, 1584, 1586, 1660, 1671	
N8-2Lc	brick gypsum mortar		TL	1730 ± 20	**later repair** after earthquake 1811	
N8-2La	brick gypsum mortar		TL	1740 ± 30		
N8-2Lb	brick gypsum mortar		TL	1805 ± 20		
N9-1L	brick gypsum mortar	1433-1454	TL	1270 ± 75	**RE-USED** bricks	lime mortar for original construction with re-used bricks (1433-1454). gypsum mortar for later repair with re-used bricks
N9-3M	lime mortar		^{14}C Cryo2sonic	Bulk: 711-745 (3.6%) 764– 1025 (91.8%) Susp _lump: 1269-1405 (95.4%)	the date is **NOT** in agreement with building age	
N9-3M	lime mortar		^{14}C Sequential dissolution Aarhus AMS Centre	1315-1356 (28.1%) 1388-1441 (67.3%)	the date is in **AGREEMENT** with building age	
N9-3L	brick lime mortar		TL	1275 ± 70	**RE-USED** bricks	
S9-1La	brick gypsum mortar	≤1433 (1404-1433)	TL	1240 ± 80	**RE-USED** bricks	lime mortar for original construction with re-used bricks (1404-1433). gypsum mortar for later repair with re-used bricks
S9-1Lb	brick gypsum mortar		TL	1250 ± 80	**RE-USED** bricks	
S9-4M	lime mortar		^{14}C Cryo2sonic	Pure lump: 1267 – 1514 (94.2%) 1600-1617 (1.2%)	the date is in AGREEMENT with building age/ later repair after earthquake 1474, 1501, 1505, 1584 or 1586	
S9-4M	lime mortar		^{14}C Sequential dissolution Aarhus AMS Centre	1424-1643 (95.4%)	poor precision in the Aarhus AMS data	
S9-4M	lime mortar		^{14}C Sequential dissolution ETH Zurigo	1328-1341 (5.2%) 1396-1439 (90.2%)	the date is in **AGREEMENT** with building age	
S9-4M	lime mortar		OSL multi grain	1140 a.C. ± 720	the date is **NOT** in agreement with building age	
S9-4M	lime mortar		OSL single grain (MAM)	960 ± 200	the date is **NOT** in agreement with building age	
S9-4L	brick lime mortar		TL	1245 ± 65	**RE-USED** bricks	

Tab. 13: absolute dating results and their interpretation.

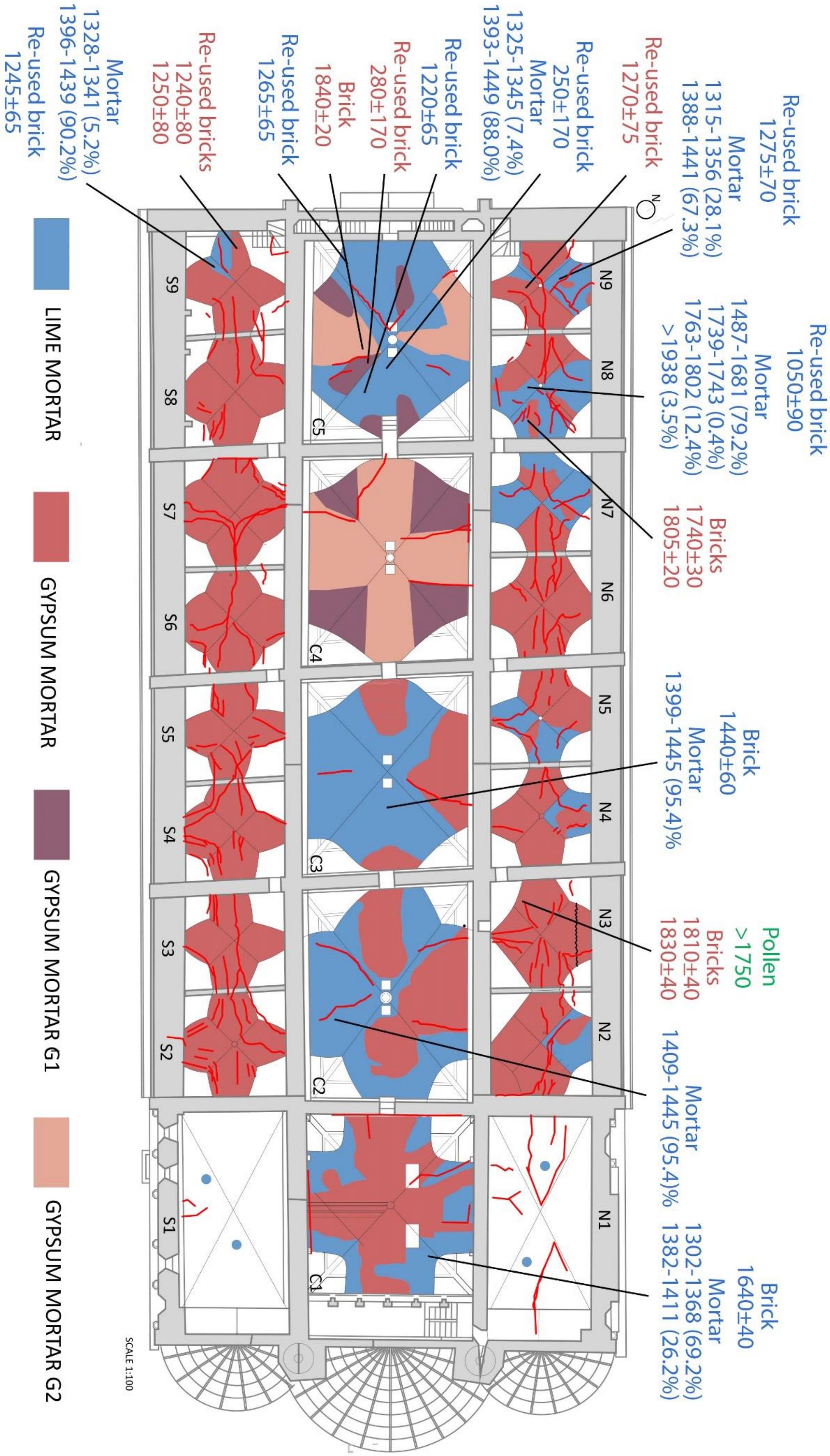

Fig. 50 mapping of the portions built using different binder with the dating results.

9. CONCLUSION OF THE CASE STUDY 1

The main objectives of this research were to clarify the vaults construction phases and to assess the damages suffered in the past. The detailed survey carried out on the extrados of the vaults binder revealed a complex and unexpected structure by the use of different mortars for the original construction and for later multiple modifications. The catalogue of earthquakes reports several seismic evets that occurred after the vaults construction, that may be the direct responsible for the reparation works, which are not documented in the historical records. An integrated approach using different absolute dating techniques of the building materials (radiocarbon dating and Optically Stimulated Luminescence for dating mortars and Thermo-luminescence to date bricks) has enabled to provide new consideration about the history of the vaults.

Petrography of mortars contributed to distinguish two phases of construction of the Modena cathedral vaults site on the basis of presence of binder related particles and composition of the sand aggregate. The bedding mortars are characterized by a large amount of BRPs and variable grain-size sand probably supplied from the Panaro River. Few samples also present *cocciopesto* added to the aggregate. The radiocarbon dating results using sequential dissolution revealed that both type of mortar has been used for the original vaults construction. The successive phase is identified by lime mortar samples characterized by the absence of BRPs and a more sorted aggregate, possibly supplied from the Secchia River. These features suggest a more sophisticated technique of mortar preparation. Unfortunately, the inability to obtain reliable radiocarbon dating result using Cryo2Sonic preparation did not allow to define the timing of the late intervention.

The comparison of the two sample preparation procedures of mortar for radiocarbon dating (Cryo2Sonic and sequential dissolution) has allowed to identify the most suitable method for lime mortars rich in carbonate aggregate. Five mortar samples were prepared and dating according to the Cryo2sonic protocol and eight after sequential dissolution. The results obtained have revealed that Cyo2Sonic procedure seems to be inadequate for radiocarbon dating of lime mortars with fine calcareous aggregate. This procedure was not able to separate the binder from the contaminants and all results obtained provided an age older than expected. The only partially satisfactory result has been obtained by dating the lime lump of the sample S9-4M, that was not prepared following the CryoSonic procedure. On the contrary, sequential dissolution has provided the most successful and reliable results. Six samples yielded an age that coincide with the chronological references

(1404-1454). The sample N8-1M is the only one that gave an age younger than the original construction age, indicating a later re-construction after damaging earthquakes. The dating of samples C3-1MLi (lime lump) and C5-4M were instead rejected. The former has the second CO_2 fraction significantly younger than the first fraction, suggesting that the analyzed lime lump could have partially carbonated after the mortar was set in place or it could contain secondary calcite that leads to a rejuvenation of the result for first fraction. Sample C5-4M has a CO_2 profile with a decreasing slope, suggesting delayed hardening. According to the radiocarbon results, the methodology of sequential dissolution seems to work better on the mortars of the Modena cathedral vaults, selecting the good fraction representative of setting moment.

The comparison of the results obtained by radiocarbon dating using sequential dissolution of lime mortars and the TL dating of bricks helped to define the history of the complex restorations. Unfortunately, the OSL dating of lime mortar did not provide reliable data due to the incomplete bleaching of the aggregate quartz grains (Sawakuchi et al. 2011).

The results revealed that lime mortar was used both as material for the original construction of the vaults in 1404-1454 and for later repairs, while the gypsum binder was used to entirely rebuild some vaults or to repair some vaults originally built using lime mortars.

Figure 51 compares and summarizes the radiocarbon dating, TL dating and pollen analysis results, showing the following conclusion.

The vaults C1, C2, C3, C5, N9 and S9 were originally built using lime mortar. Older bricks were used for the construction of most of them, except for the vault C3, built using new bricks produced in the 15th century.

Later repairs using lime mortar were carried out on the vaults C1 and N8. A partially reconstruction of the vault C1 was carried out in the 17th century, possibly as a result of the 1660 or 1671 earthquakes, while the restoration of the vault N8 was carried out immediately after the original construction, possibly as a result of the 1501, 1505, 1584, 1586, 1660 or 1671 earthquakes.

Later restoration using gypsum mortar were performed on the vaults C5, N3, N8, N9 and S9. Two different restoration phases were recognized on the vault C5. A first partially reconstruction was carried out using gypsum mortar G1 and older bricks. As gypsum mortar can not be directly dated, the re-use of older bricks did not allow to detect the timing of the vault repair and the possible triggering earthquake. A second intervention was performed using gypsum mortar G2 in the 19th century, probably to repair the damage caused by the 1811, 1828, 1832 or 1850 earthquakes.

The vault N3 was modified in the 19th century probably as a result of the 1811, 1828, 1832 or 1850 earthquakes or for mending the damages caused by the abundant snowfalls. Once again, the vault N8 was repaired in the 19th century after the 1811 earthquake. Unfortunately, it was not possible to define the restoration timing of the vaults N9 and S9 that were originally built using lime mortar and later repaired using gypsum mortar and re-used bricks manufactured in the 13th century.

Moreover, interesting information were provided by testing pollen analysis on mortars. The data obtained from the six mortar samples reflect the period during which the mortar was produced and applied. The samples display a pollen record of ornamental plants that surrounded the Modena cathedral in the medieval time and pollen findings of plants belonged to the areas nearby the city such as trees from planitial and hilly areas. A rural environment with finds of cultivated plants were also testified as evidence of the mortar production context. The sample N3-3AM shows a pollen evidence of *Ginkgo biloba*, probably trapped during the laying and the setting of the gypsum mortar. The plant is an effective chronological marker since it has arrived in Italy in the second half of the 18th century. This data is in accord with the TL dating result of the bricks embedded in the gypsum mortar, indicating that the vault N3 was modified in the 19 century.

The complex scenario identified, resulting in a patchwork of lime and gypsum mortars, and the absolute dating results obtained demonstrate that the vaults suffered much larger damage induced by earthquakes than previously assessed just by mapping fracture and crack networks. The multidisciplinary nature of the research provided also new data for the comparison of different independent dating methods.

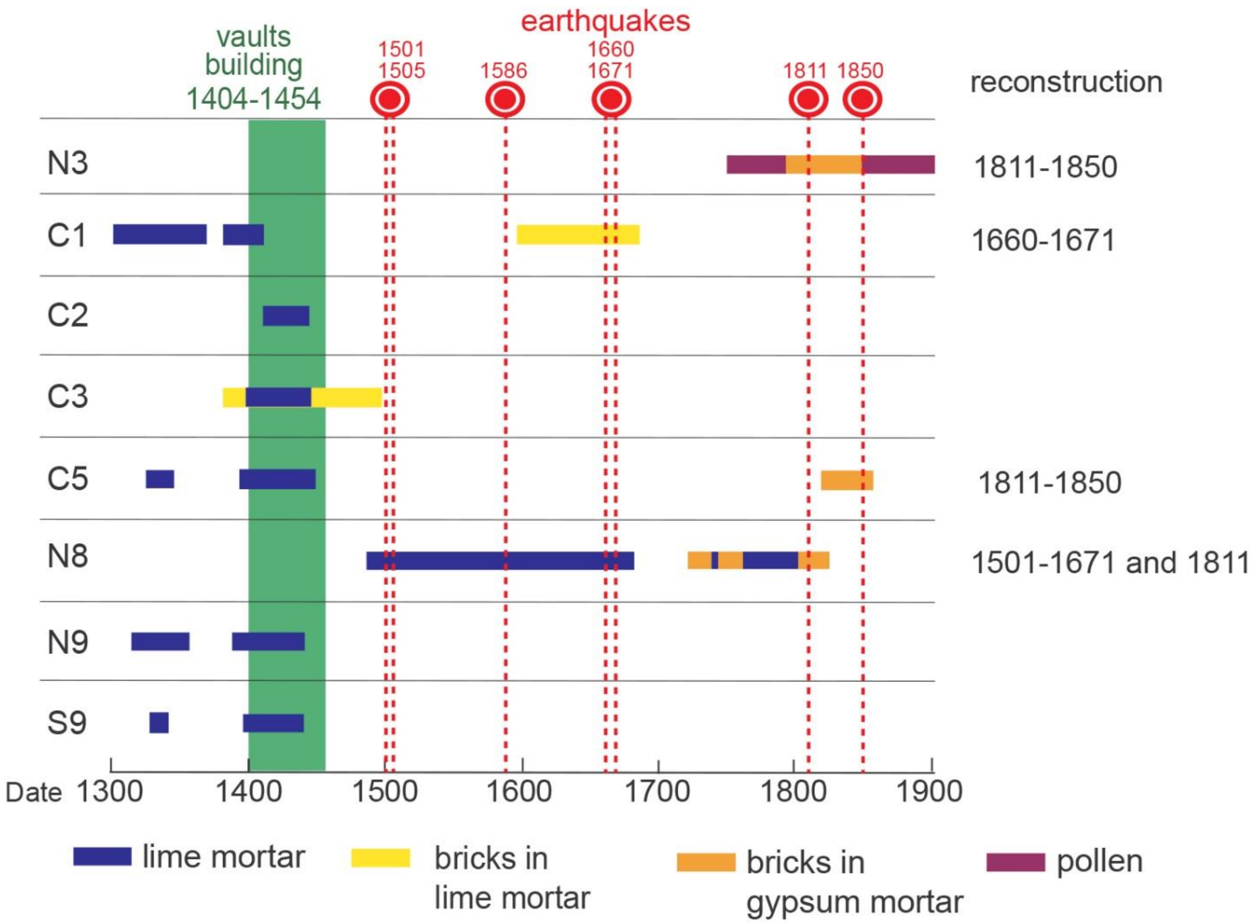

Fig. 51: overview of the absolute dating and pollen analysis results of the vaults mortar and brick samples. The radiocarbon calibrated dates of the lime mortars are marked as blue rectangle, the TL dates of bricks in lime mortar are marked as yellow rectangle while the bricks in gypsum mortar as orange rectangle and the results of pollen analysis are marked as purple rectangle. The re-used bricks dates are not reported in the figure. The building age of the vaults (1404-1454) is indicated as green vertical rectangle that matches with the radiocarbon dating results of the vaults C1, C2, C3, C5, N9 and S9 suggesting that these vaults were originally built using lime mortar. Subsequently the vaults N3, C1, C5 e N8 were partially reconstructed as consequence of several damaging earthquakes. These seismic events, marked as red vertical lines, overlap with the radiocarbon calibrated date of the vault N8 and with the TL dates of the vault N3, C1, C5 e N8. The probable reconstruction period is indicated on the right side of the figure.

<u>CASE STUDY 2: POMPEII UNESCO SITE</u>

10. INTRODUCTION AND AIMS

Some mosaic floors in houses and public spaces in Pompeii present late interventions, which were probably carried out to fill gaps in pavements to repair various types of damage. These restorations were identified in the House of *Paquius Proculus* (I, 7, 1), House of Menander (I, 10, 4), House of the Small Fountain, House VIII, 3, 24 and in the *Forum* baths (VII, 5, 2) (fig. 52). The Houses are the most ancient of Pompeii and they were built during the Samnite period (3rd century-2nd century BC).

In the House of *Paquius Proculus* the floor of the peristyle was repaired and covered with a new mortar (fig. 53A). Likewise, the floor of the peristyle and the surroundings rooms of the House of Menander show the same repair (fig. 53B). The most interesting context has been identified in the House of the Small Fountain. The mosaic floor of the *tablinum* is completely covered by a repair mortar. The perimetrical portion of the floor, decorated with meanders, is the only visible part of the original mosaic (fig. 53C). Other examples are the House VIII, 3, 24, where a big gaps were mended using this material (fig. 53E) and in the *Forum* baths where a large portion of the floor was substituted (fig. 53D) (Pisapia et al. 2018).

In order to clarify if the interventions are ancient or modern restoration, carried out just after the excavation site at the end of the 18th century, petrographic characterization, radiocarbon dating and pollen analysis have been performed.

Fig. 52: A) House of *Paquius Proculus*; B) House of Menander; C) House of the Small Fountain; D) *Forum* baths; E and F) House VIII, 3, 24.

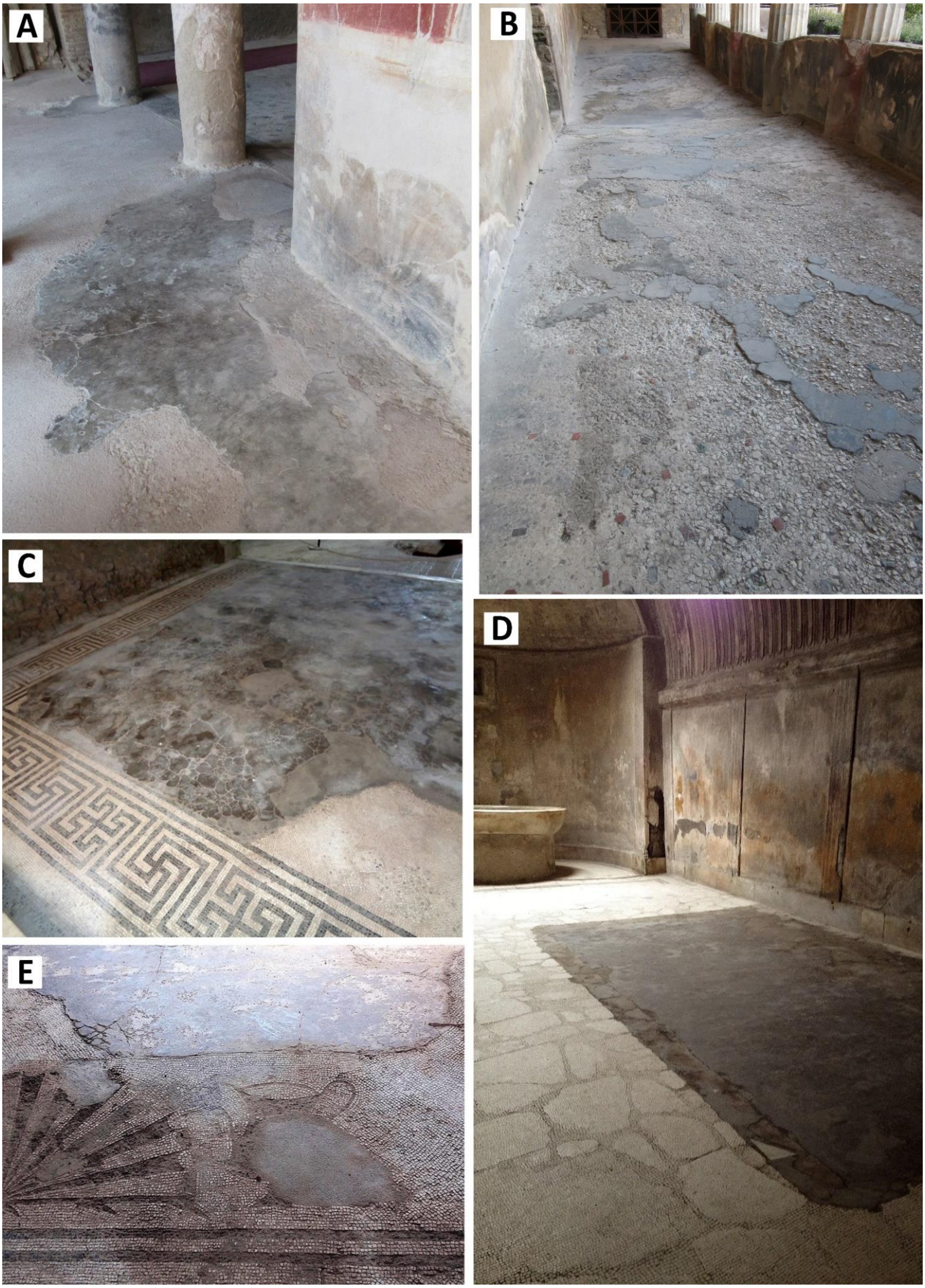

Fig. 53: A) House of *Paquius Proculus*; B) House of Menander; C) House of the Small Fountain; D) *Forum* baths; E) House VIII, 3, 24.

11. MATERIALS AND METHODS

11.1. The sampling

The sampling of the repair mortars has been carried out for each Houses (fig. 54).

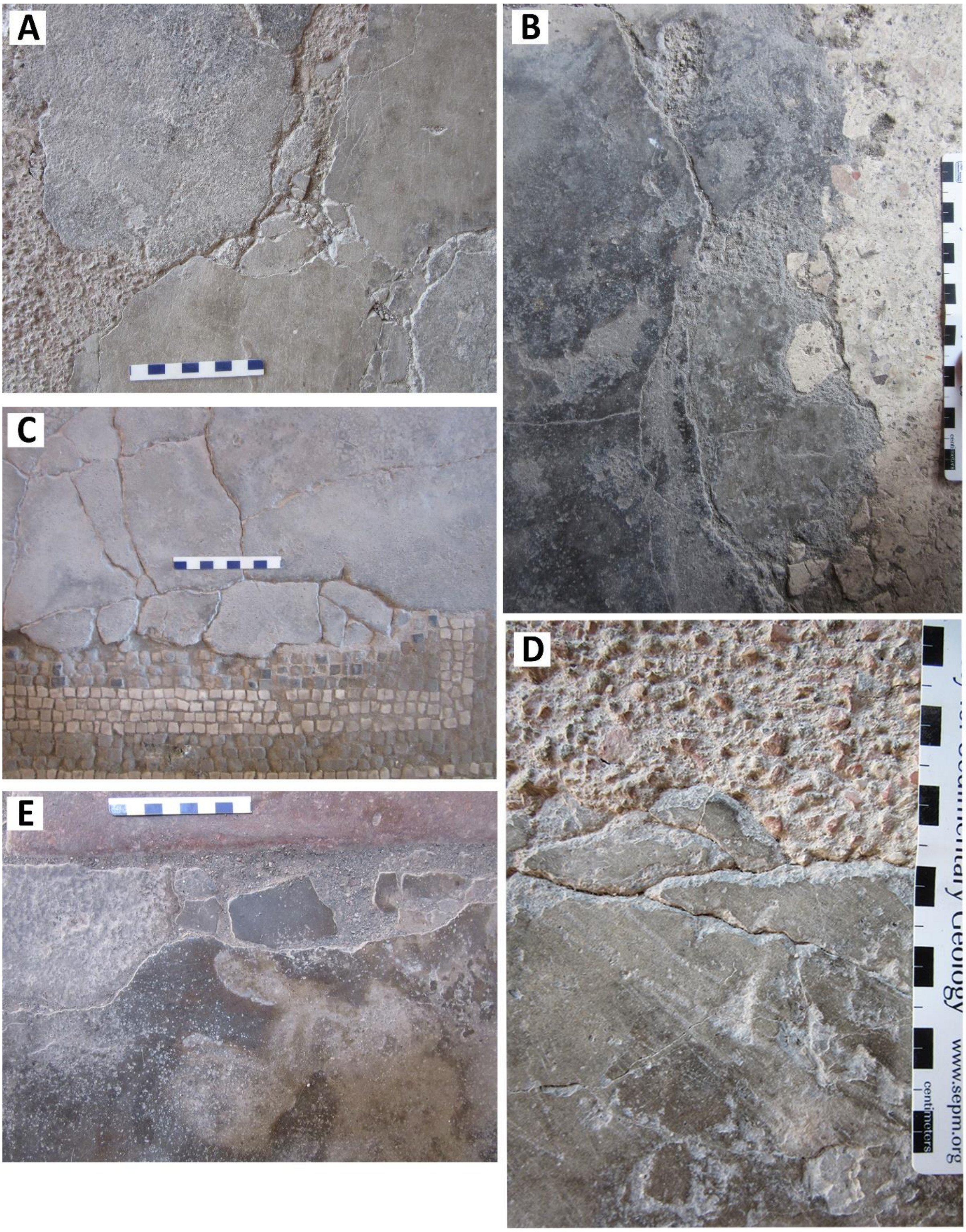

Fig. 54: sampling point of the repair mortars. A) House of *Paquius Proculus;* B) House of Menander; C) House of the Small Fountain; D) *Forum* baths; E) House VIII, 3, 24.

A total of fourteen samples have been taken. Four from House of *Paquius Proculus* (PQA, PQB, PQC, PQD), five from the House of Menander (CMA, CMB, CMC, CMD, CME), two from the House of the Small Fountain (FPB, FPC), one from the *Forum* baths (TFA) and two from the House VIII, 3, 24 (A and B).

11.2. Characterization of repair mortars

The mortar samples were vacuum impregnated with epoxy resin to obtain thin-sections, that were observed under the optical microscope in transmitted light. The main mortar features, such as the type of binder, composition of the aggregate, grain size and morphology, sorting grade, porosity and cracking, were described using as a reference the Document UNI-Normal 11176. The petrographic analysis was performed using optical microscope LEITZ Orthoplan polarizing transmitted light. The optical microscope is equipped with a Nikon Coolpix 990 digital camera for the acquisition of micrographs.

Image analysis of thin sections was performed to determine the aggregate binder ratio and the aggregate grain size by means of Image J free software (Carò e Di Giulio 2004; Michalska et al.2017; Nonni et al. 2017). The aggregate binder ratio was calculated following the recommendation produced by the RILEM TC 167-COM (2001). Three photomicrographs of about 5 mm per side for each lime mortar samples were analyzed.

11.3. AMS Radiocarbon dating by sequential dissolution

Considering the reliable results obtained using sequential dissolution procedure for the Modena cathedral vaults samples, the radiocarbon dating of the mortar samples was performed following the procedure applied at the Åbo Akademi University of Turku, Finland.

The preparation has been performed only on the sample CMA from the House of Menander that presents two layers (CMA1 and CMA2).

Both layers have been broken in a plastic bag using nipper pieces and the crushed material has been vibrated in a sieve series (mesh widths ranging between 20-500 µm). The grain-size fraction <100 µm has been subsequently wet sieved and the grain-size fraction range of 46-75 µm has been chosen for dating.

The coarser grain size fraction (300-500 µm) has been used for testing the alkalinity of the samples with 2% phenolphthalein solution (in ethanol). Sample CMA1 appeared to be with a higher alkalinity than the sample CMA2 but both colours (fig. 55) are considered acceptable.

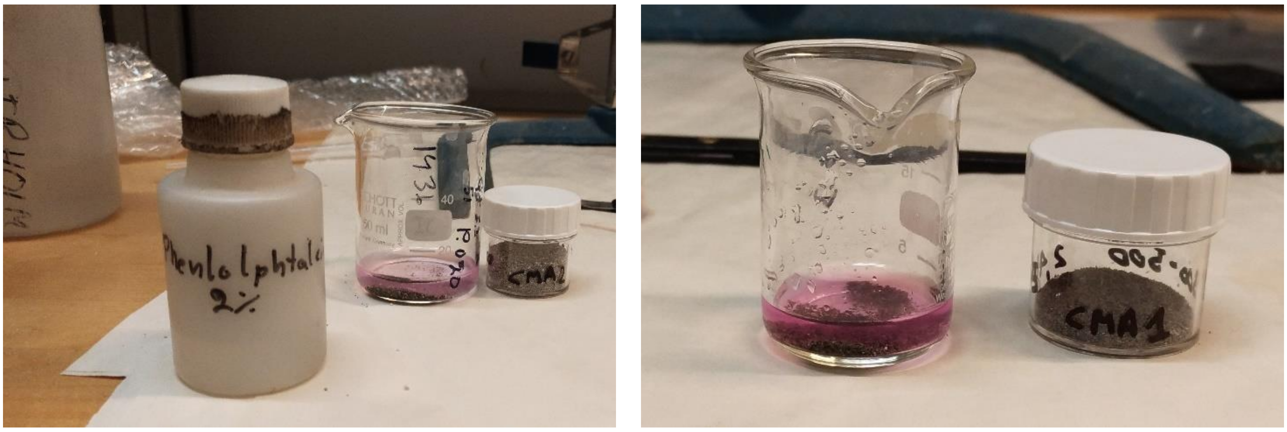

Fig. 55: alkalinity test of the samples CMA1 and CMA2.

The samples have been prepared to carbon dioxide in a specially designed preparation line shown in figure 24. The selected powders have been put into the reactor vessel and, when a sufficient vacuum is reached, around 3 mL of 85% chilled at 0°C phosphoric acid has been let in excess on the powder from a burette. Since the aim of the research is to discern if the samples are ancient or modern, large fractions were extracted to avoid strong interference from minor components and all the powder samples have been reacted. The samples behavior during the dissolution process is summarized in table 14.

The vials containing the CO_2 gas of the samples have been sent to ETH Zurich (Switzerland). The CO_2 gas has been converted to graphite for AMS ^{14}C measurements via reduction with H_2 using cobalt as a catalyst (Vogel et al. 1984). The calibration of the ^{14}C ages to calendar years has been done using the IntCal13 calibration curve (Remier et al. 2013) and the OxCal 4.3 program (Bronk Ramsey 2017). All calibrated results are reported at 95.4% confident level.

Sample	Grain-size C content *(µm)*	Sample aliquot *mg*	CO2 fraction *(nr)*	Diss. Time *(s)*	P in the CO2 line *(mbar)*	F	Calc.C cont. *(mg)*	Dating
CMA.1.1	46-75	55	1	60	8,6	0,24	0,11	
85% H_3PO_4	**3.40% C**		2	230	20,4	0,57	0,26	
0 degrees			3	900	7,0	0,19	0,09	
CMA.1.2	46-75	100	1	40	41,0	0,51	0,53	**X**
85% H_3PO_4	**5,69%C**		2	180	29,8	0,37	0,38	**X**
0 degrees			3	610	12,7	0,16	0,16	
			4	1190	5,87	0,07	0,08	
			5	1890	2,38	0,03	0,03	
CMA.2.1	Crushed	73	1	31	26,4	0,33	0,34	**X**
85% H_3PO_4	not sieved		2	635	51,7	0,647	0,67	**X**
0 degrees	**8.27 % C**		3	1115	5,76	0,072	0,07	
			4	1860	6,81	0,085	0,09	

Tab. 14: Hydrolysis data of the samples dated.

11.4. Pollen Analysis

The pollen analysis has been performed only on the repair mortar sample CMA from the House of Menander. The study has been performed by the Laboratory of Palynology and Palaeobotany of the University of Modena and Reggio Emilia (UNIMORE) following the routine method for pollen extraction already applied for Modena cathedral vaults mortars (Florenzano et al. 2012).

12. RESULTS

12.1. Results of petrographic analysis

The petrographic analyses show a high homogeneity among the samples. The samples have the same composition but they are different for grain size distribution and aggregate binder ratio. The repair mortars are characterized by a lime binder with scarce and small lime lumps (<1 mm) (fig. 56B). Underburned limestone fragments are also present (fig. 56A). The aggregate grain size is fine to medium sand, poorly sorted. The aggregate binder ratio ranges from 1 to 2.5. The composition of the aggregate is: pozzolanic fragments and singular idiomorphic crystals partially reabsorbed of pyroxene, leucite, plagioclase, sanidine and biotite. There are also many calcite nodules (fig. 58B) and traces of opaque minerals. The presence of carbonate residues resulted from the volcanic activity and they occur naturally in the volcanic ashes used to prepared mortars (Miriello et al. 2010).

The pozzolanic fragments have sub rounded shape up to 2 mm in size (fig. 57A). *Pozzolana* can be classified as volcanic *scoriae*, that could contain microcrystals of leucite, plagioclase and pyroxene (fig. 57B and C; fig. 58A). There are also fragments of pumice with microcrystals of biotite and feldspar (fig. 57E). The singular crystals of pyroxene, leucite and feldspar are always idiomorphic (fig. 57D and F). Most of the pores has irregular shapes and they are variable in size.

Three samples from House of Menander show two layers with same aggregate composition but different distribution. The first layer (aggregate binder ratio 1.5) has more aggregate than the second (aggregate binder ratio 0.8) (fig. 59). Only the sample A of the House VIII, 3, 24 is characterized by an abundant amount of crushed bricks (*cocciopesto*), finely ground (fig. 58C).

Some samples have also a thin surface layers up to 2 mm. The layer is lime-based and the aggregate is sharp glass fragments, obtained by the very fine grinding of pumice (fig. 58D).

The composition of the aggregate suggests that the volcanic materials used for the mortar production comes from primary volcanoclastic deposits of the Vesuvian area (Barberi et al. 1981; Joron et al. 1987; Di Rienzo et al. 2007; Aulinas et al. 2008) which were not reworked.

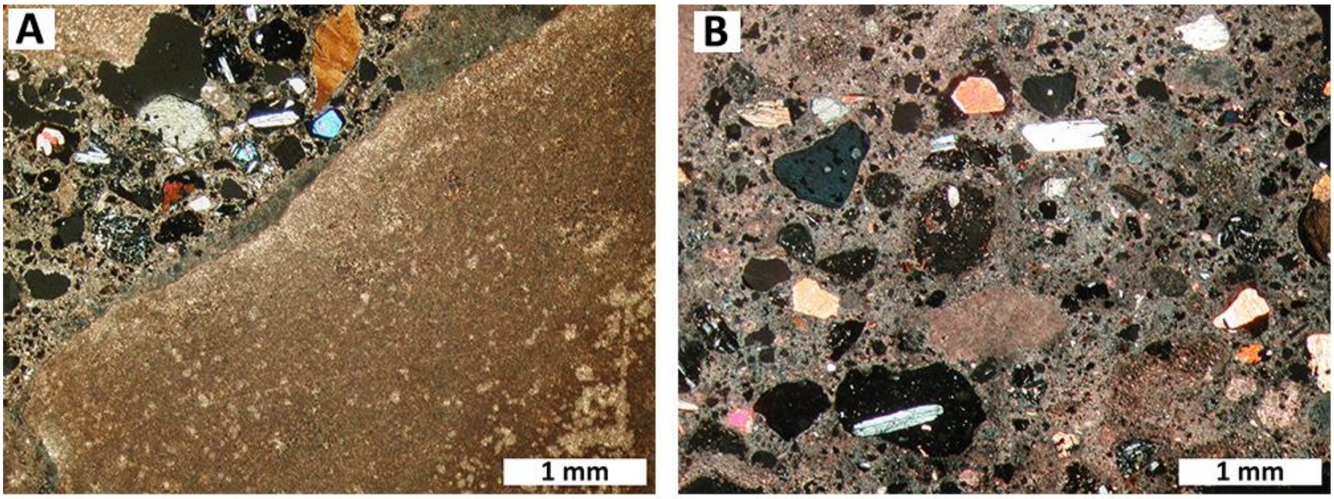

Fig. 56: photomicrograph in crossed polars of binder related particles. A) sample CMB: underburned limestone fragment that shows reaction rims that fade in the binder, sample CMB; B) sample CMB: lime lumps *sensu strictu*.

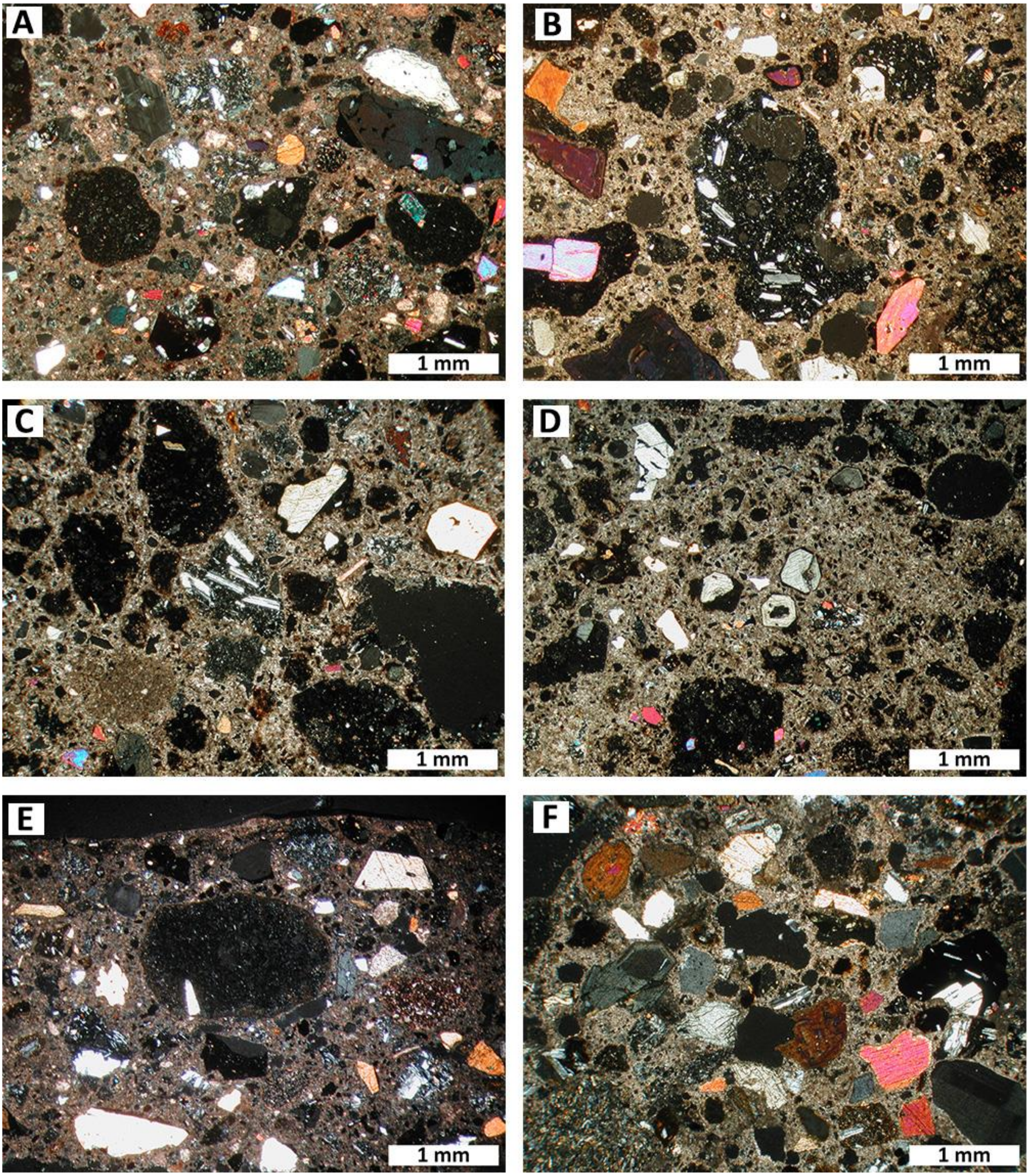

Fig. 57: photomicrograph in crossed polars of repair mortar samples. A) sample CMD, pozzolanic fragments with sub rounded shape; B) sample CMD, pozzolanic fragment with microcrystals of leucite and plagioclase; C) sample PQB, at the centre of the image is a pozzolanic fragment with microcrystals of plagioclase; D) sample PQB, at the centre of the image are singular crystals of pyroxene; E) sample PQC, fragments of pumice with microcrystals of feldspar; F) sample FPB, singular crystals of pyroxene.

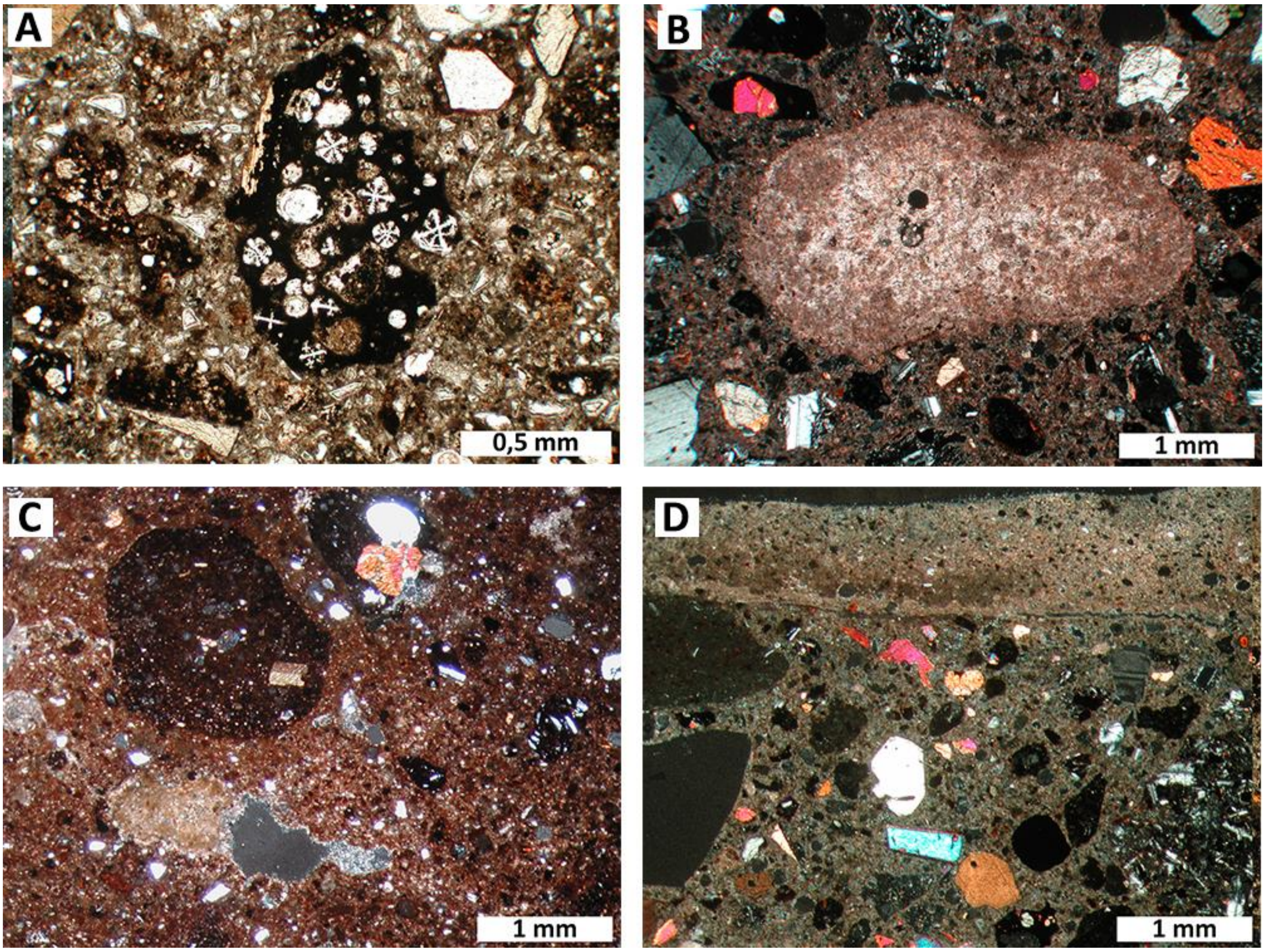

Fig. 58: photomicrograph in crossed polars of repair mortar samples. A) sample PQB, pozzolanic fragments with microcrystals of leucite chart-wheel; B) sample PQC, limestone fragment; C) sample A of the House VIII, 3, 24, *cocciopesto* finely ground; D) sample CMD, thin surface layer with sharp glass fragments, obtained by the very fine grinding of pumice.

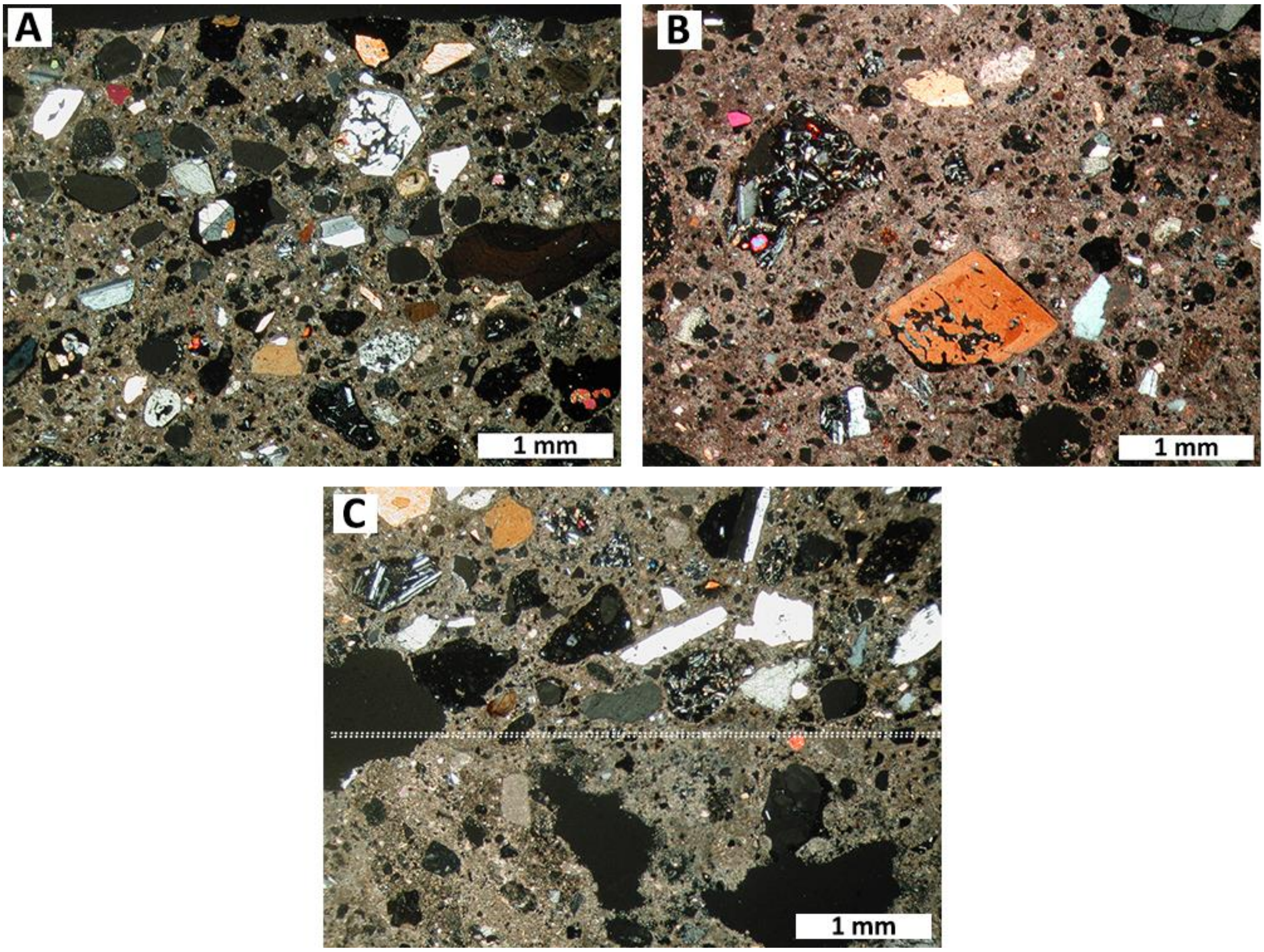

Fig. 59: photomicrograph in crossed polars of the sample CMA. The first layer (A) has more aggregate than the second (B). The transition from layer 1 to layer 2 is marked as a white line in figure C.

12.2. Results of AMS Radiocarbon dating

Results of radiocarbon dating by sequential dissolution procedure are reported in tables 15 and 16. Figures 60 and 61 show the ^{14}C profiles and the calibrated results.

Sample subsample / CO_2-fraction	Material	Grain size (µm)	Reaction time (s) from t_0	Carbon yield (tot) (%)	Fraction size (relative 1)	C-14 age (BP)	±	δ13C ‰ VPDB	Laboratory nr
CMA1.2.1	Bulk mortar	46-75	40	1,03%C	0-0.51	4717	25	-2,3	ETH-86833
CMA1.2.2			180		0.51-0.86	5256	26	-13,3	ETH-86931
CMA2.1.1	Bulk mortar	46-75	31	1,39%C	0-0.33	13810	46	-8,2	ETH-86839
CMA2.1.2			180		0.33-0.98	16198	41	-2,8	ETH-86834

carbon yield (tot) (%) = total carbon yield after about one hour of dissolution
n.r. = not reported
ETH = ETH Zurich

Tab. 15: Hydrolysis data, ^{14}C results and $d^{13}C$ values for the dated samples.

Sample	Building age	^{14}C age (BP)	Calibrated age 2σ	Notes
CMA1.2.1	1st century BC	4717 ± 25	3632-3563 BC (30.8%) 3536-3496 BC (20.8%) 3460-3376 BC (43.8%)	the date is much older than expected
CMA1.2.2		5256 ± 26	4229-4200 BC (10.8 %) 4170-4127 BC (19.7 %) 4121-4092 BC (5.9 %) 4082-3982 BC (58.9 %)	
CMA2.1.1	1st century BC	13810 ± 46	15001-14521 BC (95.4%)	the date is much older than expected
CAM2.1.2		16198 ± 41	17784-17442 BC (95.4%)	

Tab. 16: ^{14}C ages and calibrated dates.

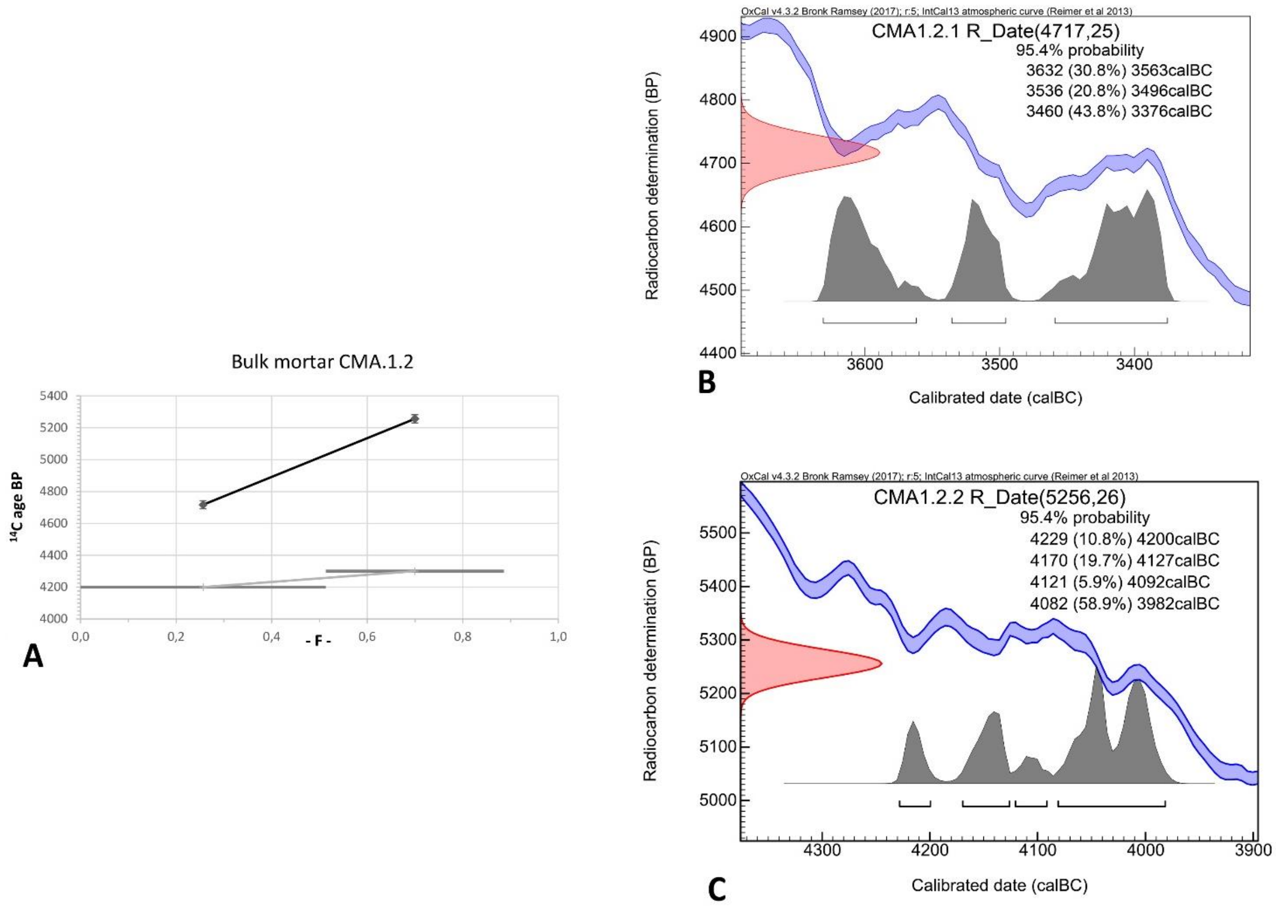

Fig. 60: A) ^{14}C age profile of the sample CMA1.2; B) calibrated result of fraction 1 (CMA1.2.1); C) calibrated result of the fraction 2 (CMA1.2.2).

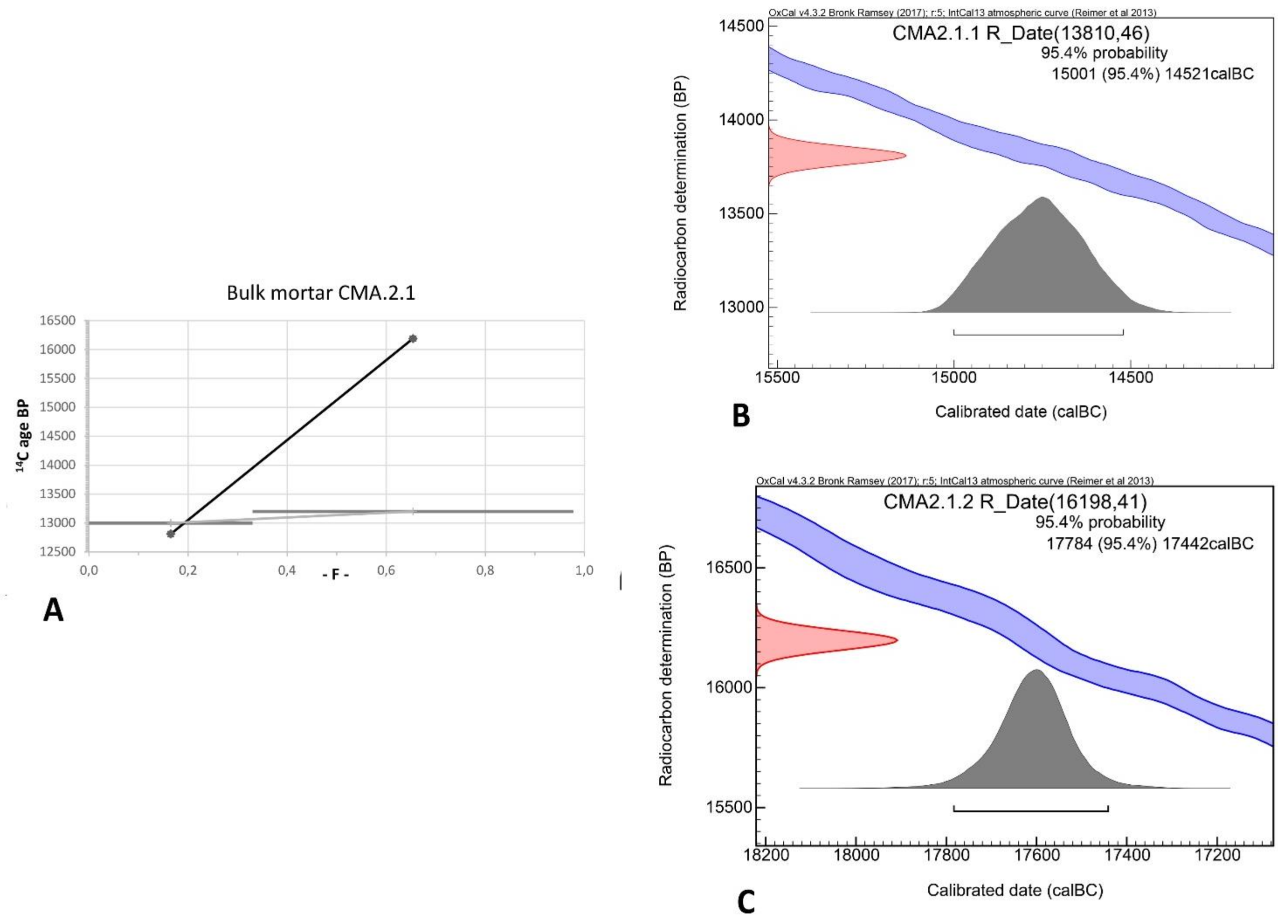

Fig. 61: A) ^{14}C age profile of the sample CMA2.1; B) calibrated result of fraction 1 (CMA2.1.1); C) calibrated result of the fraction 2 (CMA2.1.2).

The radiocarbon measurement on the samples was performed analyzing two CO_2 fractions.

Fraction 1 of the sample CMA1 yields a ^{14}C age of 4717 ± 25, calibrated 3632-3563 (30.8%), 3536-3496 (20.8%) and 3460-3376 (43.8%) BC, while the ^{14}C age of the fraction 2 (5256 ± 26 BP) corresponds with a calibrated calendar age 4229-4200 (10.8 %), 4170-4127 (19.7 %), 4121-4092 (5.9 %), 4082-3982 (58.9 %) BC (fig. 60).

The radiocarbon age of the fraction 1 of the sample CMA2 is 13810 ± 46 BP, calibrated 15001-14521 BC (95.4%) while the measurement of the fraction 2 has revealed ^{14}C ages of 16198 ± 41 BP corresponding with a calibrated calendar age 17784-17442 BC (95.4%) (fig. 61).

Both samples provided dates much older than expected (1st century BC), showing a dead carbon contamination. Since the sequential dissolution methodology has been proved efficient in eliminating the geological contribution of carbonate grains, it follows that the Pompeii mortars have been incorporated a different CO_2 source. According to Lindroos et al. (2011) this result is due to the contamination by volcanic CO_2 emission from the active Somma-Vesuvius volcano, that has affected the mortars buried in volcanic ashes after the fatal eruption in 79 AD. In this case the ^{14}C profile is biased towards an older age and it is impossible to attain the mortar setting period. As a consequence, the mortars buried under volcanic masses are not suitable for radiocarbon dating and no sample preparation procedure can remove the contamination.

12.3. Results of pollen analysis

Pollen concentration is sufficient (2569 p/g) and it is in line with what reported in works on similar materials (e.g. Langgut et al. 2013). The number of taxa identified is limited: 36.

Pollen evidence of the walnut tree (*Juglans*) and olive tree (*Olea*) has been identified in the sample. The presence of the two fruit trees seems extremely local according to the results obtained by the pollen analysis of the site Civita Giuliana (Pompeian territory) where a production system of walnuts was identified (unpublished data of the Laboratory of Palynology and Palaeobotany of the University of Modena and Reggio Emilia).

Pollen findings of ruderal plants (e.g. *Chenopodiaceae*, *Urtica dioica* type) have been also detected and they are correlated to the human activity in urban environments. Pollen of hygrophiles plants (e.g. *Alnus*, *Salix*) is present but scarce. Pollen evidence of chestnut tree (*Castanea sativa*) are associated to the piedmont sites of the Vesuvius area (Di Pasquale et al. 2010).

In addition, it is worth noting the presence of roses (*Rosa*), ornamental plant used probably in the garden of the House, and the evidence of cereals (*Hordeum* group) and commensal plants (e.g. *Papaver rhoeas* type) that attested the rural environment close to the city.

13. DISCUSSION

13.1. AMS Radiocarbon dating

Dating *pozzolana* mortars has been proven to be difficult from several studies (Lindroos 2005; Hodgins et al. 2011; Lindroos et al. 2011; Ringbom et al. 2011, 2014; Michalska and Czernik 2015; Nonni et al. 2017). Roman *pozzolana* is completely different from the normal lime mortar, it is hydraulic and can harden under water. For this reason, it was doubtful if *pozzolana* mortars would be suited for mortar dating, which depends on the interaction with atmospheric CO_2 in the hardening process. When *pozzolana* is added to the mortar, chemical reactions involving the slaked lime and the amorphous alumina-silicates of *pozzolana* occurred, increasing the mechanical resistance. *Pozzolana* mortars continue to be chemically active for a very long time and seem to produce readily soluble carbonates whenever exposed to atmospheric CO_2. The impermeable hydraulic mortar will retain pockets with un-reacted $Ca(OH)_2$ that will continue to react with CO_2 and form carbonates whenever the mortar is disturbed by breaking or crushing (Ringbom et al. 2011). Furthermore, the lower permeability to the air (and CO_2) compared to that of aerial mortars (Lindroos et al. 2011; Ringbom et al. 2011) may lead to delayed hardening. Both situations increase the risk of rejuvenation of the radiocarbon dating results.

Moreover, Lindroos et al. (2011) recognized that mortars buried under volcanic masses are not suited for dating. The main problem is the CO_2 emissions from the active Somma-Vesuvius volcano and the whole Campi Flegrei volcanic system at the Bay of Naples. If the atmospheric CO_2 was locally contaminated with excess volcanic CO_2 it is impossible to assess to what extent the ^{14}C age is influenced by radiocarbon dead material from the volcanoes. In this case the ^{14}C profile could be biased towards an older age.

However, the radiocarbon dating can be successful in discriminate the timing of the interventions.

The sample CMA from the House of Menander in Pompeii shows the same contamination widely identified in Roman mortars by Lindroos et al (2011) and contamination by dead carbon geological carbonate can be excluded given the successful sample preparation by sequential dissolution. Both fractions of the first layer of the sample provided an age ranging from 4229 to 3376 BC, that is much older than expected (1st century BC). The same for the second layer (17784-14521 BC). This means that the sample is a Roman repair mortar, extremely contaminated by volcanic CO_2 emission from the active Somma-Vesuvius volcano. The contamination, that aging the results, is originated from the volcanic masses that covered and buried the sample during the 79 AD fatal eruption of Vesuvius. Otherwise, if the sample had been a modern repair mortar, it would have yielded an age younger than expected providing the modern restoration timing.

Therefore, the repair mortars are ancient interventions probably carried out after the earthquakes of AD 62 that preceded the fatal eruption of the Vesuvius. Seneca (*Naturales Quaestiones*, Book VI) documented how the city of Pompeii has been overwhelmed in this strong earthquake, which shook all the surrounding districts as well. The earthquake was so intense that Pompeii suffered several damages and that part of the town of Herculaneum fell. In particular, the *Forum* Baths in Pompeii were strongly damaged and some modifications were performed. The bathtub of the *calidarium*, originally close to the western wall of the room, was removed and a new one was built in the north side (Pisapia et al. 2018). In this case, the repair mortar was used to fill the gap left from the previous bathtub (see fig. 52D).

13.2. Pollen analysis

The pollen spectra of the sample CMA (House of Menander) are compatible with the period before the Vesuvius eruption in AD 79. The sample displays a pollen record that testifies the human activities nearby the city of Pompeii, as walnut (*Juglans*) and olive trees (*Olea*), probably evidence of a production system, or cereal and poppy that suggest the presence of fields. Pollen of roses have been also identified as evidence of the ornamental plants that decorated the garden of the House.

The results give also an image of the vegetation surrounding the city such as the findings of chestnut tree, characteristic of the piedmont sites of the Vesuvius area.

Pollen of exotic plants that could suggest possible repairs in modern times have not been found. The archeological excavation of Pompeii started at the end of the 18th century when the import of exotic plant was widespread since 1500s, after the discovery of America. Therefore, if the repair would be a recent intervention, pollen of exotic plant should be present in the mortar sample. However, it is not possible to provide a reliable sample timing.

14. CONCLUSION OF THE CASE STUDY 2

The aim of the research was to clarify if the late interventions that covered some mosaic floors in Pompeii were an ancient or modern restoration. These repair mortar were found in important *domus* (House of *Paquius Proculus*, House of Menander, House of the Small Fountain, House VIII, 3, 24) and in the *Forum* baths and they were prepared to fill gaps in pavements to fix damages. Petrographic characterization, radiocarbon dating and pollen analysis have enabled to define the origin of the intervention.

Petrography of the repair mortars revealed a high homogeneity among the samples that display the same composition but they are different for grain size distribution and aggregate binder ratio. The samples are lime based mortars characterized by an aggregate consisting of pozzolanic fragments and singular idiomorphic crystals of pyroxene, leucite, plagioclase, sanidine, and biotite. Three samples from House of Menander show two layers with same aggregate composition but different distribution, while the sample A of the House VIII, 3, 24 is characterized by an abundant amount of crushed bricks (*cocciopesto*), finely ground. Some samples present an external surface prepared using an aggregate obtained by grinding pumice rock. The petrographic analysis suggests that the volcanic materials used for the mortar production comes from primary volcanoclastic deposits of the Vesuvian area which were not reworked.

According to the literature, Pompeii mortars buried under volcanic masses are not suitable for radiocarbon dating due to the contamination by the CO_2 emitted from the active Somma-Vesuvius volcano during the fatal eruption in 79 AD. The effect of the alteration is the ageing of the results, precluding to obtain the mortar setting period. However, the radiocarbon dating of the repair mortar sample from House of Menander was successful since the aim of the research was to discriminate the timing of the late intervention. In fact, the ^{14}C dating of the repair mortar provided an age that is much older than expected (1st century BC), suggesting that the sample is extremely contaminated by dead carbon. Since the sequential dissolution methodology has been proved efficient in eliminating the geological carbonate contaminant, it follows that the CO_2 emitted from the active Somma-Vesuvius volcano has been altered the ^{4}C results, as indicated by the literature. This means that the repair mortar is an ancient intervention that was preserved and buried under the volcanic ashes. Otherwise, if the sample has been a modern repair, it would have yielded an age younger than expected providing the modern restoration timing.

Moreover, the data obtained by testing pollen analysis on the same sample from House of Menander are compatible with the period before the Vesuvius eruption in 79 AD. The analysis revealed the presence of pollen concerning the human activity in the urban context or nearby the city of Pompeii. In particular, a local production system of walnuts and olives has been recognized and finding of cereals and poppy attested the rural environmental surrounding the city. Remarkable is also the presence of roses, probably used as ornamental plant of the garden of the House. Pollen evidence of exotic plants not belonging to the local habitat has not been found. This result is significant because the presence of pollen of exotic plants, imported from other continents since the 1500s, would indicate a modern intervention, carried out after 18th century, when the archeological excavation of Pompeii started.

In summary, the comparison of the results obtained by the different technique reveals that the late interventions are ancient restoration, probably carried out after the damaging earthquakes of 62 AD. The repairs were performed using a lime-based *pozzolana* mortar produced to fill gaps in the floors of the affected Houses.

According to these results an ancient unrecognized restoration phase is now fully recognized as another important part of the dramatic history of Pompeii, that should be preserved.

15. GENERAL CONCLUSION

The main objective of the thesis was to clarify the construction and restoration history of two case studies: Pompeii and the medieval Modena cathedral UNESCO sites.

A complex structure by the use of different mortars has been identified on the Modena cathedral vaults, suggesting late multiple modifications over time as a result of damaging earthquakes. The study provided new information about the restoration phases and new consideration about the vulnerability of the cathedral. The research was an important contribution to the anti-seismic reinforcement project, that was completed last year.

In Pompeii an ancient unrecognized restoration phase was identified. The research solved an archeological issue clarifying the origin of a repair intervention. A Roman pozzalanic mortar was produced in order to repair the damages probably caused by the earthquake of 62 AD, that preceding the fatal eruption of Vesuvius.

The thesis also allowed to make consideration about the different contamination sources that could affect the radiocarbon dating results.

Contamination by dead carbon was identified in the mortars of the Modena cathedral vaults, characterized by a fine calcareous aggregate and abundant underburned limestone relicts. The comparison of the two sample preparation procedures for radiocarbon dating (Cryo2Sonic and sequential dissolution) allowed to identify the most suitable method for eliminating the contaminant effect. According to the results, Cyo2Sonic procedure seems to be unsuitable for dating lime mortars with fine carbonate sand since this procedure is not able to separate the binder from the contaminants and all results obtained provided an age older than expected. On the contrary, sequential dissolution has provided the most reliable results, succeeding in selecting the good fraction representative of the setting moment.

Pompeii mortars show contamination by CO_2 emissions from the active Somma-Vesuvius volcano that affected the results providing ages much older than expected for roman building. This effect is characteristic of the mortars buried under volcanic masses, making them not suitable for radiocarbon dating, and no sample preparation procedure can remove the contamination. However, the radiocarbon dating is successful if the aim of the study is to discriminate the origin of the interventions, as illustrated by the research.

16. REFERENCES

Abrahamsen N., Jacobsen U., Mejdahl V., Mejdahl U. 1998. Magnetic investigations and datings of a brick kiln at Veldbaek near Esbjerg (Denmark). Physics and Chemistry of the Earth. 23 (9-10): 1015-1019.

Acidini Luchinat C., Serchia L., Piconi S. 1984. I restauri del Duomo di Modena (1875-1984). Modena: Panini, pp.394.

Addis A., Secco M., Marzaioli F., Artioli G., Chavarría Arnau A., Passariello I., Terrasi F., Brogiolo G.P. 2019. Selecting the most reliable 14C dating material inside mortars: the origin of the Padua cathedral. Radiocarbon. 61 (2): 375-393.

Aitken M.J., Tite M.S., Reid J. 1964. Thermoluminescent dating of ancient ceramics. Nature. 202: 1032-1033.

Aitken M.J., Zimmermann D.W., Fleming S.J. 1968. Thermoluminescent Dating of Ancient Pottery. Nature. 219: 442-445.

Aitken M. 1985. Thermoluminescence Dating. Oxford: Academic Press, pp. 359.

Al-Bashaireh K. 2013. Plaster and mortar radiocarbon dating of Nabatean and Islamic structures, south Jordan. Archaeometry. 55 (2): 329-354.

Ambers J. 1987. Stable carbon isotope ratios and their relevance to the determination of accurate radiocarbon dates for lime mortars. Journal of Archaeological Sciences. 14 (6): 569-576.

Andreini M., De Falco A., Giresini L., Sassu M. 2014. Structural damage in the cities of Reggiolo and Carpi after the earthquake on May 2012 in Emilia Romagna. Bulletin of Earthquake Engineering. 12 (5): 2445-2480.

Arnold L.J., Roberts R.G., Galbraith R.F, DeLong S.B. 2009. A revised burial dose estimation procedure for optical dating of young and modern-age sediments. Quaternary Geochronology. 4: 306-325.

Aulinas M., Civetta L., Di Vito M.A., Orsi G., Gimeno D., Férnandez-Turiel J.L. 2008. The “Pomici di mercato” Plinian eruption of Somma-Vesuvius: magma chamber processes and eruption dynamics. Bulletin of Volcanology. 70: 825–840.

Baraccani S., Silvestri S., Palermo M., Gasparini G., Trombetti T., Tomaso, Dib A. 2014. The assessment of the seismic behavior of the Cathedral of Modena, Italy. 2ECEES-2nd European Conference on Earthquake engineering and Seismology, Istanbul, 24-29 August.

Baraccani S., Palermo M., Silvestri S., Gasparini G., Trombetti T., Silvestri E. 2015. The structural strengthening of the Cathedral of Modena. SEWC 2015, 5th Structural Engineers World Congress: 1-5.

Baraccani S., Gasparini G., Palermo M., Silvestri S., Trombetti T. 2017. The structural behavior of the masonry vaults of the Cathedral of Modena. Proceedings of the 5th International Conference on Architecture and Civil Engineering, Singapore, 8-9 May, pp. 550-556.

Baraccani S., Palermo M., Trombetti T., DeJong M. 2019. Seismic Modelling of a Masonry Monument Including the Interaction of the Vaults, Longitudinal Walls and Soil. In Aguilar R., Torrealva D., Moreira S., Pando M.A., Ramos L.F. (eds). Structural Analysis of Historical Constructions. RILEM Bookseries, vol. 18. Springer, pp. 1099-1107.

Baracchi O. 1987. La cattedrale di Modena nei documenti della fabbrica di San Geminiano In Atti e memorie della Deputazione di storia patria per le antiche provincie modenesi. 11 (9): 157-222.

Baracchi O., Giovannini C. 1988. Il duomo e la torre di Modena: nuovi documenti e ricerche. Modena: Aedes Muratoriana, pp. 304.

Baracchi O. 1993. Volte a crociera e affreschi del Duomo: nuovi documenti del '400 e '500. Atti e memorie della Deputazione di storia patria per le antiche provincie modenesi. 11 (15): 131-156.

Barberi F., Bizouard H., Clocchiatti R., Metrich N., Santacroce R., Sbrava A. 1981. The Somma-Vesuvius Magma Chamber: a Petrological and Volcanological Approach. Bulletin of Volcanology.44 (3): 295-315.

Baronio G., Binda L. 1997. Study of the pozzolanicity of some bricks and clays. Construction and Building Materials. 11 (1): 41-46.

Baronio G., Binda L., Lombardini N. 1997. The role of brick pebbles and dust in conglomerates based on hydrated lime and crushed bricks. Construction and Building Materials. 11 (1): 33-40.

Baxter M.S., Walton A. 1970. Radiocarbon dating of mortars. Nature. 225 (5236): 937-938.

Bell W.T. 1979. Attenuation factors to absorbed dose in quartz inclusions for thermoluminescence dating. Ancient TL. 8: 2-13.

Benatti A., Bosi G., Rinaldi R., Labate D., Benassi F., Santini C., Bandini Mazzanti M. 2011. Testimonianze archeocarpologiche dallo spazio verde del Palazzo Vescovile di Modena (XII sec. d.C.) e confronto con la flora modenese attuale. Atti Società dei Naturalisti e Matematici di Modena. 142: 201-215.

Binda L., Baronio G. 1988. Survey of brick/binder adhesion in powdered brick mortars and plasters. Masonry International Journal. 2 (3): 87-92.

Böke H., Akkurt S., İpekoğlu B, Uğurlu E. 2006. Characteristics of brick used as aggregate in historic brick-lime mortars and plasters. Cement and Concrete Research. 36: 1115-1122.

Borges C., Silva A.S., Veiga R. 2014. Durability of ancient lime mortars in humid environment. Construction and Building Materials. 66: 606-620.

Bosi G., Benatti A., Rinaldi R., Dallai D., Santini C., Tomaselli M., Bandini Mazzanti M. 2015. The memory of water: archaeobotanical evidences from wetland plants of the past in the city of Modena. Plant Biosystems. 149 (1): 144-153.

Bosi G., Bandini Mazzanti M., Montecchi M.C., Torri P., Rinaldi R. 2017. The life of a Roman colony in Northern Italy: ethnobotanical information from archaeobotanical analysis. Quaternary International. 460: 135-156.

Bøtter-Jensen L., Solongo S., Murray A.S., Banerjee D., Jungner H. 2000. Using OSL single-aliquot regenerative-dose protocol with quartz extracted from building materials in retrospective dosimetry. Radiation Measurements. 32 (5-6): 841-845.

Bøtter-Jensen L., Murray A.S. 2002. Optically stimulated luminescence in retrospective dosimetry. Radiation Protection Dosimetry. 101: 309-314.

Bronk Ramsey C., Lee S. 2013. Recent and Planned Developments of the Program OxCal. Radiocarbon. 55 (2-3): 720-730.

Bronk Ramsey C. 2017. OxCal [WWW program] version 4.3. Oxford Radiocarbon Accelerator Unit: University of Oxford. Available at https// c14.arch.ox.ac.uk/oxcal/OxCal.

Bruni S., Cariati F., Fermo P., Cairati P., Alessandrini G., Toniolo L. 1997. White lumps in fifth to seventeenth century AD mortars from northern Italy. Archeometry. 39 (1): 1-7.

Bugini R., Salvatori A., Capannesi G., Sedda A.F., D'agostini C., Giuliani C.F. 1993. Investigation of the characteristics and properties of "cocciopesto" from the ancient Roman period. In Thiel M.J. Conservation of stone and other materials. Vol. 1: causes of disorders and diagnosis. Proceedings of the international RILEM/UNESCO Congress, Paris, June 29-July 1, 1993, pp. 386-393.

Candigliota E., Carpani B., Immordino F., Poggianti A. 2012. Damage to religious buildings due to the Pianura Padana Emiliana earthquake. Energia, Ambiente e Innovazione. 4-5: 58-68.

Carò F, Di Giulio A. 2004. Reliability of textural analysis of ancient plasters and mortars through automated image analysis. Materials Characterization. 53: 243-257.

Caroselli M. 2015. Mortar, plaster and brick dating: The case study of the Modena Medieval UNESCO site. PhD thesis, Università di Modena e Reggio Emilia, pp. 181.

Carran D., Hughes J.J., Leslie A., Kennedy C. 2010. Lime lump development and textural alteration during the production of mortar. Proceedings of the 2nd Historic Mortars Conference HMC2010 and RILEM TC 203-RHM Final Workshop, Prague, Czech Republic, pp. 437-445.

Cazalla O., Rodriguez-Navarro C., Sebastian E., Cultrone G., De la Torre MJ. 2000. Aging of Lime Putty: Effects on Traditional Lime Mortar Carbonation. Journal of the American Ceramic Society. 83 (5): 1070-76.

Cechák T., Gerndt J., Kubelík M., Musílek L., Pavlík M. 2000. Radiation methods in research of ancient monuments. Applied Radiation and Isotopes. 53 (4-5): 565-570.

Crane P.R., Nagata T., Mutara J., Ohi-Toma T., DuVal A., Nesbitt M., Jarvis C. 2013. Ginkgo biloba: connections with people and art across a thousand years. Curti’s Botanical Magazine. 30 (3): 239-260.

De Rienzo V., Di Vito M.A., Arienzo I., Carandente A., Civetta L., D’Antonio M., Giordano F., Orsi G., Tonarini S. 2007. Magmatic History of Somma-Vesuvius on the Basis of New Geochemical and Isotopic Data from a Deep Borehole (Camaldoli dellaTorre). Journal of Petrology. 48 (4): 753-784.

De Toni G.B. 1887. Intorno ad alcuni alberi e frutici ragguardevoli esistenti nei giardini di Padova. Atti Reale Accademia di Padova, Padova, pp. 25.

Decanini L., Liberatore D., Liberatore L., Sorrentino L. 2012. Preliminary report on the 2012, May 20, Emilia earthquake, vol.1, pp. 70. <http://www.eqclearinghouse.org/2012-05-20-italy-it/>.

Delibrias G., Labeyrie J. 1965. The dating of mortars by the carbon-14 method. 6th International Conference on Radiocarbon and Tritium Dating. Washington: Ed. Pullman: 344-347.

Dieghi C. 2009. Sources and studies for the history of the Ghirlandina. In Cadignani R. (ed) The Ghirlandina Tower. Conservation Project. Roma: Luca Sossella editore, pp. 48-65.

Di Pasquale G., Allevato E., Russo Ermolli E., Coubray S., Lubritto C., Marzaioli F., Yoneda M., Takeuchi K., Kano Y., Matsuyama S., De Simone G.F. 2010. Reworking the idea of chestnut (*Castanea sativa* Mill.) cultivation in Roman times: New data from ancient Campania. Plant Biosystems. 144 (4): 865-873.

Dolce M., Nicoletti M., Ammirati A., Bianconi R., Filippi L., Gorini A., Marcucci S., Palma F., Zambonelli E., Lavecchia G., de Nardis R., Brozzetti F., Boncio P., Cirillo D., Romano A., Costa G., Gallo A., Tiberi L., Zoppé G., Suhadolc P., Ponziani F., Formica A. 2012. The Emilia thrust earthquake of 20 May 2012 (Northern Italy): strong motion and geological observations. The national Civil Protection Department Report I, pp. 12.

Dolce M., Nicoletti M., Ammirati A., Bianconi R., Filippi L., Gorini A., Marcucci S., Palma F., Zambonelli E., Lavecchia G., de Nardis R., Brozzetti F., Boncio P., Cirillo D., Romano A., Costa G., Gallo A., Tiberi L., Zoppé G., Suhadolc P., Ponziani F., Formica A. 2012. The Ferrara arc thrust earthquakes of May-June 2012 (northern Italy): strong-motion and geological observations. The national Civil Protection Department Report II, pp. 11.

Dondi A. 1896. Notizie storiche ed artistiche del Duomo di Modena raccolte ed ordinate dal can. A. D. con l'elenco dei codici capitolari in appendice. Modena: Edizione Aldine, pp. 301.

Duller G.A.T. 1994. Luminescence dating of sediments using single aliquots: new procedures. Quaternary Science Reviews. 13: 149-156.

Duller G.A.T., Bøtter-Jensen L., Murray A.S. 2000. Optical dating of single sand-sized grains of quartz: Sources of variability. Radiation Measurements. 32: 453-457.

Duller G., Murray A.S. 2000. Luminescence dating of sediments using individual mineral grains. Andean Geology. 5: 87-106.

Duller G. 2008. Luminescence Dating: Guidelines on using luminescence dating in archaeology. Swindon: English Heritage, pp. 43.

Elert K., Rodriguez-Navarro C., Sebastian Pardo E., Hansen E., Cazalla O. 2002. Lime Mortars for the Conservation of Historic Buildings. International Institute for Conservation of Historic and Artistic Works. 47: 62-75.

Elsen J. 2006. Microscopy of historic mortar: a review. Cement Concrete Research. 36: 1416-1424.

Elsen J., Van Balen K., Mertens G. 2012. Hydraulicity in historic lime mortars: a review. In Válek J., Hughes J.J., Caspar, Groot C.J.W.P. (eds) Historic Mortars. Characterization, Assessment and Repair. Netherlands: Springer, pp. 125-139.

Fedi M.E., Bernardoni V., Caforio L., Calzolai G., Carraresi L., Manetti M., Taccetti F., Mandò P.A. 2013. Status of sample combustion and graphitization lines at INFN-LABEC, Florence. Radiocarbon. 55: 657-664.

Ferrari, P., Trevisan, G., Dallai, D. 1986. Rilevazione differenziale delle piogge polliniche nella città di Modena (msm 39) col metodo dei transects muscinali. Bollettino dell'Accademia Gioenia di Scienze Naturali. 19 (329): 147-175.

Fedi M.E., Cartocci A., Manetti M., Taccetti F., Mandò P.A. 2007. The 14C AMS facility at LABEC, Florence. Nuclear Instruments and Methods in Physics Research Section B: 259: 18-22.

Fleming S.J. 1970. Thermoluminescent dating: refinement of the quartz inclusion method. Archaeometry. 12 (2): 133-143.

Fleming S.J. 1979. Thermoluminescence techniques in archaeology. Oxford: The Clarendon Press, pp. 233.

Florenzano A., Mercuri A.M., Pederzoli A., Torri P., Bosi G., Olmi L., Rinaldi R., Bandini Mazzanti M. 2012. The significance of intestinal parasite remains in pollen samples from medieval pits in the Piazza Garibaldi of Parma, Emilia Romagna, Northern Italy. Geoarcheology. 27: 34-47.

Folk R., Valastro S. 1976. Successful technique for dating of lime mortars by carbon-14. Journal of field Archeology. 3: 203-208.

Fratini F, Pecchini E., Cantisani C. 2008. The petrographic study in the ancient mortar characterization. HMC 08. 1st Historical Mortar Conference, 24th to 27th September, Lisbon, Portugal, pp. 1-10.

Galbraith R.F., Roberts R.G., Laslett G.M., Yoshida H., Olley J.M. 1999. Optical dating of single and multiple grains of quartz from Jinmium rock shelter, northern Australia: Part I, experimental design and statistical models. Archaeometry. 41: 339-364.

Galli A., Martini M., Maspero F., Panzeri L., Sibilia E. 2014. Surface dating of bricks, an application of luminescence techniques. The European Physical Journal Plus. 129: 101-110.

Goedicke C., Slusallek K., Kubelik M. 1981. Thermoluminescence dating in architectural history: Venetian villas. Journal of the Society of Architectural Historians. 40 (3): 203-217.

Goedicke C. 2003. Dating historical calcite mortar by blue OSL: results from known age samples. Radiation Measurements. 37: 409-415.

Goedicke C. 2011. Dating mortars by Optically Stimulated luminescence: a feasibility study, Geochronometria. 38 (1): 42-49.

Göksu H.Y., Schwenk P. 2001. Investigation of the thermal stability of the 210°C TL peak of quartz and dating the components of terrazzo from the monastery church of Tergnsee. Radiation Measurements. 33 (5): 785-792.

Graziani L., Bernardini F., Castellano C., Del Mese S., Ercolani E., Rossi A., Tertulliani A., Vecchi M. 2015. The 2012 Emilia (Northern Italy) earthquake sequence: an attempt of historical reading. Journal of Seismology. 19: 371-387.

Grogler N., Houtermans F., Stauffer H. 1960. About dating of ceramics and bricks using thermoluminescence. *Helvetica Physica Acta*. 33: 595-596.

Gueli A.M., Stella G., Troja S.O., Burrafato G., Fontana D., Ristuccia G.M., Zuccarello A.R. 2010. Historical buildings: Luminescence dating of fine grains from bricks and mortar. Il Nuovo Cimento B. 125: 719-729.

Habermann D., Neuser R.D., Richter K. 2000. Quantitative high resolution spectral analysis of Mn2+ in sedimentary calcite. In Pagel M., Barbin V., Blanc P., Ohnenstetter D. (eds). Cathodoluminescence in geosciences. Springer Verlag, pp. 331-358.

Hajdas I. Bonani G., Thut J., Leone G, Pfenninger R., Maden C. 2004. A report on sample preparation at the ETH/PSI AMS facility in Zurich. Nuclear Instruments and Methods in Physics Research B. 223-224: 267-271.

Hajdas I., Lindroos A., Heinemeier J., Ringbom Å., Marzaioli F., Terrasi F., Passariello I., Capano M., Artioli G., Addis A., Secco M., Michalska D., Czernik J., Goslar T., Hayen R., Van Strydonck M., Fontaine L., Boudin M., Maspero F., Panzeri L., Galli A., Urbanova P., Guibert P. 2017. Preparation and dating of mortar samples-mortar dating inter-comparison study (MODIS). Radiocarbon. 59 (5): 1-14.

Hale J., Heinemeier J, Lancaster L., Lindroos A., Ringbom Å. 2003. Dating Ancient Mortar. American Scientist. 91 (2): 130-137.

Hayen R., Van Strydonck M., Fontaine L., Boudin M., Lindroos A., Heinemeier J., Ringbom Å., Michalska D., Hajdas I., Hueglin S., Marzaioli F., Terrasi F., Passariello I., Capano M., Maspero F., Panzeri L., Galli A., Artioli G., Addis A., Secco M., Boaretto E., Moreau C., Guibert P., Urbanova P., Czernik J., Goslar T., Caroselli M. 2017. Mortar dating methodology: assessing recurrent issues and needs for further research. Radiocarbon. 59 (6): 1859-1871.

Heinemeier J., Jungner H., Lindroos A., Ringbom Å., Von Konow T., Rud N. 1997. AMS 14C dating of lime mortar. Nuclear Instruments and Methods in Physics Research B. 123 (1-4): 487-495.

Heinemeier J., Ringbom Å., Lindroos A., Sveinbjörnsdóttir A.E. 2010. Successful AMS 14C dating of non-hydraulic lime mortars from the Medieval churches of the Åland Islands, Finland. Radiocarbon. 52 (1): 171-204.

Hodgins G., Lindroos A., Ringbom Å., Heinemeier J., Brock F. 2011. 14C Dating of Roman Mortars – Preliminary Tests Using Diluted Hydrochloric Acid Injected in Batches. Proceedings from Building Roma *Aeterna*, conference, Rome, March 23–25, 2008. In Ringbom Å., Hohlfelder R. (eds). *Commentationes Humanarum Litterarum*, *Societas Scientiarium Fennica*. 128: 209-213.

Hughes J.J., Cuthbert S.J. 2000. The petrography and microstructure of medieval lime mortars from the west of Scotland: Implications for formulation of repair and replacement mortars. Materials and Structures. 33: 594-600.

Hughes J.J., Leslie A.B., Callebaut K. 2001.The petrography of lime inclusions in historic lime based mortars. *Annales Geologiques des pays Helleniques*. 39: 359-364.

Huntley D J., Godfrey-Smith D.I, Thewalt. M.L.W. 1985. Optical dating of sediments. Nature. 313: 105-107.

Hütt G., Göksu H.Y., Jaek I., Hiekkanen M. 2001. Luminescence dating of Somero sacristy, SW Finland using the 210°C TL peak in quartz. Quaternary Science Reviews. 20 (5-9): 773-777.

Indirli M., Marghella G., Marzo A. 2012. Damage and collapse mechanism in churches during the Pianura Padana Emiliana earthquake. Energia Ambiente Innovazione. 4/5: 69-94.

ISIDe, http://iside.rm.ingv.it/: ISIDe working group (2016) version 1.0, DOI: 10.13127/ISIDe.

Ioannis Liritzis I., Singhvi A.K., Feathers J.K., Wagner G.A., Kadereit A., Zacharias N., Sheng-Hua Li S.H. 2013. Luminescence Dating in Archaeology, Anthropology, and Geoarchaeology. Springer International Publishing, pp. 70.

Joron J.L., Metrich N., Rosi M., Santacroce R., Sbrana A. 1987. Chemistry and Petrography Chemistry and Petrography of Somma-Vesuvius. In Santacroce R. (ed). Somma-Vesuvius. Roma: Consiglio Nazionale della Ricerca. Quaderni della Ricerca Scientifica. 8: 105-174.

Kennedy G.C., Knopff L. 1960. Dating by thermoluminescence. Archaeology. 13: 147-148.

Labate D. 2009. Archeology's contribution to understanding a monument. In Cadignani R. (ed) The Ghirlandina Tower. Conservation Project. Roma: Luca Sossella editore, pp. 66-77.

Labeyrie J., Delibrias G. 1964. Dating of old mortars by the carbon-14 method. Nature. 201: 742.

Langgut D., Gadot Y., Porat N. Lipschits O. 2013. Fossil pollen reveals the secrets of the Royal Persian Garden at Ramat Rahel, Jerusalem. Palynology. 37 (1): 115-129.

Lichtenberger A., Lindroos A., Raja R., Heinemeier J. 2015. Radiocarbon analysis of mortar from Roman and Byzantine water management installations in the Northwest Quarter of Jerash, Jordan, Journal of Archaeological Science. Reports 2: 114-127.

Lindroos A. 2005. Carbonate phases in historical lime mortars and pozzolana concrete: implication for 14C dating. PhD thesis, Abo Akademy University, pp.92.

Lindroos A., Heinemeier J., Ringbom Å., Braskén M., Sveinbjörnsdóttir Á. 2007. Mortar dating using AMS 14C and sequential dissolution: examples from Medieval, non-hydraulic lime mortars from the Åland Islands, SW Finland. Radiocarbon. 49 (1): 47-67.

Lindroos A., Heinemeier J., Ringbom Å., Brock F., Sonck-Koota P., Pehkonen M., Suksi J. 2011. Problems in radiocarbon dating of Roman pozzolana mortars. Proceedings from Building Roma *Aeterna*, conference, Rome, March 23–2, 2008. In Ringbom Å., Hohlfelder R. (eds). *Commentationes Humanarum Litteraru*, *Societas Scientiarium Fennica*. 128: 214-230.

Lindroos A., Ranta H., Heinemeier J., Lill JO. 2014. 14C chronology of the oldest Scandinavian church in use: an AMS/PIXE study of lime lump carbonate in the mortar. Nuclear Instruments and Methods in Physics Research B. 331: 220-224.

Lindroos A, Heinemeier J., Ringbom Å., Hodgins G., Sonk-Koota P., Sjöberg P., Lancaster L., Kaisti R., Brock F., Ranta H., Caroselli M., Lugli S. 2018. Radiocarbon dating historical mortars: lime lumps and/or binder carbonate? Radiocarbon. 60 (3): 875-899.

Lindroos A, Heinemeier J., Ringbom Å. 2019. Radiocarbon dating of lime mortars. The sequential dissolution method. In Rita Vecchiattini. Archeologia dell'Architettura, vol.24. Sesto Fiorentino: All'Insegna del Giglio, p. 11-17.

Lowe J.J., Accorsi C.A., Bandini Mazzanti M., Bishop A., Forlani L., van der Kaars S., Mercuri A.M., Rivalenti C., Torri P., Watson C. 1996. Pollen stratigraphy of sediment sequences from crater lakes (Lago Albano and Lago Nemi) and the Central Adriatic spanning the interval from oxygen isotope Stage 2 to present day. Memorie dell'Istituto Italiano di Idrobiologia. 55: 71–98.

Lugli S., Marchetti Dori S., Fontana D. 2007. Alluvial sand composition as a tool to unravel the Late Quaternary sedimentation of the Modena Plain, northern Italy. In Arribas J., Critelli S., Johnsson M.J. Sedimentary Provenance and Petrogenesis: Perspectives from Petrography and Geochemistry. United States: Geological Society of America Special Paper. 420: 57-72.

Lugli S., Marchetti Dori, S., Zolli, K., Melloni, C., Pedrazzi, S., Maiorano, C. 2010. The building materials inside the tower: stones, bricks, mortars and plasters. In Cadignani R. and Lugli S. (eds) The Ghirlandina Tower. History and restoration, Roma: Luca Sossella editore, pp. 178-189.

Lugli S., Marchetti Dori S., Caroselli M. 2013. Petrography of mortars and plasters as a tool to distinguish construction phases for the historical buildings of the Modena area (Northern Italy). Proceedings of the 3rd Historic Mortars Conference, 11-14 September 2013, Glasgow, Scotland.

Lugli S., Caroselli M., Marchetti Dori S., Vandelli V., Marzani G., Segattini R., Bianchi C., Weber J. 2016. Building materials and degradation phenomena of the Finale Emilia Town Hall (Modena): an archaeometric study for the restoration project after the 2012 earthquake. Periodico di Mineralogia. 85 (1): 59-67.

Machel H. 2000. Application of cathodoluminescence to carbonate diagenesis. In Pagel M., Barbin V., Blanc P., Ohnenstetter D. (eds). Cathodoluminescence in geosciences. Springer Verlag, pp. 271-301.

Maniero F. 2000. Fitocronologia d'Italia. Firenze: Leo S. Olschki, pp. 296.

Margalha M.G., Santos Silva A., Veiga M., Brito J., Ball R., Allen G. 2013. Microstructural changes of lime putty during aging. American Society of Civil Engineers. 25 (10): 1524-1532.

Marshall D.J. 1988. Cathodoluminescence of geological materials. Boston: Unwin Hyman, pp. 450.

Martini M., Sibilia E. 2001. Radiation in archaeometry: archaeological dating. Radiation Physics and Chemistry. 61 (3-6): 241-246.

Martini M., Sibilia E. 2006. Absolute dating of historical buildings: the contribution of thermoluminescence (TL). Journal of Neutron Research. 14: 69-74.

Marzaioli F., Borriello G., Passariello I., Lubritto C., De Cesare N., D'Onofrio A., Terrasi F. 2008. Zinc reduction as an alternative method for AMS radiocarbon dating: process optimization at CIRCE. Radiocarbon. 50 (1): 139-49.

Marzaioli F., Lubritto C., Nonni S., Passariello I., Capano M., Terrasi F. 2011. Mortar radiocarbon dating: preliminary accuracy evaluation of a novel methodology. Analytical Chemistry. 83 (6): 2038-2045.

Marzaioli F., Nonni S., Passariello I., Capano M., Ricci P., Lubritto C., De Cesare N., Eramo G., Castillo J.A.Q., Terrasi F. 2013. Accelerator mass spectrometry 14C dating of lime mortars: methodological aspects and field study applications at CIRCE (Italy). Nuclear Instruments and Methods in Physics Research B. 294: 246-251.

Mejdahl V. 1985. Thermoluminescence dating based on feldspars. Nuclear Tracks and Radiation Measurements. 10: 133-136.

Michalska D., Czernik J. 2015. Carbonates in leaching reactions in context of 14C dating. Nuclear Instruments and Methods in Physics Research B. 361: 431-439.

Michalska D., Czernik J., Goslar T. 2017. Methodological Aspect of Mortars Dating (Poznań, Poland, MODIS). Radiocarbon. 59 (6): 1891-1906.

Miriello D., Barca D., Bloise A., Ciarallo A., Crisci G.M., De Rose T., Gattuso C., Gazineo F., La Russa M. 2010. Characterization of archaeological mortars from Pompeii (Campania, Italy) and identification of construction phases by compositional data analysis. Journal of Archaeological Sciences. 37: 2207-2223.

Moore P.D., Webb J.A., Collins M.E. 1991. Pollen Analysis. 2nd ed. Oxford: Blackwell Scientific Publication, pp. 216.

Moropoulou A., Bakolas A., Anagnostopoulou S. 2005. Composite materials in ancient structures. Cement & Concrete Composites. 27: 295-300.

Murray A.S., Roberts R.G. 1997. Determining the burial time of single grains of quartz using optically stimulated luminescence. Earth and Planetary Science Letters. 152: 163-180.

Murray A.S., Wintle A.G. 1999. Isothermal decay of optically stimulated luminescence in quartz. Radiation Measurements. 30: 119-125.

Murray A.S., Wintle A.G. 2000. Luminescence dating of quartz using an improved single-aliquot regenerative-dose protocol. Radiation Measurements. 32: 57-73.

Murray A.S., Wintle A.G. 2003. The single aliquot regenerative dose protocol: potential for improvements in reliability. Radiation Measurements. 37: 377-381.

Nawrocka D.M., Michniewicz J., Pawlyta J. and Pazdur A. 2005. Application of radiocarbon method for dating of lime mortars. Geochronometria. 24: 109-115.

Nonni S., Marzaioli F., Secco M., Passariello I., Capano M., Lubritto C., Mignardi S., Tonghini C., Terrasi F. 2013. 14C Mortar Dating: The Case of the Medieval Shayzar Citadel, Syria. Radiocarbon. 55 (2-3): 514-525.

Nonni S. 2014. An innovative method to select a suitable fraction for mortar 14C dating: the Cryo2SoniC protocol, PhD thesis, Università La Sapienza, Roma, pp. 153.

Nonni S., Marzaioli F., Mignardi S., Passariello I., Capano M., Terrasi F. 2017. Radiocarbon dating of mortars with a pozzolana aggregate using the cryozonic protocol to isolate the binder. Radiocarbon. 60 (2): 1-21.

Ortega L.A., Zuluaga M.C., Alonso-Olazabal A., Inasausti M., Ibañez A. 2008 Geochemical characterization of archeological lime mortars: provenance inputs. Archaeometry. 50 (3): 387-408.

Ortega L.A., Zuluaga M.C., Alonso-Olazabal A., Murelaga X., Inasausti M., Ibanez-Exteberria A. 2012. Historic lime-mortar 14C dating of Santa María La Real (Zarautz, Northern Spain): Extraction of suitable grain size for reliable 14C dating. Radiocarbon. 54 (1): 23-36.

Pachiaudi C., Marechal J., Van Strydonck M., Dupas M., Dauchot-Dehon M. 1986. Isotopic fractionation of carbon during CO2 absorption by mortar. Radiocarbon. 28 (2A): 691-697.

Pagel M., Barbin V., Blanc P., Ohnenstetter D. 2000. Cathodoluminescence in geosciences. Springer Verlag, pp.514.

Panzeri L., 2013. Mortar and surface dating with optically stimulated luminescence (OSL): innovative techniques for the age determination of buildings. Il Nuovo Cimento. 36 (4): 205-216.

Panzeri L., Cantù M., Martini M., Sibilia E. 2017. Application of different protocols and age-models in OSL dating of earthen mortars. Geochronometria. 44: 341-351.

Panzeri L., Caroselli M., Galli A., Lugli S., Martini M., Sibilia E. 2019. Mortar OSL and brick TL dating: the case study of the UNESCO world heritage site of Modena. Quaternary Geochronology. 49: 236-241.

Parisi F., Augenti N. 2013. Earthquake damages to cultural heritage constructions and simplified assessment of artworks. Engineering Failure Analysis. 34: 735-760.

Pavia S., Caro S. 2006. Lime mortars for masonry repair: Analytical science and laboratory testing versus practical experience. In Delgado Rodrigues J, Mimoso J.M. (eds). Proceedings of International Seminar Theory and Practice in Conservation. A tribute to Cesare Brandi, Laboratorio Nacional de Engenharia Civil, Lisboa, pp. 493-500.

Pavia S., Fitzgerald B., Treacy E. 2006. An assessment of lime mortars for masonry repair. In McNally C. (ed). Concrete Research in Ireland Colloquium, Dublin, December 2005, pp. 101-108.

Pavia S. 2008. A petrographic study of mortar hydraulicity. HMC08, Historical Mortars Conference: Characterization, Diagnosis, Conservation, Repair and Compatibility. LNEC, Laboratorio General Engenharia Civil, Lisbon, September, 2008.

Pavia S., Caro S. 2008. An investigation of Roman mortar technology through the petrographic analysis of archeological material. Construction and Building Materials. 22 (8): 1807-1811.

Pecchioni E., Fratini F., Cantisani E. 2014. Atlas of the ancient mortars in thin section under optical microscope. Firenze: Nardini Editore, pp. 80.

Pesce G., Quarta G., Calcagnile L., D'Elia M., Cavaciocchi P., Lastrico C., Guastella R. 2009. Radiocarbon dating of lumps from aerial lime mortars and plasters: Methodological issues and results from S. Nicolò of Capodimonte church (Camogli, Genoa – Italy). Radiocarbon. 51 (2): 867-872.

Pesce G., Ball R. 2012. Dating of Old Lime Based Mixtures with the "Pure Lime Lumps" Technique. In Nawrocka D.M. (ed.). Radiometric Dating. InTech Open, pp. 21-39.

Pesce G.L., Ball R.J., Quarta G., Calcagnile L. 2012. Identification, extraction, and preparation of reliable lime samples for 14C dating of plasters and mortars with the "pure lime lumps" technique. Radiocarbon. 54 (3-4): 933-942.

Pesce G., Ball R. 2015. Radiocarbon dating of lime mortars. Journal of the Building Limes Forum. 22: 15-24.

Piccinini F. 2009. Notes on the construction of the Cathedral and the Ghirlandina Tower. In Cadignani R. (ed) The Ghirlandina Tower. Conservation Project. Roma: Luca Sossella Editore, pp. 42-47.

Pisapia M.S., Tirelli G., Lugli S. 2018. Una forma sconosciuta di restauro antico dei mosaici: la patinatura a Pompei. In Angelelli C., Cecalupo C., Erba M.E., Massara D., Rinaldi F., Laboranti S. (eds). Atti del XXIII Colloquio dell'Associazione italiana per lo studio e la conservazione del mosaico. Roma: Edizioni Quasar, pp. 527-534.

Pistoni G. 1977. Cesare Costa e il Duomo di Modena. In Cesare Costa: contributi di studio presentati a ricordo nel centenario della morte. Modena: Lo Scoltenna, pp. 57-64.

Preusser F., Degering D., Fuchs M., Hilgers A., Kadereit, A., Klasen N., Krbetschek M., Richter D., Spencer J. 2008. Luminescence dating: basics, methods and application. Eiszeitalter & Gegenwart / Quaternary Science Journal. 57 (1-2): 95-149.

Reille M. 1992. Pollen et spores d'Europe et d'Afrique du Nord. Marseille: Laboratoire de botanique historique et palinologie, pp. 543.

Reimer P.J., Bard E., Bayliss A., Warren Beck J., Blackwell P.G, Bronk Ramsey C., Buck C.E., Cheng H., Lawrence Edwards R., Friedrich M., Grootes P.M., Guilderson T.P., Hafildason H., Hajdas I., Hatté C., Heaton T.J., Hoffmann D.K.L., Hogg A.G., Hughen K.A., Felix Kaiser K., Kromer B., Manning S.W., Niu M., Reimer R.W., Richards D.A., Scott E.M., Southon J.R., Staff E.A., Turney C.S.M., Van der Plicht J. 2013. IntCal13 and Marine13 radiocarbon age calibration curves 0–50,000 years cal BP. Radiocarbon. 55 (4): 1869-1887.

RILEM TC 167-COM: Characterization of Old Mortars, Com-C1 Assessment of Mix Proportions in Historical Mortars Using Quantitative Optical Microscopy. Materials and Structures. 34: 387-388.

Ringbom Å., Heinemeier J., Lindroos A., Brock F. 2011.Mortar dating and Roman Pozzolana, results and interpretation. In Ringbom Å., Hohlfelder R. (eds). Proceedings from Building Roma *Aeterna*, conference in Rome, March 23-25 2008. *Commentationes Humanarum Litterarum*, *Societas Scientiarium Fennica*. 128: 187-208.

Ringbom Å., Lindroos A., Heinemeier J., Sonck-Koota P. 2014. 19 years of mortar dating: learning from experience. Radiocarbon. 56 (2): 619-635.

Rodriguez-Navarro C., Hansen E., Ginell WS. 1998. Calcium Hydroxide Crystal Evolution upon Aging of Lime Putty. Journal of American Ceramic Society. 81 (11): 3032-3034.

Rovida A., Locati M., Camassi R., Lolli B., Gasperini P. 2016. CPTI15, the 2015 version of the Parametric Catalogue of Italian Earthquakes. Istituto Nazionale di Geofisica e Vulcanologia (INGV).

Rozanski K., Stichler W., Gonfiantini R., Scott E.M., Beukens R.P., Kromer B. and Van der Plich J. 1992. The IAEA 14C intercomparison exercise 1990. Radiocarbon. 34 (3): 506.

Saccardo P.A. 1909. Cronologia della Flora italiana. Padova: Tipografia del Seminario, pp.390.

Sawakuchi A.O., Blair M.W., DeWitt R., Faleiros F.M., Hyppolito T., Guedes C.C.F. 2011. Thermal history versus sedimentary history: OSL sensitivity of quartz grains extracted from rocks and sediments. Quaternary Geochronology. 6: 261-272.

Silva J., de Brito J., Veiga R. 2009. Incorporation of fine ceramics in mortars. Construction and Building Materials. 23 (1): 556-564.

Sonninen E., Erametsa P., Jungner H. 1985. Dating mortar and bricks from the castle of Kastelholm. ISKOS. 5: 384-389.

Sonninen E., Jungner H. 2011. An improvement in preparation of mortar for radiocarbon dating. Radiocarbon. 43 (2A): 271-273.

Stefanidou M., Papayianni I. 2005. The role of aggregates on the structure and properties of lime mortars. Cement & Concrete Composites. 27: 914-919.

Stella G., Fontana D., Gueli A.M., Troja S.O. 2013. Historical mortars dating from OSL signals of fine grain fraction enriched in quartz. Geochronometria. 40 (3): 153-164.

Stella G., Fontana D., Gueli A.M., Troja S.O. 2014. Different approaches to date bricks from historical buildings. Geochronometria. 41 (3): 256-264.

Stella G., Almeida L., Basílio L., Pasquale S., Dinis J., Almeida M., Gueli A.M. 2018. Historical building dating: a multidisciplinary study of the Convento de São Francisco (Coimbra, Portugal). Geochronometria. 45: 119-129.

Stockmarr J. 1971. Tablets with spores used in absolute pollen analysis. Pollen et Spores. 1: 615-621.

Stuiver M., Smith C.S. 1965. Radiocarbon dating of ancient mortar and plaster. 6th International Conference on Radiocarbon and Tritium Dating. Washington: Ed. Pullman, pp. 338-343.

Targioni Tozzetti A. 1853. Cenni storici sulla introduzione di varie piante nell'agricoltura ed orticoltura Toscana. Firenze: Tipografia Galileana, pp. 324.

Terrasi F., De Cesare N., D'Onofrio A., Lubritto C., Marzaioli F., Passariello I., Rogalla D., Sabbarese C., Borriello G., Casa G., Palmieri A. 2008. High precision 14C AMS at CIRCE. Nuclear Instruments and Methods in Physics Research B. 266 (10): 2221-2224.

Tite M. S., Waine J. 1962. Thermoluminescent dating: a re-appraisal. Archaeometry. 5: 53-79.

Tubbs L.E., Kinder T.N. 1990. The use of AMS for dating of lime mortars. Nuclear Instruments and Methods in Physics Research. 52 (3-4): 438-441.

UNI 11176. 2016. Beni Culturali-Descrizione petrografica di una malta.

Urbanová P., Hourcade D., Ney C., Guibert P. 2015. Sources of uncertainties in OSL dating of archaeological mortars: the case study of the Roman amphitheatre Palais-Gallien in Bordeaux. Radiation Measurements. 72: 100-110.

Urbanová P., Delaval E., Dufresne P., Lanos P., Guibert P. 2016. Multi-method dating of Grimaldi castle foundations in Antibes, France. ArchéoSciences - Revue d'archéométrie. 40: 17-33.

Urbanová P., Guibert P. 2017. A methodological study on single grain OSL dating of mortars: comparison of five reference archaeological sites. Geochronometria. 44: 77-97.

Urbanová P., Michel A., Cantin N., Guibert P., Lanos P., Dufresne P., Garnier L. 2018. A novel interdisciplinary approach for building archaeology: The integration of mortar “single grain” luminescence dating into archaeological research, the example of Saint Seurin Basilica, Bordeaux. Journal of Archaeological Science: Reports. 20: 307-323.

Van der Kaars S., Penny D., Tibby J., Fluin J., Dam R., Suparan P. 2001. Late quaternary palaeoecology, palynology and palaeolimnology of a tropical lowland swamp: Rawa Danau, West Java, Indonesia. Palaeogeography, Palaeoclimatology, Palaeoecology. 171 (3-4): 185-212.

Van Strydonck M., Dupas M., Dauchot-Dehon M. 1983a. Radiocarbon dating of old mortars. In Mook W.G, Waterbolk H.T. (eds). 14C and Archeology Proceedings, PACT. 8: 337-343.

Van Strydonck M., Dupas M., Dauchot-Dehon M., Pachiaudi C., Marechal J. 1983b. A further step in the radiocarbon dating of old mortars. Bulletin Van Het Koninklijk Instituut Voor het Kunstpatrimonium. 19: 155-171.

Van Strydonck M., Dupas M., Dauchot-Dehon M., Pachiaudi C., Marechal J. 1986. The influence of contaminating (fossil) carbonate and the variations of d13C in mortar dating. Radiocarbon. 28 (2A): 702-710.

Van Strydonck M., Dupas M., Keppens E. 1989. Isotopic fraction of oxygen and carbon in lime mortar under natural environmental conditions. Radiocarbon. 31 (3): 610-618.

Van Strydonck M., Dupas M. 1991. The Classification and dating of lime mortars by chemical analysis and radiocarbon dating: A review. In Waldren W.H., Ensenyat J.A., Kennard R.C. (eds) IInd Deya International Conference of Prehistory, vol. 2, (BAR International Series 574), pp. 5-43.

Van Strydonck M.J.Y., Van der Borg K., De Jong A.F.M., Keppens E. 1992. Radiocarbon dating of lime fractions and organic material from buildings. Radiocarbon. 34 (3): 873-879.

Vogel J.S., Southon J.R., Nelson D.E., Brown T.A. 1984. Performance of catalytically condensed carbon for use in accelerator mass spectrometry. Nuclear Instruments and Methods in Physics Research Section B. 5(2): 289-293.

Weber J., Baragona A., Pintér F., Gosselin C. 2015. Hydraulicity in ancient mortars: its origin and alteration phenomena under the microscope. 15th Euroseminar on Microscopy Applied to Building Materials, 17-19 June 2015, Delft, The Netherlands.

Wintle A.G. 1973. Anomalous fading of thermoluminescence in mineral samples. Nature. 245: 143-144.

Wintle A.G. 1997. Luminescence dating: Laboratory procedures and protocols. Radiation Measurements. 27: 769-817.

Wintle A.G. 2008. Fifty years of Luminescence dating. Archaeometry. 50 (2): 276-312.

Zacharias N., Mauz B., Michael C.T., 2002. Luminescence quartz dating of lime mortars. A first research approach. Radiation Protection Dosimetry. 101 (1-4): 379-382.

Zimmerman D.W. 1971. Thermoluminescent dating using fine grains from pottery. Archeometry. 13:29-52.

Zucchini M. 1967. L'agricoltura ferrarese attraverso i secoli. Roma: G. Volpe Editore, pp. 324.